DEVELOPMENT, ORGANIZATION AND PLASTICITY OF THE ZEBRAFISH OLFACTORY SYSTEM

by

Oliver Robert Braubach

Submitted in partial fulfillment of the requirements
for the degree of Doctor of Philosophy

at

Dalhousie University
Halifax, Nova Scotia
March 2011

DALHOUSIE UNIVERSITY

DEPARTMENT OF PHYSIOLOGY AND BIOPHYSICS

The undersigned hereby certify that they have read and recommend to the Faculty of
Graduate Studies for acceptance a thesis entitled "DEVELOPMENT, ORGANIZATION
AND PLASTICITY OF THE ZEBRAFISH OLFACTORY SYSTEM" by Oliver Robert
Braubach in partial fulfillment of the requirements for the degree of Doctor of
Philosophy.

Dated: March 10, 2011

Supervisor: _____

Readers: _____

                      _____

                      _____

Departmental Representative: _____

DALHOUSIE UNIVERSITY

DATE: March 10, 2011

AUTHOR: Oliver Robert Braubach

TITLE: DEVELOPMENT, ORGANIZATION AND PLASTICITY OF THE
ZEBRAFISH OLFACTORY SYSTEM

DEPARTMENT OR SCHOOL: Department of Physiology and Biophysics

DEGREE: Ph.D.   CONVOCATION: May   YEAR: 2011

_____
Signature of Author

Für alle die dabei waren

Table of Contents

List of Tables

List of Figures

Chapter 3

Chapter 4

Chapter 5

Abstract

Olfaction is vitally important to animals in all environments and is used to identify food, habitat, conspecifics and predators. Some odors, like pheromones or the pungent smell of spoiled foods, can trigger pre-existing behavioral responses that appear to require no learning. Most odors, however, are only attended to as a result of prior experience. It is believed that different types of odors are processed in different olfactory pathways in the forebrain. This thesis examines the relationship between innate and learned olfactory behaviors and the anatomy of the neural pathways that underlie them, using the zebrafish olfactory system as a model.

I first characterized an appetitive olfactory behavior, which is displayed promptly by zebrafish when they encounter amino acid odors. A similar appetitive behavior can also be learned by the fish for another, initially neutral odorant, if it is repeatedly paired with food rewards. Zebrafish can therefore respond to, and learn to respond to certain odors. I then conducted an in-depth anatomical analysis of the structure and distribution of glomeruli in the zebrafish olfactory system. Glomeruli are spheroidal synaptic aggregates that organize and shape olfactory information that arrives in the brain. Throughout the development of zebrafish, I identified two distinct populations of glomeruli. One population consisted of 25 individually identifiable, anatomically stereotypic glomeruli that closely resembled specialized glomeruli in mammals and insects. These glomeruli were already formed during embryonic development and persisted in remarkably stable configurations throughout later developmental stages. I hypothesize that the 25 individually identifiable glomeruli constitute stable olfactory pathways (i.e., for innate olfactory behaviors). Most glomeruli, however, were anatomically variable and displayed different distributions within coarsely circumscribed regions in the zebrafish olfactory bulbs. The development of these glomeruli could be modified by sensory experience, suggesting that they may comprise plastic olfactory pathways that subserve the establishment of learned olfactory behaviors. Collectively my results show that innate and learned olfactory behaviors may indeed be represented in different olfactory pathways, and that these types of pathways may be located in both main and accessory olfactory systems.

List of Abbreviations and Symbols Used

AOB	accessory olfactory bulb
cAMP	cyclic adenosine monophosphate
cm	centimeter
CNG	cyclic nucleotide gated
cvpG	central ventroposterior glomerulus
CREB	cyclic AMP response element binding
CS	conditioned stimulus
d	day
dpf	days post fertilization
d(*p*)G	dorsal (*proto*) glomerulus, -i
dl(*p*)G	dorsolateral (*proto*) glomerulus, -i
DP	dorsal plexus
EL	early larva(e)
GAL4	yeast transcription activator protein
GFP	green fluorescent protein
G$_{olf}$	olfactory G-protein
hpf	hours post fertilization
hr	hour(s)
IR	immunoreactive / immunoreactivity
JGC(s)	juxtaglomerular cell(s)
JU	juvenile
kDa	kilodalton
KLH	keyhole limpet hemocyanin
lcG	lateral cluster glomerulus, -i
l*p*G	lateral (*proto*) glomerulus
L	liter

LIR	like immunoreactive / -immunoreactivity
LOB	left olfactory bulb
LP	lateral plexus
lvpG	lateral ventroposterior glomerulus
MC(s)	mitral cell(s)
mdG	mediodorsal glomeruls, -i
meG	medial elongated glomerulus
min	minute
ML	mid larva(e)
ml	milliliter
MOB	main olfactory bulb
m(*p*)G	medial (*proto*) glomerulus, -i
MS-222	tricaine methanosulfate
mvpG	medial ventroposterior glomerulus
µm	micrometer
NT	nervus terminalis
OB	olfactory bulb
OE	olfactory epithelium
OMP	olfactory marker protein
ON	olfactory nerve
OR(s)	olfactory receptor(s)
OSN(s)	olfactory sensory neuron(s)
PEA	phenyl-ethyl alcohol
pH	negative logarithm of hydrogen ion concentration
PBS	phosphate buffered saline
PBS-T	phosphate buffered saline containing triton
pKA	protein kinase A
ROB	right olfactory bulb
r.p.m	rotations per minute
sec	second(s)

SV$_2$	synaptic vesicle protein 2
TAAR	trace amine-associated receptor
TH	tyrosine hydroxylase
TRPC2	transient receptor potential channel 2
UAS	upstream activation sequence
UCS	unconditioned stimulus
v(*p*)G	ventral (*proto*) glomerulus, -i
vm(*p*)G	ventromedial (*proto*) glomerulus, -i
vpG	ventroposterior glomerulus, -i
VSN	vomeronasal sensory neuron
vtG	ventral triplet glomerulus, -i
V1R / V2R	vomeronasal receptor type 1 / 2
~	approximately
ºC	degree celsius
%	per cent

Acknowledgements

I would like to express my gratitude to my supervisors Dr. Roger Croll and Dr. Alan Fine for their guidance, support, patience and friendship throughout the course of my degree. It was a pleasure and a joy to work with you.

I would also like to thank past and present members of my supervisory committee, Dr. Frank Smith, Dr. William Baldridge, Dr. Douglas Rasmusson, and my external examiner Dr. Thomas Finger for their participation in this process.

A special thanks to Dr. Richard Brown for introducing me to Neuroscience.

Many thanks to members of the Croll and Fine laboratories for their friendship, insight and help; Dr. Russell Wyeth for his 'matter of factness' and Wednesday evenings, Matt Stoyek for knowing where everything is, Dr. Yi-Ling Hu for being my personal critic, Dr. Ryuichi Nakajima for being a good friend, Andrew for being Murray, Ryosuke, Ben, Tristan, Nirupa, Cecilia, Borbala and Ulli for being fun lab mates.

Thanks also to Annette and Stefan, Kazue Semba, Liz Cowley, Younes Anini, Jim Eddington, the Aquatron staff, Brian Hoyt, Mark Richard, and others who have made their time, space or equipment available for my research.

Thanks to all my friends who have experienced this process with me; Matt Naugler, Randy and Lila Naugler, Keram, Jeff, Mike and Ange, Nicole, Jenn and Mike.

Thank you Ambera for lovingly supporting my scientific endeavors and for providing me with a refuge from them.

And finally, I would like to thank my family, for supporting me for so many years in a far away country, and always providing me with a place to call home.

Chapter 1

Introduction

The sense of smell is vitally important for animals in every type of environment; it is used to search for food, to recognize habitat and conspecifics, to detect environmental hazards and predators and to respond to species-specific pheromones. In both vertebrates and invertebrates there appear to be two distinct types of olfactory behaviors. One of these is an innate olfactory behavior, such as an aversive response to spoiled foods in rodents (Kobayakawa et al., 2007), or an attraction to specific food odors in fruit flies (Ibba et al., 2010). The other olfactory behavior is learned, and is thought to occur only after animals experience odors in a certain context. For example, *Drosophila* do not normally respond to octanol, but after pairing this odor with electric shocks, the flies avoid it (Quinn et al., 1974). Similarly, mice quickly learn to respond and attend to a previously meaningless odor after it is paired with sugar (Schellinck et al., 2001).

The topic of my thesis was to examine the relationship between pre-existing and learned olfactory behaviors and the anatomy of the olfactory pathways that underlie such behaviors. I used zebrafish *Danio rerio* as a model because this animal displays tractable olfactory behaviors and has an olfactory system that is small enough to permit anatomical analysis of the entire primary olfactory pathways, consisting of the paired sensory epithelia and olfactory bulbs. It is known from mammals that different types of olfactory behaviors (i.e., innate vs learned) are processed in separate olfactory pathways, and that neural elements within these pathways differ in their form and function, both at the level of sensory transduction and odor coding in the brain. Little remains known, however, about such differences in fish and amphibians, and I thus describe multiple anatomically distinct olfactory pathways in the zebrafish. These pathways share many similarities with those in the mammalian olfactory system, which I will review briefly below in order to

provide the reader with a basic understanding of the material covered in this thesis.

1.1 Main, Accessory and Atypical Olfactory Pathways in Mammals

Rodents, which are most commonly employed in olfaction research, have an olfactory system that has been traditionally divided into two distinct pathways, the main and the accessory olfactory systems. These pathways are anatomically separate from one another, and are believed to process distinct types of olfactory information. Specifically, the main olfactory system appears to be involved mainly in processing general environmental odors (e.g., food odors) while the accessory olfactory system is most commonly linked to pheromonal communication (Dulac, 2000, Dulac and Wagner, 2006). However, despite clear differences in the anatomy of these systems, their roles in mediating olfactory behaviors may not be mutually exclusive. For example, genetic ablations of the transient receptor potential channel 2 (TRPC2, see below), a crucial component of sensorineural transduction in the accessory olfactory system, does not impact suckling behavior and male-male aggression in rodents (Wang et al., 2007, Wang et al., 2009, Brunet et al., 1996, Stowers and Logan, 2010). Both of these behaviors are triggered by pheromones, but evidently they may not depend on an intact accessory olfactory system.

It thus appears that a simple division of the vertebrate olfactory system into main and accessory pathways, although useful to study different mechanisms of olfactory processing, does not accurately describe the organization and complexity of this sensory system. Instead, it may be more instructive to consider the olfactory system as a series of independent or interdependent chemosensory pathways, each of which is specifically designed to respond to certain stimulatory chemicals. This may indeed be the case in the

rodent olfactory system, and specialized olfactory pathways could include those that are involved in sensing carbon dioxide (Hu et al., 2007, Sun et al., 2009), non-pheromonal alarm substances (Kobakayakawa et al., 2007) and temperature (Mamasuew et al., 2008). Although little is currently known about the form and function of such 'atypical' olfactory pathways, they appear to share many of the organizational features that have been established in studies of the mammalian main and accessory olfactory systems. I will therefore review the form and function of these systems below in order to provide a basic understanding of olfactory system neurobiology, which will aid the reader in understanding the material presented in later chapters of this thesis.

1.2 Odor Transduction Via OR Type Olfactory Sensory Neurons (OSNs)

The *main olfactory system* processes information about a vast number of odors related to feeding, environment and social interactions. Processing of such odors begins in the fluid lined sensory epithelium of the mammalian main olfactory organ, which houses millions of olfactory sensory neurons (OSNs) that are responsible for transforming chemical mixtures into a neural odor code. The classical OSN of the main olfactory system is a bipolar neuron that extends a single long dendrite to the surface of the sensory epithelium, where it terminates in a ciliated knob (Elsaesser and Paysan, 2007, Ache and Young, 2005). The membranes of OSN cilia are enriched with olfactory receptors (ORs), which can bind to specific odor molecules to stimulate coupling with a G-protein complex, G_{olf}. Coupling of the OR with G_{olf} stimulates enzymatic cAMP synthesis, which further leads to opening of non-selective cyclic nucleotide gated (CNG) cation channels, a cation influx, and finally, depolarization of the OSN (Ronnett and Moon, 2002, Munger et al., 2009).

Collectively, murine OSNs express 1000-1200 different ORs (Touhara and Vosshall, 2009, Buck and Axel, 1991), all of which have a seven-transmembrane domain structure characteristic of G-protein coupled receptors (Mombaerts, 2006). The most variable regions of OR genes encode transmembrane segments 3-4, and these regions may therefore contain the molecularly diverse binding pockets for different odorant molecules (Alioto and Ngai, 2005).

OSNs follow a 'one cell - one receptor' rule, and each mature sensory neuron expresses only one functional OR type (Serizawa et al., 2004). However, interactions between OR receptors and their ligands are promiscuous, and a single OR type can recognize many different odor molecules, and odor molecules can bind to many different OR types (Malnic et al., 1999). Odor quality (viz. odor type) is thus encoded in unique combinatorial (ensemble) activations of large OR sets. Furthermore, changes in odor concentration affect OR-ligand interactions, and increasing the concentration of any odor molecule increases the likelihood that it will bind to multiple OR types. Similar to odor quality, odor concentration is thus encoded in a combinatorial OR activation code (Ma and Shepherd, 2000, Buck, 2004).

OSNs that express similar ORs (and therefore respond to similar ligands) are clustered in large, non-overlapping domains in the olfactory epithelia (Mombaerts, 2006, Kobayakawa et al., 2007), but the fine organization of OSNs appears to be random (Vassar et al., 1993, Ressler et al., 1993). Nevertheless, each OSN projects a single axon to the ipsilateral olfactory bulb, and once these axons arrive in the bulb, they become highly organized (Bozza et al., 2009) and converge in spheroidal synaptic relays, the glomeruli (see OSNs and glomeruli in Figure 1A).

1.3 Organization of Main Olfactory System Glomeruli

The most fundamental feature of olfactory system organization is the massive convergence of OSN axons onto discrete ovoid to spheroidal synaptic aggregates, the glomeruli (Chen and Shepherd, 2005). Anatomical estimates in vertebrates indicate that 5000 to 25000 OSN axons converge at individual glomeruli (Chen and Shepherd, 2005, Mori and Yoshihara, 1995), and the terminals of these axons comprise dense neuropilar structures that are clearly visible on the surface of the olfactory bulbs (see glom in Figure 2A). The glomerulus proper is acellular (Kasowski et al., 1999) and consists entirely of axon shafts and their terminals, dendrites and dendritic terminals, and glial processes (Figure 1B). The most abundant synapse within the glomerulus is the axodendritic synapse formed between OSN axons and dendritic arbors from approximately 75-100 principal neurons, the mitral cells (MCs). In rats, this glutamatergic synapse accounts for approximately 75% of all neural elements in the glomerular neuropil (Kasowski et al., 1999), while the remaining synaptic contacts are formed between OSN axon terminals and / or MC dendrites with interneuron processes (for review, see Chen and Shepherd, 2005, Shepherd, 1972).

Interestingly, the distribution of synapses in individual glomeruli is not homogenous. Rather, each glomerulus appears to be compartmentalized into distinct regions that contain only axodendritic (e.g., OSN axon to MC in dashed outline in Figure 1B) or dendrodendritic contacts (Halasz and Greer, 1993, Kasowski et al., 1999). These compartments are molecularly distinguishable from one another based on their selective innervation by axons expressing different cell surface markers (Johnson et al., 1996, Treloar et al., 1996), and their selective targeting by the processes from neurochemically

distinct interneurons (Kosaka et al., 1997). Collectively, these observations suggest that the glomerular neuropil may contain multiple distinct compartments, however, the functional implications of this compartmentalization are not resolved.

The dendritic processes that innervate glomeruli arise from MCs located in the external cellular layer underlying the glomeruli and from interneurons in the juxtaglomerular space surrounding the glomerular neuropil (Figure 1B). The MCs that innervate a single glomerulus cluster together and are synaptically coupled via dendrodendritic connections (Chen and Shepherd, 2005, Shepherd, 1972). Juxtaglomerular interneurons form a ring around each glomerulus (magenta cells in Figure 1B), and are thus considered to be important determinants of glomerular structure. Indeed, juxtaglomerular cells appear to be important determinants for the development and proper maturation of the glomerulus proper (Bailey et al., 1999, Puche and Shipley, 2001, Valverde et al., 1992).

Glomeruli and the cells associated with them have been likened to cortical barrels or columns (Chen and Shepherd, 2005), and in accordance with this view, they appear to function as narrowly tuned sensory units in olfactory processing.

Function of Main Olfactory System Glomeruli

Each main olfactory bulb glomerulus is innervated with high selectivity by the axons of a single or a few OSN types (Vassar et al., 1994, Ressler et al., 1994). Each OSN expresses only a single OR type (Serizawa et al., 2004), and individual glomeruli are thus narrowly tuned to respond to a few molecular components that constitute odor mixtures (for review see Mombaerts et al., 2006). Based on their selective innervation, glomeruli thus appear to play an organizing role, in which each glomerulus collects and

organizes olfactory information from millions of widely scattered OSNs, into a few sensory units that are located in fixed positions on the surface of the olfactory bulb (Buck, 2004). Indeed, optophysiological data confirm this idea, showing that different odors activate unique, but repeatable spatial patterns of activity among glomeruli (Wachowiak and Cohen, 2001, Uchida et al., 2000, Stewart et al., 1979, Sharp et al., 1975, Moulton, 1976), and it is thus believed that these activity patterns represent an orderly 'odor code' that can be read by integrating regions in the brain.

In addition to their role as organizing modules, glomeruli and the cells associated with them, apparently play roles in sharpening the olfactory input. For example, glomeruli with similar tuning cluster together (Johnson and Leon, 2007, Friedrich and Korsching, 1998) and are interconnected by a network of inhibitory juxtaglomerular interneurons (e.g., Figure 1B). In a group of similarly tuned glomeruli, multiple units will be activated by the same odor molecules, but with varying intensities. Those glomeruli that are most sensitive to the odor molecules will exert a strong inhibitory effect on weaker-activated glomeruli in their surround, thereby reducing 'background noise'. Such lateral inhibition appears to depend strongly on the activity of juxtaglomerular interneurons, which are instructed by neighbouring glomeruli to inhibit stimulus transmission in MC dendrites (Figure 1B; for review see Wachowiak and Shipley, 2006). Coincidentally, strongly activated MCs can synchronize their firing patterns via dendrodendritic synapses formed between their dendrites, thereby enhancing their output and the contrast of the relevant olfactory signal (Yokoi et al., 1995, Chen and Shepherd, 2005).

Odor representations (glomerular ensemble activity) in the mammalian main olfactory bulb are dynamic and subject to modulation by experience. For example, olfactory conditioning can lead to changes in glomerular activity (Wilson and Leon, 1988, Johnson et al., 1995) and morphology (Woo et al., 1987, Kerr and Belluscio, 2006). Furthermore, axon terminals can compensate for odor deprivation by enhancing neurotransmitter release probability (Tyler et al., 2007), and long-term potentiation can be induced between OSN axon terminals and mitral cell dendrites (Yuan, 2009), and between dendrodendritic connections of mitral cells (Zhou et al., 2006, Pimentel and Margrie, 2008, Satou et al., 2006, Satou et al., 2005). Thus, there are multiple synaptic connections within and between glomeruli and all of these appear to be modifiable by experience. It is because of these connections that glomeruli in the main olfactory bulbs are believed to be neural substrata that contribute to the acquisition and retention of learned olfactory behaviors.

1.4 Odor Transduction in the Accessory Olfactory System

The mammalian accessory olfactory system is traditionally viewed as the substrate responsible for processing pheromonal inputs and eliciting behaviors of an innate (e.g., pre-existing) type (Dulac, 2000). Pheromones are large organic compounds, which are sensed by sensory neurons (VSNs) in the vomeronasal sensory organ, separate from the main olfactory organ (blue and magenta cells in Figure 1C). VSNs are morphologically and molecularly distinct from OR-type receptors (above) and they express vomeronasal receptor types 1 and 2 (V1R, V2R), each of which couple to distinct G-protein complexes containing the subunits $G\alpha_{i2}$ and $G\alpha_o$, respectively (Zufall and

Leinders-Zufall, 2007, Touhara and Vosshall, 2009). When activated, V1R and V2R couple with a distinct G-protein complex, leading to activation of a phospholipase C signalling cascade, ultimately leading to the opening of transient receptor potential cation channels (e.g., TRPC2) to depolarize the VSNs (Munger et al., 2009). In rodents, the numbers of functional V1R (200) and V2R (280) genes is much less than that of the OR-type receptors, and in humans there appear to be only 25 functional pheromone receptor genes (Touhara and Vosshall, 2009), suggesting that only very few (if any) of the hundreds of purported human pheromones that are commercially available may trigger their desired effects.

The tuning of V2R-type receptors to particular pheromone compounds appears to be very narrow and interactions between this receptor type and its ligands may not occur in a combinatorial manner (compare to OR type above). For example, optophysiological recordings from isolated VSNs showed that V2R-expressing VSNs responded with high specificity to potential pheromones, without becoming more promiscuous to other ligands as concentrations were increased (Leinders-Zufall et al., 2000). Based on these and other findings (for review, see Touhara and Vosshall, 2009), V2R-expressing VSNs have been hypothesized to be 'specialist' sensory receptors that function in a 'one receptor - one ligand' fashion, and thus respond only to a few behaviorally relevant chemical ligands (Luo and Katz, 2004). Neural pathways that are downstream from V2R may thus be equally sensitive to certain types of pheromone compounds, which is very different from the combinatorial odor codes used to encode chemical stimuli in the main olfactory system.

1.5 Organization of the Accessory Olfactory Bulb

The surface of the accessory olfactory bulbs (AOB) consists of spheroidal synaptic relays in which the axons from VSNs synapse with mitral cells (Figure 1C). The organization of these glomeruli, however, is very different from that of MOB glomeruli. AOB glomeruli are much smaller (Meisami and Safari, 1981), and are organized in large and vaguely circumscribed regions (Wagner et al., 2006). Furthermore, AOB glomeruli can be targeted by the axons of up to 20 different VSN types (Belluscio et al., 1999, see also Rodriguez et al., 1999), and be non-selectively innervated by mitral cells that extend extensive dendritic arbors towards several glomeruli at once (Takami and Graziadei, 1991, Takami and Graziadei, 1990, Mori et al., 1983). This arrangement suggests that AOB glomeruli do not merely represent the activation of certain vomeronasal receptor types, but that they integrate incoming olfactory information from multiple receptor types to produce a pheromone 'identity code' (Dulac and Wagner, 2006).

Recent recordings from mitral cells in the mouse AOB have identified cells that respond with high selectivity to certain pheromone components, as well as others that appear to encode mixtures of such chemicals (Meeks et al., 2010). Indeed, in many animals it appears that pheromones are blends of chemicals (Wyatt, 2010, Sorensen et al., 1998) and glomeruli in the accessory olfactory system may thus be wired towards detecting not only individual chemical constitutents, but specific chemical blends, which ultimately comprise pheromone signals.

Thus, the main and accessory olfactory systems of mammals appear to employ different mechanisms of sensorineural transduction and odor coding; the main olfactory system appears to be broadly tuned towards detecting a vast number of odors in a

changing environment, while the accessory olfactory pathway may be more specialized and tuned towards a limited range of species-specific odors.

1.6 'Atypical' Olfactory Pathways in the Main Olfactory Bulb

In addition to the above-mentioned main and accessory olfactory systems, there are several 'specialist' olfactory pathways that are distinct in their anatomy, function and their roles in mediating olfactory behaviors (for review see Stowers and Logan, 2010). For example, the main olfactory system of rats contains a small number of 'atypical' glomeruli that together comprise a 'modified glomerular complex'. This complex is located along the boundary of the MOB and AOB, and is selectively activated by suckling pheromone in rat pups (Teicher et al., 1980, Greer et al., 1982). Unlike the widespread combinatorial activation of 'typical' MOB glomeruli (above), the activation of sensory units within the modified glomerular complex is highly localized and appears to be non-combinatorial (Greer et al., 1982). Furthermore, the development of the modified glomerular complex precedes that of other MOB glomeruli and this olfactory pathway appears to be completely differentiated and functional at the time of birth, when much of the MOB is still disorganized and devoid of glomeruli proper (Greer et al., 1982).

Similarly, 'necklace glomeruli' are also located in the MOB, and unlike other MOB glomeruli, these glomeruli resemble a string of beads, in which each glomerulus is contacted *en passant* by incoming sensory neuron axons (Luo, 2008). Necklace glomeruli are sensitive to semiochemicals released in urine (Cockerham et al., 2009) and have been additionally linked to CO_2 sensing (Hu et al., 2007). The sensory neurons that innervate the necklace glomeruli are unique, and unlike canonical OSNs and VSNs (above), they do

not appear to employ G-protein coupled receptors in sensorineural transduction (Luo, 2008). Furthermore, necklace glomeruli are innervated by multiple OSN classes, including OSNs (above), and may therefore integrate information across different olfactory pathways (Cockerham et al., 2009). Thus, both the modified glomerular complex and necklace glomeruli comprise specialist olfactory subsystems within the MOB, involved in processing of highly select stimuli, or subserving a modulatory role between different olfactory pathways.

As discussed below, fish are faced with an olfactory environment that similarly diverse as that of terrestrial mammals, but we do not yet understand how the fish olfactory system processes the many different types of odors present in the aquatic environment.

1.7 The Olfactory Environment of Fish

The olfactory environment of fish is rich in dissolved chemicals and many of these are unspecialized metabolic biproducts that convey information about food, habitat and conspecifics (Derby and Sorensen, 2008). In addition, many species are known to employ specific pheromones to signal the availability of potential mates or the presence of predators (Sorensen et al., 1998). There exists considerable variability among the known behavioral significance of odors within and between species, and these are reviewed in detail elsewhere (Hara, 1994, Derby and Sorensen, 2008). Below I will focus on odors known be involved in feeding and social communication in zebrafish and related species.

Amino Acids and Feeding

Amino acids emanate from foods that are high in protein and as such are favored

and actively sought by many fish (Derby and Sorensen, 2008). Upon encountering an amino acid, many fish will promptly initiate appetitive swimming behaviors, which include chemotactic swimming; this behavior manifests itself as a series of alternating turns, presumably as the fish are adjusting their position while following an amino acid gradient within an odor plume (Valentincic et al., 2000a). Appetitive swimming behaviors ultimately lead the animals to the source of the odorant, and once the fish is exposed to a certain threshold concentration of amino acids (e.g., at the source of the odor) it displays reflexive snapping and biting behaviors, both of which are presumably mediated by the gustatory system (Valentincic and Caprio, 1997, Valentincic and Caprio, 1994a). Behavioral responses to amino acids have been documented in many fish (Hara, 2006, Hara, 1994, Hamdani and Døving, 2007, Derby and Sorensen, 2008), and to my knowledge there exists a consensus that these chemicals are involved mainly in feeding.

Pheromones and Bile Acids

Fish are highly sensitive to bile acids and pheromones, which are actively released by individuals and used as social signals. For example, in lampreys, trout, salmon and kokopu, bile acids are released during mating season in order to attract conspecifics to the spawning grounds (Li et al., 2002, Fine et al., 2004, Døving et al., 1980). In this role, bile acids are considered to be migratory pheromones, which complement the function of sex pheromones that are released locally at the spawning grounds (below).

A more global function (e.g., applies to all fish) for bile acids may be their employment as 'signature mixtures' (Wyatt, 2010). 'Signature mixtures' are used to recognize kin, to discriminate sex and age of kin, to discriminate kin from other species, and for shoaling and other non-sexual aggregating behaviors (Sorensen and Stacey,

2004). Furthermore, bile acid mixtures appear to be used to refine certain pheromone signals. For example, bile-acids may be co-released with sex-pheromones in minnows, all of which appear to employ the same or similar sex pheromones (Derby and Sorensen, 2008); co-release of a conspecific 'signature mixture' along with sex-pheromone may then enable the fish to discriminate mating signals from their own species over those emanating from other species. Similarly, alarm pheromones, which are released from the skin of injured fish to signal predation (Waldman, 1982, Jesuthasan and Mathuru, 2008, Døving and Lastein, 2009), are also co-released with additional odors, including bile acids and amino acids (Derby and Sorensen, 2008). A fish may then perceive the alarm pheromone as a warning signal, the bile acids as cue that the warning signal is from a conspecific, and will then presumably be able to interpret the amino acid as a non-food odor.

Thus, the olfactory environment of fish is complex and fish are continuously faced with odor mixtures consisting of potentially conflicting information from which the fish need to identify and discriminate the relevant cues from an otherwise noisy olfactory environment. Unlike most mammals, fish accomplish all this in a single compact olfactory system.

1.8 The Olfactory System of Fish

The odors discussed above are transduced into neural information in bilateral olfactory epithelia that are often folded into symmetric rosette-shaped structures (Hansen and Zeiske, 1993, Hansen et al., 2005), located within small pits anterior to the eyes (see OE in Figure 2B). The olfactory pits, or nostrils, are covered by several folds of skin, which together comprise a funnel that facilitates water flow to the olfactory epithelium

(Cox, 2008). The surfaces of the olfactory epithelia are lined with OSNs (Figure 2C) and each of these sends an axon via the olfactory nerve to two compact and bilaterally symmetric olfactory bulbs (OB in Figure 2B), where they target the dendrites of postsynaptic mitral cells within spheroidal glomeruli (glom in Figure 2A).

The olfactory system of many teleost fish (e.g., zebrafish) is smaller and less complex than that of mammals. Fish have between 50-100 OR types (Hashiguchi and Nishida, 2007, Alioto and Ngai, 2005) and therefore a less diverse repertoire of OSNs and glomeruli (Korsching et al., 1997). Furthermore, there is no gross separation of olfactory pathways into main and accessory components. Instead, amino acids, bile acids and pheromones are processed in parallel olfactory pathways in a single olfactory system (Figure 3).

Amino Acids Are Processed in a Lateral Olfactory Pathway

The diverse odors discussed above are transduced by different populations of sensory receptor cells, which send axons to distinct regions of the olfactory bulb, the lateral and medial olfactory bulbs (Laberge and Hara, 2001, Hamdani and Døving, 2007).

Physiological evidence suggests that amino acids (and nucelotides) are transduced by microvillous OSNs (see green cells in Figure 3) in zebrafish (Lipschitz and Michel, 2002), carp (Thommesen, 1983), catfish (Hansen et al., 2003) and trout (Sato and Suzuki, 2001). Microvillous cells express V2R type odorant receptors and TRPC2 channel subunits (Sato et al., 2005), in addition to the G-protein G_q (Hansen et al., 2003). Interestingly, all of these molecules are linked to pheromone pathways in mammals (above), but in fish, microvillous cells appear to mediate mostly feeding (but see Zippel et al., 1997).

The axons of microvillar cells project almost exclusively to the lateral olfactory bulbs of zebrafish (Sato et al., 2005, Koide et al., 2009, Castro et al., 2006). As expected, the lateral glomeruli (see green glomeruli in Figure 3) are sensitive to amino acid-odors in adult (Hamdani et al., 2001b, Hamdani et al., 2001a, Fuss and Korsching, 2001, Friedrich and Korsching, 1998, Friedrich and Korsching, 1997), and newly hatched larval fish (Li et al., 2005a). Genetically silencing microvillous cells in zebrafish, by expressing tetanus toxin in their axon terminals, disrupts food-searching behavior (Koide et al., 2009). Furthermore, chemical mutagenesis that results in malformations of lateral glomeruli, disrupts behavioral attraction to some amino acids (Vitebsky et al., 2005). Collectively, these data support the role of microvillous cells and lateral glomeruli in mediating amino acid-evoked food searching behaviors in zebrafish.

Bile Acids and Pheromones are Processed in a Medial Olfactory Pathway

Bile acids appear to be transduced mainly by ciliated OSNs (Thommesen, 1983, Hansen et al., 2003, Døving et al., 2011). These cells (red cells in Figure 3) have long dendrites with a characteristic ciliated knob that protrudes towards the epithelial surface (Hansen and Zielinski, 2005, Hansen et al., 2003, Frontini et al., 2003, Celik et al., 2002, Belanger et al., 2003). The cilia are enriched with the OR-type olfactory receptors that are linked to the G-protein G_{olf}, suggesting that the cilia are the sites of odor transduction. Ciliated OSNs also express the olfactory marker protein OMP (Sato et al., 2005, Celik et al., 2002), and the CNG subunit A2 (Sato et al., 2005), and thus closely resemble the OR-type OSNs in mammals.

A third receptor cell type, the crypt cell, appears to be unique to fish (Hansen and Finger, 2000, Hansen and Zielinski, 2005). This ovoid cell (blue cells in Figure 3) is

located superficially in the sensory epithelium and easily discriminated from the above-mentioned sensory neurons because of its round shape, lack of a long dendritic protrusion and the presence of a small crypt at its apical membrane (Hansen and Finger, 2000). Crypt-cells in catfish express $G_{\alpha o}$ (Hansen et al., 2003), which is associated with pheromonal communication in mammals, and they are thought to be responsible for transducing pheromones in fish (Hamdani et al., 2008, Hamdani and Døving, 2007).

Both, ciliated OSNs and crypt sensory neurons project axons to the medial olfactory bulbs (Sato et al., 2005, Morita and Finger, 1998, Hamdani and Døving, 2007, Hamdani and Døving, 2002, Frontini et al., 2003) and there is ample evidence to show that medial glomeruli are sensitive to bile acids (Nikonov and Caprio, 2001, Hansen et al., 2003, Friedrich and Korsching, 1998, Døving et al., 1980) and pheromones (Sorensen et al., 1991, Lastein et al., 2006, Hamdani and Døving, 2003, Fujita et al., 1991). It is, however, unclear how bile acids and pheromones are processed in the medial olfactory bulbs.

Data from Friedrich and Korsching (1998) suggest that bile acids activate large overlapping sets of medial glomeruli, and that they may be encoded in a combinatorial manner, while candidate sex pheromones activate small and sharply demarcated 'glomerular modules' that may correspond to certain identifiable glomeruli (see also, Baier and Korsching, 1994). Extracellular recordings indicate that sex pheromones preferentially activate posteromedial regions of the olfactory bulbs (Lastein et al., 2006), but it is unclear which, and how many different types of glomeruli reside within these regions. Furthermore, single unit recordings in posteromedial regions respond to skin extract that contains alarm pheromone (Hamdani and Døving, 2003), but it is again

unclear how such responses relate to actual glomeruli.

Thus, there exists a functional dichotomy between the lateral and medial olfactory bulbs of fish, but little remains known about the contributions of individual glomeruli within lateral and medial olfactory bulbs to olfactory coding and the production of olfactory behavior.

1.9 Thesis Objectives

The purpose of this thesis was to characterize a zebrafish olfactory behavior and map the underlying neural circuitry to permit future physiological studies aimed at linking whole-animal behavior with cellular neurobiology. In doing so, I initially identified pre-existing and learned olfactory behaviors (Chapter 2). I then used a variety of anatomical tools to describe in the zebrafish olfactory system in unprecedented detail, describing the distribution (Chapter 3), detailed morphology (Chapter 4) and development (Chapter 5) of glomeruli in this olfactory system. Collectively, my results suggest that odors are encoded in two anatomically distinct olfactory pathways that appear to be suitable substrates for initiating pre-existing (i.e., innate) and learned olfactory behaviors.

Figure 1. Schematic overview of the olfactory system. The sensory epithelium is on the left hand side and the brain is on the right hand side. (**A**) Odors are transduced into neural information by randomly scattered OSNs in the sensory epithelium. Each OSN projects a single axon to the olfactory bulb and selectively innervates a glomerulus. (**B**) The glomerulus proper (grey area) consists of pre- and postsynaptic terminals of neural processes that arise from different cell types outside of the glomerulus. Each glomerulus is compartmentalized (small dashed circles) into distinct regions containing different types of input and / or modulatory synapses. General environmental odors and pheromones are processed mainly in different pathways, the main (**A**) and (**C**) accessory olfactory systems.
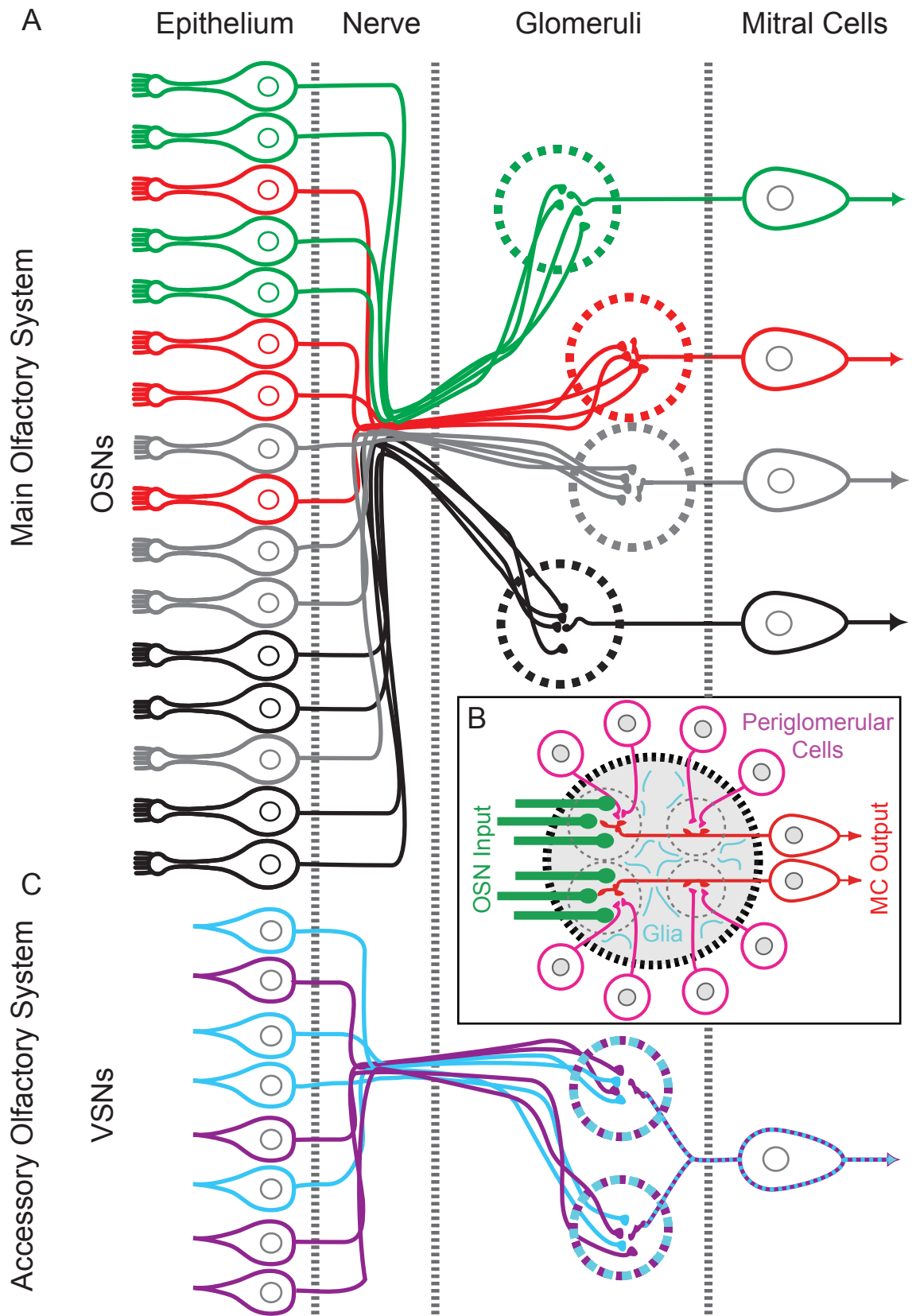
Figure 1 - Schematic Overview of the Olfactory System

Figure 2. Gross Anatomy of the Zebrafish Olfactory System. (**A**) The surface of the zebrafish olfactory bulbs is innervated by hundreds of OSN axons (green) that terminate in spheroidal glomeruli (glom). Shown in magenta are the synaptic terminals of the OSN axons, the glomerulus proper, revealed via staining against the synaptic vesicle protein 2 (SV_2). (**B**) Dorsal view of a zebrafish head with the skull cap removed to expose the olfactory epithelia (OE), olfactory nerve (ON) and olfactory bulbs (OB). (**C**) The olfactory epithelia are lined with olfactory sensory neurons (OSNs) that extend ciliated dendrites to the epithelial surface (dashed line). OSNs are visualized here via staining against a cellular protein (calretinin). For more information on the anatomical labels and staining procedures, refer to Chapter 3.
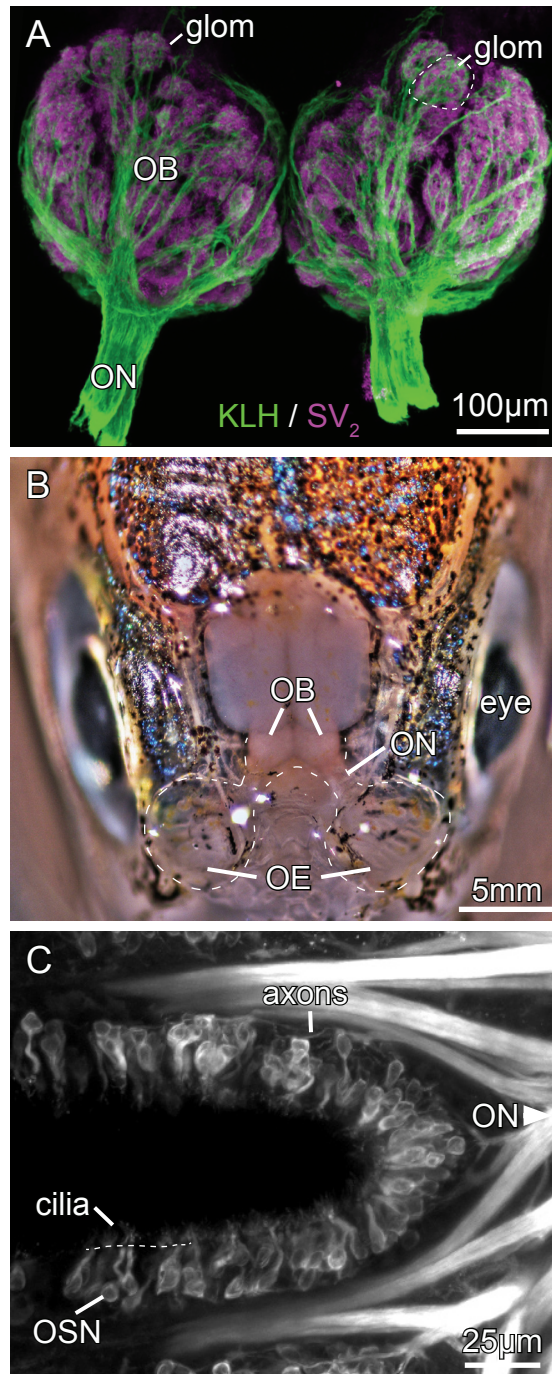
Figure 2 - Gross Anatomy of the Zebrafish Olfactory System

Figure 3. Schematic overview of the fish olfactory system. Non-pheromonal and pheromonal odors transduced in parallel pathways in a common olfactory system. Distinct cell types transduce different odors; microvillous OSNs (green) are amino acid-sensitive, ciliated OSNs (red) are bile acid-sensitive and (crypt cells, blue) presumably respond to pheromones. Aside from their innervation of medial (red, blue) and lateral (green) olfactory bulbs, little is known about the targets of the OSN axons in the olfactory bulbs. The schematic shows only the coarse organization of the fish olfactory system.
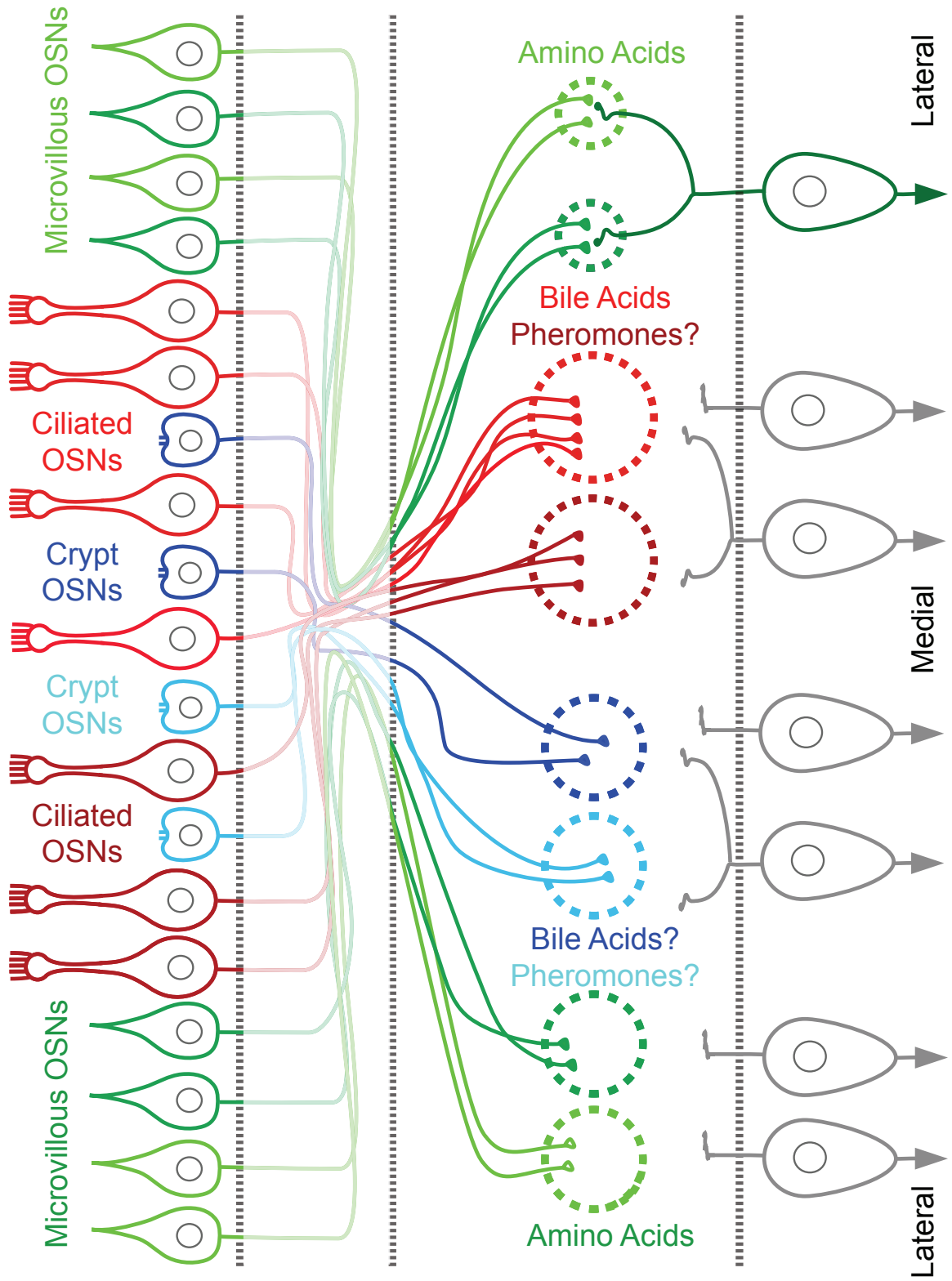
Figure 3 - Schematic Overview of the Fish Olfactory System

Chapter 2

Classical Conditioning of Zebrafish Olfactory Behaviors

2.1 Summary

The zebrafish olfactory system is an attractive model for studying neural processing of chemosensory information. Here we characterize a zebrafish olfactory behavior and its modification through learning, using an apparatus consisting of a circular flow-through tank that allows controlled administration of odorants. When exposed to the amino acids L-alanine and L-valine, naïve zebrafish responded with appetitive swimming behavior, which we measured as the number of $>90^o$ turns made during 30 s observation periods. Such an appetitive response was not observed when naïve zebrafish were exposed to an unnatural odorant, phenylethyl alcohol (PEA). Repeated pairing of amino acids or PEA (conditioned stimuli; CS) with food flakes (unconditioned stimuli; UCS) increased odorant-evoked appetitive swimming behavior in all fish tested. The zebrafish also learned to restrict this behavior to the vicinity of a feeding ring, through which UCS were administered. When both nares were temporarily occluded, conditioned fish failed to respond to odorants, confirming that these behaviors were mediated by olfaction. These results represent the first demonstration of a classically conditioned appetitive response to a behaviorally neutral odorant in fish. Furthermore, they complement recent demonstrations of conditional place preferences in fish. By virtue of its robustness and simplicity, this method will be a useful tool for future research into the biological basis of olfactory learning in zebrafish.

2.2 Introduction

The zebrafish is an attractive model for studying the molecular and cellular bases of behavior. Many of the advantages that have led to the widespread use of zebrafish in developmental biology (Fishman, 2001) apply equally well to studies of neural substrates of behavior. *In vivo* cellular neurobiology of zebrafish can be directly correlated with whole animal behavior (Fetcho et al., 2008), and recent work suggests that zebrafish can be employed for studying neural mechanisms underlying olfactory-driven behaviors. In particular, there has been considerable progress toward elucidating the genetics (Vitebsky et al., 2005, Sato et al., 2005), neurophysiology (Yaksi et al., 2007, Tabor et al., 2004), development (Whitlock and Westerfield, 1998, Li et al., 2005a) and structure (Fuller et al., 2006, Byrd and Brunjes, 1995) of the zebrafish olfactory system. Additional evidence that zebrafish olfactory behaviors can be conditioned (Valentincic et al., 2005) suggests that this animal may also be a useful model for *in vivo* study of neural mechanisms underlying behavioral plasticity.

Several species of fish, including zebrafish, have been successfully conditioned to associate odorants with aversive stimuli. In the conditioned cardiac reflex paradigm, for example, odorants are paired with electric shocks to which fish respond with decreased heart rates. Using this method, it was demonstrated that catfish (Little, 1981) can associate single amino acid odorants with aversive stimuli, and also discriminate among these odorants. Similarly, Manteifel and Karelina (1996) demonstrated that goldfish can be conditioned to avoid flavored food particles following injections with lithium chloride. This aversion was partially blocked after occlusion of the nostrils, demonstrating an involvement of the olfactory system (Manteifel and Karelina, 1996). In another

paradigm, Suboski et al. (1990) demonstrated that zebrafish can be conditioned to respond with defensive behaviors to previously neutral odorants, by specifically pairing these neutral odors with alarm pheromones released by injured conspecifics (Suboski et al., 1990). Both sensory preconditioning and second order conditioning experiments suggest that the learning of alarm behaviors was mediated by classical conditioning (Hall and Suboski, 1995).

A positive reinforcement paradigm for conditioning freely swimming fish to odorants was first demonstrated using catfish (Herbert and Atema, 1977). Later experiments showed that innate appetitive swimming could be conditioned through repeated pairings of amino acid odorants with food rewards, leading to increased food searching behavior in response to the conditioned odorants. By these means, it was demonstrated that catfish can discriminate between individual amino acids, and mixtures thereof (Valentincic et al., 1994, Valentincic et al., 2000b, Valentincic et al., 1996). Similar discrimination between amino acids has apparently also been observed in zebrafish (Valentincic et al., 2005). Finally, in an unrelated paradigm, it has been shown that goldfish discriminate and localize odorant sources in order to obtain food (Zippel et al., 1993). Thus, teleost fish can exhibit both classical and operant conditioning in positive reinforcement olfactory paradigms.

We describe a new, simple and robust positive reinforcement paradigm to condition zebrafish to associate odorants with the occurrence and location of feeding. Using this paradigm, we demonstrate for the first time that zebrafish can be similarly conditioned both to amino acids and a neutral, unnatural odorant, and that they can acquire conditional place preference in response to such odorants.

2.3 Methods

2.3.1 Animals

Zebrafish were bought locally (AquaCreations, Halifax, NS, Canada) and housed as groups of 20-25 fish in 40 L aquaria for a minimum of 2 weeks before experimentation. All fish were maintained in carbon-filtered, dechlorinated tap water (Dalhousie University Aquatron) at 27 ± 0.5^0 C, on a 12 hr day / 12 hr night cycle, and were fed daily with Nutrafin staple fish food (Hagen Incorporated, Montreal, QC, Canada). The size of animals used for conditioning experiments was 3 ± 0.5 cm, and both male and female fish were used. Preliminary studies indicated no sex differences in performance. Animal husbandry and all behavioral experiments were conducted in accordance with guidelines for the use of laboratory animals set by the Canadian Council for Animal Care.

2.3.2 Apparatus

For the duration of behavioral conditioning and subsequent testing, zebrafish were kept individually in white polypropylene buckets (IPL Products Ltd., Troy, MI, USA; diameter = 28.5 cm; Figure 4). These opaque cylindrical buckets were mounted on 2 m high shelves on rubber pads, to minimize the likelihood of the fish detecting the experimenters' presence. Lighting was provided by cool-white fluorescent lights (Osram) mounted 1 m above the buckets and diffused through tracing paper that covered the tanks except for a small hole for a camera lens.

Each bucket was equipped with a flow-through system, which replaced its entire volume of water (4 L) approximately every 40 sec throughout each day. Eight water inflows were located at 10 cm intervals along the underside of a circular hose (I.D. = 1.5

cm) located near the bottom edge of each bucket. The water outflow consisted of a polyvinyl chloride (PVC) standpipe (I.D. = 4.5 cm; height = 8 cm) in the middle of the bucket, over which a wider PVC sleeve (I.D. = 8 cm; height = 12 cm) with equally spaced horizontal slits was fitted. This configuration provided uniform drainage of the 8 cm-deep water column and minimized turbulence.

Odorants were injected into the main water inflow via a Y-connector. The connecting tubes (I.D. = 0.5 cm) were approximately 1 m long to allow remote application of odorants. Food flakes were also administered remotely, through a funnel and tube that terminated in a floating feeding ring (I.D. = 4 cm) that was tethered to the wall of the bucket and remained in the same location throughout the duration of the experiment. The location of the floating feeding ring was varied between buckets.

2.3.3 Odorants

The amino acids L-alanine and L-valine (BioChemika > 99.0% purity; Sigma Chemical Co, Oakville, ON, Canada), and the synthetic fragrance phenylethyl alcohol (PEA; International Flavors & Fragrances Incorporated, Jacksonville, FL, USA), were dissolved freshly before each of four trials during a training session and injected into the perfusion system as 10 mL aliquots with 6×10^{-2} M odorant concentration for amino acids, and 1×10^{-4} M odorant concentration for PEA. Preliminary experiments with dye infusions and spectroscopic measurements established that concentrated aliquots reached a nearly homogeneous 1000-fold dilution throughout the bucket 5 sec after injection into the system. The final stimulus concentrations to which the fish were subjected to were thus $\sim 6 \times 10^{-5}$ M for amino acids and $\sim 1 \times 10^{-7}$ M for PEA; these concentrations were similar to the effective odorant concentrations previously determined for zebrafish

2005, Harden et al., 2006, Friedrich and Korsching, 1997). Dye injections also indicated

a further 10,000-fold reduction of stimulus concentration within 4 min of washout.

2.3.4 Assessment of Pre-Existing Odorant Responsiveness

All odorants used in this study were tested before conditioning experiments to

determine if they evoked pre-existing responses in freely behaving fish. A single fish

was placed in the experimental apparatus 24 hrs prior to testing and deprived of food

throughout this acclimatization. On the testing day, single odorants were injected, and

their ability to elicit increased numbers of $>90^{o}$ turns, indicative of appetitive swimming

behavior (Valentincic et al., 2000, Valentincic and Caprio, 1994), was monitored. For

each odorant, fish (n = 10) were tested in four trials spaced approximately 3 hrs apart.

No food rewards were given in any of these trials. Fish used in these tests were not used

for further experiments.

2.3.5 Conditioning

Zebrafish were acclimatized individually to the apparatus and then food-deprived

as described above. Next, fish were trained daily in three sessions (approximately 2-3 hrs

apart) of four trials each. At the onset of each trial, an odorant (conditioned stimulus,

CS) was injected into the water inlet of a bucket. After 35 sec (5 sec odorant infusion

plus 30 sec observation), a single flake (~ 2 mg) of fish food (unconditioned stimulus,

UCS) was dropped into the feeding ring. A trial was completed when the fish retrieved

the food reward. If the fish failed to retrieve the food reward 30 sec after it was

administered, no score was given and the trial was repeated. Inter-trial intervals were of

at least 15 min durations. Training to single odorants consisted of a total of 60 trials,

conducted over the course of five days.

"Probe" tests were performed 24-48 hrs after the last training session. These tests consisted of four probe trials conducted approximately in 3 hr intervals, over the course of a single day. The probe trials were conducted in an identical manner to training trials, but no food was given to the fish at the end of the trials. Ten fish were used for each odorant conditioning experiment; they were not used for any other experiments.

2.3.6 Control Experiments

To test whether olfactory learning was dependent on the specific pairing of odors and food rewards, odors were injected without subsequent presentation of food rewards. This experiment was conducted on the same schedule as the actual olfactory conditioning experiments (see above). Feeding, however, was explicitly unpaired with the administration of odors and occurred at various times during the 3 hr inter-trial intervals with a total of 12 flakes of fish food given to each fish daily.

To assess the possible involvement of the mechanical stimuli in producing learned associations with feeding, odorant solutions were replaced with water alone, as a CS. The fish were given food after every such water infusion, and the conditioning schedule was identical to the one used during odorant conditioning (see above).

In order to assess possible involvement of gustation in producing conditioned behaviors, separate groups of fish were conditioned to odorants as described above. Following the last training session, however, individual fish were removed from the behavioral tanks and anaesthetized by immersion in 0.02% ethyl-aminobenzoate methanesulfonate salt (MS-222; Sigma) for 10 min. The fish were then wrapped in a soft, wet cloth previously soaked with 0.02% MS-222, and placed under a dissecting microscope. A fine tube that delivered a constant flow (~3-4 mL / min) of water

containing 0.02% MS-222 was then placed in the mouth of the fish to irrigate the gills.

Several coats of N-butyl-2-cyanoacrylate (Histoacryl® tissue glue; B. Braun Vet Care

GmbH, Tuttlingen, Germany) were then applied to the outside of one or both nares using

a fine plastic tip and both, the anterior and posterior opening to the nares were occluded.

This glue hardened within minutes, and individual fish were then placed in a 4 L bath

containing fresh water. Fish revived quickly, and were then returned to the experimental

tanks. The tissue glue generally remained in place for up to 48 hrs, after which it often

dissociated from the nares. Fish were therefore tested 24 hrs after glue application.

These tests were identical to the probe trials conducted at the end of odorant conditioning

experiments (see above). For each odorant we tested 10 fish with bilaterally occluded

nares as well as 8 fish that had only a unilateral occlusion of their nares.

2.3.7 Data Acquisition and Analysis

All experiments were recorded with a video camera mounted over the

experimental chambers, and recordings were stored on videotape. Recordings were

started 35 sec prior to odorant infusion, and continued until shortly after fish retrieved the

food reward (up to a maximum of 30 sec following food presentation).

Using these video recordings, we monitored several behavioral variables

throughout training and testing periods. Appetitive swimming behavior was quantified as

the number of times that fish completed $>90^o$ turns within 120 msec during a 30 sec

observation period. We used this variable to assess the baseline behavioral activity of

fish before every trial, as well as odorant-evoked appetitive food searching behavior. We

also measured the percentage of time that fish spent within each of the bucket's four

quadrants (Figure 4) before and after odorant infusions. These quadrants were drawn on

the video screen relative to the location of the feeding ring. Specifically, the *reward* quadrant was defined as the quadrant with boundaries equidistant from each side of the feeding ring. The two *adjacent* and one *opposite* of the reward quadrant were assigned accordingly (Figure 4).

For all statistical tests and graphical representations, raw data were pooled to session means (four trials). Statistical analyses were carried out in SPSS version 10.0 (SPSS Inc., Chicago, IL, USA). One-way analyses of variance (ANOVA) for repeated measures were performed to identify change in the performance of animals throughout the course of conditioning (within subject effects) and interactions between pretrial and odorant-evoked behaviors during training (between subject effects). Statistical significance was set at $p < 0.05$ for all of these tests. To determine when within and between subject effects became statistically significant during conditioning we conducted a post hoc Dunnett's Test, in which each training session was compared to others in the same experiment (e.g., we compared the performance of animals during the first training session and the probe trials). The significance level for post hoc tests was set at $p < 0.05$.

Quantitative graphic assessment of zebrafish locomotion was carried out by using Matlab (The MathWorks Inc., Natick, MA, USA). Specifically, mean images of representative video clips were subtracted from individual frames to produce a series of "motion-enhanced" images. A threshold was then applied to each frame, producing binary frames showing a white fish against a black background (Wyeth and Willows, 2006a, Wyeth and Willows, 2006b). The binary frames were averaged over the entire video, and the resulting pixel values coded using a false-color lookup table, with the color scale units reflecting the mean presence of fish per frame. The false color image was

then overlaid on a raw video frame by setting all false color pixels below a minimum transparency. All thresholds and other parameters were kept constant for processing of different videos.

2.4 Results

2.4.1 Only Amino Acids Trigger Pre-Existing Appetitive Swimming

During acclimatization and between training sessions, zebrafish often remained stationary at varying locations in the apparatus and generally displayed only minimal numbers of $> 90^{\circ}$ turns (see pretrial behavior in Figure 5). When untrained fish were exposed to the amino acids L-alanine or L-valine, they responded with appetitive swimming behavior consisting of a significant increase in the numbers of $> 90^{\circ}$ turns during the odorant administration period (both amino acids, $p < 0.001$, RM ANOVA; Figure 5). No such increase in appetitive swimming behavior was evoked when naïve zebrafish were exposed to PEA ($p = 0.263$, RM ANOVA). During these tests zebrafish did not localize preferentially to any of the quadrants within the experimental chamber (not shown).

2.4.2 Conditioned Increases in Appetitive Swimming

Repeatedly pairing either L-alanine or L-valine with feeding (Figure 6A & C) led to significant overall effects of training on the number of $> 90^{\circ}$ turns exhibited by zebrafish during presentation of the odorants (both amino acids, $p < 0.001$, RM ANOVA), but not during the pretrial periods ($p_{ala} = 0.293$; $p_{val} = 0.149$, RM ANOVA). Appetitive swimming behavior evoked by L-alanine and L-valine was elevated in the final probe trials when compared either to odorant-evoked behavior during the first training session (both amino acids, $p < 0.05$, Dunnett's Test), or to the pretrial swimming behavior during these probe trials (both amino acids, $p < 0.05$, Dunnett's Test).

When repeated exposures of L-alanine or L-valine were explicitly unpaired with the food presentation, no increases in the numbers of $> 90^o$ turns in response to the odorants were observed over training sessions (Figure 6B & D).

Conditioning zebrafish to the synthetic odorant PEA also produced a significant increase in odorant-evoked appetitive swimming behavior (Figure 6E). Specifically, conditioning increased the number of $> 90^o$ turns observed during PEA presentations ($p < 0.05$, RM ANOVA), but not during pretrial periods ($p = 0.063$, RM ANOVA). During probe trials, the number of odorant-evoked $> 90^o$ turns was significantly elevated from the initial odorant-evoked appetitive response ($p < 0.05$, Dunnett's Test), and from the pretrial behavior during the probe trials ($p < 0.001$, Dunnett's Test). Repeatedly exposing zebrafish to PEA without subsequently administering food rewards did not lead to an increase in the number of $> 90^o$ turns (Figure 6F).

2.4.3 Odorant-Driven Localization to the Feeding Ring

When untrained fish were exposed to an odorant they swam in variable paths across the four compartments of the apparatus (Figure 7A), and eventually retrieved the food reward from the feeding ring. Conditioning fish to L-alanine or L-valine resulted in a significant main effect of training, with fish spending progressively more time in the reward quadrant (L-alanine: $p < 0.001$; L-valine $p < 0.05$, both RM ANOVA; Figure 7B-D, Figure 8A & C). This trend was preserved in the final probe trials, during which fish spent significantly more time in the reward quadrant than during odorant infusions at the beginning of the experiment (both, $p < 0.001$ in Dunnett's Test).

In pretrial observation periods during training, we also observed that zebrafish were located mostly in the reward quadrant, with a significant main effect of training (L-

alanine: p < 0.001; L-valine p < 0.05, both RM ANOVA; Figure 8A & C). No interaction was observed between pretrial and odorant-induced localization to the reward quadrant in either amino acid conditioning group (not shown). Crucially, however, pretrial localization of the fish to the reward quadrant was abolished during probe trials conducted 24-48 hours after training (Figure 8A). A subsequent analysis revealed that pretrial localization to the reward quadrant decreased rapidly after the first probe test whereby odorant-driven localization did not decrease (Figure 9A & B). Thus, pretrial localization to the reward quadrant was quickly extinguished during probe tests but conditioned-odorant evoked reward quadrant localization was more robust.

When zebrafish were repeatedly exposed to L-alanine or L-valine without subsequently being fed, we did not observe an effect of training on localization to the reward quadrant (Figure 8B & D). Instead, fish spent varying amounts of times in all areas of the apparatus.

As with the amino acids, conditioning zebrafish to PEA led to a significant main effect of training, in which the fish spent progressively more time in the reward quadrant (p < 0.05 in RM ANOVA). This localization was preserved during probe trials (p < 0.05 in Dunnett's Test; Figure 8E). During training, no difference between pretrial- and PEA induced localization to the reward quadrant was observed. Once again, pretrial localization seen during training was abolished in the probe trials, and a significant difference was found between the pretrial behavior and that occurring after presentation of the conditioned odorant (p < 0.05, Dunnett's Test; Figure 8E, 9C). When repeated PEA infusions were not paired with feeding, no preferential localization to the reward

quadrant developed over training, and fish spent similar amounts of time in all areas of the apparatus (Figure 8F).

2.4.4 Control Experiments Using Water as Conditioned Stimulus

In control experiments where odorants were replaced with water alone as the conditioned stimulus, fish failed to develop the behavioral profile described above. Repeated pairings of water infusions with feeding did not lead to a progressive increase the number of $> 90^{\circ}$ turns observed at any time during training or testing ($p = 0.362$, RM ANOVA; Figure 10A). Moreover, zebrafish in this experimental group did not develop a significantly increased preference for the reward quadrant during training, either before or during water infusions ($p = 0.107$, RM ANOVA; Figure 10B).

2.4.5 Necessity of Olfaction for Conditioning

In a final series of experiments in which conditioned zebrafish were temporarily rendered anosmic, their responses to odorants were significantly reduced. Specifically, before occlusion of their nares, the zebrafish displayed significantly more appetitive swimming behavior in response to conditioned odorants than they did during the pre-trail period before odorant presentation (Figure 11A). These responses were similar to those observed in conditioned fish from other groups. Following bilateral occlusion of their nares, however, the fish responded to odorant infusions with significantly fewer $> 90^{\circ}$ turns (L-alanine: $p < 0.001$, L-valine: $p < 0.05$, PEA: $p < 0.05$ all RM ANOVA), and no difference was observed between swimming behavior before vs. after odorant presentation (see post-occlusion in Figure 11A). In a separate group of conditioned fish in which only one naris was occluded, as a control for analyzing the effects of this

manipulation per se, we observed that the appetitive swimming response to conditioned odorants did not differ from that seen prior to the occlusion (Figure 11B).

Finally, prior to occlusion of their nares, conditioned fish also responded to odorant infusions with significant localization to the reward quadrant. Following occlusion of their nares, however, the fish responded to infusions of the conditioned odorant with significantly less localization to the reward quadrant (L-alanine: $p < 0.001$, L-valine $p < 0.05$, PEA: $p < 0.05$, all RM ANOVA; Figure 12A) and no difference in localization between pretrial periods and odorant-evoked behavior could be observed. Again, if we occluded the nares of the fish only unilaterally, the conditioned response to odorant infusions was unaffected, and the animals localized preferentially to the reward quadrant following odorant infusions, significantly more than what was observed in *pretrial* periods, just as in unoccluded conditions (Figure 12B).

2.5 Discussion

We describe a simple positive reinforcement paradigm to condition olfactory behaviors of zebrafish. Using this paradigm, we demonstrate that zebrafish are capable of forming associations between both natural and synthetic odorants and feeding. Conditioned responses to amino acids were evident as a significant increase in the numbers of $>90^{\circ}$ turns, indicative of appetitive swimming behavior (Valentincic et al., 2000b). While initially unresponsive to PEA, conditioned zebrafish also displayed a significant appetitive response to this odorant. During conditioning, the fish further learned to target swimming behavior reliably to the reward quadrant of the apparatus. For all odorants tested, we also demonstrated that a functional olfactory system is necessary to elicit these conditioned behaviors, as bilateral occlusion of the nares prevented conditioned fish from responding to odorant infusions.

Our results complement and extend recent studies that have demonstrated the ability of fish to learn in a variety of olfactory paradigms. We confirm a previous suggestion that pre-existing appetitive responses of zebrafish to amino acid odorants can be potentiated through odorant conditioning (Valentincic et al., 2005), as has also been shown in several other species of fish (Valentincic et al., 1994, Valentincic et al., 2000b, Valentincic et al., 1996). Our work also complements observations that goldfish can acquire more complex olfactory behavioral repertoires in which they learn to discriminate and approach different odorant sources (Zippel et al., 1993). In addition, our results complement the observation that zebrafish can be classically conditioned to associate previously neutral odorants with naturally occurring alarm pheromones (Suboski et al., 1990, Hall and Suboski, 1995).

2.5.1 Potentiated Versus Newly Acquired Appetitive Responses

A major result of this study is the finding that olfactory conditioning led to increased odorant-evoked appetitive responses in all fish tested regardless of odorant. Due to the inherent stimulus properties of the different conditioned stimuli (L-alanine, L-valine, PEA), these conditioned behaviors may have arisen due to different learning processes. The amino acids triggered significant appetitive responses in naïve zebrafish, and may not be regarded as behaviorally neutral olfactory stimuli. The conditioned increase in amino acid-evoked appetitive swimming behavior that we observed thus did not represent classical Pavlovian conditioning, in which a contingency develops between a behaviorally *neutral* stimulus and one of prior significance to the animal. Therefore, the robust increase in appetitive swimming behavior that results from conditioning zebrafish to amino acids represents not an acquired olfactory stimulus response but a potentiation of a pre-existing chemosensory behavior.

To investigate if zebrafish are capable of acquiring a *classically conditioned* appetitive response, we employed the synthetic odorant PEA as a conditioned stimulus. This fragrance was previously shown to elicit olfactory neural activity in salmon (Hasler et al., 1978) and zebrafish (Harden et al., 2006), but to be behaviorally neutral in both species. Our results confirm the behavioral neutrality of PEA, as it elicited no significant increase in appetitive behaviors in naïve fish. More importantly, we demonstrated that zebrafish can indeed be classically conditioned to associate this neutral chemical stimulus with feeding. To our knowledge, this is the first demonstration of a *classically conditioned* appetitive behavioral response in fish, although Suboski *et al.* (1990)

classically conditioned zebrafish in a negative reinforcement paradigm by pairing PEA with a chemical predatory stimulus.

The conditioned PEA-evoked appetitive response that we have observed was remarkably similar to the pre-existing appetitive response displayed by adult zebrafish following exposures to amino acids. This observation suggests that the appetitive swimming response is a general behavioral mechanism that is not only inherently linked to the perception of certain odorants, but may develop for appropriate chemical stimuli repeatedly associated with feeding. It must then also be considered that the *pre-existing* appetitive response of adult zebrafish to amino acid that we observed could be a result of previous, repeated conditional exposures to these compounds, emanating from normal food sources during rearing. It has been shown that larval zebrafish respond to amino acids just as they begin to feed (Lindsay and Vogt, 2004), thus providing evidence that these fish *innately* respond to amino acids. Nevertheless, it remains unclear how or if ongoing exposure to amino acids during the life history of the fish alters their behavioral responses.

2.5.2 Targeting Swimming Behavior to the Location of Feeding

In addition to increased appetitive swimming behavior, a conditioned place preference for the location of feeding develops nearly identically in fish conditioned to amino acids or PEA. Place preferences develop following repeated pairings of unconditioned stimuli with previously neutral sets of environmental spatial cues. As a result, animals approach or avoid conditioned environmental features (Tzschentke, 1998). Place conditioning has been previously demonstrated in a paradigm in which zebrafish were rewarded with psychoactive substances for entering a specific compartment within a

choice chamber (Darland and Dowling, 2001, Ninkovic and Bally-Cuif, 2006). During olfactory conditioning in our paradigm, zebrafish develop two distinct place preferences for the reward quadrant. Firstly, as observed during training in *pretrial* periods, the repeated administration of food alone is sufficient for the fish to develop an association between the feeding ring and the rewarding properties of food; the fish localize to the region of the feeding ring throughout training sessions, regardless of the presence of an odorant. During all of training, the localization of fish to the reward quadrant may therefore be dominated by this association alone. Crucially, however, the extinction of this place preference is rapid (e.g., Figure 9), and it does not persist throughout probe tests. It is during these during probe tests that the second, *conditional*, place preference can be observed. Here the zebrafish do not localize preferentially to the feeding ring in pretrial observation periods. Only following the infusion of a conditioned odorant, which signals the availability of a reward from the feeding ring, do fish approach the feeding ring and remain in the reward quadrant, thereby displaying a stimulus-dependent conditioned place preference. Thus, the fish have learned a place preference that is *conditional* on odorant presentation.

2.5.3 Sensory Systems Involved in Conditioned Olfactory Behavior

When water infusions were presented as the conditioned stimulus instead of odorants, the zebrafish did not respond to the stimulus, even though it was repeatedly paired with feeding. This suggests that small differences in water inflow associated with the odorant infusions were undetectable or simply not attended to while developing conditioned behaviors. We therefore rule out an involvement of mechanoreceptors, such as those along the lateral line (Ghysen and Dambly-Chaudiere, 2007), in producing the

conditioned behaviors examined in our study. Similarly, when zebrafish were rendered anosmic by blocking their nares, they did not respond to odorant infusions with conditioned food searching behaviors. While the gustatory system may still have been activated by the odorant infusions (Kotrschal, 2000), our data clearly indicate that it did not play a significant role in responding to the conditioned stimuli. We therefore conclude that olfaction was the primary, and perhaps the sole sensory modality mediating responses to the conditioned stimulus.

Our data indicate, however, that the visual system likely played a significant role in producing the conditioned behaviors. This was particularly evident during training in *pretrial* observation periods, when the fish showed a significant place preference for the reward quadrant (see above). As no other sensory cues, including odorants, were present during these pretrial observation periods, it appears that the place preference was visually driven. Notably, this visual place-preference occurred independent of significant appetitive swimming behaviors, as pretriale swimming behavior was very low throughout training.

Together, these results suggest that the conditioned olfactory behaviors that we have observed here involve multi-component behavioral adaptations that require both olfactory and visual memories. When an odorant was introduced into the apparatus, olfactory and visual systems acted synergistically to target appetitive swimming behavior to the reward quadrant. Odorant infusions resulted in a nearly homogenous distribution of the chemical stimulus, which unconditioned animals sampled randomly to search for possible sources of the odorant. Conditioned fish, however, responded to this stimulus with appetitive swimming behavior that was clearly restricted to the reward quadrant.

Thus, they may have employed their olfactory system to initially sense imminent feeding, and thereafter used a visual memory to target appetitive food searching behavior to the recalled feeding locus. In our artificial environment lacking directional chemical cues (e.g., chemical gradients or clearly delineated odorant plumes), this behavioral adaptation ultimately allowed the fish to circumvent costly, random odorant sampling behaviors and instead fixate these to the reward quadrant, the location of anticipated feeding.

2.5.4 Conclusions

Our study confirms that zebrafish can learn complex behavioral tasks quickly and reliably in a standard conditioning paradigm. We are beginning to understand both the cellular mechanisms that underlie olfactory processing in the forebrain of zebrafish (Friedrich, 2006) and the genetic makeup of this system (Sato et al., 2005). Exploitation of the paradigm developed here provides a simple and robust method of studying multi-modal learning processes involving olfaction. It should now be possible to link olfactory-driven behaviors with *in vivo* neurobiology to uncover the mechanisms that underlie the establishment and maintenance of learned chemosensory behaviors.

Figure 4. Overview of the behavioral apparatus as viewed from a camera mounted above the setup. Water entered the bucket through regular inflows along a circular inflow hose (**A**). A centrally located standpipe (**B**), covered by a larger sleeve with equally spaced slits, allowed for uniform drainage of water from the system. Food pellets were administered remotely into a floating feeding ring (**C**).
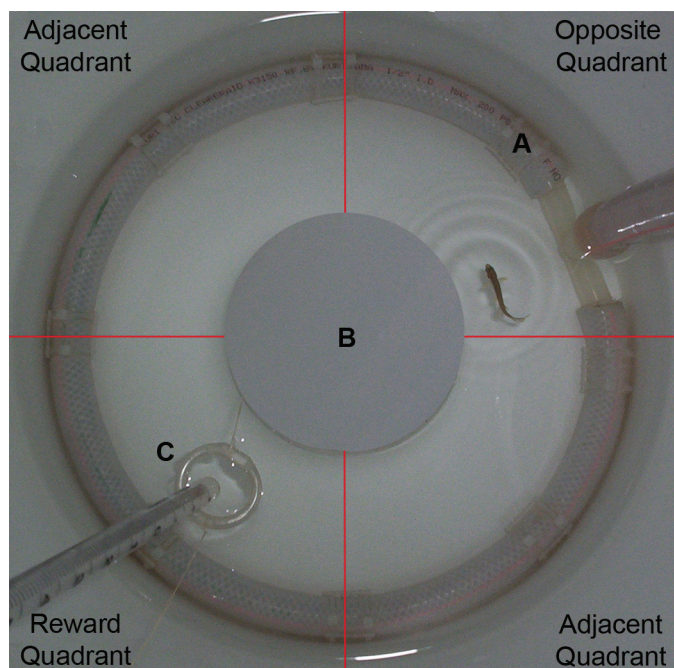
Figure 4. Overview of the Behavioral Apparatus as Viewed From a Camera Mounted Above the Setup

Figure 5. Pre-existing behavioral responses to amino acids and phenylethyl alcohol. Fish displayed very little swimming behavior for the 30 sec before odorant infusions (pretrial behavior = 3.41 ± 1.38 turns / 30 sec). Natural odorants L-alanine and L-valine elicited significant increases in appetitive swimming in all fish tested (see text). No increase in appetitive swimming was observed following exposure of the fish to PEA. All data are shown as the mean $>90^0$ turns per session and their standard errors.
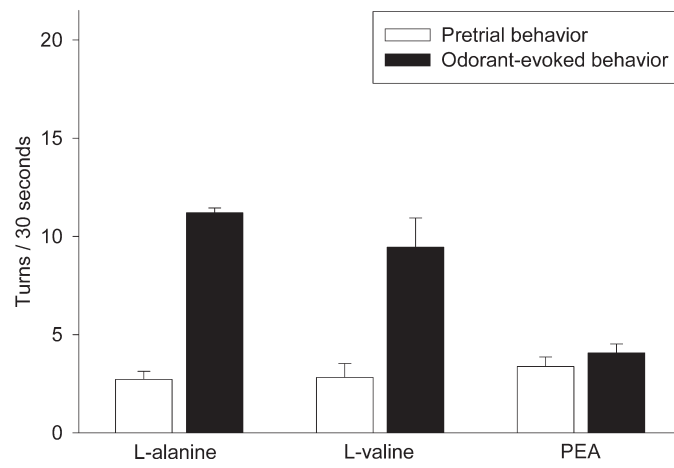
Figure 5. Pre-Existing Behavioral Responses to Amino Acids and Phenylethyl Alcohol

Figure 6 Conditioned increases in appetitive swimming behavior as a result of repeated pairings of odorants with food rewards. Pairing amino acids (**A**, **C**) and PEA (**E**) with food rewards led to a robust increase in odorant-evoked appetitive swimming. In contrast, repeated administrations of unreinforced odorants did not increase appetitive swimming behaviors (**B**, **D**, **F**). A mild increase in appetitive swimming was also apparent during the pretrial periods during reinforcement conditioning (**A, C, E**). This was notably absent in pretrial periods preceding the probe tests and also during unreinforced conditioning (**B, D, F**). All data are shown as the mean $>90^{0}$ turns per session and their standard errors.
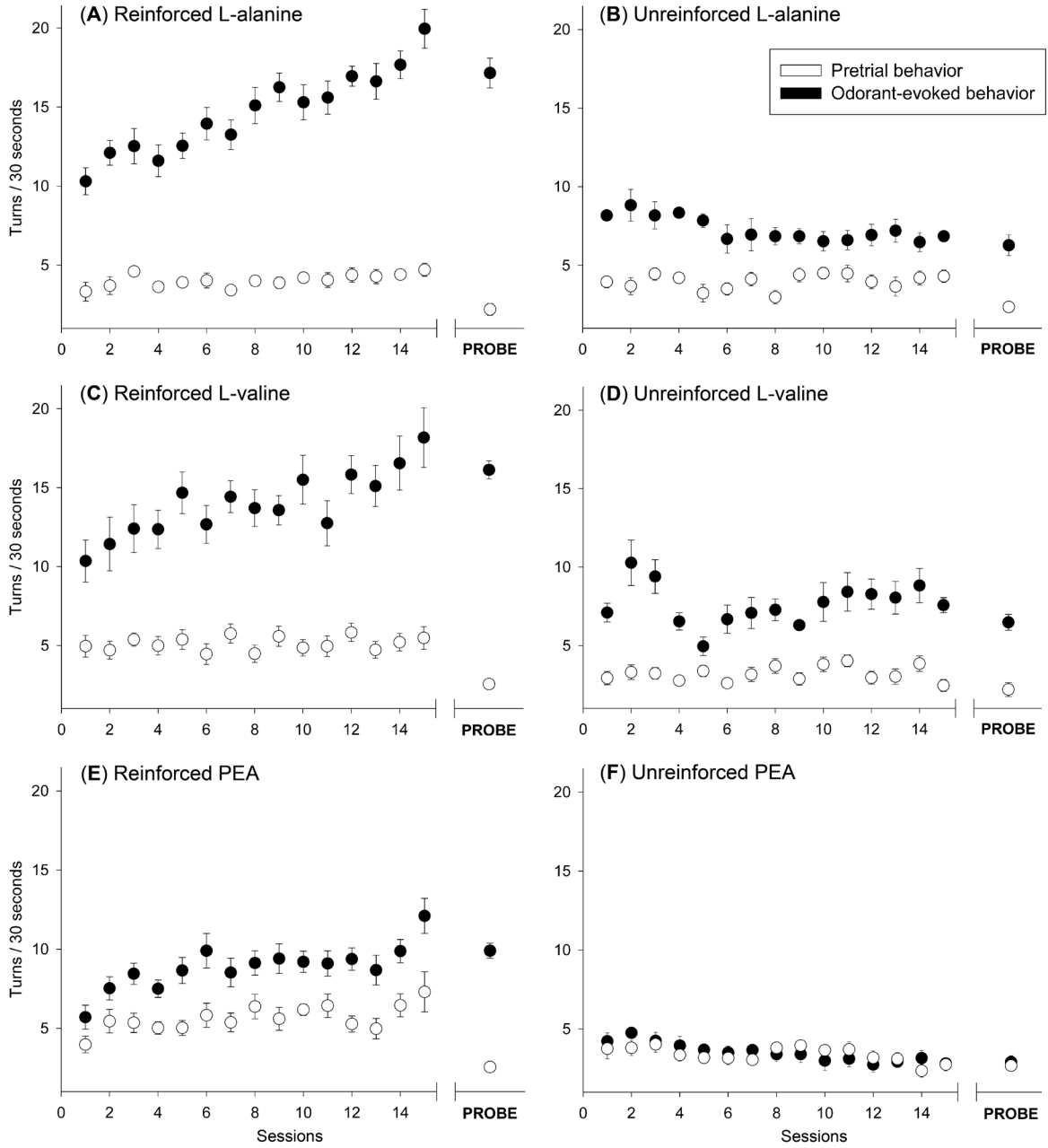
Figure 6. Conditioned Increases in Appetitive Swimming Behavior as a Result of Repeatedly Pairing Odorants With Food Rewards

Figure 7. False color images depicting the location of fish during training trials at various times during olfactory conditioning. At the onset of olfactory conditioning (L-alanine), odorant-evoked food searching behavior was variable and occurred across all 4 quadrants (**A**). After 5 sessions, some zebrafish showed heightened but non-specific appetitive swimming (**B**). After 8 sessions fish localized odorant-evoked appetitive swimming increasingly to the reward quadrant (**C**). With further training, this targeted food search became more apparent (**D**). Scale refers to the time (sec) that background pixels were occupied by the image of the moving fish.
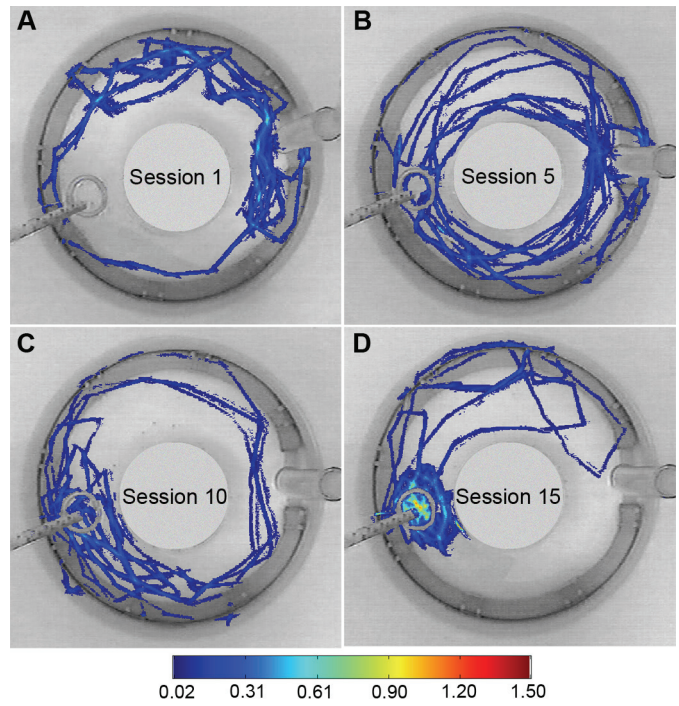
Figure 7. False Color Images Depicting the Location of Fish During Training Trials at Various Times During Olfactory Conditioning

Figure 8. The amount of time spent near the feeding ring increases as a result of pairing amino acids (**A**, **C**) and PEA (**E**) with reward administration through the feeding ring. This was also apparent during pretrial observation periods, and continued throughout training. During probe tests, the fish did not localize preferentially to the reward quadrant unless odorants were infused (**A**, **C**, **E**). When zebrafish were repeatedly exposed to unreinforced odorants they failed to develop a preference to the reward quadrant (**B**, **D**, **F)**. The dashed line indicates the chance probability (25%) of the fish's localization to the reward quadrant. All data are shown as the mean percentage of session time that the fish spent in the reward quadrant and their standard errors.
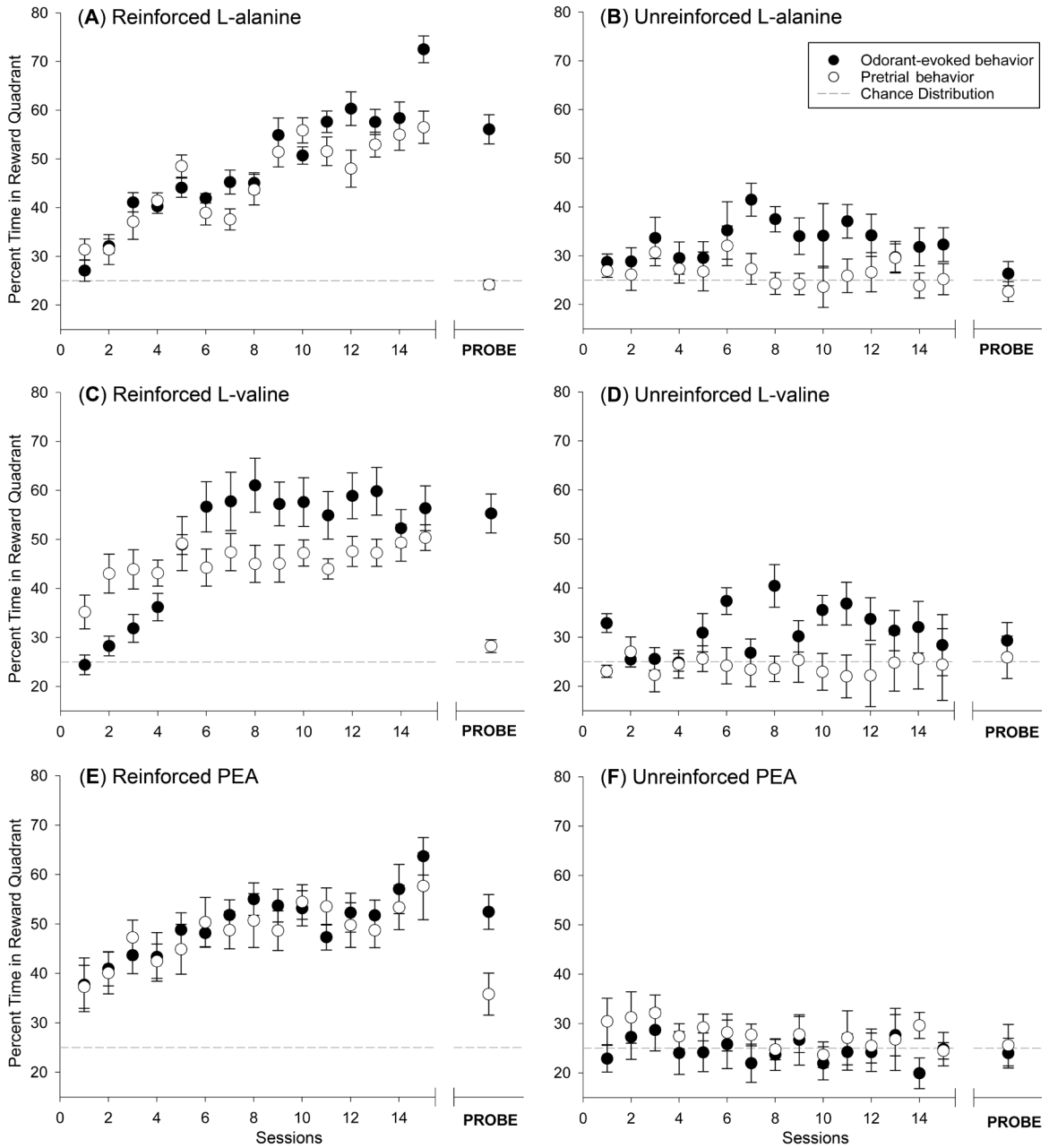
Figure 8. The Amount of Time Spent Near the Feeding Ring Increases as a Result of Pairing Amino Acids and PEA With Reward Administration Through the Feeding Ring

Figure 9. Trial-by-trial analysis of probe sessions shows different rates of extinction in odorant-evoked and pretrial place preferences. Localization of the zebrafish to the feeding ring was similar for pretrial and odorant-evoked behavior in the first 'probe' test (**A**, **B**, **C**). However, pretrial localization to the reward quadrant decreased significantly with further, unrewarded testing (L-alanine: $p < 0.05$; L-valine $p < 0.05$; PEA $p < 0.001$) whereas odorant-evoked localization to the reward quadrant did not decrease.
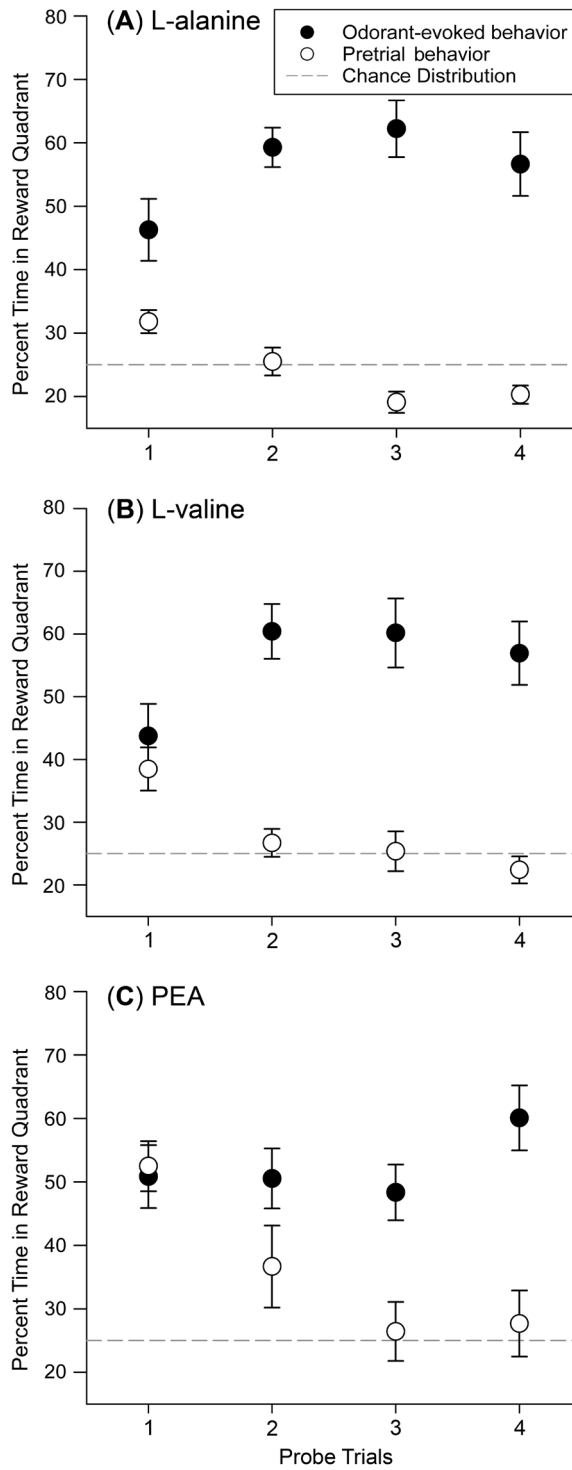
Figure 9. Trial-By-Trial Analysis of Probe Sessions Shows Different Rates of Extinction in Odorant-Evoked and Pretrial Place Preferences

Figure 10. Water injections paired with feeding failed to induce conditioned behaviors. Repeated pairing of water injections with feeding did not lead to a progressive increase in appetitive swimming behavior (**A**), nor did fish develop a progressive preference for the feeding ring (**B**). The dashed line in (**B**) indicates the chance probability (25%) of the fish's localization to the reward quadrant. Data are shown as the means per session and their standard errors (units as indicated).
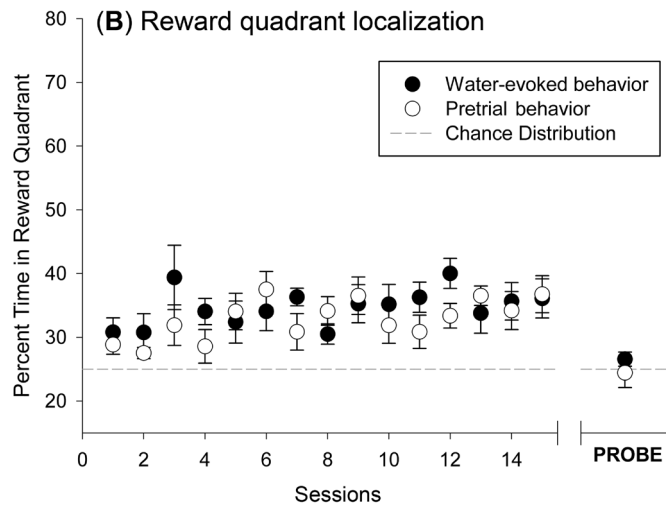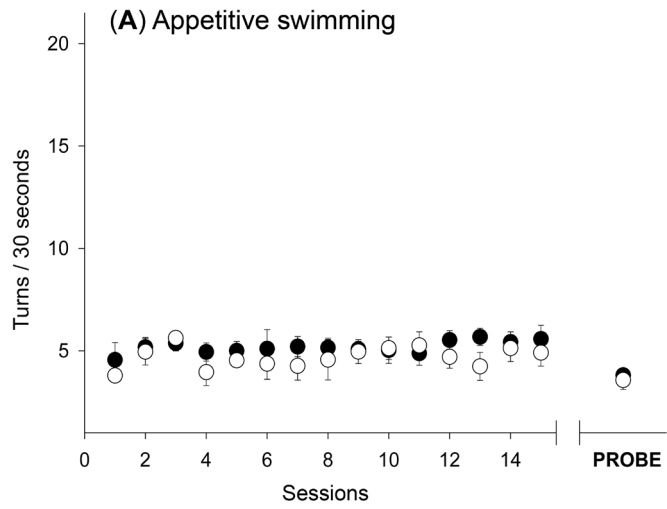
(A) Appetitive swimming

(B) Reward quadrant localization

Water-evoked behavior
Pretrial behavior
Chance Distribution

Figure 10. Water Injections Paired With Feeding Failed to Induce Conditioned Behaviors

61

Figure 11. Conditioned fish with bilaterally occluded nares did not respond to L-alanine, L-valine or PEA. All fish responded to odorant infusions with significant appetitive swimming before the occlusion (**A**). Occluding the nares of another group of conditioned fish only unilaterally did not decrease odorant-evoked appetitive swimming behavior (**B**). All data are shown as the mean $>90^0$ turns per session and their standard errors.
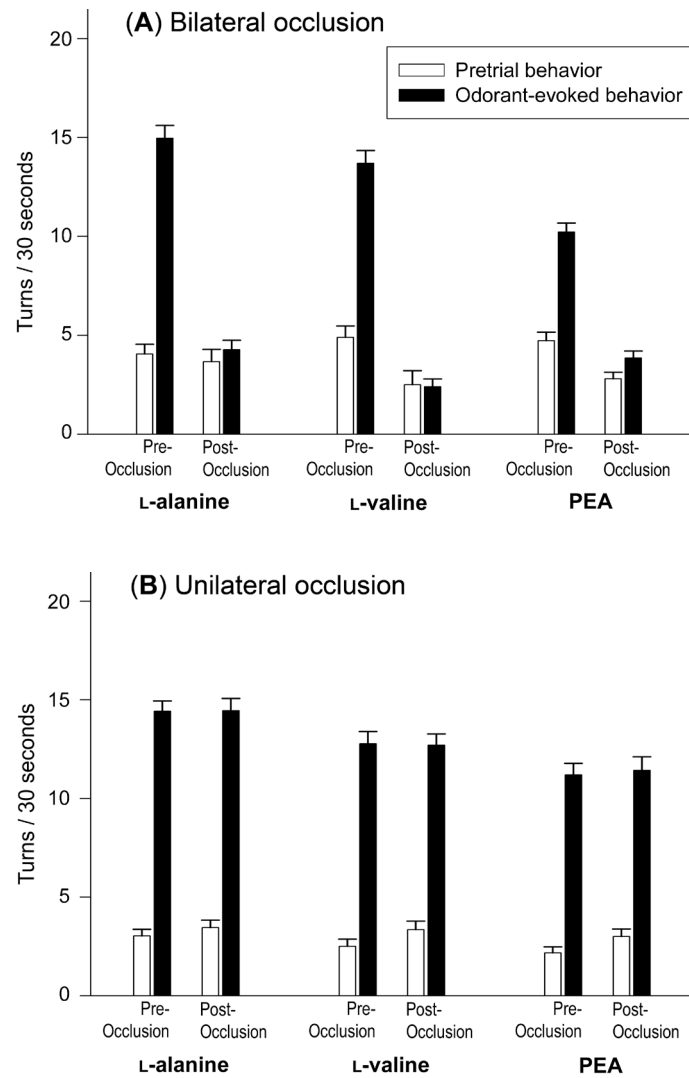
Figure 11. Conditioned Fish With Bilaterally Occluded Nares Did Not Respond to L-alanine, L-valine or PEA

63

Figure 12. Odor evoked localization to the reward quadrant does not occur in zebrafish with bilaterally occluded nares (**A**). Occluding the nares of conditioned fish only unilaterally did not decrease odorant-evoked localization to the feeding ring (**B**). The dashed line indicates the chance probability (25%) of the fish's localization to the reward quadrant. All data are shown as the mean percentage of session time that the fish spent in the reward quadrant and their standard errors.
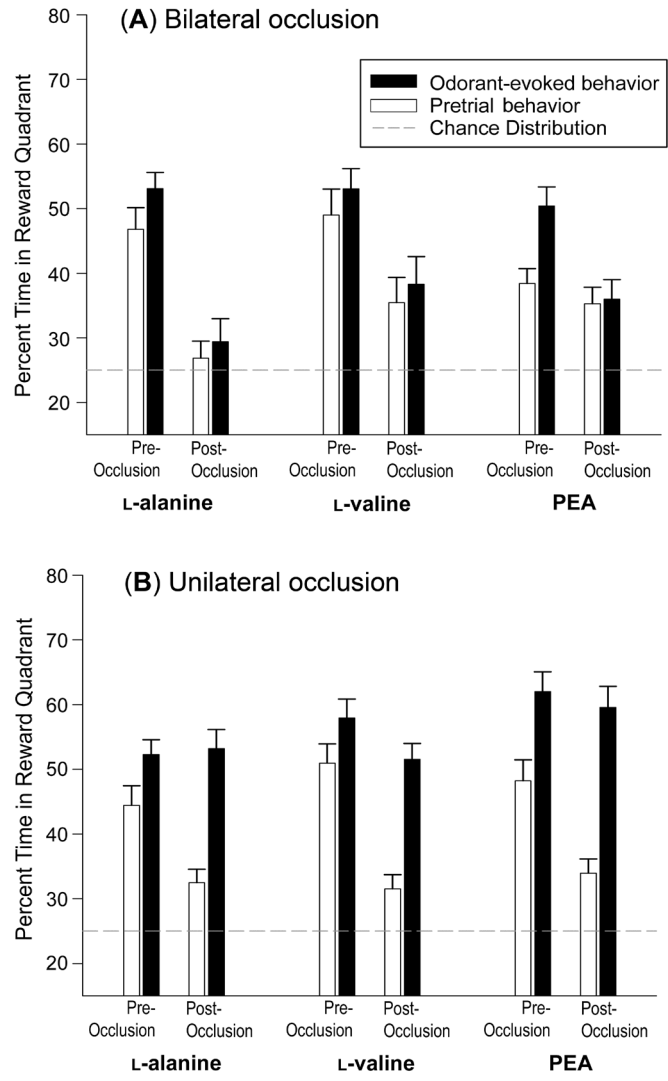
Figure 12. Odor Evoked Localization to the Reward Quadrant Does Not Occur in Zebrafish With Bilaterally Occluded Nares

Chapter 3

Distribution and Functional Organization of Glomeruli in the Zebrafish Olfactory System

3.1 Summary

Odors are transduced by thousands of narrowly tuned olfactory sensory neurons (OSNs) in the olfactory epithelia. Each OSN expresses a single odorant receptor (OR) and projects an axon to a spheroidal glomerulus in the olfactory bulb. Glomeruli in turn are innervated by axons of only one or a few OSN types and their combinatorial activations by odor molecules may be regarded as OR activation maps. Knowledge about the distribution of glomeruli is thus fundamental to understanding olfactory information processing. In the present study we created a comprehensive overview of the morphology and functional organization of glomeruli in the zebrafish olfactory system. We first mapped the coarse organization of glomeruli in whole zebrafish olfactory bulbs stained with antibodies against G-protein subunits and calcium binding proteins. Using complementary markers, we then examined the detailed distributions of glomeruli within identified functional subdivisions. In total, we identified 140 glomeruli that could be separated based on several anatomical features. Specifically, 25 large glomeruli were unambiguously identifiable in the olfactory bulbs of all or most animals; these glomeruli were scattered throughout the olfactory bulbs and were innervated by diverse OSNs, including crypt cells that are known to be involved in pheromonal communication. The remaining glomeruli were innervated by ciliated olfactory sensory neurons; most of these glomeruli were small, anatomically variable and indistinguishable from one another in tightly packed clusters in the medial and dorsolateral olfactory bulbs. Our results are, to our knowledge, the most detailed description of a teleost olfactory system and are among the first to specifically link repeatably identifiable glomeruli with their purported functions.

3.2 Introduction

The olfactory system processes information about a vast number of odorants related to habitat, feeding, conspecifics, and predation. Odors are transduced into neural signals by hundreds (zebrafish: Korsching, 2005, Alioto and Ngai, 2005) and thousands (mice: Buck and Axel, 1991) of different types of olfactory sensory neurons (OSNs), each of which expresses only one functional odorant receptor (OR) type (Serizawa et al., 2004, Mombaerts, 2004). OSNs that express the same OR type are scattered widely throughout the sensory epithelia, but their axons project with great precision to synaptic targets in the olfactory bulbs, the glomeruli. Each glomerulus is innervated by only one or at most a few OSN types (Vassar et al., 1994, Ressler et al., 1993) and is thus narrowly tuned to respond to particular molecular components of odors (Mori et al., 2006, Fuss and Korsching, 2001). Odor quality thus appears to be encoded in combinatorial activations of distinct glomerular ensembles, and these activation patterns may be regarded as 'OR activity maps' (Wachowiak and Cohen, 2001, Vosshall et al., 2000, Stewart et al., 1979, Sharp et al., 1975, Moulton, 1976, Friedrich and Korsching, 1998).

Insects like *Drosophila melanogaster*, *Apis melifera* and *Manduca sexta* have small olfactory systems that contain very few glomeruli (~100), and because of their small numbers, most glomeruli in these species have already been catalogued in standardized anatomical atlases (Rybak et al., 2010, Masante-Roca et al., 2005, Laissue et al., 1999, Huetteroth and Schachtner, 2005, Galizia et al., 1999). Because of such knowledge, physiological and molecular analysis of olfactory information processing in insects is proceeding at a rapid pace, and importantly, certain types of behavior can now be directly linked to the function of individually identifiable glomeruli (Suh et al., 2004, Suh et al.,

2007, Ibba et al., 2010).

In contrast, the mapping of glomeruli in vertebrates has proven to be far more challenging. Mice, which are the species most commonly employed to study vertebrate olfaction, have large and complex olfactory bulbs, each containing between 1800 and 2000 anatomically indistinct glomeruli (Mombaerts, 2006). Due to their sheer number, only a fraction of murine glomeruli have been individually identified, mapped and studied repeatedly (e.g., Schaefer et al., 2001, Potter et al., 2001, Oliva et al., 2008, Jones et al., 2008).

An increasingly attractive alternative for studying the neurobiology of vertebrate olfaction is the zebrafish, *Danio rerio*. This species is advantageous for this purpose because it is economical, small, amenable to genetic manipulations and suitable for *in vivo* optophysiological experiments. Each zebrafish olfactory bulb has been reported to contain only 80 glomeruli (Baier and Korsching, 1994), and these are segregated in distinct regions, and known to process different types of odors. For example, amino acids (food odors) are processed by a distinct group of lateral glomeruli (Friedrich and Korsching, 1997), while bile acids (social odors) are transduced by ventromedial glomeruli (Friedrich and Korsching, 1998). Despite the apparent simplicity of the zebrafish olfactory system, however, very little is known about the identity and contribution of individual glomeruli to producing olfactory behaviors. We believe that this is due to the lack of a comprehensive anatomical atlas that describes the coarse organization and the detailed distribution of individual glomeruli.

The present study was therefore undertaken to catalogue zebrafish glomeruli in more detail than has been previously attempted (Baier and Korsching, 1994). We first

69

studied the functional organization of glomeruli (e.g., division of lateral vs medial glomeruli) by labeling olfactory bulbs with antibodies against G-protein subunits and calcium binding proteins, which recognize molecules in certain OSN classes and their axons. Using general structural markers we then studied the detailed distributions of glomeruli within identified functional subdivisions. Overall, we obtained unprecedentedly detailed images of glomeruli in whole-mounted olfactory bulbs, and estimate that the total number of glomeruli is approximately 140 per olfactory bulb, regardless of sex. Of these glomeruli we were able to unambiguously identify 25 in each olfactory bulb, because they were relatively large, stereotypically arranged and uniquely labeled by different combinations of neurochemical markers. The remaining glomeruli were much smaller and varied in morphology and numbers, but were always located in certain regions. However, these units were generally anatomically indistinguishable from one another. Collectively, these data depict what appear to be multiple distinct olfactory processing streams.

3.3 Methods

3.3.1 Animals

Wild type zebrafish (AB strain: University of Oregon) were maintained at Dalhousie University according to standard guidelines (Nüsslein-Volhard and Dahm, 2002). Briefly, fish were kept at 27.5^{o}C on a 12 hour light / 12 hour dark schedule in 10L holding tanks (Aquatic Habitats, Apopka, FL, USA) that were continuously supplied with a drip of fresh dechlorinated water, which was filtered through a series of biofilters and a charcoal filter. The fish were fed several times daily with staple fish food (Omega Sea, Sitka, Alaska, USA) and live brine shrimp (Salt Creek, Salt Lake City, Utah, USA). All experiments were conducted on adult zebrafish that were three months or older and between 2-3 cm in length. A total of 17 zebrafish were used to create the images and numerical data shown in this manuscript. Animals were handled according to procedures outlined in the guide to the care and use of laboratory animals, established by the Canadian Council for Animal Care.

3.3.2 Tissue Preparation

Zebrafish were killed by immersion in cold water (< 4°C for ~1 minute) and decapitated. The skull caps were removed and exposed brains were fixed by immersion in fresh 2% paraformaldehyde (PFA; Electron Microscopy Sciences, Hartfield, PA, USA) in phosphate buffered saline (PBS: 100mM Na$_2$HPO$_4$, 140mM NaCl, pH 7.4) for six hours at room temperature, or overnight at 4°C. The tissue was next washed five times over two hours in PBS before dissecting the heads further to isolate the brain and olfactory epithelia. These were then placed in a PBS-based blocking solution containing 0.25% Triton X-100, 2% dimethyl sulfoxide, 1% bovine serum albumin and 1% normal

goat serum (PBS-T; all from Sigma) for ≥ 12 hours at 4°C. Unless noted otherwise, PBS-T was used for all subsequent wash steps, each of which comprised minimally five rinses in PBS-T over a period of approximately four hours.

3.3.3 Antibody Characterization

We employed a combination of antibodies (Table 1) to label OSN axons and their synaptic terminals, both of which are abundant in glomeruli (Chen and Shepherd, 2005). We used an antibody against keyhole limpet hemocyanin (KLH), which has been used previously in zebrafish and trout (Riddle and Oakley, 1992, Fuller et al., 2006) to label an unknown epitope in OSN axons. We counterstained some preparations with anti-synaptic vesicle protein 2 (SV_2), which labels axon terminals in the core of each glomerulus (Koide et al., 2009).

To characterize the functional organization of glomeruli, we employed antibodies against G-protein α subunits and calcium binding proteins. These proteins are selectively expressed in certain OSN classes and permit discrimination of these neurons and their axons in the sensory epithelium and the olfactory bulbs (Hansen et al., 2003). We used anti-$G_{\alpha\ s/olf}$ (Table 1), which recognizes a 42-45kDa protein in the olfactory epithelium of lampreys (Frontini et al., 2003) and catfish (Hansen et al., 2003), to label ciliated OSNs and axons as has been shown in larval zebrafish (Koide et al., 2009). We also tested anti-$G_{\alpha q\ /\ 11}$ and anti-$G_{\alpha o}$ (Table 1), which label microvillous and crypts cells in catfish (Hansen et al., 2003) and anti-$G_{\alpha i-3}$ as an additional marker for microvillous receptor neurons (Hansen et al., 2005). To our knowledge, none of these antibodies were used in zebrafish before, and we thus performed control experiments (below).

To complement these labels, we also used anti-calretinin (Table 1), which

recognizes a 28-29kDA protein in zebrafish (Germana et al., 2007, Castro et al., 2006) and is useful for identifying ciliated and microvillous OSNs (Sato et al., 2005). Finally, we used anti-S_{100} (Table 1), which recognizes a 10kDa protein in zebrafish tissue and appears to label crypt-like cells in this species (Germana et al., 2007).

3.3.4 Whole-Mount Immunocytochemistry

Mixtures of primary antibodies were diluted 1:50-1:200 in PBS-T, and brains were incubated in these solutions for seven days at 4°C with gentle agitation. Longer incubation periods (three to four weeks) improved staining and were performed when possible. Brains were next washed and then incubated in a mixture of appropriate secondary antibodies conjugated to Alexa Fluor dyes (Invitrogen, Burlington, ON, Canada). These antibodies were used at a final dilution of 1:100 in PBS-T, and brains were incubated in these solutions for five to seven days at 4°C.

Before mounting, all brains were rinsed three times in PBS containing 0.25% Triton and then an additional three times in just PBS. The brains were then immersed in a 3:1 solution of glycerol to 0.1M Tris buffer (pH 8.0) containing 2% n-propyl gallate (all from Sigma) for a minimum of 24 hours for clearing. Afterwards, the tissue was mounted in fresh glycerol solution between coverslips separated with stacks of coverslip fragments. Slides were then sealed with nail polish and stored at 4°C prior to being viewed with a confocal microscope.

3.3.5 Immunocytochemistry on Cryosections

Olfactory epithelia were removed from fixed skulls (4% PFA for 12 hours) and immersed in 20% sucrose in PBS for 12 hours. Isolated epithelia were then placed in embedding medium (Tissue Tek Optimal Cutting Temperature Medium, Fisher

Scientific, Ottawa, ON, Canada), quickly frozen, and cryosectioned at 8μm. The sections were collected on gelatin-coated slides, and air-dried for 30 minutes before being postfixed in 4% PFA for another 30 minutes. After three washes in PBS containing 0.3% Triton X-100 the sections were blocked with the same PBS based solution, additionally containing 10% normal goat serum, for 30 minutes.

Mixtures of primary antibodies (Table 1) were diluted 1:500 in PBS-T and placed directly onto each tissue section; the slides were then transferred to a humid chamber and incubated overnight at room temperature. The next day, sections were rinsed with PBS-T three times for 20 minutes each, and solutions of appropriate secondary goat antibodies conjugated to Alexa Fluor dyes (1:250 dilution; Invitrogen) were placed on top of the sections and left for five hours at room temperature. Sections were then washed four times with PBS-T before being mounted in fresh glycerol mounting medium (see above). The slides were then coverslipped and viewed with a confocal microscope.

3.3.6 Antibody Controls

The labeling patterns achieved with each of the antibodies were consistent with previous reports that used these same antibodies and similar immunocytochemistry protocols in zebrafish or related species (see above). We therefore conducted preadsorption controls only for antibodies that had not previously been used in zebrafish. These antibodies were rabbit anti-$G_{\alpha o}$, anti-$G_{\alpha i-3}$, and anti-$G_{q/11}$ antibodies (Table 1). Synthetic peptides for each antibody were obtained from Santa Cruz Biotech and were added at 200ug/ml to 1:200 dilutions of primary antibody solution, preadsorbed for 24 hours at room temperature and then spun for 10 min at 5000 rpm in a bench top centrifuge. Several fixed brains were incubated in the supernatant and processed as

described above; none of these brains exhibited immunolabelling. Finally, we also conducted negative controls by processing brains without incubation in primary antibodies; none of the specimens exhibited detectable fluorescence.

3.3.7 Microscopy and Image Processing

Specimens were viewed with a Zeiss LSM 510 META laser scanning confocal microscope (Carl Zeiss Inc., Thornwood, NY, USA) and serial optical sections were obtained from the olfactory bulbs at 1μm intervals to a maximum depth of 100μm. Where required, optical sections were obtained from multiple sides of the whole-mounted tissue (i.e., dorsal, lateral, ventral, and medial). Optical sections were viewed and processed with ImageJ (http://rsb.info.nih.gov/ij). Photomicrographs shown here are superimposed stacks of optical sections to a depth indicated in each figure panel. Images were assembled into plates using Photoshop and InDesign and diagrams accompanying these images were created with Illustrator (Adobe Systems Inc., San Jose, CA, USA).

Three-dimensional reconstructions shown in supplemental movies were created from raw confocal data with the ImageJ 3D viewer (Schmid et al., 2010). Data were resampled to 512 x 512 formats (from 1024 x 1024) prior to rendering reconstructions and pixel detection thresholds were adjusted where necessary. Movies were recorded in ImageJ and annotated and edited in Apple Keynote.

3.3.8 Identification and Classification of Glomeruli

Glomeruli were identified based on the following anatomical criteria. A structure was considered a glomerulus if it possessed visible OSN axons that targeted and encircled a roundish structure. In specimens that were counterstained with synaptic labels, each glomerulus furthermore had to co-localize with an aggregate of SV_2 IR

puncta indicative of the synaptic neuropil in the glomerular core. We first conducted a series of preliminary experiments to determine if different labels correctly represented the numbers and distributions of glomeruli. We identified anti-KLH and anti-SV$_2$ as reliable labels for all glomeruli in the olfactory bulb, while anti-calretinin was useful to label glomeruli in certain, but not all regions (see results). Staining with all other antibodies was not nearly as detailed, and we thus based our morphological analysis on specimens that were stained with the above-mentioned antibodies.

Glomeruli were counted and measured by stepping through optical sections and tracing outlines of the fibrous innervation of identified units with the freehand drawing tool in ImageJ. We obtained all measures from single optical sections in which the maximal circumferences of glomeruli in question were shown. A representative example of such tracings is provided in Supplemental Movie 1. Average counts and sizes of glomeruli were based on observations from at least five fish of each sex. All data are presented as 'per bulb' averages of glomerular numbers and sizes. These averages were obtained separately for left and right olfactory bulbs but did not differ in preliminary comparisons. However, unless noted otherwise, data cited in this manuscript are obtained from measurements in the left olfactory bulbs.

Glomeruli that could be unambiguously identified in 70% of the specimens examined were assigned specific names (e.g., dorsal glomerulus dG$_1$), while the remaining units were only assigned to appropriate regions (e.g., dorsal glomerulus dG$_x$). Glomerular nomenclature was adopted from a previous description (Baier and Korsching, 1994) but modified in several instances to provide consistency.

3.3.9 Statistical Analysis

Numbers and sizes of glomeruli were pooled across animals (female vs male) according to their identity (e.g., individually identifiable dG_1) or the region in which they were located (e.g., indistinguishable dG_x). Throughout this chapter these data are presented as means and their standard deviations. To determine if differences in glomerular size were statistically significant, we compared pooled anatomical data from individually identifiable or indistinguishable glomeruli via a one-way analysis of variance (ANOVA). Possible differences in anatomical variability among numbers of different types of glomeruli were evaluated through Levene's test for equality of variances, and where significant, we further evaluated variances among glomeruli through a series of Student's t-tests. All statistics were analyzed with SPSS software (Chicago, IL, USA).

3.4 Results

3.4.1 Anatomy of Different OSN Types

Antibodies against different G-protein α subunits and calcium binding proteins labeled morphologically distinct cell types throughout the olfactory epithelium (OE). Anti $G_{\alpha\ s/olf}$ faintly labeled cells with round somata that were located deep in the epithelium. A slender dendrite extended from each $G_{\alpha\ s/olf}$ immunoreactive (IR) cell to the epithelial surface and terminated in an intensely IR knob (Figure 13B, green arrowheads). Many $G_{\alpha\ s/olf}$ IR cells also labeled with the calretinin antibody (Figure 13B, white arrowheads) and all of these cells were widespread but without any evident organization. The calretinin antibody also labeled another type of cell; this cell was located mid-way through the depth of the epithelium and bore a short, stout dendrite that extended towards the epithelial surface (Figure 13D; red arrowhead).

$G_{\alpha o}$ IR was present in a few scattered cells located near the surface of the epithelium (Figure 13C, cyan arrowhead). The somata of such cells appeared to be slightly larger than that of other OSNs (compare to soma indicated by white arrowhead in Figure 13C) and each $G_{\alpha o}$ IR cell possessed a single short stout dendritic protrusion. Finally, we observed a few S_{100} IR oval cells with thin cilia-like protrusions (white arrowhead in Figure 13D). These cells were scattered throughout the tissue and were also located near the epithelial surface.

Two other G-protein α subunit antibodies (anti $G_{\alpha i-3}$ and anti $G_{\alpha q/11}$) did not produce unambiguous labeling in the olfactory epithelia, but labeled OSN axons ($G_{\alpha i-3}$) and taste receptor cells ($G_{\alpha q/11}$) as shown in Supplemental Figure 1. The KLH antibody, which we used as general marker for OSN axons also did not produce unambiguous labeling of

OSN somata (not shown).

3.4.2 Coarse Organization of Glomeruli

OSN axons fasciculated in the olfactory nerve and then targeted specific regions of the olfactory bulb in a coarse topographic manner. For example, OSN axons that originated in the medial OE gave rise to a distinct axon bundle that was clearly distinguishable from other bundles, as it extended into the medial olfactory bulbs (see medial ON in Figure 14). In contrast, those axons that originated in the lateral sensory epithelium targeted the lateral olfactory bulbs (lateral ON in Figure 14). Despite this organization we observed many small axon bundles that originated in medial and / or lateral regions of the olfactory epithelia but crossed over to the other side once inside the olfactory bulb (arrows in Figure 14).

In the olfactory bulbs, OSN axons selectively targeted one of nine anatomically distinct glomerular aggregates, or clusters. These clusters were easily distinguished from one another by means of their selective innervation by neurochemically distinct OSN families and also by their separation from one another by areas devoid of glomeruli. Glomeruli on the dorsal olfactory bulb surface were thus organized into the dorsal cluster (dG), the dorsolateral cluster (dlG), the dorsal cluster associated glomeruli (dcaG) and the mediodorsal cluster (mdG; all in Figure 15A$_1$). All dorsal glomeruli uniformly displayed KLH like immunoreactivity (LIR; Figure 15A$_2$), and dG and dlG furthermore labeled with antibodies against calretinin and G$_{\alpha \text{ s/olf}}$ (see dG and dlG in Figures 15A$_3$, 15B$_2$). The dcaG labeled inconsistently, but in specimens in which we achieved labeling, they displayed KLH LIR (Figure 15A$_2$) and also G$_{\alpha \text{ s/olf}}$ IR (Figure 15B$_2$), but never calretinin IR. The innervation to mdG displayed KLH LIR (compare mdG in Figure 15A$_2$ to 15B$_1$)

in addition to highly specific labeling of some mdG (discussed below).

Glomeruli on the ventral olfactory bulb surface were organized into three anatomically distinct regions, the ventral (vG), ventromedial (vmG) and ventroposterior (vpG) clusters, and all displayed uniform KLH LIR (Figures $16A_1$ and $16A_2$). Innervation to the vG and vmG appeared to arise from the same axon bundle (arrowheads in Figure $16A_1$), but these glomeruli were not uniformly labeled. The vG, which were located several micrometers beneath the olfactory bulb surface, labeled with anti $G_{\alpha\ s/olf}$ but not anti calretinin (compare structures indicated by arrowheads in Figures $16B_2$ and $16B_3$ and see Supplemental Movie 2). In contrast, the vmG were innervated by $G_{\alpha\ s/olf}$ *and* calretinin IR axons, but the anti $G_{\alpha\ s/olf}$ labeling was much dimmer than that of anti calretinin (arrowheads in Figure $16B_1$). Finally, with the exception of a single glomerulus that was consistently targeted by calretinin IR axons (lvpG in Figure $16A_3$, $16B_3$), the vpG labeled only with anti KLH (compare vpG in Figure $16A_1$, $16B_1$).

The lateral cluster glomeruli (lcG) were best visualized from a lateral perspective (Figure 17). Most of the lcG and the nerve-plexus like innervation to the posterolateral olfactory bulbs (lateral plexus, LP) were labeled with the anti calretinin antibody (see lcG and LP in Figure $17A_3$, $17B_3$). However, a single large lateral glomerulus (lcG_1) labeled with anti KLH and anti $G_{\alpha\ s/olf}$ (lcG_1 in Figures $17A_2$ and $17B_2$) but not anti calretinin (lcG_1 in Figure $17A_3$, $17B_3$) antibodies.

Finally, glomeruli on the medial olfactory bulb surface were also easiest to visualize in bulbs that were lying on their side (Figure 18). These medial glomeruli (mG in Figure $18A_1$) appeared to be uniformly labeled by the anti KLH (Figure $18A_2$) and anti $G_{\alpha\ s/olf}$ antibodies (Figure $18B_2$), but were only partially innervated by calretinin IR axons

(compare arrowheads in Figures $18A_2$ and $18A_3$).

The coarse organization of glomerular clusters described here was highly stereotypic and essentially the same in all animals, regardless of sex. However, the individual glomeruli that were located in different glomerular clusters differed not only in their OSN innervation patterns, but also in their sizes and distributions as described below.

3.4.3 Fine Organization of Glomeruli

We identified 137 ± 6 and 140 ± 8 glomeruli in the each olfactory bulb of adult female (n = 7 left bulbs) and male zebrafish (n = 5 left bulbs; Table 2), respectively. We obtained these estimates by stepping through optical sections of whole-mounted olfactory bulbs and tracing and counting the outlines of glomeruli as shown in Supplemental Movie 1. Approximately 20% of these glomeruli could be identified and mapped as distinct individuals across all or most specimens examined, and their outlines are traced, named and / or numbered in Figures 15-18 (e.g., dG_1 in Figures $15A_3$ and $15B_3$). The remaining 80% of glomeruli could not be unambiguously identified across specimens but could be recognized as residents of glomerular clusters. These glomeruli are traced with dashed lines or are indicated otherwise throughout subsequent sections of this chapter (e.g., mG_x in Figure $18A_2$). We discuss these types of glomeruli separately.

3.4.4 Individually Identifiable Glomeruli

Glomeruli that could be unambiguously identified in at least 70% of the olfactory bulbs of the same (i.e., left and right) and different zebrafish of either sex generally shared the following anatomical features. Their OSN innervation labeled with an antibody against a G-protein α subunit *or* calcium binding protein (e.g., lcG_1 in Figures

17B$_2$), but not with both (e.g., see lcG$_1$ in Figure 17B$_3$; with exception of vtG$_{1-3}$ and vmG$_2$ in Figures 16B$_2$ and 16B$_3$), and in several cases with none of the neurochemical markers that we tested (e.g., mvpG in Figure 16A$_2$ vs. 16B$_{2-3}$). The average cross-sectional area of these glomeruli (n = 25, see Table 2) was approximately 1670μm^2, which was significantly larger than the average size of the remaining glomeruli (~485μm^2; p<0.001, ANOVA). Indeed, individually identifiable glomeruli constituted the 14 largest units in the olfactory bulbs of both male and female zebrafish and were located mainly the medial regions of the olfactory bulbs.

Individually identifiable mdG

The mdG are recognizable as a roughly triangular, bilaterally symmetric cluster in the dorsal olfactory bulbs (mdG in Figure 15A$_2$). We identified six mdG with very similar arrangements in almost all specimens studied, regardless of sex (Table 2). The mdG were often stacked on top of one another, which made it difficult to discern all six units from a single view plane (e.g., dorsal view in Figure 15A$_2$). However, if the bulbs were additionally viewed from their medial surface, all mdG became visible (Figure 18A$_2$). All mdG displayed uniform KLH IR (Figure 15A$_2$), but only some of these glomeruli were innervated by axons that labeled additionally with neurochemical markers. Specifically, mdG$_2$ and mdG$_5$ were selectively innervated by S$_{100}$ IR fibers (Figure 19A) and G$_{αo}$ IR processes (Figure 19B), respectively. The innervation to both of these glomeruli appeared to originate from multiple axon stalks (see arrowheads in Figures 19A), which occasionally crossed the midline of the olfactory bulbs (arrow in Figure 19A). The innervation to the remaining mdG did not label with any other antibodies that we tested in this study.

82

Individually Identifiable dcaG

The dorsal cluster associated glomeruli (dcaG) were located approximately >30μm beneath the dorsal olfactory bulb surface (see dcaG in Supplemental Movie 3). The dcaG were occasionally arranged as a row of 5 glomeruli along the caudal edge of the olfactory bulbs (see $dcaG_{1-5}$ on the right side of Figure 20D), as reported previously by Baier and Korsching (1994). However, it was more common for the dcaG to be located within a diffuse neuropil (see left side of Figure 20D), which appeared to contain additional glomeruli anterior to the location of the known dcaG (see dashed tracing in Figure 20D). Overall, we were able to identify five dcaG in at least 70% of the animals examined (Table 2), and we thus treat these as individually identifiable glomeruli.

Individually identifiable $lcG_{1,3,4}$

Some of the largest and most stereotypic glomeruli were located on the lateral olfactory bulb surface ($lcG_{1,3,4}$ in Figure 21A-D). The lcG_1 was located on the caudal edge of the lateral cluster (Figure 21A; see also Figure $17A_2$) and was identifiable in every animal (Table 2). Like other lcG, this glomerulus was innervated by axons from the lateral fiber bundle (see arrowheads in Figure 21A), however, unlike the other lateral glomeruli, lcG_1 was innervated by $G_{\alpha\,s/olf}$ but not calretinin IR axons (Figure $17B_1$).

The lcG_3 (Figures 21A and 21B) and lcG_4 (Figure 21D) were similarly large (Table 2), repeatedly identifiable and innervated by axons from the lateral fiber bundle. The innervation of these glomeruli, however, was calretinin IR and not $G_{\alpha\,s/olf}$ IR (compare lcG_3 in Figures $17B_3$ and $17B_2$).

Individually identifiable vpG

The medial (mvpG), central (cvpG) and lateral (lvpG) ventroposterior glomeruli

(Figure 16A$_2$) were among the largest and most consistently identifiable glomeruli in the olfactory bulbs of both female and male zebrafish (see Table 2). The lvpG was innervated by calretinin IR axons in all animals (e.g., see Figure 16A$_3$, 16B$_3$), but the innervation to the cvpG and mvpG was not labeled with any of the G-protein α subunit or calcium binding protein antibodies that we used in this study, suggesting that they may be innervated by another, neurochemically distinct set of OSNs.

Individually Identifiable vmG$_{1-3}$ and vtG$_{1-3}$

Glomeruli in the ventral olfactory bulbs labeled with different combinations of antibodies against G-protein α subunits and calcium binding proteins, but they were also morphologically diverse and differed significantly in size (e.g., compare vmG$_{1-3}$ and vtG$_{1-3}$ to vmG$_x$ in Figure 16A$_3$). The only individually identifiable glomeruli in the ventral olfactory bulbs were the three ventral triplet glomeruli (vtG$_{1-3}$) and the three ventromedial glomeruli (vmG$_{1-3}$). The innervation to all of these glomeruli stained very well with anti-calretinin (e.g., Figures 16A$_3$ and 16B$_3$), and with exception of vmG$_1$ and vmG$_3$ these glomeruli also displayed G$_{\alpha \text{ s/olf}}$ IR (compare Figures 16B$_2$ and 16B$_3$). In both female and male zebrafish, the vtG and vmG comprised the largest glomeruli in the vmG and vG clusters, but they were noticeably smaller than most other individually identifiable glomeruli (e.g., compare to vpG in Table 2).

Other Individually Identifiable Glomeruli

We identified two additional glomeruli in the olfactory bulbs of all animals examined. The dorsal glomerulus 1 (dG$_1$) was not a particularly large unit, but was nevertheless identifiable by its strong staining with anti calretinin, and its characteristic shape (dG$_1$ in Figures 15A$_3$ and 15B$_3$). The medial elongated glomerulus (meG) was

located between ventromedial and medial Glomerular clusters and was only visible in specimens that were stained with anti-KLH (compare Figures 18A$_2$ and 18A$_3$).

3.4.5 Anatomically Indistinguishable Glomeruli

Approximately 80% of glomeruli in the olfactory bulbs of female and male zebrafish could not be identified consistently and unambiguously in tissue from the same (left and right bulbs) or different animals. These glomeruli shared the following anatomical features. Their OSN innervation almost always labeled with antibodies against the G-protein α subunit $G_{\alpha\ s/olf}$ *and* the calcium binding protein calretinin. Moreover, while the morphologies and sizes of these glomeruli varied substantially, they were always much smaller than the glomeruli discussed above, with an average cross-sectional area of approximately 485μm^2 (p < 0.001, ANOVA). All of these glomeruli were tightly packed in glomerular clusters.

Indistinguishable dG

We found approximately 15 glomeruli in the diffusely innervated dorsal cluster (dG) in the anterodorsal olfactory bulb (Table 2; see dG in Supplemental Movie 3). With the exception of dG$_1$ (discussed above), these glomeruli varied considerably in their numbers and individual morphologies and were thus indistinguishable. The actual numbers of identified dG ranged from 10-21 and 14-20 in female (n = 7) and male (n = 5) zebrafish, respectively. Examples of such morphological variations are further illustrated in Figure 20, where dG$_x$ with cross-sectional areas ranging from 512μm^2 (arrows in Figure 20B) to 175μm^2 (arrowheads in Figure 20C) are depicted.

Indistinguishable dlG

The dorsolateral glomeruli (dlG) accounted for approximately one third of the total

glomerular population and these units were among the smallest glomeruli in the bulbs of female and male zebrafish (Table 2). All dlG_x were located in a thin sheet on the dorsal olfactory bulb surface (Supplemental Movie 3). Morphological variations, although common, were not as profound as in other areas (dG, above) and the dlG appeared to have rather homogeneous appearances (see dlG on the left side of Figure 20B). Occasionally, we found dlG that appeared to resemble one another in the left and right olfactory bulbs of single animals (see arrowheads in Figure $15A_2$), but these same glomeruli were not recognizable in other animals.

Indistinguishable vmG and mG

The vmG (Figures $16A_2$ and $16A_3$) and mG (Figure $18A_2$) were very small glomeruli that were located in adjacent and separately innervated regions on the ventromedial and medial olfactory bulb surfaces, respectively. The OSN axons that innervated the vmG and mG were labeled with anti-calretinin (Figures $16A_3$ and $18A_3$) and anti $G_{\alpha \, s/olf}$ (Figures $16B_2$ and $18B_3$); however, the calretinin labeling often appeared to be much stronger than that achieved with anti $G_{\alpha \, s/olf}$ (e.g., vmG in Figure $16B_1$).

Individual vmG_x in the left and right olfactory bulbs of single animals generally mirrored each other (see red lines in Figure $16A_3$), but there were always glomeruli that could only be detected unilaterally (see red arrowheads in Figure $16A_3$); however these glomeruli differed from animal to animal and it was therefore not possible to unambiguously identify them.

Indistinguishable vG

A group of relatively large, but irregularly distributed ventral glomeruli (vG_x) was located >10μm below the ventral olfactory bulb surface. These sparse glomeruli could be

found anywhere between the olfactory nerve entry and the ventroposterior glomeruli (see vG_x in Figure 22B and 22C; see also Supplemental Movie 2). Unlike other indistinguishable glomeruli, the vG_x labeled only with anti $G_{\alpha \, s/olf}$ but not anti calretinin, and the vG_x were also larger than most other indistinguishable glomeruli (Table 2). However, these glomeruli were diffusely innervated, arranged in variable manners and thus not identifiable between animals.

Indistinguishable lcG

In addition to the large and stereotypic $lcG_{1,3,4}$ discussed above, we detected a few lcG_x that labeled only with the calretinin antibody and were on average smaller than the individually identifiable lateral glomeruli (Table 2; $p < 0.05$, ANOVA). The shapes and sizes of these lcG_x varied substantially (compare lcG_x in Figure 21A and 21D) as did their locations and numbers. Much of the perceived variability among the lcG_x could be due to the diffuse innervation of the lateral olfactory bulbs (e.g., compare dlG and the lateral glomeruli in Figure 21A). Indeed, several relatively large lcG_x, located approximately 25μm below the lateral olfactory bulb surface (Figure 21D), were easier to identify because they were not surrounded by a dense neuropil. However, without a specific label, these units could not be identified in different animals.

3.4.6 Stereotypy Versus Variability of Identifiable and Indistinguishable Glomeruli

Thus far we have described two classes of glomeruli that can be discriminated based on their size and the neurochemistry of their OSN innervation. All glomeruli displayed some degree of anatomical variability, but individually identifiable glomeruli appeared to be present in every animal and varied only occasionally, while differences in the numbers of indistinguishable glomeruli were common in every cluster. We therefore

compared the pooled variance among 25 individually identifiable glomeruli to that of the

$G_{\alpha\ s/olf}$ IR and calretinin IR glomeruli in the dG, vmG, mG, vG and lcG clusters, each of

which contained similar or fewer numbers of glomeruli. An overall comparison between

these variances was indeed statistically significant ($p < 0.05$, Levene's test) and further

comparisons indicated that the variability in the number of glomeruli in the dG, vmG,

mG and lcG_x was increased over that in the 25 individually identifiable glomeruli (all $p <$

0.05, Student's t). Thus, glomeruli in the zebrafish olfactory system differ not only based

on size and innervation, but also by their degree of anatomical stereotypy and variability.

3.5 Discussion

We have taken advantage of the small and compact zebrafish olfactory system to create, what is to our knowledge, one of the most detailed descriptions of the anatomical organization of olfactory glomeruli in a lower vertebrate (see also, Gaudin and Gascuel, 2005, Byrd and Brunjes, 1995, Baier and Korsching, 1994, Hansen et al., 2003). We identified approximately 140 glomeruli in each olfactory bulb of female and male zebrafish, and based on several anatomical features we could categorize these glomeruli as either one of two types. The first type consisted of 25 enlarged glomeruli that were highly stereotypic in position and arrangement and thus unambiguously identifiable in nearly all animals. These glomeruli were innervated by axons from distinct types of ciliated, microvillous and / or crypt OSNs. The other type of glomerulus (85% of total) was smaller on average and arranged in tight clusters in several individually identifiable regions of the olfactory bulbs. Across animals, these units were indistinguishable from one another, and most small glomeruli were innervated uniformly by calretinin IR and $G_{\alpha \ s/olf}$ IR axons from ciliated OSNs. We believe that these two types of glomeruli comprise several different olfactory pathways.

3.5.1 Previously Known and Newly Identified Glomeruli

The sensory input to a glomerulus consists of the axons and terminals of hundreds (insects: Hildebrand and Shepherd, 1997) to thousands of OSNs (vertebrates: Mombaerts, 2006; Mori and Yoshihara, 1995), and the convergence of these axons onto discrete spheroidal locations is the most fundamental anatomical feature of the olfactory system (Chen and Shepherd, 2005). Labeling OSN axons and / or their terminals with anatomical or functional probes is thus a valid and established method to study the

structure, distribution, function and development of glomeruli (e.g., Wachowiak et al., 2009, Sato et al., 2005, Li et al., 2005b, Koide et al., 2009, Friedrich and Korsching, 1998, Feinstein et al., 2004, Bozza et al., 2004, Bellmann et al., 2010).

In a previous description of glomeruli in the zebrafish olfactory system, Baier and Korsching (1994) employed a lipophilic axon tracer to non-selectively label OSN axons that innervate glomeruli. Similar to our data, the authors of this study identified 22 glomeruli that were individually identifiable within and between adult zebrafish (see Table 2). Indeed, our descriptions of individual types of glomeruli are very similar. For example, both we and Baier and Korsching could identify five dorsal cluster associated glomeruli (dcaG) in the dorsoposterior olfactory bulbs (e.g., Figure 20D). Moreover, our descriptions of anatomically indistinguishable glomeruli are also similar. We identified between 44-50 dlG in the olfactory bulbs of female and male zebrafish and these were located in the same region in which Baier and Korsching previously identified 49 glomeruli (e.g., see dlG in Figure 20A). These and other data compared in Table 2 are therefore highly consistent.

However, our data further complement the present understanding of the anatomy and functional organization of olfactory glomeruli in zebrafish and related species. We provide new and highly detailed data depicting the neurochemistry of OSN innervation to *all* glomeruli. For example, we identified lcG_1 as a functionally distinct unit within the lateral cluster; this glomerulus was evidently different from other lateral glomeruli as it labeled with an antibody against $G_{\alpha \, s/olf}$ and not, like other lcG, with the anti-calretinin antibody (Table 2). Thus, by employing a combinatorial labeling approach, we confirmed not only the coarse organization of glomeruli described in previous studies

(zebrafish: Sato et al., 2005, catfish: Hansen et al., 2003; lamprey: Frontini et al., 2003), but describe several individually identifiable, neurochemically distinct units throughout the olfactory bulbs.

Our study additionally complements previous anatomical data by identifying a significant number of additional glomeruli. To our knowledge, none of the previously available descriptions of the olfactory system in zebrafish and related species (trout: Riddle and Oakley, 1992; catfish: Hansen et al., 2003; lamprey: Frontini et al., 2003) has produced data with as much resolution of structural detail as we show throughout our results. For example, Baier and Korsching (1994) described 80 diffusely organized glomeruli, but we found 140 glomeruli, all of which were identifiable as separately innervated spheroidal structures with sharp boundaries. We determined that most newly identified glomeruli (~ 45) were located in the anterior and medial olfactory bulbs (e.g., dG, mG, vmG in our study), regions that were previously thought to be aglomerular nerve plexi (e.g., see Kosaka and Hama, 1982b). For example, we identified ~15 dG in the anterodorsal olfactory bulb, a region that other authors have described as 'aglomerular anterior plexus' in zebrafish (Baier and Korsching, 1994) and lamprey (Frontini et al., 2003, see also Table 2). We believe that our ability to detect additional glomeruli in this and other regions was due to the improved labeling obtained with certain antibodies, as well as our exhaustive confocal imaging of all surfaces of whole-mounted olfactory bulbs. Thus, even the smallest glomeruli were clearly identifiable in tissue that was labeled with anti-KLH or anti-calretinin (e.g., see mGx in Figure 6A$_2$), but these same glomeruli were hardly visible when we stained tissue with anti-G$_{\alpha \text{ s/olf}}$ (e.g., see mG in Figure 6B$_2$) or lipophilic tracers (pers. observation), both of which had been

used in previous descriptions of fish glomeruli (Hansen et al., 2003, Frontini et al., 2003, Baier and Korsching, 1994). Furthermore, most small glomeruli were only visible if they were viewed from the correct perspective (e.g., medial glomeruli viewed on the medial surface), which was not done in previous studies (but see Sato et al., 2005, Koide et al., 2009). We therefore suggest that future studies exploit the techniques that we have established here in order to accurately characterize the anatomy and distributions of glomeruli in related species.

Nevertheless, the 140 glomeruli that we identified did not cover the entire olfactory bulb surface and significant parts of the glomerular layer indeed appeared to be plexus-like. For example, we could not identify glomeruli proper on the posterolateral olfactory bulb surfaces. This region may contain microglomeruli (Meyerhof and Korsching, 2009, Korsching, 2005), but we were not able to resolve such structures, even in careful analysis of individual optical sections. A possible explanation may be that zebrafish microglomeruli consist of merely one or a few axon terminals, as do microglomeruli in orthoptera (Ignell et al., 2001). Anti-KLH does not appear to label axon terminals (pers. observations), and may therefore not be an adequate label for microglomeruli. We hope to resolve this issue and determine a suitable label for microglomeruli in future studies (see Chapter 4).

3.5.2 Relationships Between Chemosensory Receptor Types and Glomeruli

In mammals (Vassar et al., 1994, Mombaerts, 1996) and presumably also in fish (Hamdani and Døving, 2007), each olfactory glomerulus is innervated by axons of one or at most a few OSN types. The number of functional OR genes in these animals may thus be predictive of the number of glomeruli in the olfactory bulbs.

OR and V2R type receptors and glomeruli

Approximately 143 functional chemosensory receptor sequences have been linked to the zebrafish olfactory system (Alioto and Ngai, 2005). Of these, 102 encode OR-like olfactory receptors (Hashiguchi and Nishida, 2007). OR-like receptors are linked to G_{olf}-expressing OSNs (Sato et al., 2005), which we explicitly link to ~ 100 glomeruli in the ventromedial and dorsolateral olfactory bulbs (Table 2). Thus, the numbers of OR type receptors and the glomeruli that they presumably innervate, correlate well with one another.

An additional 46 V2R-type chemosensory receptors have been identified in zebrafish (Hashiguchi and Nishida, 2007). In zebrafish, V2R-type receptors are expressed by microvillous cells, which project their axons almost exclusively to the lateral olfactory bulbs (Sato et al., 2005). We have been able to detect only ~ 20 lateral glomeruli, suggesting that additional V2R-expressing microvillous neurons innervate the posterolateral plexus (above). Indeed, data from Friedrich and Korsching (1997) indicate that posterolateral olfactory bulb is responsive to stimulation by amino acids in a manner that is complementary to the responses recorded in the anterolateral olfactory bulb, where we find the lateral glomeruli lcG_x.

TAAR-type chemosensory receptors

An additional 100 trace amine-associated receptor (TAAR) gene sequences are expressed in the zebrafish olfactory epithelium (Hashiguchi and Nishida, 2007). TAARs belong to a specific family of G-protein coupled receptors and may be involved in pheromonal communication in mammals (Liberles and Buck, 2006) and fish (Hashiguchi and Nishida, 2007; Yambe et al., 2006). We and others (Miyasaka et al., 2009) believe

that TAARs may be expressed in crypt sensory neurons, a sensory receptor cell type that may also be involved in pheromonal communication in fish (Hamdani et al., 2008, Hamdani and Døving, 2007). We have identified at least two glomeruli that are innervated by crypt cells, the mdG_2 and mdG_5 and we describe seven additional glomeruli ($mdG_{1,3,4,6}$, meG, cvpG, mvpG) in the putatively pheromone-responsive medial olfactory bulbs. Based on our results it appears that none of these seven glomeruli are innervated by OR-type and V2R-type OSNs and, by exclusion, it is thus plausible that they are innervated by TAAR-expressing crypt cells.

However, if all TAAR-associated glomeruli were innervated according in a 'one glomerulus - one receptor' fashion, then there would have to be approximately 100 additional glomeruli in the olfactory bulbs (240 total), significantly more than we or others (Baier et al., 1994) have described. As an alternative hypothesis, we suggest that individual pheromone-sensitive glomeruli are innervated by multiple TAAR type chemosensory cells. It is known from mammals that pheromone-responsive glomeruli in the AOB can be innervated by the axons from as many as 20 different V2R type vomeronasal sensory neurons (Rodriguez et al., 1999, Belluscio et al., 1999) and we thus reason that pheromonal glomeruli in zebrafish may be wired in a similar manner. However, additional experiments are needed to elucidate this (see Chapter 4).

To summarize, our anatomical data correspond well to known numbers of OR and V2R type olfactory receptors, and it appears that these receptor types may be represented in a nearly 1:1 ratio by glomeruli, as is also the case in insects (Vosshall et al., 2000), but not mammals (Mombaerts, 2006). In contrast, the TAARs may not be represented in such a manner and instead multiple TAAR-expressing cells may innervate individual

glomeruli at once.

3.5.3 Are Large Glomeruli Part of Specialized Olfactory Pathways?

We show that the cross-sectional area of zebrafish olfactory glomeruli can range from 400-4000μm^2 (see also, Baier and Korsching, 1994). Similarly diverse size ranges have been documented for glomeruli in trout (Riddle and Oakley, 1992), lampreys (Iwahori et al., 1987, Frontini et al., 2003), *Xenopus laevis* (Nezlin and Schild, 2000, Nezlin et al., 2003, Gaudin and Gascuel, 2005), mammals (St John and Key, 2001, Pinching and Powell, 1971, Meisami and Bhatnagar, 1998) and insects (Masante-Roca et al., 2005, Kazawa et al., 2009).

Pheromone-Responsive Glomeruli

The olfactory systems of mammals and insects contain specialized olfactory pathways consisting of small numbers of 'atypical' glomeruli, which are identifiable based on unique anatomical features not shared with other, generally more numerous, glomeruli. For example, the main olfactory bulbs of rodents contains an anatomically stereotypic (Shinoda et al., 1989), neurochemically distinct (Jastreboff et al., 1984, Zheng et al., 1987) 'modified glomerular complex', which has been linked to suckling behavior in rat pups (Greer et al., 1982). Similarly, pheromone-responsive glomeruli in insects are fewer in number, but larger than glomeruli that respond to plant odors, and based on their stereotypic arrangements these units are identifiable in animals of the same and related species (Sorensen et al., 1998, Kleineidam et al., 2005, Hildebrand and Shepherd, 1997, Galizia and Rössler, 2010, Christensen and Hildebrand, 1987, Boeckh et al., 1987).

We believe that the enlarged and individually identifiable glomeruli described in our study also comprise specialized olfactory pathways. For example, the mdG, meG,

vpG, vtG_{1-3} and vmG_{1-3} are all comparably large, labeled with distinct combinations of antibodies against G-protein α subunits, and are furthermore situated in the pheromone-responsive medial olfactory bulbs (Hanson et al., 1998, Hamdani and Døving, 2007, Hamdani and Døving, 2003). Indeed, optophysiological recordings indicate what appear to be specific glomeruli in the ventromedial olfactory bulbs as regions sensitive to zebrafish candidate sex pheromones (Friedrich and Korsching, 1998). Thus, there are several converging lines of evidence to support a role of the large mdG, meG, vpG, vtG_{1-3} and vmG_{1-3} in pheromone processing.

Possible Specialist Glomeruli lcG_3 and lcG_4

The lcG_3 and lcG_4 are among the largest and most stereotypic glomeruli, but these glomeruli reside in the amino acid-responsive lateral cluster and presumably play a role in feeding (Koide et al., 2009), not pheromonal processing. Ibba et al. (2010) have recently provided direct evidence for glomerular enlargement as a result of a species-specific adaptation to a food source in insects. Related data indicate that fish may possess similarly specialized glomeruli. Specfically, Nikonov and Caprio demonstrated that catfish have a population of OSNs (Nikonov and Caprio, 2007a), olfactory bulb neurons (Nikonov and Caprio, 2004), and lateral forebrain neurons (Nikonov and Caprio, 2007b) that are highly tuned and respond selectively to a few neutral and basic amino acid odorants, suggesting that these amino acids may be encoded in a specific labeled line olfactory pathway. Optophysiological recordings in zebrafish (Friedrich and Korsching, 1997) similarly show 1-2 specific 'glomerular modules' that respond preferentially and with little overlap to neutral amino acids, and our interpretation is that these data describe either lcG_3 or lcG_4. Finally, zebrafish appear to be innately attracted to certain amino

acids and these attractive behaviors are abolished in larvae that have malformed lateral glomeruli (Vitebsky et al., 2005). Based on these data, we believe that lcG_3 and / or lcG_4 may be specifically tuned towards certain types of amino acids that may be main components of the zebrafish diet; being highly receptive to these compounds would evidently be advantageous for the survival of zebrafish.

3.5.4 Anatomical Variability of Small But Not Large Glomeruli

We observed significant anatomical variability among the calretinin IR and $G_{\alpha\ s/olf}$ IR small glomeruli in the medial and dorsolateral olfactory bulbs. Throughout our study we tried to minimize experimental errors that could underlie such variations by selecting only well-stained preparations for analysis, confirming our findings with multiple complementary labels (e.g., anti-KLH and anti SV_2), and repeating the same analysis in several olfactory bulbs. Yet, we still observed anatomical variations among these glomeruli, and we thus believe that they are of biological origin.

Variations in the numbers of glomeruli are common, and errors in the estimated numbers of glomeruli can range from 20% of detectable units in frogs (Nezlin and Schild, 2000) and moths (Kazawa et al., 2009), to approximately 10% in bees (Flanagan and Mercer, 1989), moths (Masante-Roca et al., 2005, Couton et al., 2009) and ants (Kleineidam et al., 2005). Similarly, the numbers and distributions of glomeruli also vary in the main (Strotmann et al., 2000, Schaefer et al., 2001, Royal and Key, 1999) and accessory olfactory system of rodents (Meisami and Bhatnagar, 1998).

The sources of anatomical variations (or stereotypy) have not been determined, but may be of developmental origin. There exists significant morphological variability during the development of glomeruli in mice (Royal and Key, 1999, Potter et al., 2001)

and sensory experience can furthermore influence their maturation during postnatal development (Zou et al., 2004, Zheng et al., 2000, Oliva et al., 2008, Kerr and Belluscio, 2006). Sensory experience could similarly shape the assembly of the glomerular map in zebrafish, but to our knowledge, no study has yet assessed this in detail. However, if sensory experience indeed contributes to the development of morphological variations in the olfactory system, then an important question arises as to why large glomeruli are not as variable. If these glomeruli are indeed specialized (see above), then they may develop under more guidance from genetically programmed events, as is often reasoned for innate behavioral circuits (for review, see Su et al., 2009). Given our extensive understanding of anatomical details in the zebrafish olfactory system, we believe that such questions can now be addressed (see Chapter 5).

3.5.6 Summary and Conclusion

We have provided a detailed anatomical description of the zebrafish olfactory system and our data indicate that glomeruli exist as diverse types, beyond the simplified functional dichotomy of lateral glomeruli that are involved in feeding and medial glomeruli that are involved in social communication. We will next attempt to specifically examine the structure of the pre- and postsynaptic compartments of individually identifiable and indistinguishable glomeruli in order to determine if these units are wired in a similar manner as representative specialist and generalist glomeruli in mammals and insects (Chapter 4).

Table 1. List of antibodies, their sources and staining protocols

Table 1.

Antibody	Immunogen / Host	Source	Fixation
General labels (1:100 in PBS-T)			
Anti-keyhole-limpet-hemocyanin (KLH)	hemocyanin from keyhole limpets / rabbit	Sigma (H0892)	2% PFA
Anti-synaptic vesicle protein 2 (SV_2)	ommata synaptic vesicles / mouse	Developmental Studies Hybridoma Bank (Iowa City, IA, USA)	2% PFA
OSN class specific Labels (1:50-100 in PBS-T)			
Anti-$G_{\alpha\, s/olf}$	rat c-terminus (seq: 377-394) / rabbit	Santa Cruz Biotech (Santa Cruz, CA, USA) sc-383	2% PFA
Anti-$G_{\alpha\, o}$	rat divergent domain (seq: 105-124) / rabbit	Santa Cruz sc-387	2% PFA
Anti-$G_{\alpha\, i-3}$	rat c-terminus (seq: 345-354) / rabbit	Santa Cruz sc-262	2% PFA
Anti-$G_{\alpha q\, /\, 11}$	mouse common domain (seq: 115-133) / rabbit	Santa Cruz sc-392	2% PFA
Anti-calretinin	recombinant human calretinin / mouse	Swant (Bellinzona, Switzerland) 6B3	2% PFA
Anti-S_{100}	cow S_{100} protein / rabbit	Dako (Glostrup, Denmark) Z 0311	2% PFA

Table 2. Summary of numbers, sizes, and innervation of glomeruli in this study and comparison with previously identified glomeruli in zebrafish and other species.

Table 2.

Glomerular Cluster / *Glomerulus*	Glomeruli per Bulb ♀ (n = 7)	♂ (n = 5)	Area (μm²) ♀	♂	Innervation	Previous Description / *name*
Dorsal glomeruli						
dG₁	1	1	742 ± 81	713 ± 70	calret	Baier and Korsching, 1994 (adult zebrafish); Frontini et al., 2003 (adult lamprey) / *not identified*
dGₓ	14.6 ± 3.5	16.2 ± 2.7	384 ± 70	488 ± 100	$G_{\alpha\,s/olf}$ / calret	*anterior plexus* (no glomeruli identified)
Dorsolateral glomeruli	♀ (n = 8)	♂ (n = 6)	♀	♂		
dlGₓ	49.6 ± 4.5	44.3 ± 4	252 ± 82	360 ± 88	$G_{\alpha\,s/olf}$ / calret	Baier and Korsching, 1994 (adult zebrafish); Koide et al., 2009 (larval zebrafish) / *glomeruli of the dorsal cluster in adult; posterior glomeruli (pG) in larva*
Dorsal cluster associated glomeruli	♀ (n = 7)	♂ (n = 5)	♀	♂		
dcaG₁	1	1	932 ± 394	1000 ± 494	$G_{\alpha\,s/olf}$	Baier and Korsching, 1994 (adult zebrafish) / *dcaG₁*
dcaG₂	0.7 ± 0.5	0.7 ± 0.5	828 ± 242	1052 ± 329	$G_{\alpha\,s/olf}$	*dcaG₂*
dcaG₃	0.9 ± 0.3	0.7 ± 0.5	838 ± 396	1163 ± 504	$G_{\alpha\,s/olf}$	*dcaG₃*
dcaG₄	0.7 ± 0.5	0.8 ± 0.3	878 ± 337	1263 ± 510	$G_{\alpha\,s/olf}$	*dcaG₄*
dcaG₅	1	0.7 ± 0.4	1139 ± 572	1303 ± 510	$G_{\alpha\,s/olf}$	*dcaG₅*

102

Table 2. continued

	♀	♂	♀	♂		
Mediodorsal glomeruli	(n = 8)	(n = 6)				Baier and Korsching, 1994 (adult zebrafish); Dynes and Ngai, 1998 and Koide et al., 2009 (larval zebrafish)
mdG_1	1	1	1277 ± 341	1396 ± 653	?	*mediodorsal posterior glomerulus₁ (mdpG₁) in adult; medial glomerulus₁ (mG₁) in larva*
mdG_2	1	1	2216 ± 644	2350 ± 730	S_{100}	*mdpG₂ in adult; mG₂ in larva*
mdG_3	0.9 ± 0.2	1	1356 ± 346	1809 ± 630	?	*not identified in adult; mG₃ in larva*
mdG_4	1	1	1554 ± 591	1901 ± 846	?	*not identified in adult; mG₄ in larva*
mdG_5	1	1	1380 ± 243	1509 ± 458	$G_{\alpha o}$	*not identified in adult; mG₅ in larva*
mdG_6	0.9 ± 0.2	0.7 ± 0.5	1800 ± 438	1844 ± 313	?	*medial anterior glomerulus (maG) in adult; mG₆ in larva*
Lateral cluster glomeruli	(n = 7)	(n = 5)				Baier and Korsching, 1994 (adult zebrafish); Dynes and Ngai, 1998 and Koide et al., 2009 (larval zebrafish)
lcG_1	1	1	2940 ± 151	3783 ± 557	$G_{\alpha\,s/olf}$	*glomerulus 1 of the lateral chain (lcG₁) in adult; lateral glomerulus₁ (lG₁) in larva*
lcG_2	0.1 ± 0.3	0.5 ± 0.6	1796	1509 ± 154	calret	*lcG₂ in adult; lG₂ in larva*
lcG_3	1	1	2148 ± 517	2578 ± 275	calret	*lcG₃ in adult; lG₃ in larva*
lcG_4	1	1	3190 ± 512	4085 ± 675	calret	*lcG₄ in adult; lG₄ in larva*
lcG_5	0.3 ± 0.4	0.25 ± 0.5	1480 ± 783	2012	calret	*lcG₅ in adult; not identified in larva*
lcG_x	12 ± 2.4	10 ± 2	878 ± 224	776 ± 195	calret	*not identified*
Ventroposterior glomeruli	(n = 10)	(n = 6)				Baier and Korsching, 1994 (adult zebrafish, goldfish); Dynes and Ngai, 1998 (larval zebrafish)
$lvpG$	1	1	2797 ± 429	2699 ± 406	calret	*not identified*

Table 2. continued

	♀	♂	♀	♂		
vpG	1	1	2201 ± 547	2296 ± 878	?	vpG in adult and larva
mvpG	0.9 ± 0.3	1	2397 ± 857	3116 ± 927	?	not identified
Ventral Triplet glomeruli	♀ (n = 10)	♂ (n = 5)	♀	♂		Baier and Korsching, 1994 (adult zebrafish)
vtG_1	0.7 ± 0.5	1	921 ± 264	923 ± 197	calret	vtG_1
vtG_2	1	1	1248 ± 308	1155 ± 304	$G_{\alpha s/olf}$ / calret	vtG_2
vtG_3	1	0.6 ± 0.5	1027 ± 350	797 ± 221	calret	vtG_3
Ventromedial glomeruli	♀ (n = 10)	♂ (n = 5)	♀	♂		Baier and Korsching, 1994 (adult zebrafish)
vmG_1	1	1	1076 ± 333	912 ± 328	calret	ventromedial glomerulus
vmG_2	0.7 ± 0.5	1	936 ± 146	956 ± 331	$G_{\alpha s/olf}$ / calret	not identified
vmG_3	0.8 ± 0.4	1	1208 ± 226	944 ± 284	calret	not identified
vmG_x	16 ± 2	15 ± 3	331 ± 73	344 ± 71	$G_{\alpha s/olf}$ / calret	not identified
Ventral glomeruli	♀ (n = 7)	♂ (n = 6)	♀	♂	$G_{\alpha s/olf}$	Baier and Korsching, 1994 (adult zebrafish); Frontini et al., 2003 (adult lamprey); anterior plexus (zebrafish), ventral cluster (lamprey)
vG_x	8.6 ± 1	11.4 ± 2.3	718 ± 188	775 ± 163		
Medial glomeruli	♀ (n = 7)	♂ (n = 5)	♀	♂		not identified
mG_x	17.8 ± 3.6	16.8 ± 3.3	343 ± 110	323 ± 117	$G_{\alpha s/olf}$ / calret	not identified
Medial elongated glomerulus	♀ (n = 7)	♂ (n = 5)	♀	♂	?	Baier and Korsching, 1994 (adult zebrafish)
meG	1	1	1562 ± 477	2457 ± 364		meG
	137 ± 6 (n = 7)	**140 ± 8 (n = 5)**				

Figure 13. OSN types in the olfactory epithelium of zebrafish. The olfactory epithelia of mature zebrafish are located on numerous lamellae that are folded into a rosette-shaped olfactory organ. (**A**) Schematic of a horizontally sectioned olfactory rosette, where grey area indicates sensory epithelium and white area is non-sensory epithelium. The dark bands in the middle of panels **B-D** are the midlines of lamellae and epithelial surfaces face up and down. (**B**) $G_{\alpha\ s/olf}$ and calretinin IR OSN were found throughout the sensory epithelium. Cells that were $G_{\alpha\ s/olf}$ IR often expressed calretinin IR as well (white arrowheads). (**C**) Anti-$G_{\alpha\ o}$ labeled cells with relatively large soma (cyan arrowhead). (**D**) S_{100} IR was sparse, but was strong in oval cells with small hair-like protrusions (white arrowhead). Scale bar in **D** also applies to **B** and **C**.
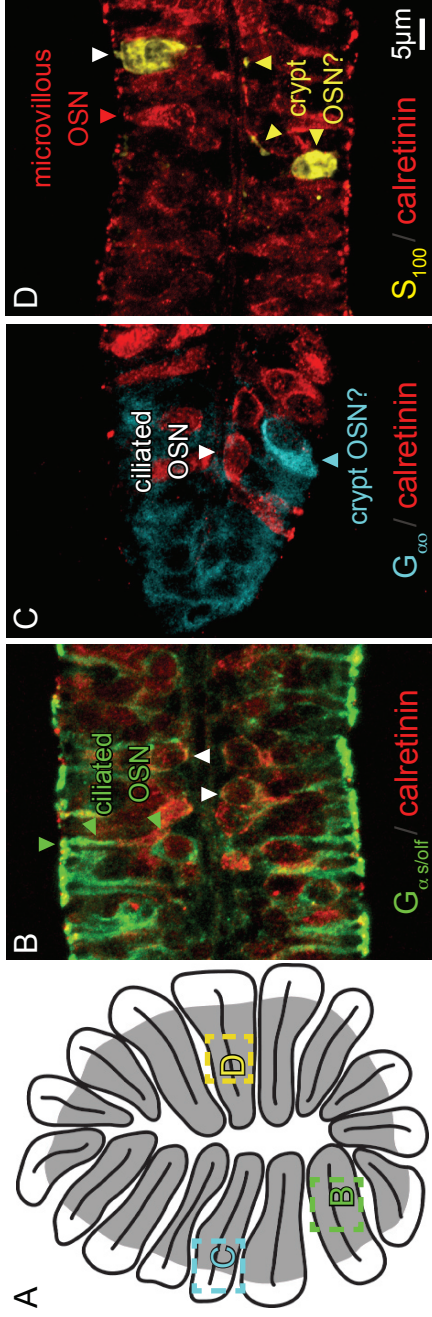
Figure 13. OSN Types in the Olfactory Epithelium of Zebrafish

Figure 14. A whole-mounted zebrafish olfactory system viewed from the ventral side. The olfactory epithelia (OE) are separated from the olfactory bulbs (OB) by a short olfactory nerve (ON). OSN that reside in the ventromedial and ventrolateral parts of the olfactory epithelium project their axons to the olfactory bulb in a topographic manner. The dashed line in the ON shows the separation of medial and lateral nerve bundles.
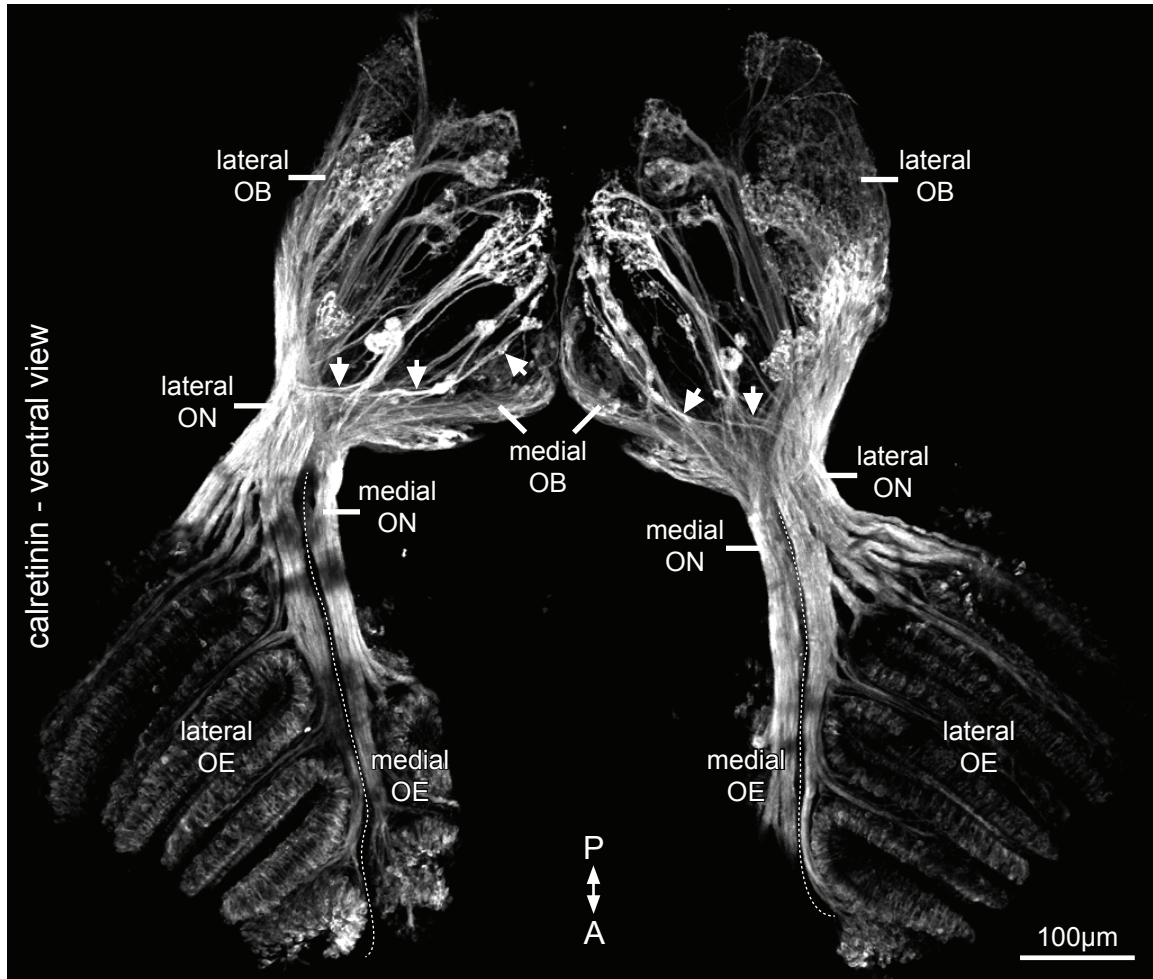
Figure 14. A Whole Mounted Zebrafish Olfactory System Viewed From the Ventral Side

Figure 15. Overviews of the dorsal olfactory bulb surface labeled with different antibody combinations. Glomerular clusters are traced with dashed lines in **A** and **B**, and individually identifiable glomeruli are traced with solid lines and are numbered. (**A$_2$**) Labeling with the general marker anti-KLH reveals the entire OSN afferent innervation to the dorsal olfactory bulbs. (**A$_3$**, **B$_3$**) Anti calretinin and (**B$_2$**) anti G$_{\alpha\ s/olf}$ antibodies label only the dorsal (dG) and dorsolateral (dlG) but not the mediodorsal (mdG) glomeruli. Some individual glomeruli label with one antibody but not another, as indicated (e.g., dcaG in **B**). Scale bars in **A$_3$** and **B$_3$** apply to all panels in each column.

Figure 15. Overviews of the Dorsal Olfactory Bulb Surface Labeled With Different Antibody Combinations

110

Figure 16. Overviews of the ventral olfactory bulb surface labeled with different antibody combinations. Tissue is the same as shown in Figure 15, but was rotated. (**A₂**) Labeling with the general marker anti-KLH reveals the entire OSN afferent innervation to the ventral olfactory bulbs. (**A₃**, **B₃**) Anti calretinin labeled ventromedial (vmG) but not ventral glomeruli (vG arrowheads in **B₃**), as well as the lateral ventroposterior glomerulus (lvpG in **A₃**). (**B₂**) $G_{\alpha \text{ s/olf}}$ IR axons innervate the vmG and the vG (arrowheads in **B₂**). Glomerular clusters are traced with dashed lines in **A₁** and **B₁**, and individually identifiable glomeruli are traced with solid lines and numbered throughout the figure plate. Scale bars in **A₃** and **B₃** apply to all panels in each column.
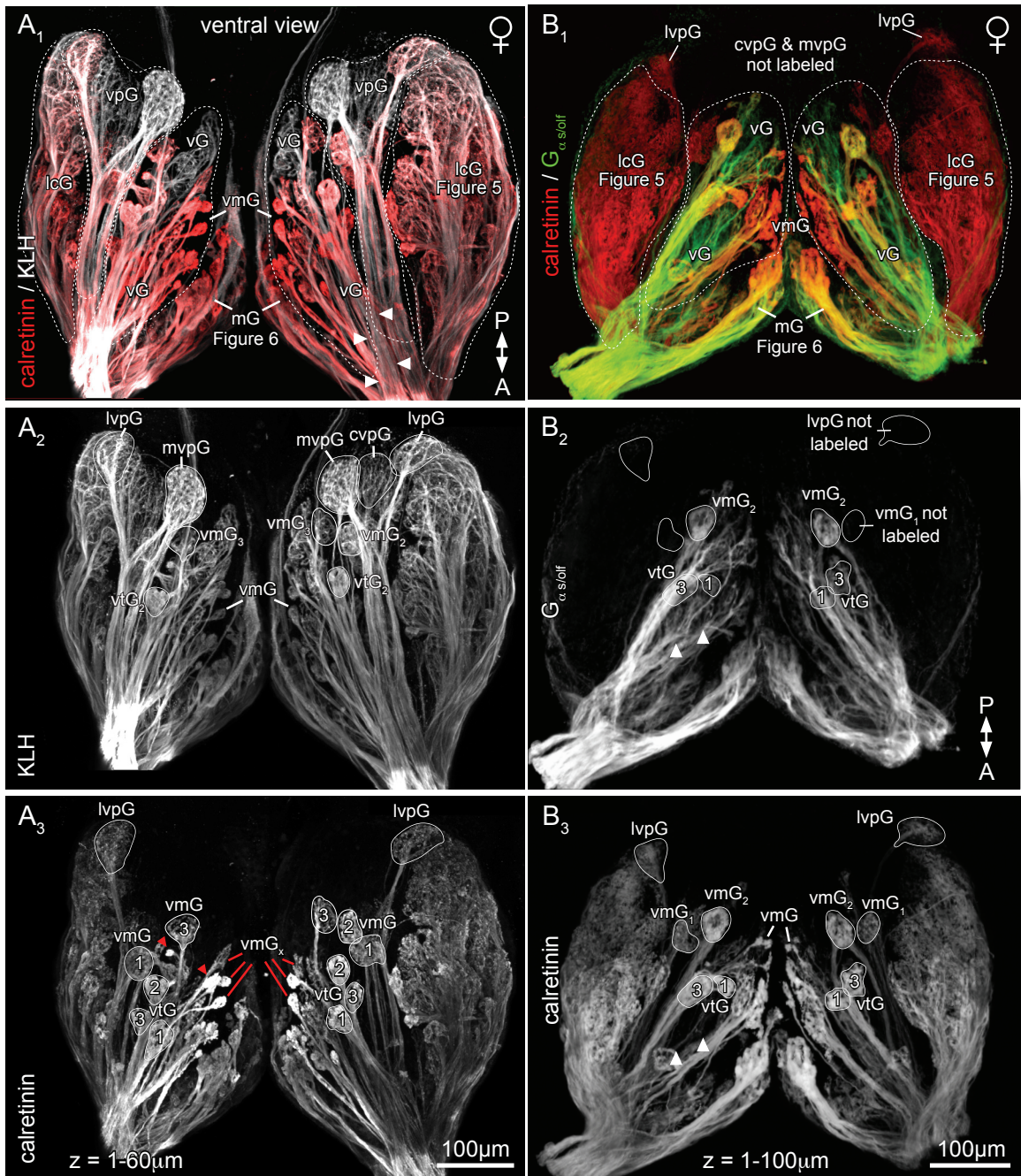
Figure 16. Overviews of the Ventral Olfactory Bulb Surface Labeled with Different Antibody Combinations

Figure 17. Overviews of the lateral olfactory bulb surface labeled with different antibody combinations. Tissue is the same as shown in Figures 15 and 16 but was rotated. Most lateral cluster glomeruli (lcG) are innervated by calretinin IR axons (**A₃, B₃**) but are devoid of $G_{\alpha\ s/olf}$ IR (**B₂**). However, lcG_1, one of the largest glomeruli in this cluster, is innervated by $G_{\alpha\ s/olf}$ IR (**B₂**), but not calretinin IR axons (indicated in **B₃**). Much of the lateral olfactory bulb surface was devoid of glomeruli and instead consisted of a diffuse aggregate of OSN axons. We refer to this region as lateral plexus (LP). Glomerular clusters are traced with dashed lines in **A₁** and **B₁**, and individually identifiable glomeruli are traced with solid lines and numbered throughout the figure plate. Scale bars apply to all panels within each column.

Figure 17. Overviews of the Lateral Olfactory Bulb Surface Labeled With Different Antibody Combinations

114

Figure 18. Overviews of the medial olfactory bulb surface labeled with different antibody combinations. The tissue is the same as shown in Figures 15 through 17 but was rotated. The medial glomeruli (mG) are small and variably innervated by calretinin IR and $G_{\alpha \, s/olf}$ IR axons (see arrowheads in **B₂** and **B₃**). The medial elongated glomerulus (meG) was visible in nearly all specimens examined. This glomerulus labeled with the anti KLH antibody (**A₂**), but did not label with anti calretinin or anti $G_{\alpha \, s/olf}$ antibodies (**A₃**, **B₂**, **B₃**). Also visible are the mediodorsal glomeruli, which label only with the anti KLH antibody (mdG in **A₂**). Glomerular clusters are traced with dashed lines in **A₁** and **B₁**, and individually identifiable glomeruli are traced with solid lines and numbered throughout the plate. Scale bars in each column apply to all panels.
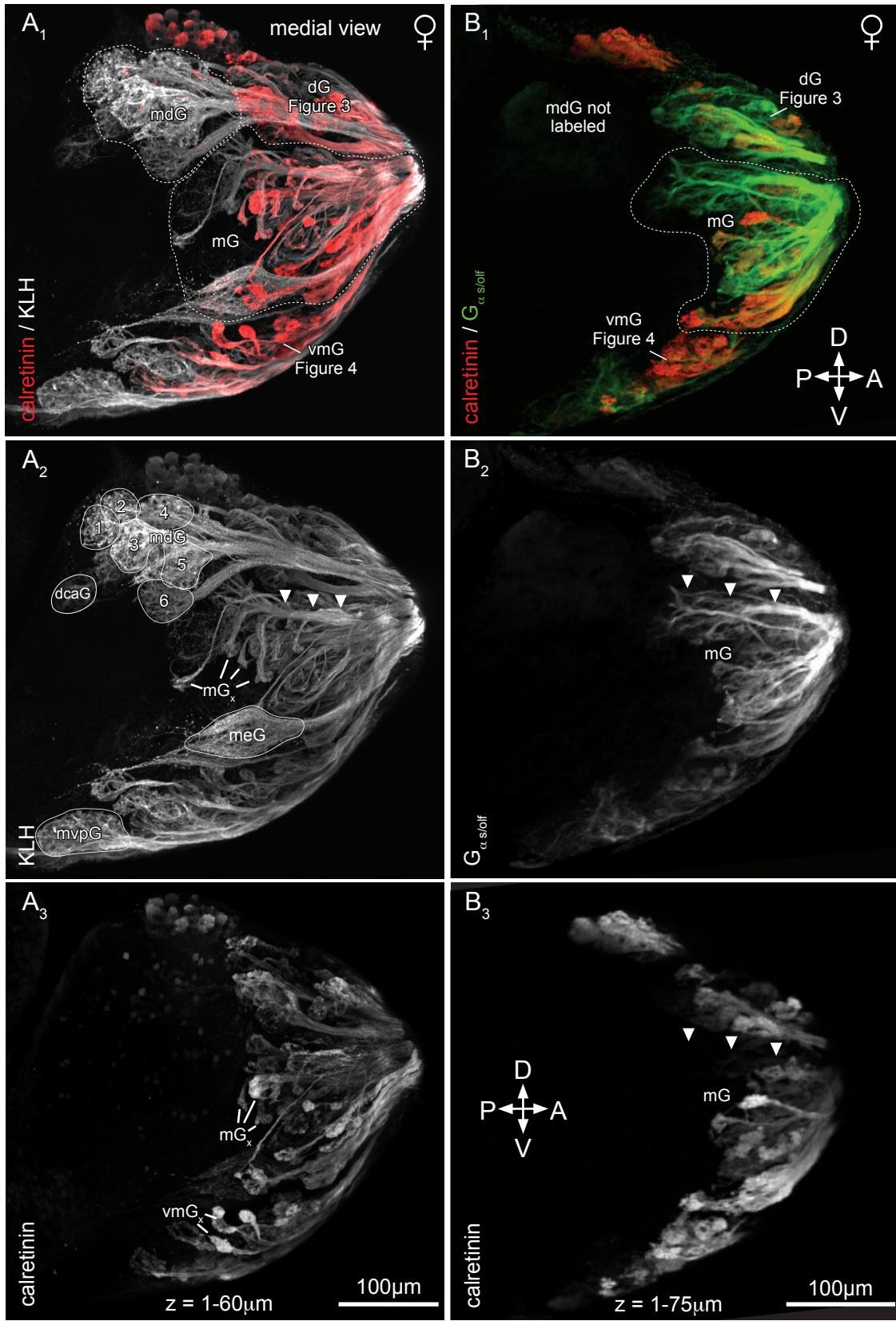
Figure 18. Overviews of the Medial Olfactory Bulb Surface Labeled With Different Antibody Combinations

116

Figure 19. (**A**, **B**) Specific innervation of mediodorsal glomeruli (mdG) by S_{100} IR and $G_{\alpha o}$ IR axons. The innervation to these glomeruli appeared to originate from multiple areas in the olfactory epithelium and we routinely observed S_{100} IR and $G_{\alpha o}$ IR axons to arrive at these glomeruli via different routes (arrowheads in **A**). Glomerular clusters are traced with dashed lines, and individual mdG tracings were omitted for clarity.
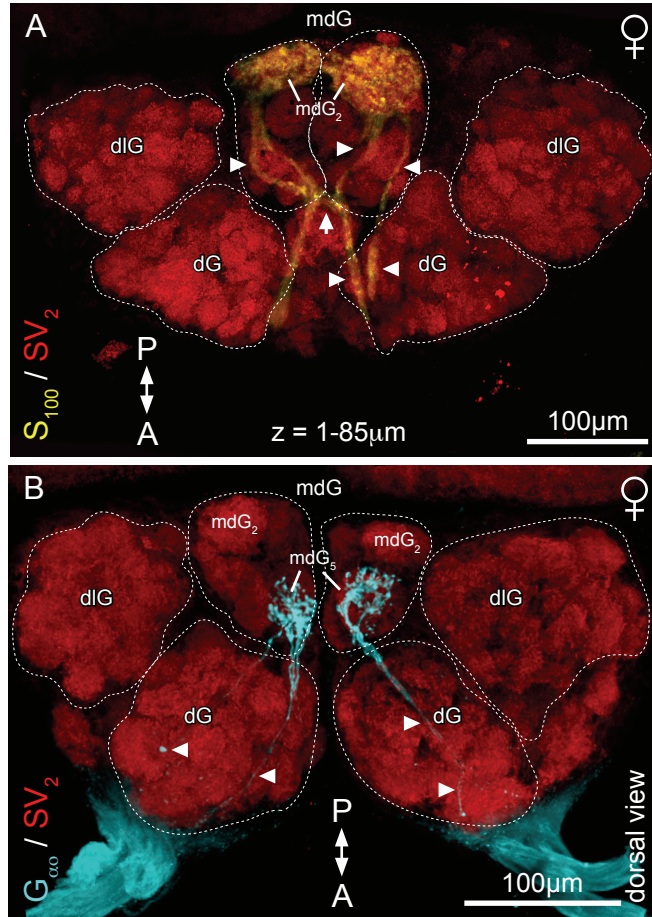
Figure 19. Specific Innervation of Mediodorsal Glomeruli (mdG) by S_{100} IR and $G_{\alpha o}$ IR Axons

Figure 20. Individually identifiable and indistinguishable glomeruli on the dorsal olfactory bulb surface. **B-D** are stepwise projections of 10-20 serial, 1μm thick optical sections. The outlines of glomeruli are traced with solid (white) and dashed (red) lines to indicate individually identifiable and indistinguishable glomeruli, respectively. (**B**) The dorsolateral (dlG) are indistinguishable from one another (traced only on one side for clarity). The dorsal glomeruli (dG) are anatomically diverse and vary in shapes and sizes (compare arrows in **B** to arrowheads in **C**). (**D**) The dorsal cluster associated glomeruli (dcaG) were sometimes arranged in a row of 5 units (see dcaG$_{1-5}$ on the right side of **D**), but were often located within a diffuse neuropil that was faintly labeled (see dcaG on the left side of **D**). Scale bar in **D** applies to all panels.
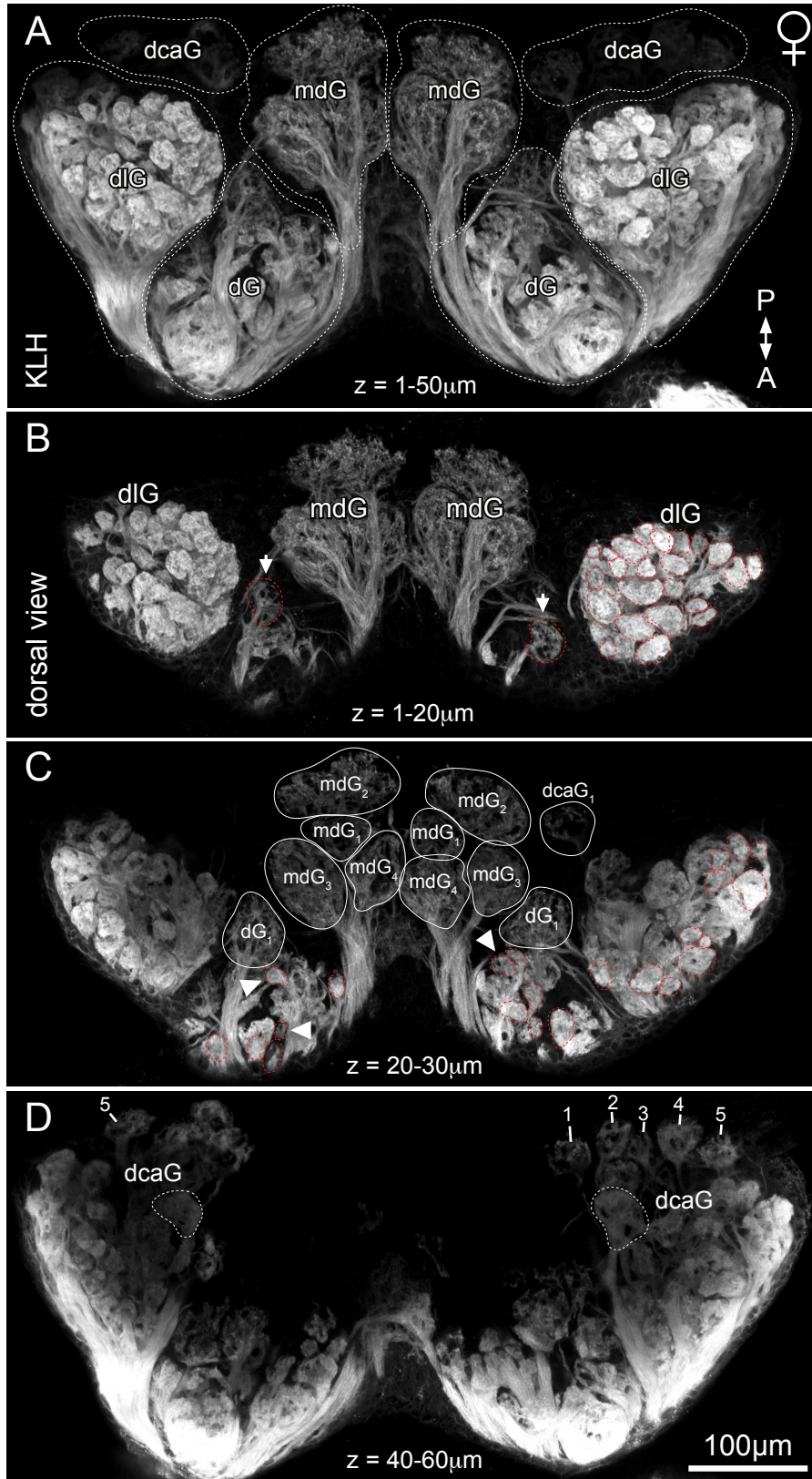
Figure 20. Individually Identifiable and Indistinguishable Glomeruli on the
Dorsal Olfactory Bulb Surface

120

Figure 21. Individually identifiable glomeruli in the lateral olfactory bulbs. **B-D** are stepwise projections of 2-6 serial optical sections (1μm thick) from the whole-mounted tissue obtained from laterally mounted specimens. The lateral cluster contained some of the largest and most stereotypic units in the olfactory bulb ($lcG_{1,3,4}$) in addition to variably sized lcG_x (dashed outlines). The lateral plexus (LP) was diffusely innervated and appeared to be devoid of glomeruli proper. Scale bar in **D** applies to all panels.
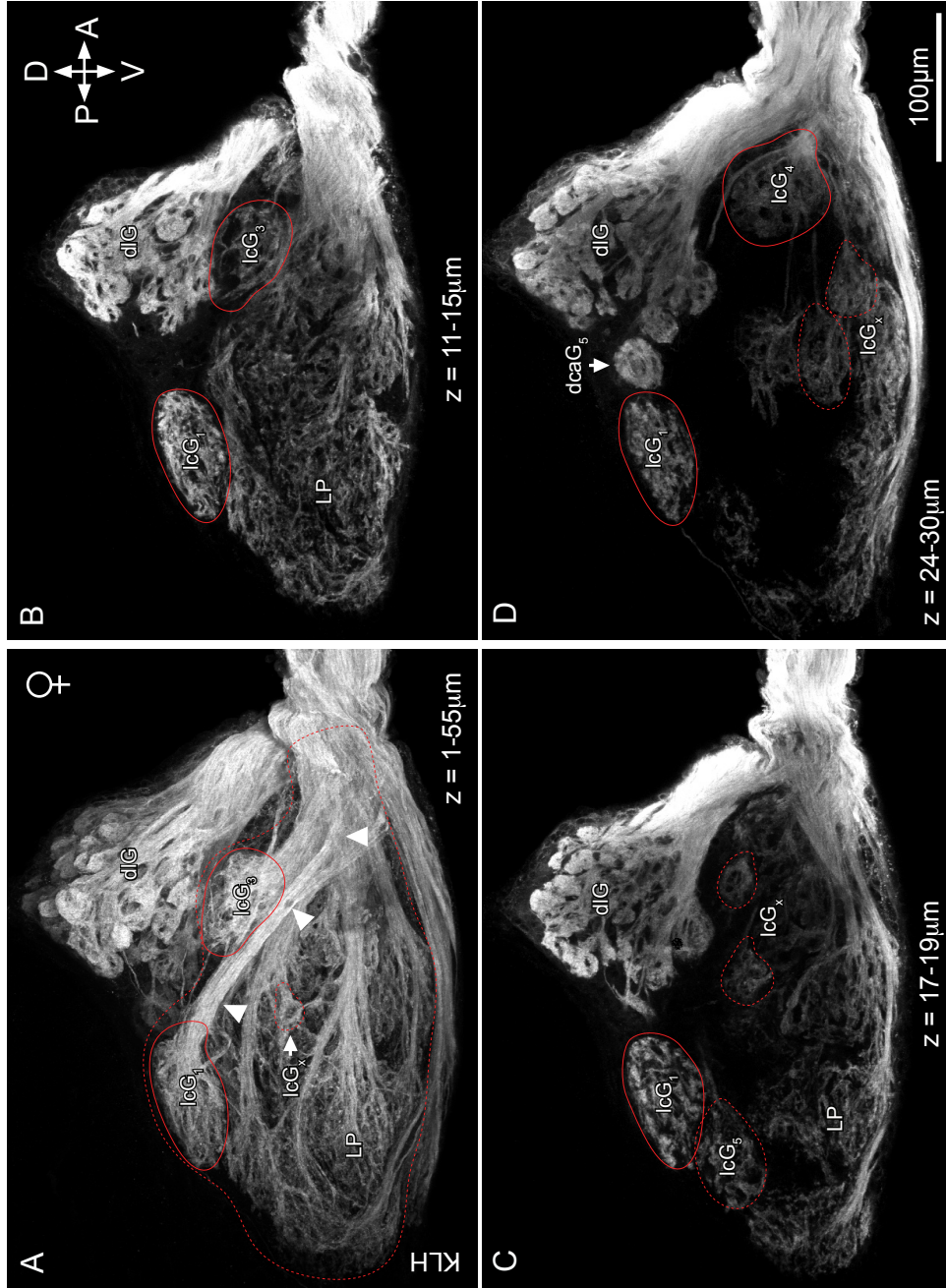
Figure 21. Individually Identifiable Glomeruli in the Lateral Olfactory Bulbs

Figure 22. Distinct labeling of ventral glomeruli with antibodies against calretinin and $G_{\alpha \, s/olf}$. **B-C** are stepwise projections of 9-14 serial optical sections (1μm thick) from the whole-mounted tissue. Glomeruli in the ventral olfactory bulbs are diverse, consisting of the small ventromedial glomeruli (see bright red vmG in **A**) and also several ventral glomeruli (vG_x) that were innervated only by $G_{\alpha \, s/olf}$ IR axons. These vG_x were located beneath the axon bundles that traverse the ventral olfactory bulb surface (**B-C**). Other identifiable glomeruli are also labeled in **A**. Scale bar in **C** applies to all panels.
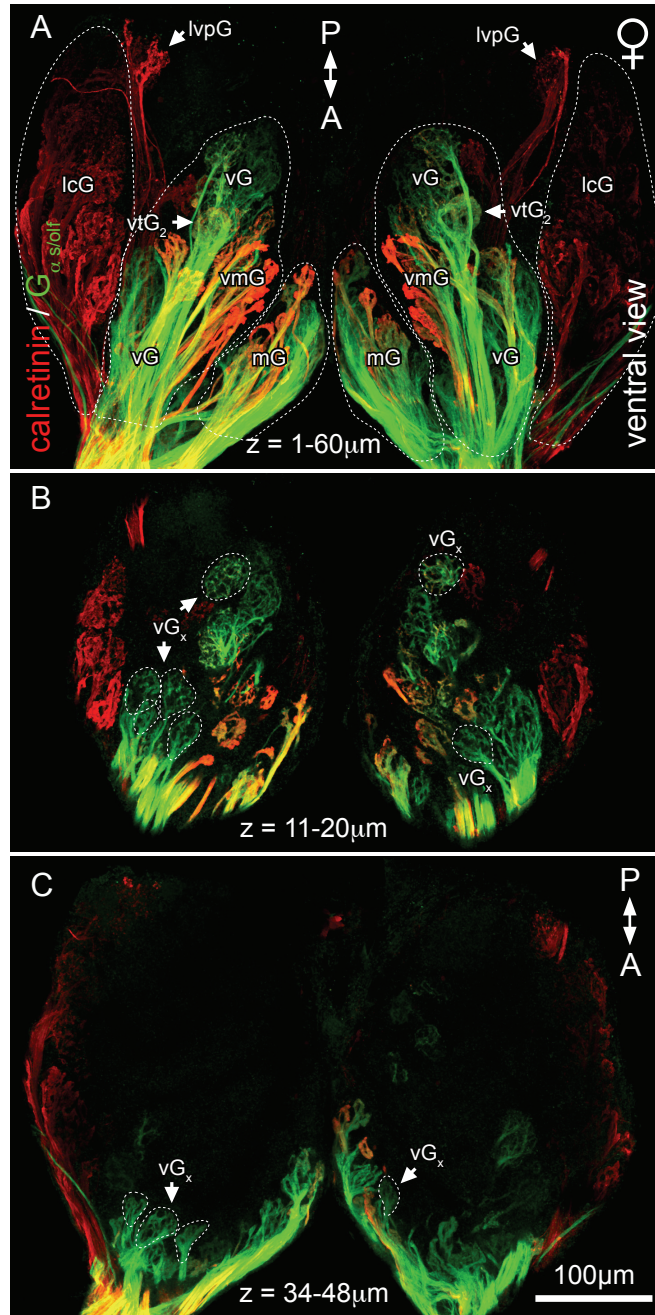
Figure 22. Distinct Labeling of Ventral Glomeruli With Antibodies Against Calretinin and $G_{\alpha\,s/olf}$

Supplemental Figure 1. Labeling of OSN axons and tastebuds with anti $G_{\alpha\ i\text{-}3}$ and anti $G_{\alpha/q11}$ antibodies. (**A, B**) The $G_{\alpha\ i\text{-}3}$ antibody diffusely labeled the innervation to almost all glomeruli. Shown are whole-mounted olfactory bulbs of a juvenile, circa 50-day old zebrafish, from their ventral (**A**) and dorsal sides (**B**). Glomeruli are partitioned into several anatomically distinct regions (dashed outlines, discussed in results). Almost all of these regions are targeted by $G_{\alpha\ i\text{-}3}$ IR fibers, except for fibers innervating the mediodorsal glomeruli (mdG in **B**). We did not pursue these findings further, because the $G_{\alpha\ i\text{-}3}$ antibody produced labeling in only a fraction of specimens and inconsistently labeled tissue if fixation and other treatments were slightly varied. (**C**) The $G_{\alpha\ q11}$ antibody labeled tastebuds (arrowheads) on the lips, skin and barbels. Shown in **C** are the lips of a 20-day old whole-mounted zebrafish viewed from the dorsal side. The tissue was counterstained with anti-SV_2, which labels a small punctate region in the basal membrane of the taste receptor cells. The reference bar (anterior and posterior) on the bottom left is valid for all images and the scale bar in **B** also applies to **A**.
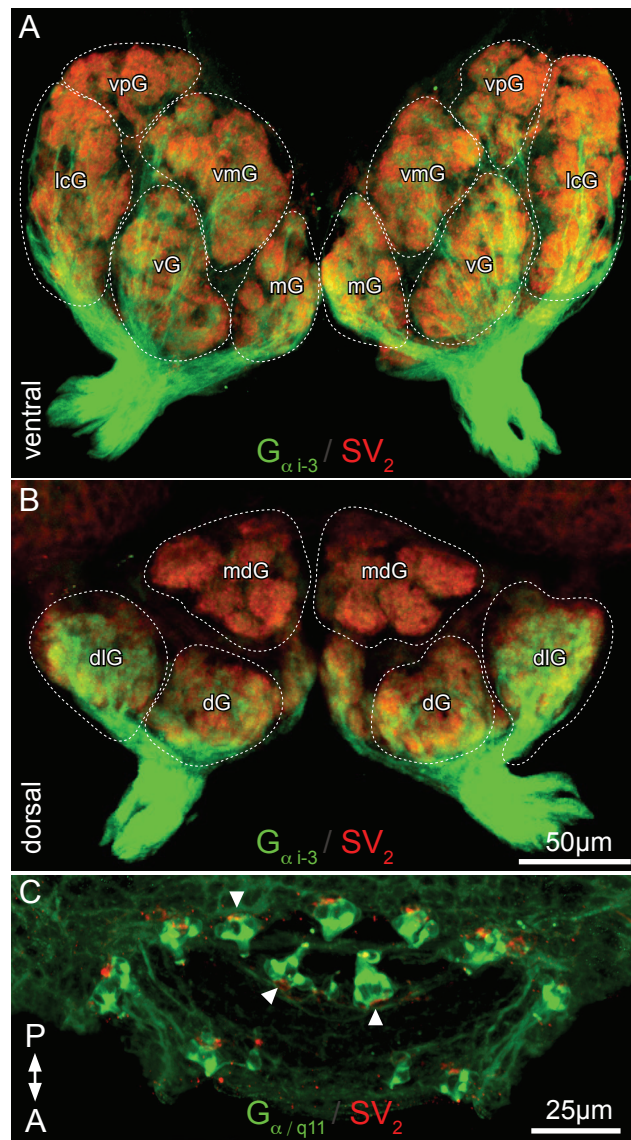
Figure S1. Labeling of OSN Axons and Tastebuds With Anti $G_{\alpha i\text{-}3}$ and Anti $G_{\alpha / q11}$ Antibodies

Chapter 4

Organization of Pre- and Postsynaptic Compartments
of Zebrafish Olfactory Glomeruli

4.1 Summary

The olfactory bulbs of zebrafish contain approximately 140 glomeruli, which are spheroidal synaptic aggregates that organize and relay the odor code originating from sensorineural transduction by thousands of olfactory sensory neurons (OSNs). Glomeruli involved in processing different types of olfactory information apparently differ in anatomy and function, but no such differences have been examined in detail in the zebrafish. In the present study we examined the organization of the pre- and postsynaptic glomerular compartments of different-sized glomeruli in the zebrafish olfactory system. We found large glomeruli that were innervated either by one or multiple OSN axon bundles while their postsynaptic compartments were innervated either by uniglomerular mitral cells (MCs) and / or multiglomerular MCs, innervating one or several glomeruli, respectively. Medium-sized glomeruli were each innervated by one visible OSN axon bundle and postsynaptically by dendrites from uniglomerular MCs; these glomeruli were furthermore interconnected by a diffuse network of interneurons. Small glomeruli were all separately innervated by distinct OSN axon bundles, but their postsynaptic compartments almost always consisted of dendrites from multiglomeruar MCs. Finally, we examined the detailed anatomy of microglomeruli in the lateral and dorsal nerve plexus. Presynaptically, microglomeruli consisted of only a few OSN axon terminals and these made synaptic contacts with extensively branching MC dendrites. Our data confirm that there exist wiring differences among differently sized glomeruli in zebrafish.

4.2 Introduction

Animals are confronted by a vast array of odors that carry information about habitat, food, conspecifics and predation. These different types of olfactory information are processed in anatomically distinct olfactory pathways, which project to different regions of the brain (Dulac and Wagner, 2006, Tohuhara and Vosshall, 2009). In mammals, general odorants (e.g., food odors) are transduced into neural information in the main olfactory epithelium by millions of olfactory sensory neurons (OSNs), each of which expresses only one of approximately 1200 (mice) available odorant receptor (OR) types (Serizawa et al., 2004, Buck, 2004, Buck and Axel, 1991). Each OSN projects a single axon to the main olfactory bulb (MOB) where it fasciculates with axons of the same type, selectively innervating a small number of MOB glomeruli (Sakano, 2010). Each mammalian glomerulus is in turn innervated by the axons of a single, or at most a few OSN types (Mombaerts, 2006). Glomerular output is conveyed by mitral cells (MCs) that have only a single apical dendrite that arborizes entirely within a single glomerulus (Shepherd, 1972, Kishi et al., 1982, Dhawale et al., 2010); feedforward and feedback synaptic modulation between secondary dendrites of adjacent MCs and local interneurons shape this output by mechanisms not fully understood (Wilson, 2008, Wachowiak and Shipley, 2006, Spors and Grinvald, 2002, Laurent et al., 2001, Friedrich and Laurent, 2001, Friedrich, 2006). Each MOB glomerulus may thus be regarded as a discrete and narrowly tuned sensory channel that processes information about individual components of chemical mixtures that constitute odors.

In contrast, pheromones are transduced by an unrelated set of odorant receptors in a completely different region in the nasal cavity, the vomeronasal organ (for review, see Dulac, 2000), and OSNs from this organ project axons to glomeruli in the accessory olfactory bulb (AOB). AOB glomeruli differ from those in the MOB in that they are much smaller and only diffusely organized structures (Meisami and Bhatnagar, 1998), and significantly, in that they can receive input from as many as 10-20 different OSN types at once (Belluscio et al., 1999, see also Rodriguez et al., 1999). Furthermore, the output of AOB glomeruli differs from that of MOB glomeruli, with MCs in the AOB possessing extensive dendritic arbors that may innervate multiple glomeruli at once (Takami and Graziadei, 1991, Takami and Graziadei, 1990, Meisami and Bhatnagar, 1998, Jia et al., 1999). AOB glomeruli may thus have a capacity to integrate incoming information from molecular components that comprise pheromonal signals.

The olfactory glomeruli of zebrafish are anatomically and functionally similar to their mammalian counterparts, but they are significantly fewer in number. There are only ~ 140 glomeruli in each zebrafish olfactory bulb (in contrast to ~1800 in mice, Mombaerts, 2006) and about 20% of these are individually identifiable (Chapter 3). However, unlike in most mammals, the zebrafish olfactory system is not divided into separate MOB and AOB components, and glomeruli involved in the processing of food odors, non-pheromonal social odors and pheromones are all arranged in closely apposed regions in the small and compact olfactory bulbs. For example, amino acids, which signal the availability of food, activate glomeruli in the lateral olfactory bulbs, and bile acids, which are involved in habitat and conspecific recognition, the medial glomeruli (Friedrich

130

and Korsching, 1998, Friedrich and Korsching, 1997).

Zebrafish olfactory glomeruli may be further discriminated from one another based on their size. Most glomeruli have diameters ranging from 10 to 70 micrometers; most of these glomeruli are innervated by the axons of ciliated OSNs and are tightly packed in certain regions of the olfactory bulbs. Due to variations in their numbers and morphology, these glomeruli are indistinguishable from one another (Chapter 3). In contrast, about 20% of glomeruli are larger than 70μm in diameter and are scattered throughout different regions of the olfactory bulbs. These glomeruli are highly stereotypic in their numbers and appearance, and at least two of them are targeted by axons of crypt sensory neurons, which appear to be involved in pheromonal processing (Hamdani et al., 2008, Hamdani and Døving, 2007). Based on these observations it is plausible that small and large glomeruli constitute separate olfactory pathways.

In the present study, we examined the anatomical organization of pre- and postsynaptic compartments of different-sized zebrafish glomeruli and determined that these glomeruli are distinctly wired. Most large glomeruli were innervated by multiple OSN axon bundles that converged onto dendrites of uniglomerular MCs, but a few large units were innervated by single OSN axon bundles that innervated the dendrites of uniglomerular and / or multiglomerular MCs. Small glomeruli were never targeted by more than one OSN bundle, and the postsynaptic compartment of these units almost always contained dendrites from multiglomerular MCs. We discuss the significance of these findings in view of known and hypothesized functions of individual glomeruli.

4.3 Methods

4.3.1 Animals

Zebrafish (AB strain, University of Oregon) were maintained at Dalhousie University according to standard guidelines (Nüsslein-Volhard and Dahm, 2002). Briefly, the fish were kept at 27.5^{o}C on a 12:12 hour light-dark schedule in 10L holding tanks (Aquatic Habitats, Apopka, FL, USA) that were continuously supplied with a drip of dechlorinated fresh water, filtered through a series of biofilters and a charcoal filter. The fish were fed several times daily with staple fish food (Omega Sea, Sitka, Alaska, USA) and live Artemia (Salt Creek, Salt Lake City, Utah, USA). Zebrafish used for experiments were all adults and 2-3cm in length. Experiments were conducted according to procedures outlined in the guide to the care and use of laboratory animals, established by the Canadian Council for Animal Care.

4.3.2 Tissue preparation

Zebrafish were killed by immersion in cold water ($< 4^{o}$C) for ~ 1 minute (Wilson et al., 2009) and decapitated. The skull caps were then removed to expose the brains, and heads were fixed by immersion in fresh 2% paraformaldehyde (PFA; Electron Microscopy Sciences, Hartfield, PA, USA) in phosphate buffered saline (PBS: 100mM Na_2HPO_4, 140mM NaCl, pH 7.4) for 6 hours (PFA) at room temperature, or overnight at 4°C. The tissue was next washed five times over 2 hours in PBS before further dissecting the heads to isolate the brains. These were then placed in a PBS-based blocking solution containing 0.25% Triton X-100, 2% dimethyl sulfoxide, 1% bovine serum albumin and 1% normal goat serum (PBS-T; all reagents from Sigma) for $\geq$ 12 hours at 4°C. Unless noted otherwise, PBS-T was used for all subsequent wash steps, each of which consisted

of at least five rinses over a period of ~ 4 hours.

4.3.3 Antibody Characterization

We used a variety of antibodies to label cellular structures associated with glomeruli (Figure 23 and Table 3). An antibody against keyhole limpet hemocyanin (KLH; Table 3) has been used previously in zebrafish and trout as a reliable, but non-specific marker for a currently unknown molecule in or on OSN axons (Fuller et al., 2005; Riddle and Oakley, 1992). To label synaptic elements in the core of glomeruli (Figure 23), we used anti-synaptic vesicle protein 2 (SV_2; Table 3), which has been used previously for this purpose in zebrafish (Koide et al., 2009). We also used anti tyrosine hydroxylase (TH; Table 3) to label juxtaglomerular interneurons and their innervation of glomeruli, as was previously demonstrated in zebrafish (Fuller et al., 2005). Finally, we employed anti-calretinin (Table 3), which correctly recognizes a 28-29 kDA protein in zebrafish (Castro et al., 2006; Germana et al., 2007), to label OSN axons in certain regions of the olfactory bulbs.

The labeling that we achieved with each antibody was highly consistent with previous reports (see results) and we did not conduct further control experiments. To control for non-specific staining from our secondary antibodies, we processed brains without incubation in primary antibodies. None of the specimens exhibited detectable fluorescence.

4.3.4 Immunohistochemistry and Mounting

Brains were incubated in mixtures of two primary antibodies, diluted 1:50 - 1:200 in PBS-T (Table 3), for 4-7 days at 4°C with gentle agitation. The brains were then washed

in PBS-T and incubated in a mixture of secondary antibodies conjugated to Alexa Fluor dyes (1:50 in PBS-T; Invitrogen, Burlington, ON, Canada), for 4-5 days at 4°C.

Prior to mounting, all brains were washed three times in PBS containing 0.25% Triton and then three times in PBS. The brains were then immersed in a 3:1 solution of glycerol to 0.1M Tris buffer (pH 8.0) containing 2% n-propyl gallate (all from Sigma) for a minimum of 24 hours for clearing. The tissue was then whole-mounted in fresh glycerol between coverslips separated with stacks of coverslip fragments (to minimize tissue compression) and then sealed with nail polish.

4.3.5 Axon Tracing

To study the organization of MC dendrites in the postsynaptic compartment of glomeruli, we labeled MCs and OSN axons via combined retrograde and anterograde tracing with lipophilic axon tracers. Fish were killed and heads were fixed in 4% PFA overnight at 4°C. After several rinses in PBS, overlying tissues were removed to expose the olfactory epithelia and ventral telencephalon. Using a razor blade, we next made a small incision on the ventral surface of the caudal telencephalon, perpendicular to the lateral and medial olfactory tracts that contain MC axons. With a glass pipette pulled to a fine tip, we then placed crystaline 1,1'-dioctadecyl-3,3,3',3'-tetramethylindocarbocyanine (DiI; Invitrogen) into this cut, removing any misplaced or excess crystals with a filter paper. To label the OSN axons, we dipped the tips of fine forceps into a drop of 1,1'-dioctadecyl-3,3,3',3'-tetramethylindodicarbocyanine perchlorate solution (DiD 5mg / 5mL in dimethyl formamide; Invitrogen), and then gently squeezed the olfactory nerve with the stained forceps to apply the dye.

Specimens were then transferred to PBS containing 0.5% PFA and stored in a dark chamber at 37°C. Under these conditions, the tracers spread into the olfactory bulbs within 48 hours. After this incubation, any non-neural tissue was removed and the isolated brains were mounted on a coverslip in a drop of PBS, because preliminary experiments revealed that DiI spread into surrounding tissue in specimens that were mounted in glycerol-based media. Brains were carefully arranged with forceps (i.e., ventral or dorsal side facing the slide), coverslipped and then sealed with nail polish.

4.3.6 Identification of Mitral Cells in Axon Tracing Experiments

Application of lipophilic tracers into the medial and / or lateral olfactory tracts led to labeling of the MCs, along with other types of glomerular output neurons and the terminal nerve. We focused specifically on the glomerular innervation by MCs, which we defined as cells with soma diameters ranging from 8-13μm (Fuller et al., 2006) and dendritic projections that overlap with OSN terminals within a glomerulus. We could easily distinguish somata associated with the nervus terminalis (NT) from MCs, because the NT somata were much larger (22 ± 3μm diameter in n = 4 fish) and clustered in a characteristic location near the olfactory nerve (see also, Edwards et al., 2007). Ruffed cells differ from bulbar output neurons in that they have a large and characteristic 'ruff' at the initial segment of the axon (Fuller and Byrd, 2005, Arevalo et al., 1991, Alonso et al., 1987) and, unlike MCs, the dendrites of ruffed cells are not targeted by OSN axons (Kosaka and Hama, 1979, Fuller and Byrd, 2005). Tufted cells are another type of glomerular output neuron that appear to have smaller somata than MCs and appear to be located in superficial layers of the olfactory bulbs that normally do not contain MCs (hamster: Macrides and Schneider, 1982). We thus excluded from our analysis cells that

were smaller than 8μm in diameter and located in superficial layers of the olfactory bulb (~1-15μm; depending on the diameter of the glomerulus). Finally, local interneurons do not project axons outside of the olfactory bulbs and we thus assume that they were not labeled by our dye applications (in the telencephalon).

4.3.7 Microscopy and Image Processing

Specimens were viewed with a LSM 510 META laser scanning confocal microscope (Carl Zeiss Inc., Thornwood, NY, USA). To achieve optimal visualization of glomeruli, we repositioned and remounted the specimens to permit imaging from different viewing planes (i.e., ventral, dorsal and lateral). Images presented in this report are projections of optical sections, collected at 1μm intervals, to a depth indicated in each figure (maximum depth of 100μm). Projections were created with ImageJ (http://rsb.info.nih.gov/ij) and images were adjusted for brightness and contrast in Photoshop and assembled into plates in InDesign. Diagrams were created with Illustrator (all from Adobe Systems Inc., San Jose, CA, USA).

4.3.8 Data Acquisition and Analysis

We viewed and analyzed our data as described in Chapter 3. Briefly, glomeruli were defined as ovoid to spheroidal structures that were targeted and encircled by axons connected to the olfactory nerve. Measurements for individual glomeruli were obtained by tracing the outlines of individual units in single optical sections showing their maximum diameter. Throughout this manuscript we provide the cross-sectional area and the Feret diameter as measures for the approximate size of glomeruli and associated cell types. The Feret diameter represents the longest distance between any two points along the traced outline of glomeruli (i.e., maximum diameter) and is standard measurement

option in ImageJ. We also determined the numbers of MCs associated with glomeruli by tracing their processes from the soma into the core of glomeruli during step-by-step analyses of optical sections. Relevant MCs were counted and measured by tracing their somata with the ImageJ freehand tracing tool. Anatomical data describing the numbers and sizes of glomeruli were obtained from different tissue samples as those used to describe MC numbers, sizes and their associations with glomeruli. This is because most of the measurements for the presynaptic anatomical features were obtained from immunohistochemistry experiments, which were incompatible with axon tracing experiments.

For statistical comparisons, numbers and sizes of glomeruli were pooled across animals and according to size, where large glomeruli were all units with diameters from 70-100μm, medium-sized glomeruli those with diameters from 35-55μm and small glomeruli with diameters ranging from 20-30μm. To determine if differently sized glomeruli were innervated by different numbers of MCs, we compared pooled anatomical data from multiple animals (above) through a one-way analyses of variance (ANOVA). Similarly, comparisons between the diameters of certain types of glomeruli and related neural elements (e.g., their postsynaptic compartment) were also compared via a one-way ANOVA. All statistics were analyzed with SPSS software (Chicago, IL, USA).

4.4 Results

4.4.1 Organization of the Presynaptic Glomerular Compartment

Axonal innervation of the zebrafish olfactory bulbs was compartmentalized in eight anatomically distinct regions, which we refer to as glomerular clusters (Figure 24). Each glomerular cluster was individually identifiable based on its selective innervation by discrete OSN axon bundles, such as the axons that innervated the medial glomeruli (mG; arrowheads in Figure 24A$_1$) or the dorsolateral glomeruli (arrowheads in Figure 24B$_1$). Furthermore, presynaptic elements of individual glomerular clusters were physically separated from one another, which was evident in tissue that was counterstained with an antibody against the synaptic vesicle protein 2 (SV$_2$; see dim border between dG, dlG and mdG in Figure 24B$_2$). The layout of these clusters is summarized in Figures 24A$_4$ and 2B$_4$. We will next discuss details about the innervation and presynaptic neuropil of different-sized glomeruli within these clusters.

4.4.2 Patterns of OSN innervation

Large Glomeruli

Based on the criteria that a glomerulus had to be roughly spherical and innervated by axons from the olfactory nerve, we identified a range of differently sized glomeruli (see also Chapter 3). Large glomeruli (diameter $\sim$ 70-100μm; area $\sim$ 2500-4800μm^2; see Table 4), such as the medial ventroposterior glomerulus (mvpG in Figure 24A$_{1-3}$), were consistently identifiable in stereotypic locations throughout the olfactory bulbs, as individuals or small clusters. The mvpG, in particular, was easily recognized in the ventral olfactory bulbs as a bilaterally symmetric unit that was completely encased by a meshwork of KLH LIR fibers (Figures 25A$_1$ and 25A$_2$). Importantly, each mvpG was

138

innervated by two or more anatomically separate OSN axon bundles that were clearly distinct from one another and only converged at the glomerulus (arrows in Figures $25A_1$ and $25A_2$). Another large unit, the lateral cluster glomerulus 1 (lcG_1) was located in a completely different region of the olfactory bulb, but was similarly innervated by multiple axon bundles that appeared to originate from different regions of the olfactory nerve; several small axon bundles emerged from the lateral olfactory nerve (arrowheads in Figure 25B) while another one originated in the dorsolateral olfactory nerve (arrows in Figure 25B).

Not all large glomeruli were, however, innervated by multiple axon bundles. The lcG_4, which was located in the same cluster as lcG_1 (Figure 25C), was innervated by a *single* thick axon bundle (arrowhead in Figure 25C). These observations, along with data from other large glomeruli, are summarized in Table 4.

Medium-sized Glomeruli

Medium-sized glomeruli, with diameters ranging from 35-55μm (Table 4), were anatomically diverse and located in several areas of the olfactory bulbs, including the dorsal (dG), lateral (lcG), ventral (vG) and ventromedial (vmG) clusters (see Figure 24). Most of these glomeruli were located several micrometers beneath the OSN axons that traverse the olfactory bulb surface and they were thus best seen in optical sections from intermediate depths of the glomerular layer (Figure 26). Most medium-sized glomeruli had varied shapes and appearances and were therefore indistinguishable (see vG_x and vmG_x in Figure 26 and Table 4). However, we could identify the medium-sized ventral triplet (vtG_{1-3}) and ventromedial glomeruli (vmG_{1-3}), which we have previously described (see Chapter 3 and also Baier and Korsching, 1994). Recognizing these glomeruli

139

without specific neurochemical markers (e.g., see Chapter 3) was difficult, and they are thus only partially shown in Figure 26. Overall, however, we did not observe any medium-sized glomeruli that were innervated by more than one axon bundle.

Small Glomeruli

Glomeruli with diameters from 20-30μm were the most abundant (Table 4) and were tightly packed in the dorsolateral glomerular cluster (dlG in Figure 24B$_1$). The dlG were largely indistinguishable from one another (Figures 27A$_1$ and 27$_2$); each dlG was roughly spheroidal and uniformly KLH LIR and appeared to be separately innervated by a single small bundle of OSN axons. These axon bundles were well visible as they defasciculated from one another well before reaching their target glomerulus (e.g., see arrows in Figure 27A$_{1-2}$). None of the dlG were innervated by more than one OSN axon bundle.

The smallest glomeruli (diameter: ~10μm) were located in the medial (mG) and ventromedial (vmG) clusters (see Figure 24A$_1$). These units often labeled only faintly with the KLH antibody and could therefore not be unambiguously identified (see arrowheads in Figure 27B$_1$). To study the anatomy of these units in more detail, we employed an antibody against the calcium binding protein calretinin, a known label for OSN axons that project to the medial and ventromedial regions of the olfactory system (Castro et al., 2006). Anti calretinin labeled several small glomeruli that arose from a common fiber stalk (see arrowheads in Figure 27B$_2$); this stalk defasciculated very close to the glomeruli, which were identifiable as separate aggregates of calretinin IR puncta.

Lateral Plexus

OSN axon innervation of a significant portion of the olfactory bulbs was poorly

organized and terminated in a fibrous neuropil that has previously been described as an aglomerular nerve plexus (Chapter 3; Baier and Korsching, 1994). One representative example, the lateral plexus (LP), occupied the posterolateral surface of each olfactory bulb (Figure 28A, see also Figure 25B). Viewed as a projection of serial optical sections (Figure 28A), the LP indeed resembled a disorganized aggregate of OSN axons, but when we examined partial projections of such data, many axonal terminals were visible. Some of these terminals resembled the vmG described above (arrowheads in Figure 28B) and were indeed similarly sized (diameter = $9.5 \pm 0.7\mu m$; n = 45). However, smaller terminals (diameter = $2.7 \pm 0.2\mu m$; n = 27), which apparently originated from individual axons (arrows in Figure 28C), were much more common and distributed throughout the LP without any visible organization.

Thus, the data presented above demonstrate clear anatomical differences in the axonal innervation of different-sized glomeruli. With the exception of microglomeruli in the lateral plexus, OSN innervation of glomeruli is very well organized, and individual glomeruli are each separately targeted and innervated by a distinct bundle of OSN axons.

4.4.3 Organization of the Glomerular Synaptic Tuft

Large Glomeruli

We next used a monoclonal antibody against the synaptic vesicle protein 2 (SV_2; Table 3) to study the organization of presynaptic terminals of OSNs and juxtaglomerular interneurons (JGCs) in the core of glomeruli (i.e., the area inside GLOM in Figure 23), a compartment we refer to as the glomerular tuft. In large glomeruli, SV_2 IR puncta were abundant and tightly packed in the glomerular tuft (see mdG_6 in Figure 29A$_2$); SV_2 IR puncta were delimited by a border devoid of labeling, indicating that the presynaptic

compartments of large glomeruli were isolated from their surroundings.

Because anti-SV_2 labels both the terminals of OSN axons and the terminals of JGC processes (Figure S2), we also examined the JGC innervation of glomeruli, by staining olfactory bulbs with anti-TH (Table 3). Large glomeruli like the vpG (e.g., Figure $24A_1$) contained TH IR puncta that were surrounded by an area of very little labeling (Figure $29B_1$), suggesting that there is little overlap between the JGC innervation of the vpG and surrounding units. Indeed, many of the TH IR puncta in the vpG tuft appeared to originate from JGCs with short, unbranched processes that were closely apposed to and appeared to exclusively innervate the vpG (arrowheads in Figure $29B_{1-2}$ and 29C), but not other adjacent units.

Interestingly, some large glomeruli were nearly devoid of TH IR puncta. The glomerular tuft of the mvpG, for example, always contained visibly fewer TH IR puncta than the vpG, even though the mvpG was similarly sized and directly adjacent (compare mvpG and vpG in Figure $S3A_1$). Similarly, the lcG_1 appeared to be almost devoid of TH IR, while the tufts of the nearby $lcG_{2,3}$ were strongly TH IR (Figure $S3C_1$).

Small Glomeruli and Medium-Sized Glomeurli

The glomerular tufts of medium-sized glomeruli (not shown) and small units like the dlG also labeled strongly with the SV_2 antibody, and SV_2 IR resembled spheroidal glomerular tufts that were separated from one another by borders of weaker labeling (see arrows in Figure $30A_2$). In contrast to large glomeruli (above), borders between individual tufts we not devoid of labeling, but instead stained, although weaker than the tufts, with the SV_2 antibody. This suggests either the OSN afferent input or interneuron innervation overlaps between adjacent dlG.

In anti-TH labeled tissue, the dlG indeed appeared to be very diffuse and we could not identify discrete glomerular tufts (compare Figure 30A$_2$ with 30B$_2$). This diffuse JGC innervation appeared to originate from JGC with long processes that branched multiple times and innervated overlapping regions that were approximately 40μm in diameter (see 'multiple dlG' in Figure 31A). The average diameter of dlG axon innervation is only ~ 20μm (Table 4) and it thus appears that the axon input of these glomeruli converges onto an interconnected network of JGC.

Dorsal Plexus

The dorsal plexus, which was located among glomeruli in the dorsal cluster (dG in Figure 24B$_3$), contained several well-organized aggregates of synaptic terminals (see arrowheads in Figure 32A$_2$). However, the axonal innervation to the dorsal plexus was very diffuse, and did not resemble glomeruli as we describe them above, therefore suggesting that this region may contain glomeruli that are not detectable based on their OSN innervation alone. In contrast to well-organized SV$_2$ IR puncta, JGC-associated TH IR puncta were very diffuse and not organized into spheroidal compartments (Figure 32B$_2$). Thus, as observed in small glomeruli (above), microglomeruli in the dorsal plexus may be interconnected by a shared pool of interneurons and their processes.

To summarize, our data show that the synaptic terminals of OSN axons and JGC processes are well organized in large glomeruli, and apparently do not overlap among these units. In contrast, JGC (but not OSN) innervation of the medium and small glomeruli has a diffuse appearance, suggesting that glomeruli in these regions may be interconnected by the processes of JGC. Finally, both the OSN innervation and JGC innervation of the glomerular plexi appeared to be diffuse.

4.4.4 Organization of the Postsynaptic Glomerular Compartment

Application of lipophilic dyes to the medial and / or lateral olfactory tracts (MOT and LOT) led to varying degrees of MC labeling that permitted us either to determine the coarse organization of the MC network (in heavily labeled specimens as shown in LP in Figure S4C$_1$) or to identify distinct MC types in association with certain glomeruli (in sparsely labeled specimens as shown in lcG on the right side of Figure S4A$_1$). In the following descriptions we refer to MCs that innervated a single glomerulus as uniglomerular MCs, while multiglomerular MCs were those that extended dendrites to more than one glomerulus.

Large Glomeruli

Most large glomeruli were innervated by a dense network of dendrites that originated from several closely apposed, apparently uniglomerular MCs. For example, the mvpG was innervated by 6 - 7 MCs with somata that were approximately 15μm in diameter (see mvpG and MC in Figures 33A$_2$ and 33A$_5$ and Table 4). The MC dendrites within mvpG intermingled tightly and could not be discriminated from one another, but overlapped very well with the area that was encased by the OSN innervation, both in superficial (Figure 33A$_3$) and in deep parts of the glomerulus (Figure 33A$_6$). The border between the dendritic neuropil of mvpG and adjacent unit was delimited by an unlabeled band, suggesting little overlap between dendrites of adjacent ventroposterior glomeruli. Similarly, the postsynaptic compartment of lcG$_3$ contained the dendrites from approximately 6, apparently uniglomerular MCs (see lcG$_3$-associated MCs in Figure 33B$_{2,5}$).

All large glomeruli were innervated by uniglomerular MCs, but we additionally

identified some units that contained dendrites from multiglomerular MCs. Thus, glomeruli in the mediodorsal cluster (mdG in Figure 24B$_1$) were innervated by dendrites from uniglomerular and mutliglomerular MCs. The uniglomerular MCs were, similar to our descriptions above, closely associated with each mdG (see asterisks in Figure 34A$_{1-2}$). In contrast, somata from multiglomerular MCs were each located at a distance from the glomeruli (see MC$_1$ and MC$_2$ in Figure 34A$_{1-2}$). One MC that we frequently saw in association with mdG had a large cell body and two thick dendrites that extended towards separate targets (MC$_1$ in Figure 34B$_1$). Given the diffuse organization of dendrites in this area it was difficult to distinguish the targets of MC$_1$ dendrites, but they appeared to extend towards the mdG$_1$ and the mdG$_3$ (arrowheads in Figure 34B$_2$). Similarly, MC$_2$ (Figure 34C$_1$) projected a thin branching dendrite towards the mdG, and one dendritic branch terminated in the tuft of mdG$_1$ while the other branch targeted mdG$_3$ (arrowheads and tracings in Figure 34C$_{1-2}$). We have summarized our observations on the innervation of large glomeruli by uniglomerular and multiglomerular MCs in Table 4 (see 'MC type').

Medium Glomeruli

Medium-sized glomeruli appeared to be innervated exclusively by uniglomerular MCs, and on average there were fewer MCs associated with each medium glomerulus when compared to large glomeruli (Table 4; $p < 0.05$, ANOVA). For example, between 3-4 MCs innervated the vtG$_2$; these MCs each extended a single dendrite that branched extensively and overlapped fully with the area encased by the axonal innervation of vtG$_2$ (see MC in Figure 35A$_{2-3}$).

The morphology and arrangement of vtG$_2$-associated MCs was remarkably similar

in the olfactory bulbs of different animals, as shown by three representative examples in Figures 35A$_2$, 35B$_2$, 35C$_2$. These cells had similar-sized somata, similar locations and similar orientations, and all appeared to contribute equally extensive dendritic arborizations to the glomerular tuft of vtG$_2$. Other MC also innervated this glomerulus but their locations varied (not visible in Figure 35).

Small Glomeruli

Small glomeruli (see dlG and vmG in Figure 24) were innervated mainly by multiglomerular MCs. In the dlG and vmG, the dendrites of these cells intermingled and formed dense circular aggregates (dashed outlines in Figure 36A$_2$) with diameters of approximately $38 \pm 6\mu m^2$ (n = 7), which is larger than the average diameter of OSN inputs to the dlG (~20μm in Table2; $p < 0.05$) or mG (~15μm in Table 4; $p < 0.001$). Thus, axonal innervation to multiple small glomeruli may converge, at least in part, in the postsynaptic glomerular compartment.

Indeed, in sparsely labeled preparations in both the dlG and mG, we found many MCs with dendrites that branched multiple times and formed small contacts with multiple glomeruli (see vmG$_x$ and associated MC in Figure 36B$_{2-3}$). We analyzed the MC innervation of 49 dlG, and estimate that most dlG are innervated by two multiglomerular MC (see Table 4). In contrast, the smaller vmG are on average innervated by only 0.4 ± 0.3 MC (Table 4). Interestingly, we also observed a small number of uniglomerular MC in the dlG and vmG clusters; these cells often extended dendritic arbors that were larger than the small glomeruli (compare tracings of OSN input and dendrite in Figure 36C$_3$).

Lateral Plexus

The lateral glomerular plexus was innervated by diverse MCs, and we observed

146

cells that resembled uniglomerular MC (MC in Figure 37A$_2$) and multiglomerular MC (MC in Figure 37B$_2$) in this region. The MC type shown in Figure 37B$_2$ was particularly common; these cells had large dendritic arbors that extended up to 100μm from the soma (see traced area in Figure 37B$_2$) and many small OSN axon terminals and varicosities (e.g., microglomeruli described above) thus intermingled and co-localized with the dendrites of such MCs (arrowheads in Figure 37B$_{1,3}$). Occasionally, the MCs in the plexus-like regions appeared to form organized dendritic compartments. An example of such a compartment is depicted in Figure 37C$_2$ (see traced area). Such compartments overlapped either with innervation that resembled glomeruli (arrow Figure 37C$_1$) or multiple small terminals that are characteristic of the lateral plexus (e.g., see Figure 28C).

Thus, the MC innervation of different-sized glomeruli varies. With a few exceptions (mdG), the large and medium-sized glomeruli were innervated by uniglomerular MCs. In contrast, small glomeruli and the diffusely organized axonal terminals in the glomerular plexi were innervated mostly by dendrites from multiglomerular MCs, targeting multiple sensory inputs at once.

4.5 Discussion

The olfactory systems of vertebrates and invertebrates are capable of detecting and discriminating a vast number of odors, and different types of olfactory information appear to be transduced and encoded in anatomically and functionally distinct olfactory pathways. For example, in both rodents and insects, food odors and pheromones are processed by glomeruli that differ in their location, size, OSN innervation, neurochemistry, and the structure of their postsynaptic compartment (for reviews see Hildebrand and Shepherd, 1997, Munger et al., 2009, Stowers and Logan, 2010, Galizia and Rössler, 2010, Dulac and Wagner, 2006). Glomeruli in the olfactory system of fish are similarly diverse and differ in their sizes and shapes (Chapter 3, Riddle and Oakley, 1992, Iwahori et al., 1987, Frontini et al., 2003, Baier and Korsching, 1994), their innervation by neurochemically distinct OSNs (Chapter 3, Sato et al., 2005, Hansen et al., 2003, Frontini et al., 2003) and their innervation by postsynaptic MCs (Miyasaka et al., 2009, Kosaka and Hama, 1982a, Fuller et al., 2006). In the present study we provide a comprehensive overview of the organization of both pre- and postsynaptic compartments of differently sized glomeruli in zebrafish. We describe what appear several different types of glomeruli and, as discussed below, believe that these glomeruli provide different but complementary mechanisms for olfactory processing.

4.5.1 Structure of Olfactory Glomeruli

The canonical olfactory glomerulus is a spheroidal acellular aggregate of synaptic terminals from OSN axons, MC dendrites and interneuron processes (vertebrates, Chen and Shepherd, 2005, Kasowski et al., 1999; insects, Hildebrand and Shepherd, 1997). Each glomerulus is innervated by only one, or at most a few different OSN types, and

because of their selective innervation, glomeruli are narrowly tuned to a small range of odors (Mombaerts, 2006). The output of a glomerulus typically consists of a pool of uniglomerular MCs, each of which extends a single primary dendrite into a glomerular tuft (Shepherd, 1972, Kishi et al., 1982, Dhawale et al., 2010). Based on their wiring, glomeruli may thus be regarded as a functionally distinct, narrowly tuned sensory channel that relay information about specific molecular components of odors to the brain.

Glomeruli of fish and amphibians, although similar to the description above, differ from typical glomeruli in several respects. For example, the boundaries of glomeruli in fish (Frontini et al., 2003, Kosaka and Hama, 1982b) and amphibians (Nezlin and Schild, 2000) are not delineated by periglomerular interneurons and their synaptic tufts are often poorly delimited. In zebrafish, for example, much of the glomerular layer appears to lack glomeruli proper, and instead consists of large and diffuse nerve plexus-like areas that are targeted without visible organization by OSN axons (Chapter 3, Baier and Korsching, 1994). Furthermore, studies describing the innervation of fish glomeruli by MCs have provided conflicting evidence, suggesting that glomeruli in fish are either innervated by multiglomerular MCs (Friedrich and Laurent, 2001, Kosaka and Hama, 1982b), or by multiglomerular and uniglomerular MCs (Fuller et al., 2005, Miyaska et al., 2005). Similarly, functional evidence in zebrafish suggests that odors can elicit sharply defined activity foci (i.e., single glomerulus) or activate overlapping sets of glomeruli on the surface of the olfactory bulbs (Friedrich and Korsching, 1998). Based on such data, a clear definition of the term 'glomerulus' has been difficult to establish in the olfactory systems of fish and amphibians (see also Nezlin et al., 2003). Based on the results from our study, we propose that zebrafish olfactory glomeruli are multiple distinct types of

anatomically and functionally distinct synaptic relays that all contain the basic constituents of glomeruli proper.

Large and medium glomeruli are analogues of 'classical glomeruli'

The large and medium-sized glomeruli that we describe closely resemble glomeruli in the main olfactory system of rodents (i.e., canonical glomerulus described above). All large and medium-sized glomeruli were anatomically distinguishable from one another, by means of their selective OSN axon innervation and clearly delimited presynaptic tufts. Moreover, the postsynaptic compartment of these glomeruli almost always consisted of dendrites from uniglomerular MCs. Glomeruli in the main olfactory system of rodents also have clearly distinguishable synaptic tufts (Kasowski et al., 1999) and these glomeruli are generally innervated by dendrites from uniglomerular MCs (Shepherd, 1972, Kishi et al., 1982, but see Cockerham et al., 2009). Indeed, our anatomical data depicting the presynaptic glomerular compartment of large and medium-sized glomeruli are remarkably similar to data describing glomeruli in the rat olfactory system (Kasowski et al., 1999). Nevertheless, some differences exist between our data and descriptions of rodent glomeruli. For example, we and others (Nezlin et al., 2003) did not observe a characteristic ring of interneurons in the juxtaglomerular space surrounding individual glomeruli (e.g., see Kasowski et al., 1999). Moreover, unlike glomeruli in rats (Halasz and Greer, 1993, Kasowski et al., 1999), we did not observe any visible segregation of glomeruli into distinct functional compartments. However, despite these differences, large and medium-sized glomeruli were clearly distinct from one another, innervated by distinguishable OSN axon bundles and MC pools, and we thus suggest that these units represent glomeruli proper that have been described in the rodent and insect olfactory

150

systems (Hildebrand and Shepherd, 1997; Chen and Shepherd, 2005; Tohuhara and Vosshall, 2009, Wagner and Dulac, 2006).

Glomerular Plexus and Microglomeruli

We believe that 'microglomeruli' in the glomerular plexi in the lateral and dorsal zebrafish olfactory bulbs (see also Korsching, 2005) also constitute functional units of olfactory processing. Our results show that the OSN termini that comprise the microglomeruli overlapped with MC dendrites and interneuron processes, which are the fundamental components of the olfactory glomerulus (Shepherd, 1972, Chen and Shepherd, 2005, Kasowski et al., 1997, Hildebrand and Shepherd, 1997). Indeed, optophysiological recordings indicate that the microglomeruli in the lateral glomerular plexus of zebrafish are functional and respond to a broad range of amino acids (Friedrich and Korsching, 1997). It remains unclear, however, what the precise function of individual microglomeruli is, but they may add additional odor processing capabilities to more narrowly tuned large glomeruli in their surround (see below).

Glomerular plexi and microglomeruli have been suggested to be unique to fish (see also Baier and Korsching, 1994, Korsching, 2005, Kosaka and Hama, 1982b), but there appear to be morphologically analogous structures in both mammals and insects. For example, the accessory olfactory bulb of rodents consists of diffusely organized glomeruli, which are smaller than those in the main olfactory system (Meisami and Bhatnagar, 1998), innervated by axons from multiple OSN types (Wagner et al., 2006, Belluscio et al., 1999, Rodriguez et al., 1999) and diffusely targeted by mitral cell dendrites (Takami and Graziadei, 1991, Jia et al., 1999). Interestingly, both the lateral plexus in zebrafish (Sato et al., 2005) and the mammalian AOB (Dulac, 2000) are

innervated by V2R type OSNs, suggesting that their diffuse organization may originate in the use of a common molecular receptor type (see discussion below). Another possible analogue of the glomerular plexus may be the microglomeruli in the antennal lobes of orthoptera; these contain thousands of microglomeruli, which are all very small spheroidal structures that appear to consist of single or at most a few OSN axon terminals (Ignell et al., 2001). While the AOB and antennal lobe microglomeruli indeed have a remarkably similar appearance and the plexus microglomeruli in zebrafish, more research is needed to further examine a possible link between the form and function of these structures. Below, we discuss the possible functions of the different types of glomeruli identified in this study.

4.5.2 Integration of Pheromone Blends by Large Glomeruli

Steroidal and gonadal pheromones used in intraspecies communication are multicomponent mixtures that are released by fish in variable temporal and intensity patterns (Sorensen et al., 1998, Jesuthasan and Mathuru, 2008), and fish apparently respond to certain ratios of pheromone components (Sorensen et al., 1998). This suggests that pheromone blends may need to be integrated in the olfactory system. Based on data presented here and in our previous present study (see Chapter 3), we believe that large medial glomeruli suit such an integrative role. Specifically, we observed that the lcG_1, mdG and vpG were all innervated by multiple OSN axon bundles that arose from distinct regions of the olfactory nerve. It is possible that these axon bundles originate from a single OSN type that is widely dispersed across the olfactory epithelium, however, this idea is not in agreement with our observation that the similarly large lcG_3 and lcG_4, which are all innervated by a single thick bundle of OSN axons (see below). We

therefore hypothesize that the separate OSN bundles that innervate large medial glomeruli arise from OSNs that express different OR types.

ORs play a fundamental role in OSN axon routing and axons that express the same or similar ORs fasciculate and form glomeruli, while unlike axons remain separate from one another (Sakano, 2010, Mombaerts, 2006, Feinstein and Mombaerts, 2004, Feinstein et al., 2004). Thus, the above-mentioned large glomeruli may be innervated by axons expressing distinct ORs, which prevent the fasciculation of these axons, even if they traverse the olfactory bulb very close to one another (notice the proximity of axons indicated by arrowheads in Figure 25B). Pheromone-responsive glomeruli in mammals are similarly innervated by axons from multiple OSN types (Rodriguez et al., 1999, Belluscio et al., 1999), and given that pheromone-responsive glomeruli in fish may need to integrated multiple types of olfactory information we hypothesize that the mdG_2, vpG and lcG_1 may resemble glomeruli in the rodent accessory olfactory system (Figure 38A).

An alternative, but similar model may describe the function of the mdG. We do not know what the OSN innervation patterns to most mdG are (Table 2), but we observed that these glomeruli were innervated by uniglomerular *and* multiglomerular MCs (Figure 38B). Pheromone-responsive glomeruli in mammals (Takami and Graziadei, 1990, Jia et al., 1999) and insects (Galizia and Rössler, 2010) are similarly innervated by uniglomerular and multiglomerular MCs, and physiological data from accessory olfactory pathways in both mammals (Meeks et al., 2010) and insects (Christensen and Hildebrand, 1997) describe glomerular output neurons that respond to both, individual chemical components of a pheromone mixture as well as blends of these components that resemble the naturally occurring pheromone product (e.g., Figure 38B).

Thus, our descriptions of enlarged medial glomeruli correspond to anatomical and functional features of pheromone-responsive units in mammals and insects and we thus hypothesize that these glomeruli are involved in producing responses to steroid and gonadal pheromones.

4.5.3 Combinatorial Coding of Bile Acid Odors in mG and vmG

Bile acids are actively released by many species of fish (Hara, 1994, Derby and Sorensen, 2008) and are important in conspecific recognition. Every fish appears to secrete a unique bile acid 'signature mixture' (Wyatt, 2010) that permits its identification and discrimination among members of the same and other species. Bile acids appear to be common in the aquatic environment (Derby and Sorensen, 2008) and the glomeruli that encode them must therefore be able to detect a wide range of bile acid odors while being able to discriminate minute differences among them for conspecific recognition.

Bile acid-sensitive regions in zebrafish (Friedrich and Korsching, 1998) and other species (Hansen et al., 2003, Hamdani and Døving, 2007, Derjean et al., 2010), are located in the ventromedial olfactory bulbs, where we have identified the small mG and vmG (see also Chapter 3). These glomeruli appear to be ideally suited to encode and discriminate the diverse bile acid signatures mixtures of fish. The sensory inputs to both mG and vmG are small and numerous, providing sufficient input channels for encoding the diverse range of bile acid odors. Moreover, these glomeruli are innervated by G_{olf}-expressing, OR-type ciliated sensory neurons (Chapter 3), and OR-type OSNs appear to encode odors in a combinatorial manner (Malnic et al., 1999). Combinatorial odor coding implies that each OR can bind to multiple odor molecules and multiple odor molecules can bind to each OR (Figure 38C), enabling OR-type OSNs to encode vast

numbers of different odorants based on different combinations of ligand interactions (Buck, 2004). Indeed, optical imaging data from zebrafish show that bile acid odors evoke overlapping combinatorial activity patterns in regions containing the mG and vmG in zebrafish (Friedrich and Korsching, 1998).

Interestingly, we observed that the sensory input to nearly all mG and vmG converges onto multiglomerular MCs. This is in contrast to glomeruli that are innervated by OR-type OSNs in the main olfactory bulb of mammals; these glomeruli are innervated by uniglomerular MCs (Shepherd, 1972, Dhawale et al., 2010), which appear to be similarly tuned as their OSN input, and much of the integration of olfactory information is thus thought to occur in other regions of the brain (Stettler and Axel, 2009, Lei et al., 2006, Apicella et al., 2010). MCs in the mG and vmG clusters, on the other hand, may integrate large amounts of converging sensory information, and may be capable of discriminating and filtering information about certain bile acid odors prior to sending the information to other regions of the brain.

Thus, social odors appear to be processed in two different subsystems in the medial olfactory bulbs. Steroids and gonadal pheromones appear to be processed by sparse large glomeruli that are innervated by OSNs that we have previously linked to putative pheromone chemoreceptors (see Chapter 3 discussion). In contrast, bile acids appear to be encoded in a combinatorial processing system that is wired to detect a large range of odors. Both of these systems appear to have a capacity to integrate or extract chemical components that constitute behaviorally relevant odorants.

4.5.4 Specialist lcG_3 and lcG_4 for Detection of Amino Acids?

The lateral olfactory bulbs contain some of the largest and most stereotypic glomeruli (lcG_3 and lcG_4), the medium-sized and anatomically variable lcG_x and a diffusely organized lateral plexus (below). All of these structures are, to our knowledge, innervated by microvillous sensory neurons, which express V2R-type olfactory receptors and are responsive to amino acids and nucleotides. In mammals, V2R-type receptors appear to be very narrowly tuned (Leinders-Zufall et al., 2000, Touhara and Vosshall, 2009), and appear to encode chemical information in non-combinatorial manners, where ligand-receptor interactions are highly specific and limited. V2R-type receptors may thus pose restrictions on the information that can be transmitted to the olfactory system, and the tuning of microvillous cells and the lateral glomeruli that they innervate may be relatively narrow.

The lcG_3 and lcG_4 are each innervated by a single thick bundle of OSN axons, and both glomeruli appear to be innervated exclusively by uniglomerular mitral cells, implying that these glomeruli may comprise sensory channels that faithfully relay specific types of odor information to the brain (Figure 38D). Indeed, such glomeruli appear to reside in the lateral olfactory bulbs of catfish; these animals have OSNs (Nikonov and Caprio, 2007a), olfactory bulb units (Nikonov and Caprio, 2004), and lateral forebrain units (Nikonov and Caprio, 2007b) that all respond with restricted tuning to certain types of amino acids. Additionally, optical imaging data from Friedrich and Korsching (1997) indicate that amino acids elicit specific activity foci in regions near lcG_3 and lcG_4 (Friedrich and Korsching, 1997); these regions appear to be responsive to several amino acids, but respond with near-uniform activations to all of these, suggesting

that they may relay a simple 'yes / no signal' that informs the animal about the presence of certain types of amino acids. Additional discrimination among amino acids may then require additional lateral glomeruli (below).

4.5.5 Lateral Plexus for Amino Acid Discrimination?

In this study we provide detailed anatomical descriptions of the microglomeruli in the lateral plexus of the posterolateral olfactory bulb (see also, Baier and Korsching, 1994). These microglomeruli are only diffusely organized and their sensory input consists of widely dispersed OSN axon terminals. As discussed above, olfactory pathways that are innervated by V2R-type expressing OSNs may not be suitable for combinatorial odor coding, and may thus be restricted, given the narrow range of responsiveness of V2R-types receptors (Leinders-Zufall et al., 2000). We believe that the wiring of the lateral plexus represents an adaptation to this limitation. Few OSN axons that innervate the lateral plexus coalesce and form glomeruli, which would carry a uniform sensory message to certain postsynaptic targets. Instead, axons within the lateral plexus are widely scattered and thus distribute their narrow inputs over a wider range of postsynaptic targets (Figure 38E). The end result of this setup appears to be a combinatorial odor coding system that could circumvent the presumably narrow tuning to the lateral olfactory bulbs by V2R-type receptors. Data from Friedrich and Laurent (2001) confirm this idea and show that individual MCs in the lateral plexus receive inputs from many different OSN, which they can discriminate from one another.

Thus, in summary, lateral glomeruli appear to consist of two distinct populations that play different, but possibly complementary roles in odor coding. The lcG_3 and lcG_4 may represent a stable olfactory pathway that conveys a simple yes / no signal about the

presence of certain abundant components in the animals food source; additional discrimination among such components could then be provided by the combinatorial coding system in the lateral plexus. Optophysiological data are in agreement with this hypothesis; they show that many different amino acids elicit activity in certain 'hotspots' in the lateral olfactory bulb, while each amino acid triggers its own unique combinatorial activation surrounding these hotspots (Friedrich and Korsching, 1997).

4.5.6 Summary

We describe several distinct types of glomeruli throughout the olfactory system; these glomeruli appear to employ distinct but similar mechanisms of odor coding and may act in synergy to provide information about both presence and type of odorant. We will next investigate how these pathways develop, hypothesizing that the stable pathways (lcG_3 and lcG_4) may develop early in the life of an animal, while the dynamic pathways (lateral plexus) arise later as the animal becomes active and learns certain chemical features of its environment.

Table 3. List of antibodies and tracers, their sources and staining protocols

Table 3

Antibody	Immunogen / Host	Source	Fixation	Prior use in fish
OSN axon labels (1:100 in PBS-T)				
Anti keyhole-limpet-hemocyanin (KLH)	hemocyanin from keyhole limpets / rabbit	Sigma Chemical Co. (H0892)	2% PFA	Fuller et al. (2005), Riddle and Oakley (1992)
Anti calretinin	recombinant human calretinin / mouse	Swant (Bellinzona, Switzerland) 6B3	2% PFA	Miyasaka et al. (2005), Castro et al. (2006)
Synaptic label (1:100 in PBS-T)				
Anti synaptic vesicle protein 2 (SV_2)	ommata synaptic vesicles / mouse	Developmental Studies Hybridoma Bank (Iowa City, IA, USA)	2% PFA	Koide et al. (2009)
JGC labels (1:100-1:200 in PBS-T)				
Anti tyrosine hydroxylase (TH)	purified rat TH / mouse	ImmunoStar	2% PFA	Fuller et al. (2005)
Anti tyrosine hydroxylase (TH)	denatured rat TH / rabbit	Millipore (Etobicoke, ON, Canada)	2% PFA	Edwards et al. (2007)
Anti GABA	BSA conjugated GABA / rabbit	Sigma	2% PFA	Li et al. (2005)
Axonal Tracers				
DiI carbocyanine tracer	n / a	Invitrogen (Burlington, ON Canada)	4% PFA	Baier and Korsching (1994)
DiD	n / a	Invitrogen	4% PFA	n / a

Table 4. Summary of morphological data from large, medium and small glomeruli. Glomeruli are arranged alphabetically. Number per bulb refers to how many glomeruli are located in each olfactory bulb. Axon bundles refers to the number of distinct axon bundles that innervate a single glomerulus. All data are the mean and standard deviations derived from indicated numbers of specimens.

Table 4.

Glomerulus (animals)	Number per bulb	Feret diam. (μm)	Cross-sectional area (μm^2)	Axon bundles	Number of MC (animals)	MC Feret diameter (μm)	MC Type
Large Glomeruli							
lcG$_1$ (n = 6)	1	85	3650 ± 582	2	6 (n = 1)	14.3	uMC
lcG$_3$ (n = 5)	1	74 ± 9	2590 ± 672	1	7 ± 0.8 (n = 4)	12.6 ± 2	uMC
lcG$_4$ (n = 5)	1	99 ± 3	4800 ± 400	1	4.5 ± 0.7 (n = 3)	17.8 ± 2	uMC
mdG$_1$ (n = 7)	1	80 ± 5	3234 ± 176	?	6 ± 0.8 (n = 2)	14.4	uMC / mMC
mdG$_2$ (n = 7)	1	77 ± 8	2950 ± 381	2 - 3	6.5 ± 2 (n = 2)	12.9 ± 2.3	uMC / mMC
mdG$_3$ (n = 7)	1	72 ± 6	2902 ± 486	?	4 ± 1.4 (n = 2)	12.5 ± 1.6	uMC / mMC
mdG$_4$ (n = 7)	1	75 ± 2	3251 ± 105	?	6 ± 1.4 (n = 2)	13.9 ± 1.1	uMC / mMC
mvpG (n = 7)	1	76 ± 4	2813 ± 331	2	6.6 ± 0.5 (n = 3)	15.1 ± 0.6	uMC
vpG (n = 5)	1	80 ± 2	2994 ± 205	2	6.5 ± 0.7 (n = 2)	15.3 ± 1	uMC
lvpG (n = 6)	1	85	3051 ± 407	2	6 (n = 1)	14.1	uMC
Medium Glomeruli							
vG$_x$ (n = 5)	7.5 ± 1.3	44 ± 6	829 ± 353	1	3.5 ± 1.2 (n = 4)	11.3 ± 1.2	uMC
vtG$_1$ (n = 5)	0.8 ± 0.3	45 ± 12	854 ± 146	1	3.2 ± 0.9 (n = 4)	12.5 ± 1.1	uMC
vtG$_2$ (n = 5)	1	52 ± 11	1287 ± 342	1	3.2 ± 0.9 (n = 5)	13.9 ± 2.6	uMC

Table 4 continued.

	Small Glomeruli						
dlG_x (n = 6)	47.1 ± 7.2	20 ± 4	235 ± 88	1	1.7 ± 0.7 (n = 4)*	10.7 ± 1	uMC / mMC
vmG_x (n = 5)	13.7 ± 4.6	15 ± 3	136 ± 46	1	0.4 ± 0.3 (n = 3)*	11.7 ± 0.8	uMC / mMC

* We identified the mitral cell innervation of 22 dlG_x in n = 4 animals and 14 vmG_x in n = 3 animals.

Figure 23. Organization of the pre- and postsynaptic compartments of glomeruli. Glomeruli contain axon shafts (green) and synaptic terminals (magenta) of OSN and juxtaglomerular interneurons (JGC, red) inside the glomerular core, (glomerular tuft). Mitral cell (MC, red) dendrites innervate the postsynaptic compartment. Not shown are granule interneurons, which laterally connect MCs outside of the glomerulus. Arrows in the diagram illustrate one hypothesized function of some JGC (lateral inhibition). Unless indicated otherwise, the colors used in this schematic are also used in anatomical data throughout this manuscript.

Figure 23. Organization of the Pre- and Postsynaptic Compartments of Glomeruli

165

Figure 24. Coarse organization of the presynaptic compartment of zebrafish glomeruli. Overviews of ventral (A_{1-4}) and dorsal (B_{1-4}) olfactory bulb surfaces and their partitioning into distinct aggregates (clusters) of glomeruli. (A_{1-4}) Glomeruli that are visible via ventral views of whole-mounted olfactory bulbs are segregated into five anatomically distinct regions, the medial (mG), lateral (lcG), ventral (vG), ventromedial (vmG) and ventroposterior (vpG) clusters. (B_{1-4}) The dorsal olfactory bulbs are partitioned into dorsal (dG), dorsolateral (dlG) and mediodorsal glomeruli (mdG). All images are projections of serial optical sections acquired at 1μm intervals to the indicated depth. A_4 and B_4 summarize the coarse organization of glomeruli.

Figure 24. Coarse Organization of the Presynaptic Compartment of Zebrafish Glomeruli

167

Figure 25. OSN innervation of large glomeruli. Large glomeruli like the mvpG (A_1, A_2) and lcG$_1$ (**B**) were innervated by several distinct axon bundles that apparently originated from different parts of the olfactory nerve (arrows and arrowheads in A_{1-2}, **B**). Other large glomeruli, like the lcG$_4$, were only innervated by a single axon bundle (see arrowhead in **C**). All images are projections of serial optical sections acquired at 1μm intervals to the indicated depth. Insets are schematic overviews of olfactory bulb surfaces and red circles show the location of depicted glomeruli.
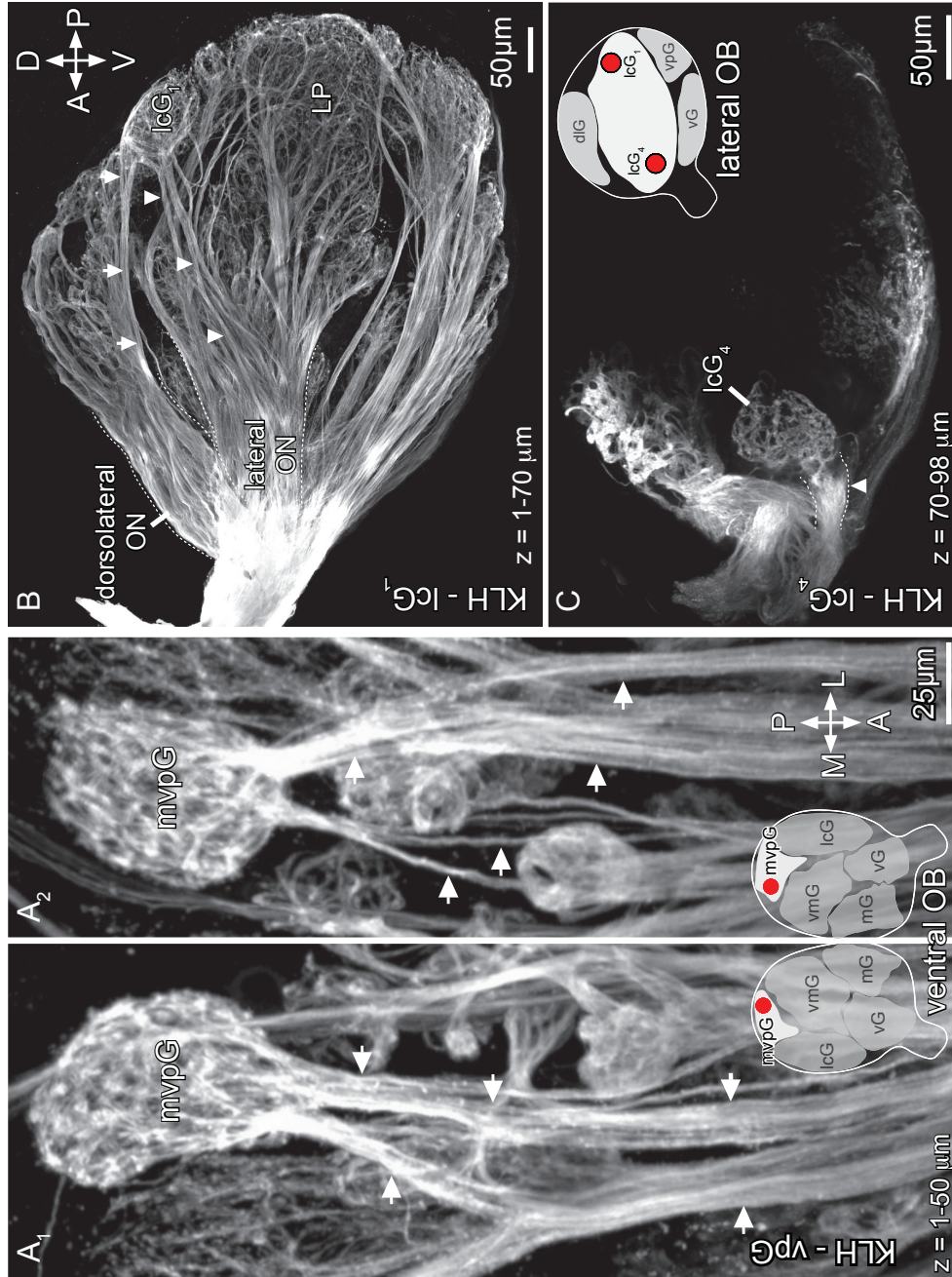
Figure 25. OSN Innervation of Large Glomeruli

169

Figure 26. OSN innervation of medium glomeruli. Medium-sized glomeruli were anatomically diverse and located beneath the olfactory nerve layer. The ventral triplet glomeruli (vtG$_{1-3}$) and some ventromedial glomeruli (vmG$_{1-2}$) were occasionally identifiable in anti-KLH labeled tissue. The large ventroposterior glomeruli are also visible (indicated). The image shows a projection of 6 optical sections obtained at 1μm intervals beginning 16μm below the olfactory bulb surface. Red circles in inset show the location of depicted glomeruli with reference to glomerular clusters.
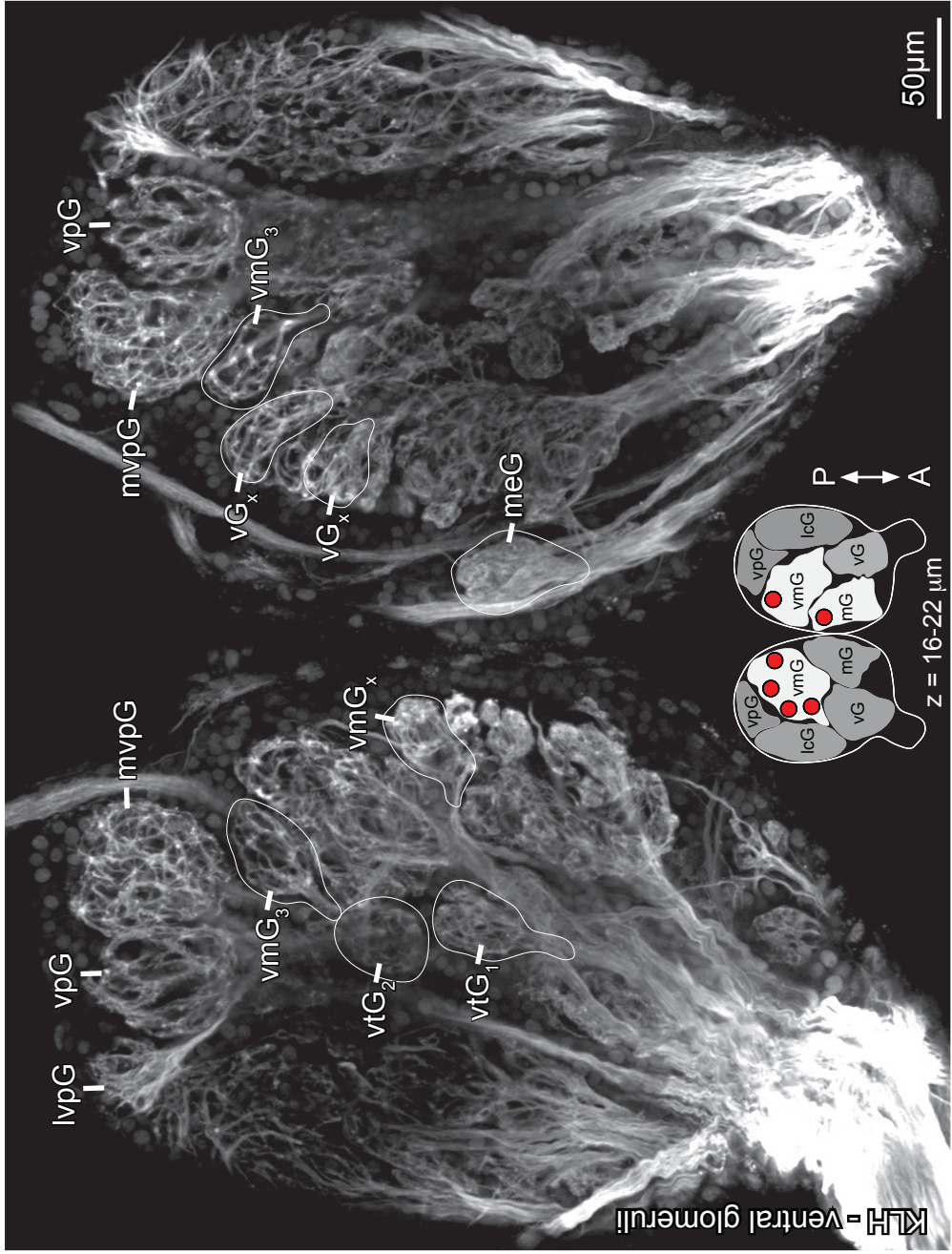
Figure 26. OSN Innervation of Medium Glomeruli

171

Figure 27. OSN innervation of small glomeruli. The majority of glomeruli were small and tightly packed inside anatomically distinct clusters such as the dorsolateral cluster (left and right bulbs from same fish in **A$_{1-2}$**). All glomeruli in this cluster were separately innervated (follow arrows in **A$_{1-2}$**). The smallest glomeruli were located in the medial (mG) and ventromedial (vmG) clusters. These units were only faintly KLH LIR (arrowheads in **B$_1$**) but labeled well with the calretinin antibody (arrowheads in **B$_2$**). All images are projections of serial optical sections acquired at 1μm intervals to the indicated depth. Insets show regions containing the depicted glomeruli (red).
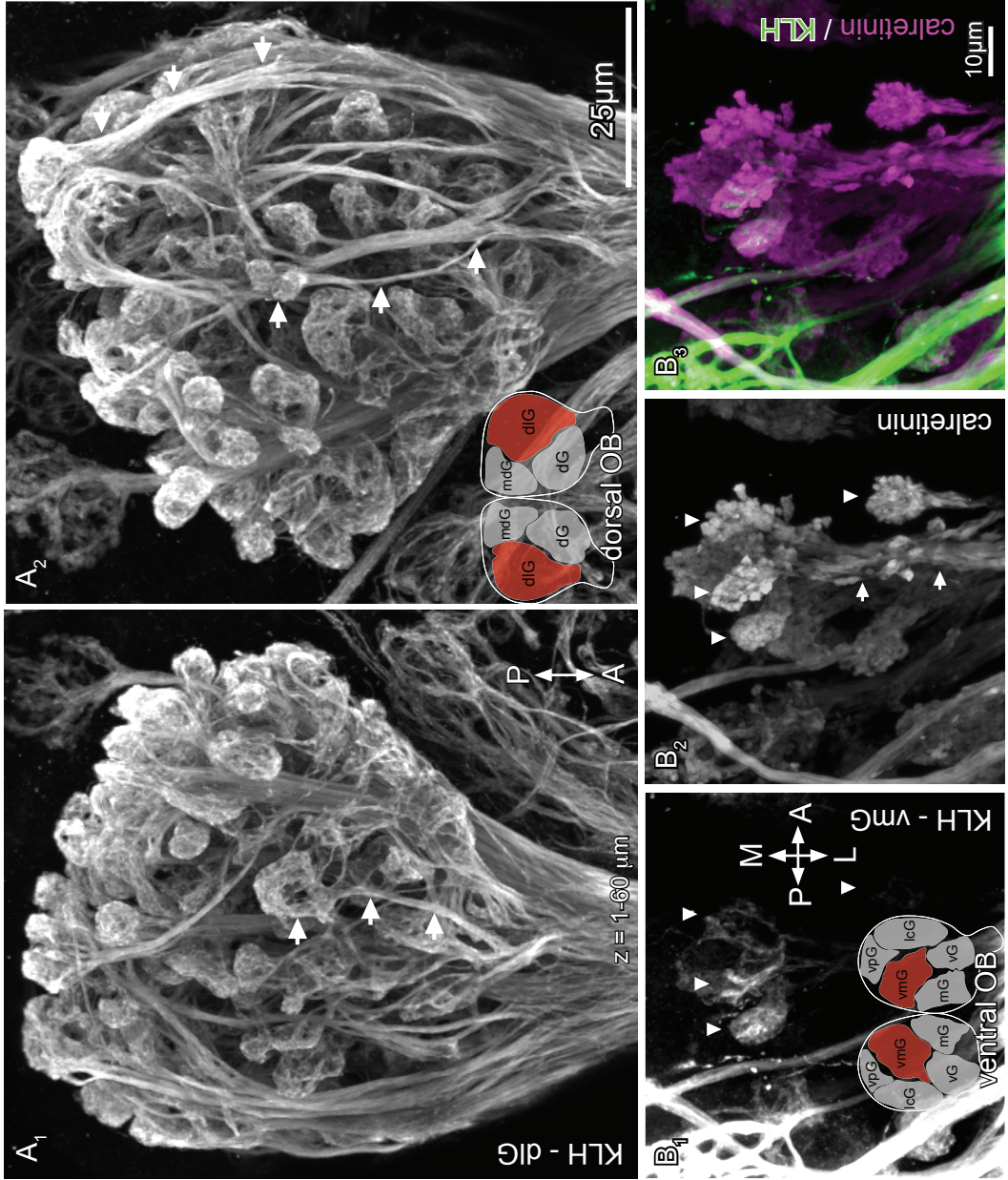
Figure 27. OSN Innervation of Small Glomeruli

Figure 28. OSN innervation of the lateral plexus. (**A**) OSN innervation to the posterolateral olfactory bulb surface was poorly organized and formed a diffuse lateral plexus (LP), containing many small glomerulus-like axon terminals (arrowheads in **B**) and even smaller varicosities that appeared to originate from single axons (arrows in **C**). All images are projections of serial optical sections acquired at 1μm intervals to the indicated depth. Inset shows location of LP in lateral olfactory bulb.
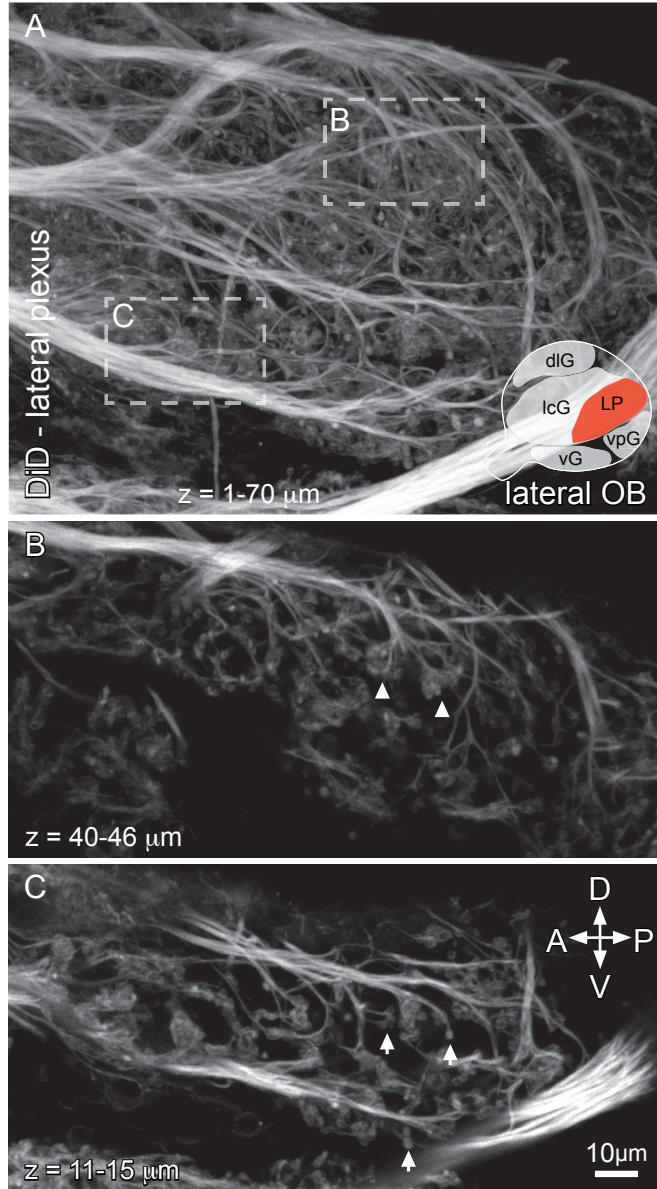
Figure 28. OSN Innervation of the Lateral Plexus

Figure 29. Presynaptic compartment of large glomeruli and innervation by juxtaglomerular interneurons (JGCs). Large glomeruli like the mediodorsal glomerulus 6 (mdG$_6$) possessed synaptic tufts that were separated from their surroundings by a border devoid of SV$_2$ labeling (**A$_2$**). The synaptic tuft overlapped with the area innervated by OSN fibers, but KLH IR and SV$_2$ IR puncta co-localized only poorly (very few white pixels in **A$_3$**). The glomerular tuft also contained TH IR terminals (**B$_1$**, **C**) from juxtaglomerular interneurons that appeared to exclusively innervate certain large glomeruli (arrowheads in **B$_1$**, **C**). Colored circles in insets show the location of depicted glomeruli with reference to glomerular clusters.

Figure 29. Presynaptic Compartment of Large Glomeruli and Innervation by Juxtaglomerular Interneurons

177
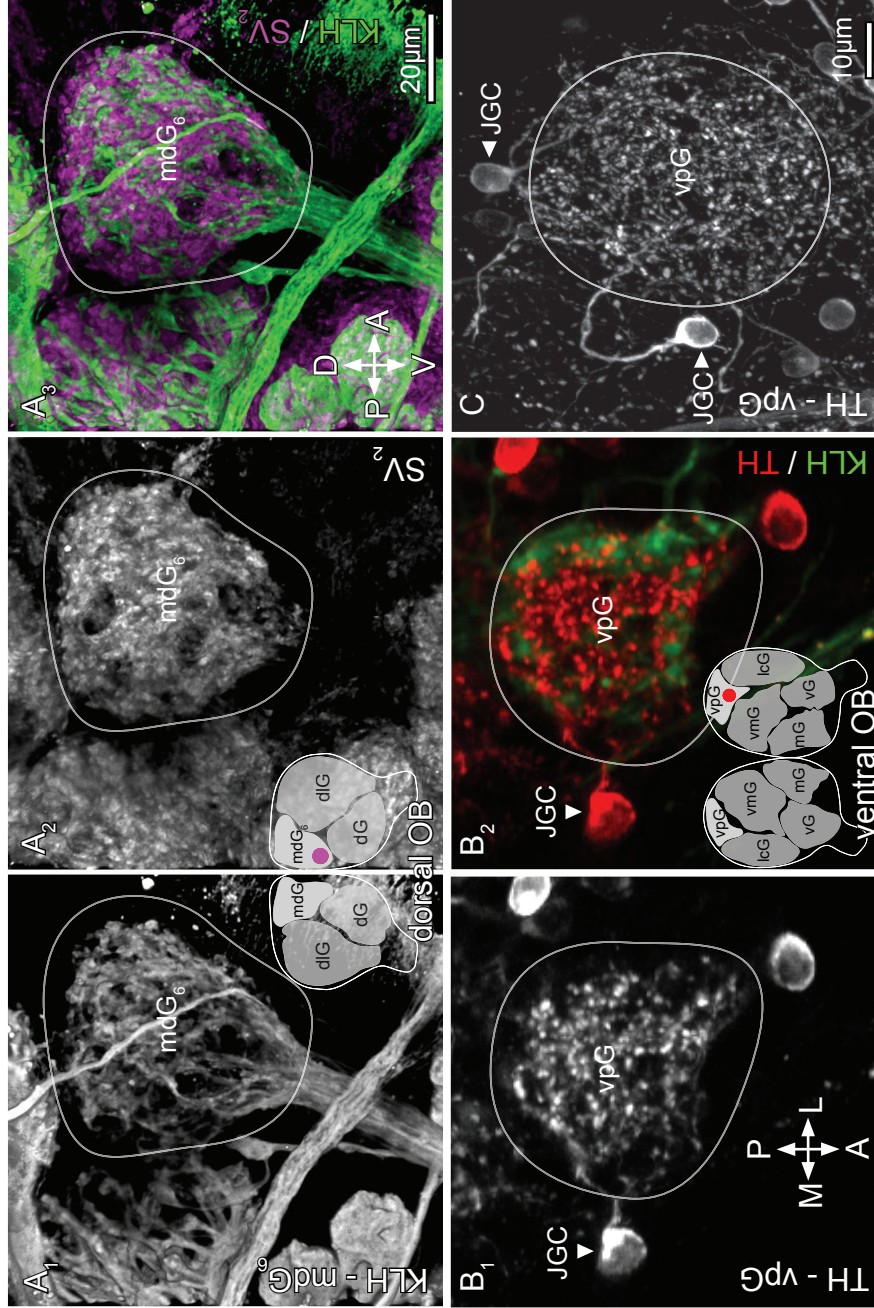
Figure 30. Presynaptic compartment of small glomeruli and innervation by juxtaglomerular interneurons (JGCs). Glomeruli in the dorsolateral cluster (dlG in A_{1-3}) had spheroidal synaptic tufts separated by a border with much weaker labeling (arrows in A_2). Staining the same regions with anti-TH produced only a diffuse picture in which glomerular tufts were not visible where they would be expected based on OSN innervation (compare arrowheads in B_{1-2}). Insets show regions containing these glomeruli (red and magenta).

Figure 30. Presynaptic Compartment of Small Glomeruli and Innervation by Juxtaglomerular Interneurons

179

Figure 31. Juxtaglomerular cells (JGC) associated with small dorsolateral glomeruli. JGC somata were located far from their targets (the dlG), along the edge of the dlG cluster (dashed line), but extended long branched processes (arrowheads) to diffuse areas inside the dlG cluster. Areas innervated by JGC were larger than the size of dlG OSN input (see multiple dlG in **A**). Inset shows location of the dlG (red).
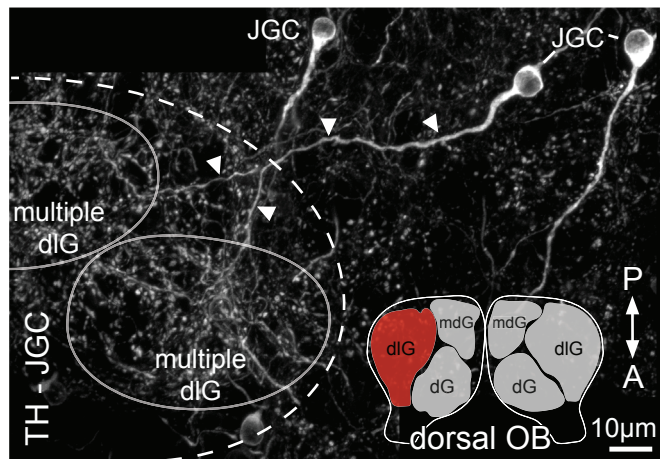
Figure 31. Juxtaglomerular Interneuron Types
Associated With Small Dorsolateral Glomeruli

Figure 32. Presynaptic compartment of the dorsal glomerular plexus and innervation by juxtaglomerular interneurons (JGCs). The dorsal plexus was only diffusely targeted by OSN axons and it was difficult to identify glomeruli proper based on KLH IR (see arrowheads in A_1), but counterstaining with anti-SV_2 revealed anatomically distinct synaptic tufts in these areas (arrowheads in A_2). In contrast, TH IR in the same region was dim and not organized into distinct glomerular tufts (B_2). Insets show location of the dG (red and magenta).
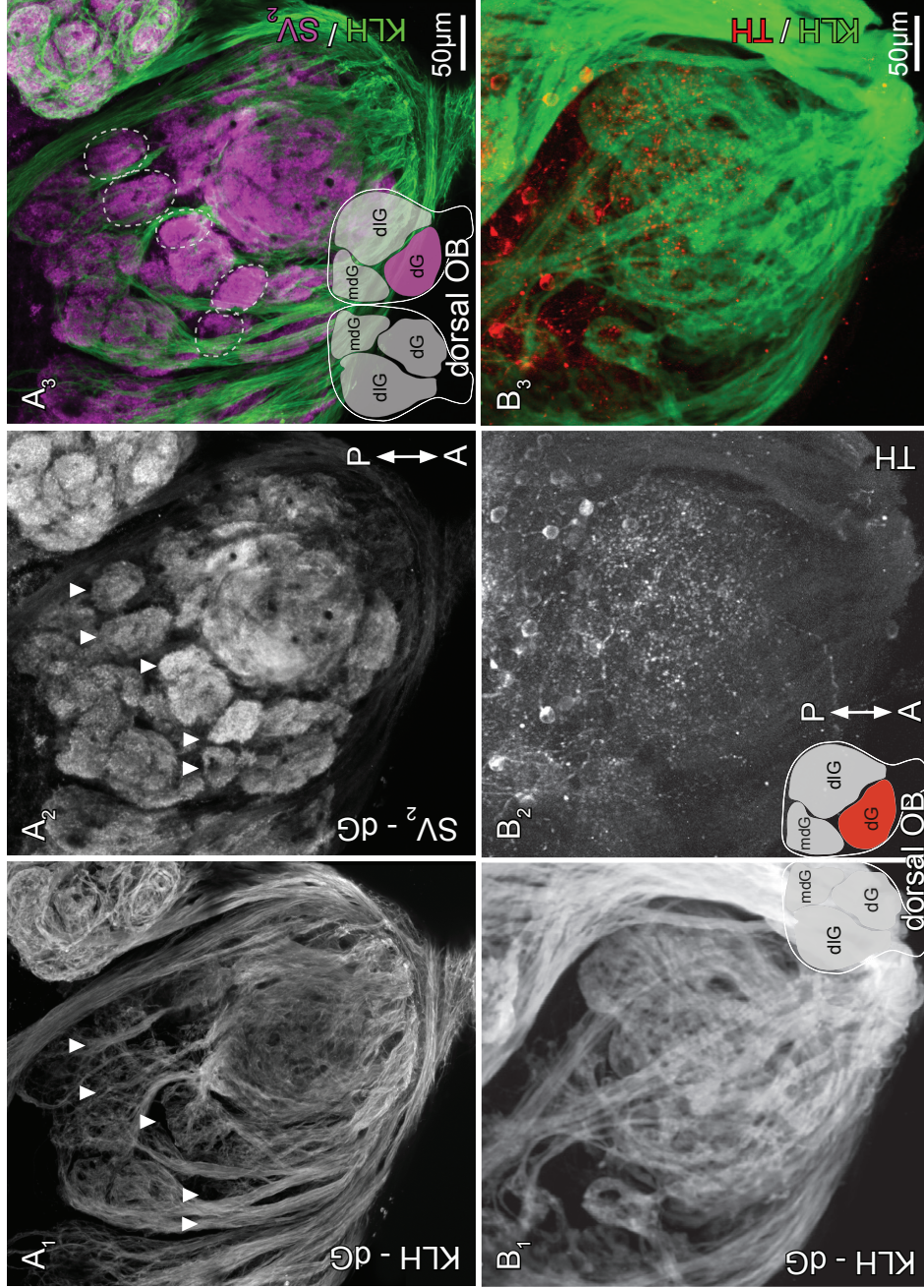
Figure 32. Presynaptic Compartment of the Dorsal Glomerular Plexus and Innervation by Juxtaglomerular Interneurons

Figure 33. Innervation of the postsynatpic compartment of large glomeruli by uniglomerular mitral cells. The medial ventroposterior glomerulus (mvpG) was innervated by 6-7 uniglomerular MCs, some are shown in **A$_2$**, **A$_5$**. Dendrites of these MCs overlapped fully with the area encircled by OSN axons, in superficial (**A$_3$)** and deep regions (**A$_6$**) of the mvpG. MC innervation of the lateral cluster glomerulus 3 (lcG$_3$) was similarly structured (**B$_1$-B$_6$**). Colored circles in insets show the location of depicted glomeruli with reference to glomerular clusters.

Figure 33. Innervation of the Postsynatpic Compartment of Large Glomeruli by Uniglomerular Mitral Cells

185
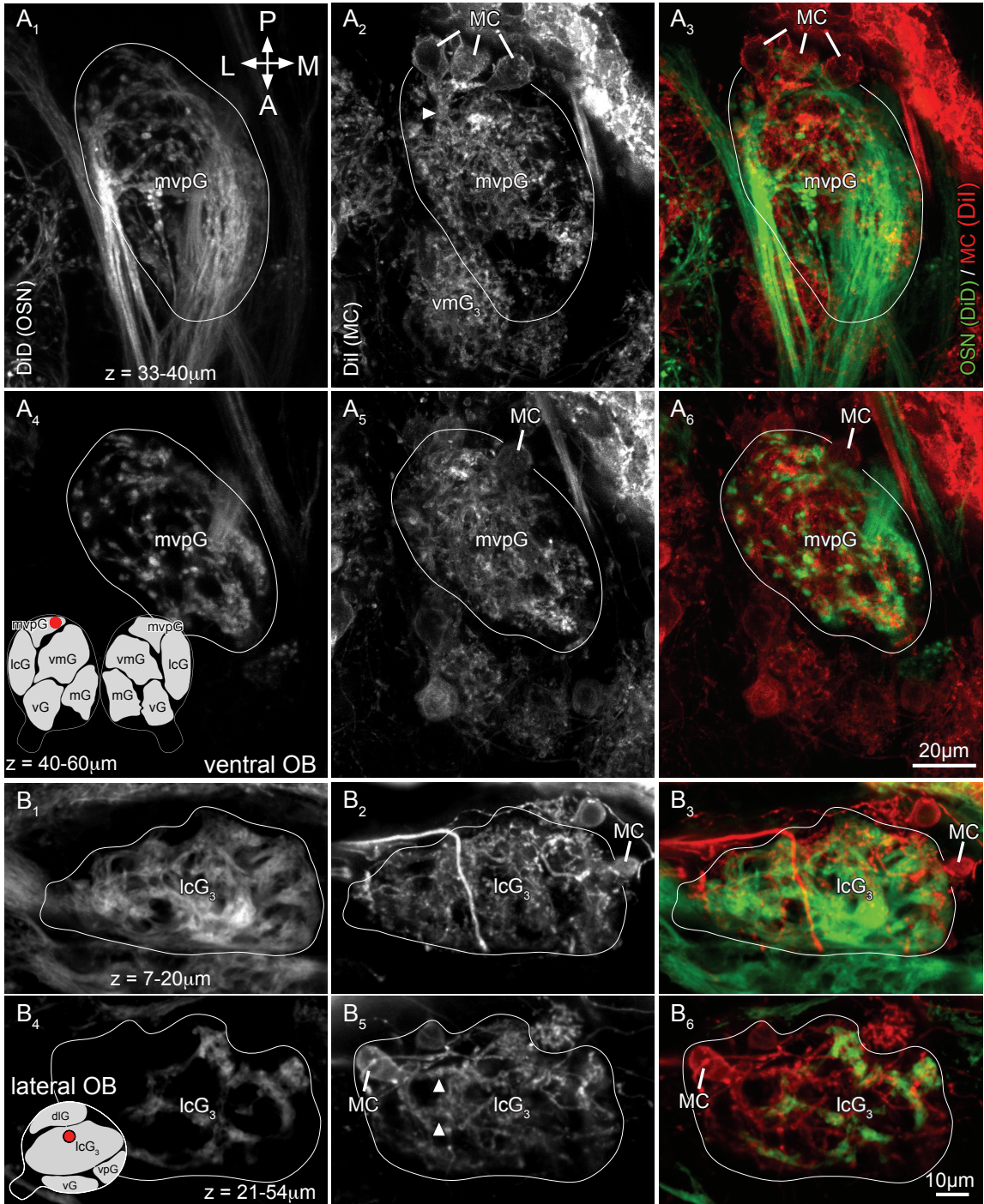
Figure 34. Innervation of the postsynatpic compartment of the large mediodorsal glomeruli (mdG) by uniglomerular and multiglomerular mitral cells. The mdG were targeted by dendrites from uniglomerular and multiglomerular MCs. Uniglomerular MCs (asterisks in A_{1-2}) were near each glomerulus, while multiglomerular MCs were located further away (MC_1 and MC_2 in A_1). Notice that this image depicts a medial view of the olfactory bulb; the bulbs were separated at their midline and imaged laying on their medial sides. Colored region in insets shows the location of mdG.
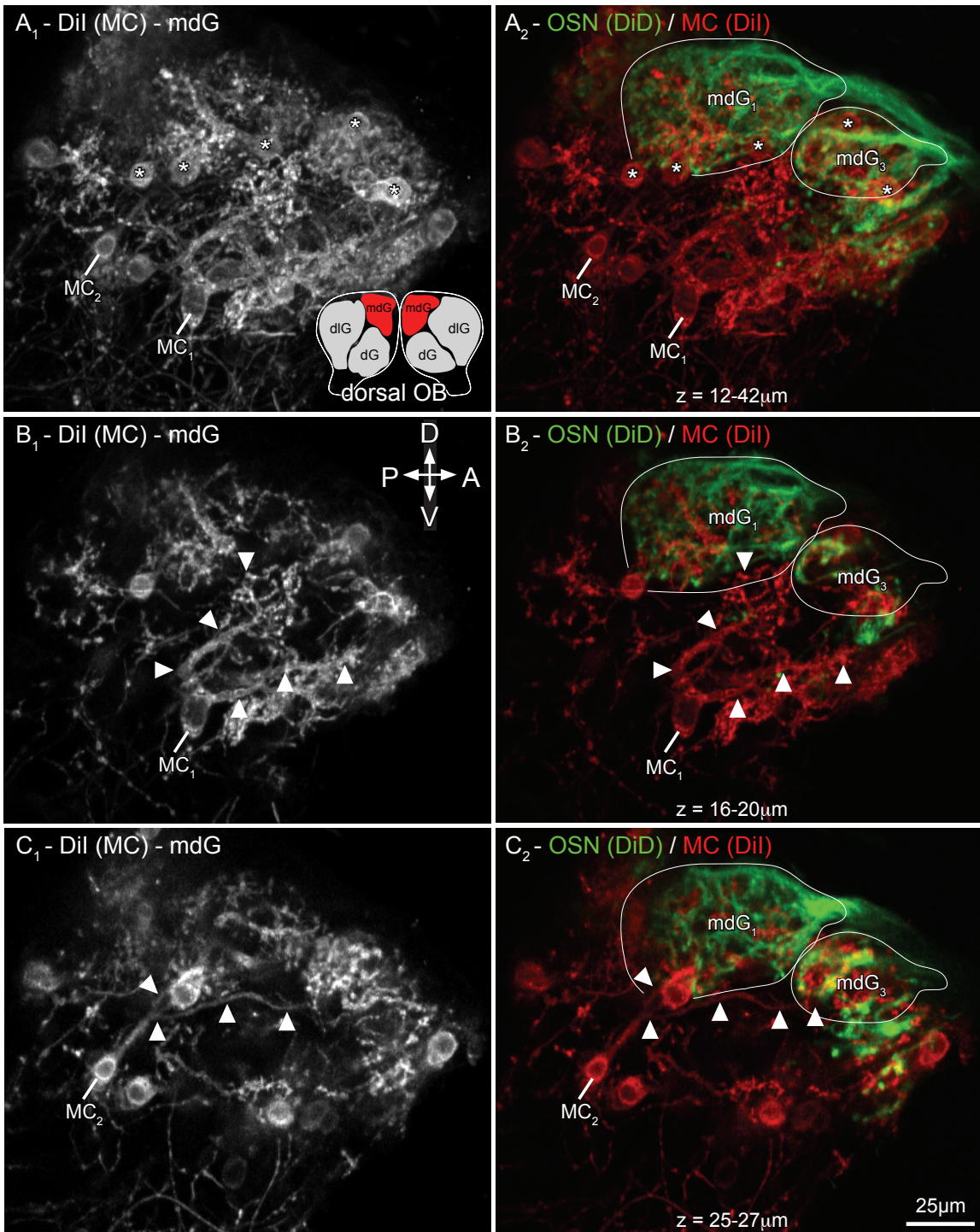
Figure 34. Innervation of the Postsynaptic Compartment of Large Mediodorsal Glomeruli by Uniglomerular and Multiglomerular Mitral Cells

Figure 35. Innervation of the postsynatpic compartment of medium-sized glomeruli by uniglomerular mitral cells. The innervation of medium-sized glomeruli, such as the ventral triplet glomerulus 2 arose from uniglomerular MCs (MC in $\mathbf{A_2}$, $\mathbf{B_2}$, $\mathbf{C_2}$). The arrangement of a single MC was similar for the vtG$_2$ shown in tissue from three different fish ($\mathbf{A_2}$, $\mathbf{B_2}$, $\mathbf{C_2}$); all images are from the left olfactory bulbs and the same orientation. The colored circle in the inset shows the location of depicted glomeruli with reference to glomerular clusters.
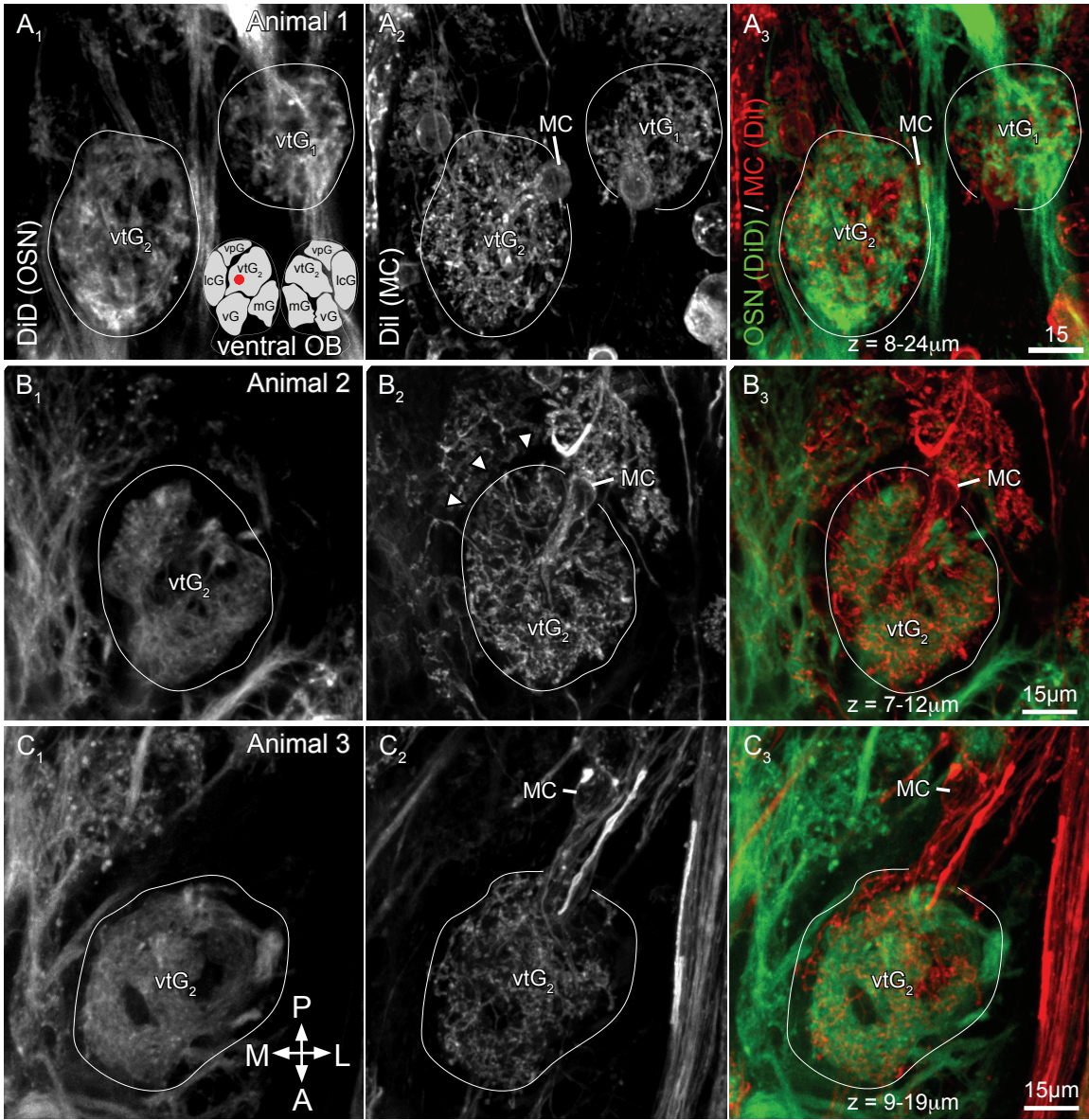
Figure 35. Innervation of the Postsynatpic Compartment of Medium-Sized Glomeruli by Uniglomerular Mitral Cells

189

Figure 36. Innervation of the postsynatpic compartment of small glomeruli by multiglomerular mitral cells. Small glomeruli were often innervated by intermingled dendrites of several multiglomerular MCs (traced area in A_2). The MCs that were associated with small glomeruli almost always formed multiple dendritic tufts that overlapped with OSN termini (see MC and vmG_x in B_{1-3}). Also associated with small glomeruli were some uniglomerular MCs with dendritic arborizations that were larger than the corresponding axonal input (C_{1-3}). Shaded areas in insets show location of the depicted glomerular clusters.
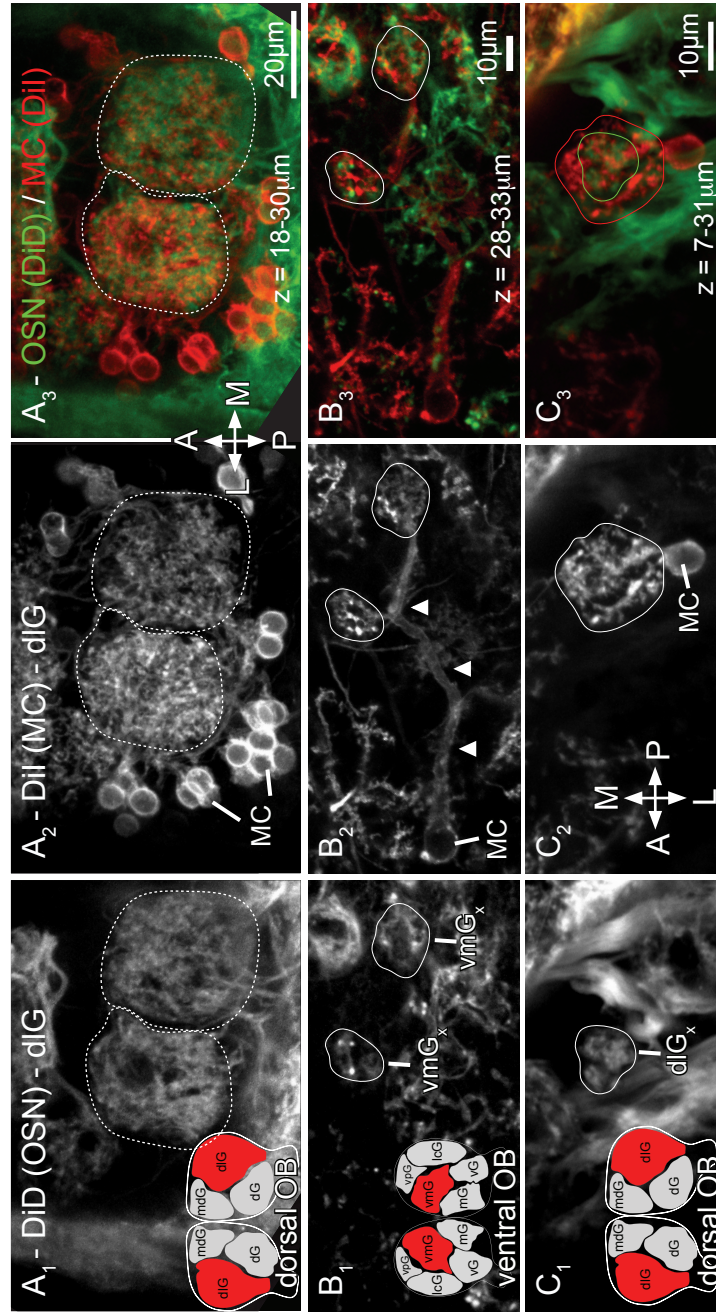
Figure 36. Innervation of the Postsynatpic Compartment of Small Glomeruli by Multiglomerular Mitral Cells

191

Figure 37. Innervation of the lateral plexus (LP) by variable mitral cell types. The postsynaptic compartment of LP was innervated by a diverse pool of uniglomerular (A_2) and multiglomerular (B_2) MCs. Regardless of MC type, many small axon terminals contacted each individual MC. Occasionally the dendrites of multiple MC intermingled to form distinct roundish compartments (see traced tuft in C_2). All abbreviations are listed in Table 1. Inset shows the location of the LP in red.
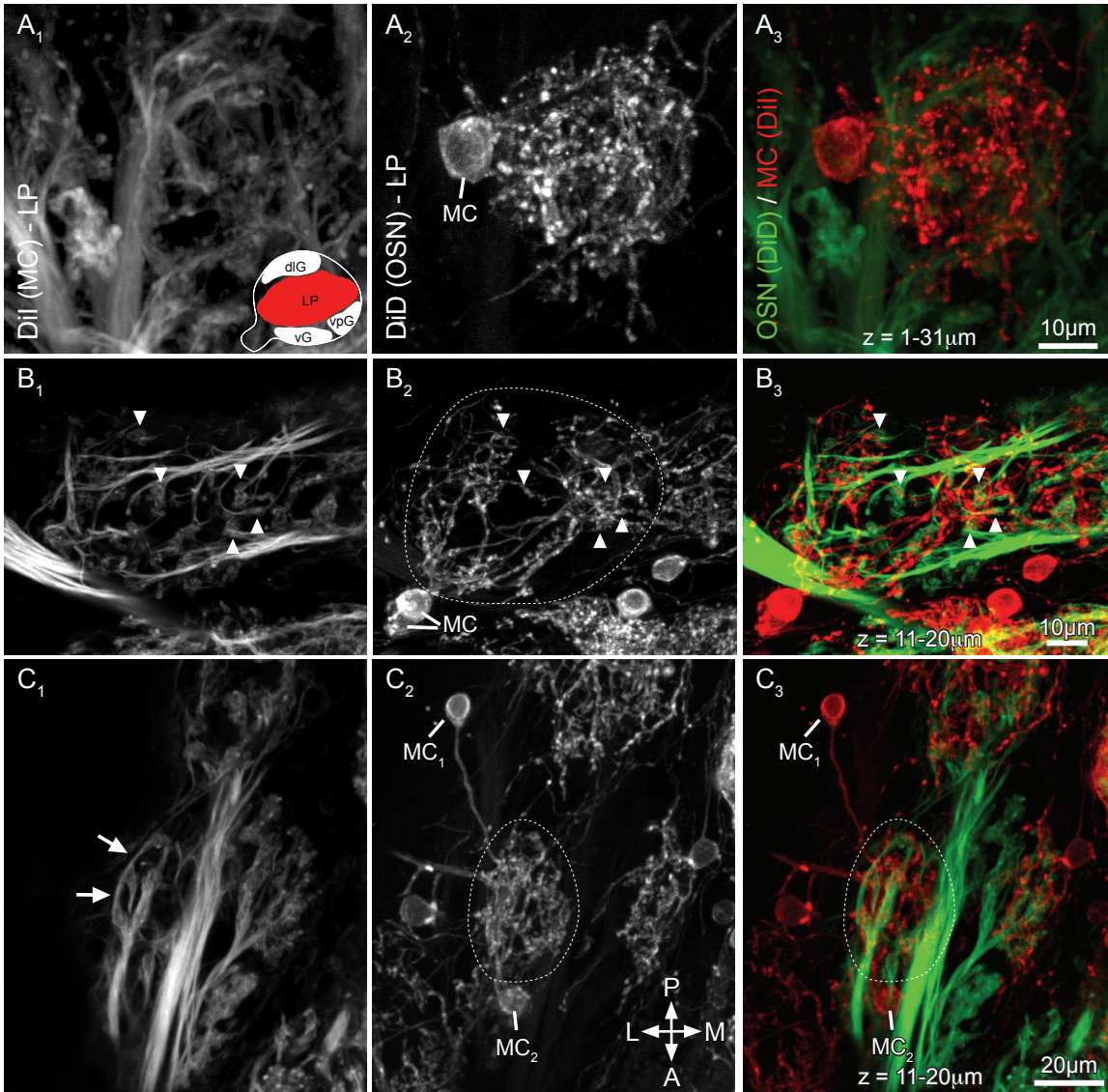
Figure 37. Innervation of the Lateral Plexus by Variable Mitral Cell Types

193

Figure 38. Summary of different types of glomeruli in the zebrafish olfactory system. Glomeruli that encode social odors are green and glomeruli that encode food odors are shaded red. (**A**, **B**) Possible pheromone-responsive glomeruli may integrate information arising from multiple receptor types to produce a pheromone 'identity code'. (**C**) Incoming sensory information also converges onto mitral cells in small glomeruli, suggesting an integrative function. (**D**) Large lateral glomeruli may represent labeled line pathways that faithfully transmit odor signals to the brain. (**E**) The diffusely organized lateral plexus (microglomeruli) resemble a combinatorial odor coding system.
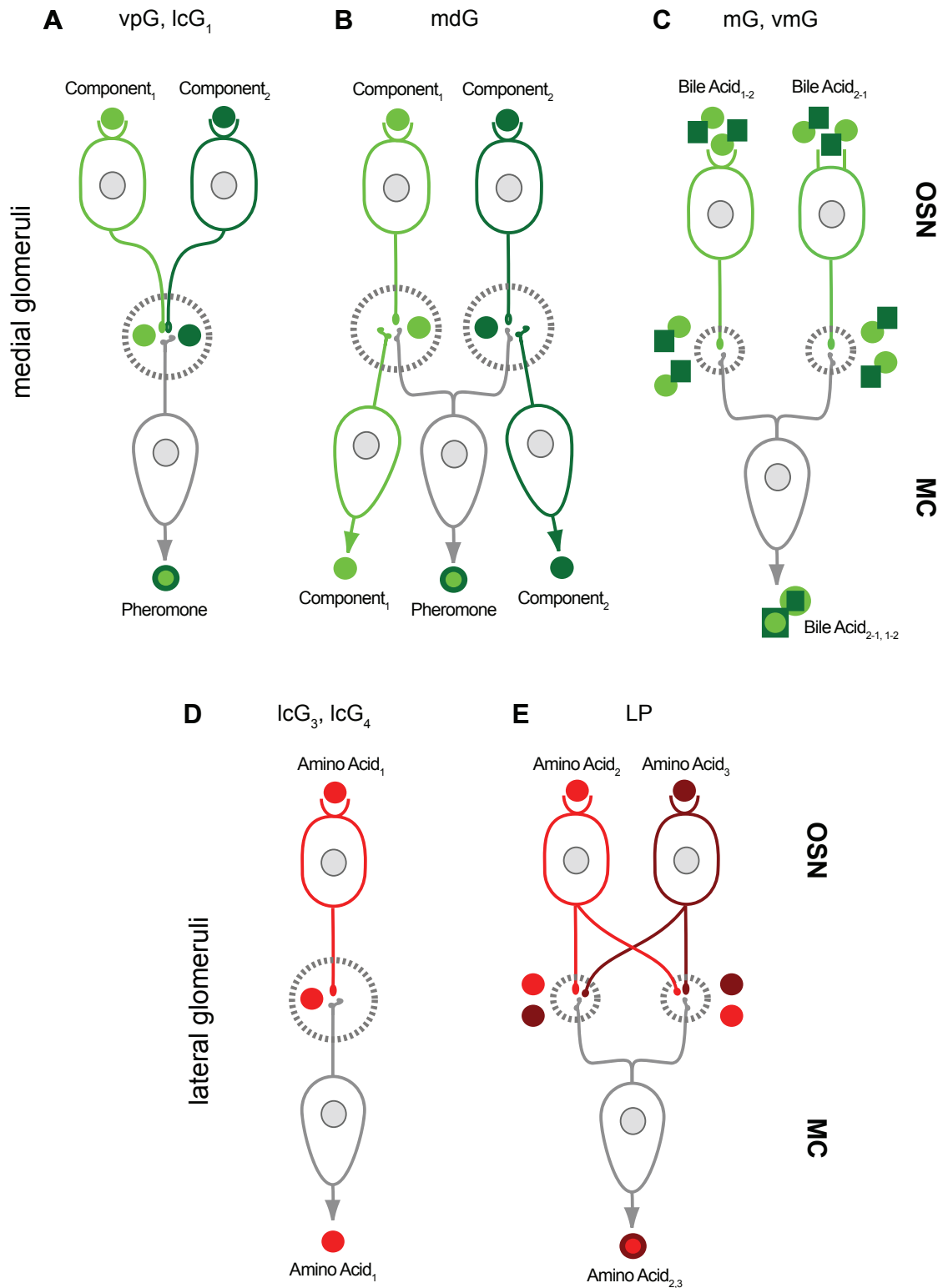
Figure 38. Summary of Different Types of Glomeruli in the Zebrafish Olfactory System

195

Supplemental Figure 2. A glomerular tuft double labeled with anti SV_2 and anti TH antibodies. Anti-TH (**A**) and anti-SV_2 (**B**) labeling co-localized in much of the glomerular tuft, suggesting that a significant portion of the synaptic terminals inside the core of a glomerulus represents the innervation by juxtaglomerular interneurons (JGC). This image depicts a medium-sized ventral glomerulus (vG_x) in an olfactory bulb of a larval zebrafish (approximately 20 days old).
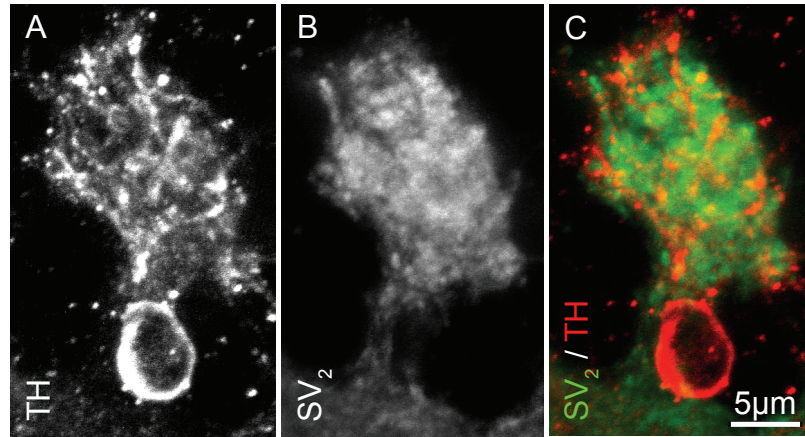
Figure S2. A Glomerular Tuft Double Labeled with Anti SV$_2$ and Anti TH Antibodies

Supplemental Figure 3. Overview of juxtaglomerular (JGC) interneurons and their innervation of glomeruli in ventral (**A**), dorsal (**B**) and lateral (**C**) olfactory bulbs. TH IR was diffuse and did not permit identification of glomerular clusters and / or individual glomeruli (compare to anti-SV_2 labeling in Figure 24). Most JGC somata were located in areas devoid of glomeruli, such as the border region between lcG and vmG (see arrows in **A$_2$**). TH IR in the glomerular tufts of some large glomeruli varied consistently; the mvpG always contained less TH labeling than the adjacent vpG (**A$_1$**), and the tuft of lcG$_1$ always contained less TH IR than the lcG$_{2,3}$ (**C$_1$**).
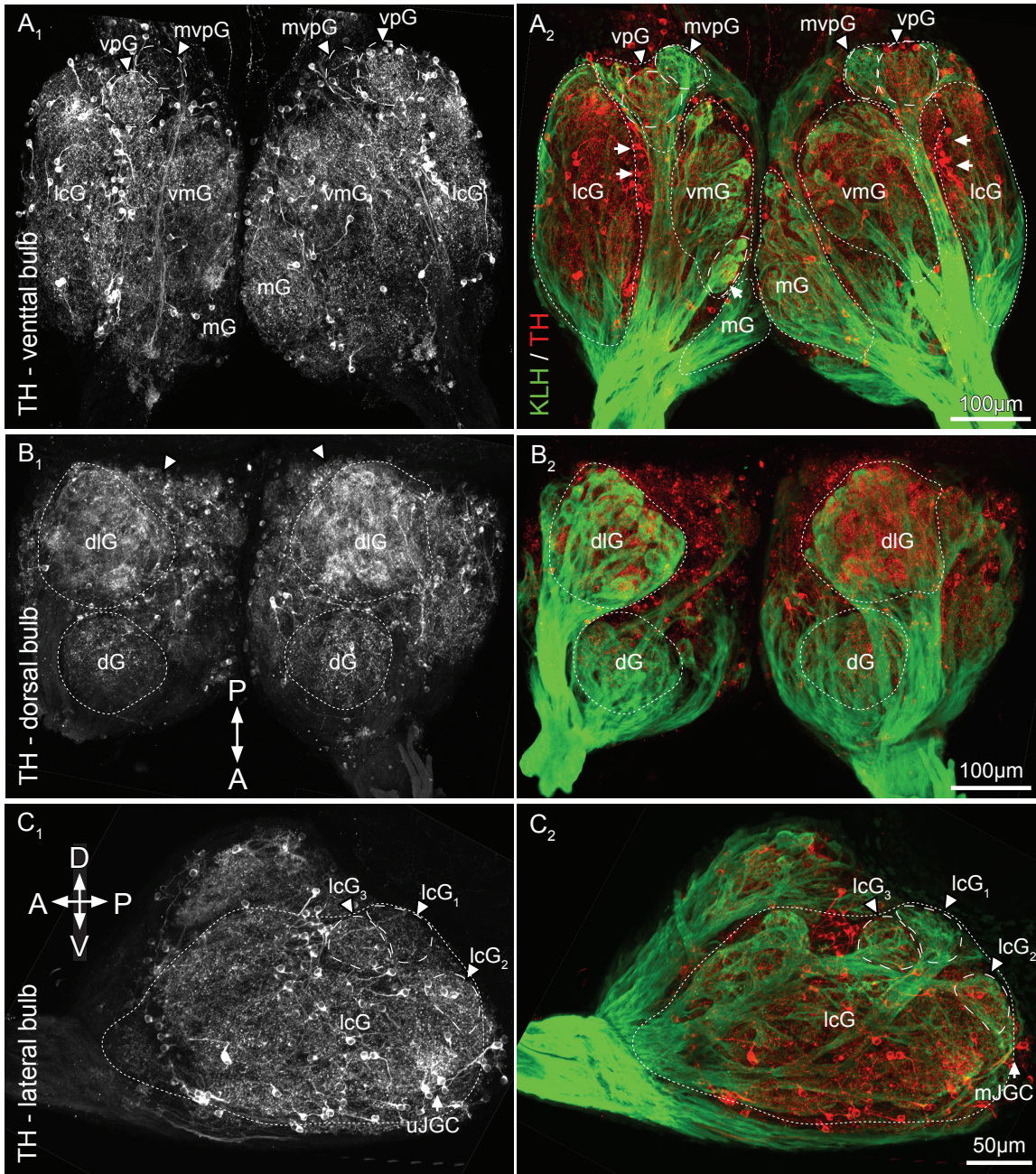
Figure S3. Overview of Juxtaglomerular Interneurons and Their Innervation of Glomeruli in Ventral, Dorsal and Lateral Olfactory Bulbs

Supplemental Figure 4. Overview of mitral cells (MCs) and their innervation of glomeruli in ventral (**A**), dorsal (**B**) and lateral (**C**) olfactory bulbs. MC in some areas appeared to be completely labeled (see lateral plexus LP in C_1) and in other cases MC labeling was incomplete (e.g., the single MC indicated by an arrowhead in A_1). Structures labeled by the dye application included the medial olfactory tract (MOT in A_1), and the nervus terminalis (NT in A_1), both of which were easily distinguished from other structures.
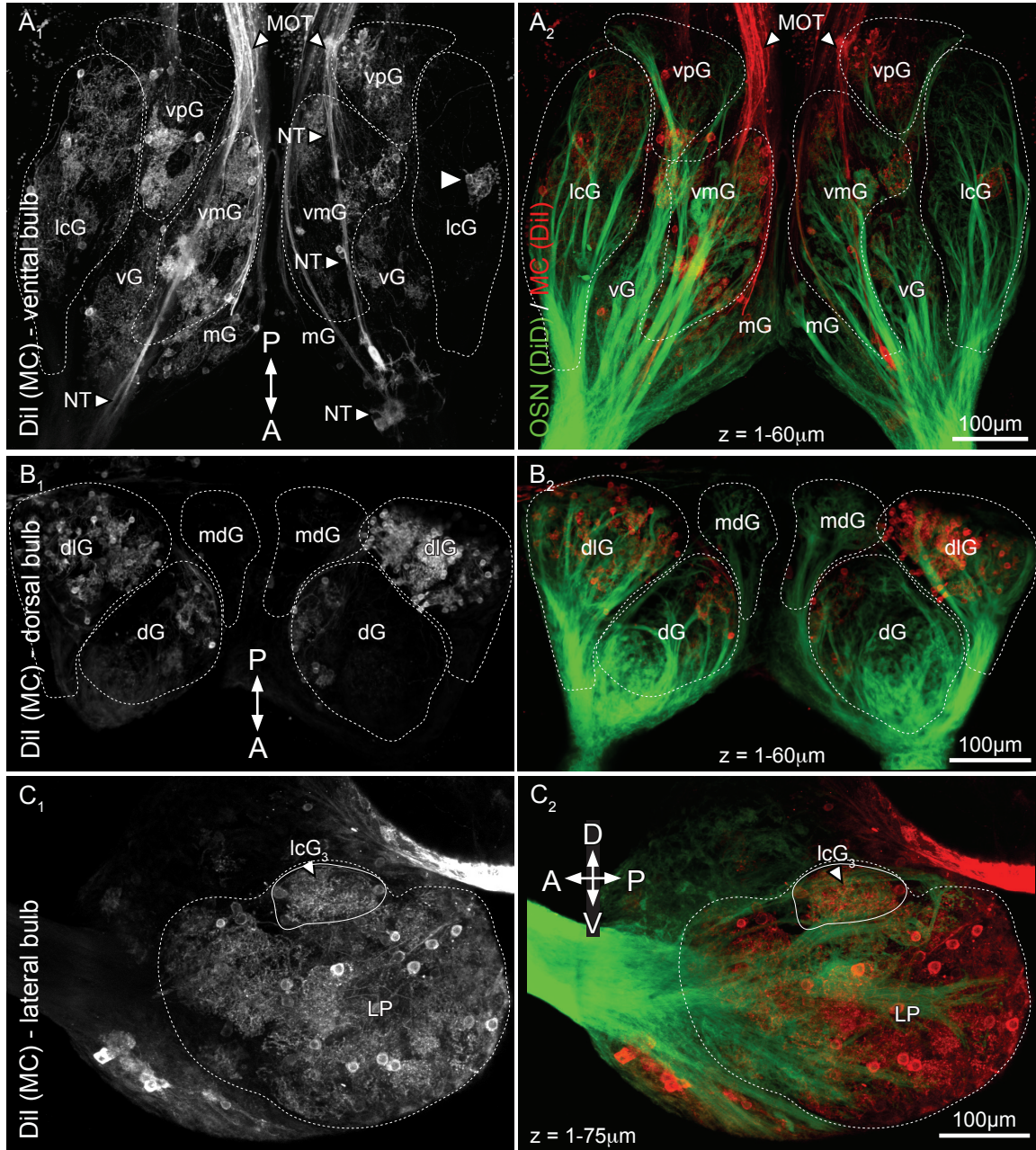
Figure S4. Overview of Mitral Cells and Their Innervation of Glomeruli in Ventral, Dorsal and Lateral Olfactory Bulbs

Chapter 5

Development and Plasticity of Different Types of Glomeruli

5.1 Summary

Vertebrates have the ability to detect and discriminate large sets of odorants, and different types of olfactory information, such as pheromonal cues or food odors, are transduced by different sensory neuron populations that innervate glomeruli in separate olfactory pathways. We have recently identified two anatomically distinct populations of glomeruli in the zebrafish olfactory system that may constitute such olfactory pathways. Thus, we described a small group of particularly large glomeruli that were identifiable in almost all animals examined, while the remainder of glomeruli (80% of total) was comparably small and anatomically indistinguishable. In the present study we examined and compared the development of these two different glomerular populations. The largest glomeruli, consisting of putative pheromonal glomeruli and a small set of amino-acid responsive glomeruli, were among the first to differentiate and in 72 hour embryos they already attained a configuration that closely resembled their mature appearance. The cross-sectional area of these glomeruli continued to increase throughout the end of larval development, at which time they were among the largest units in the olfactory system. In contrast, the more numerous, small and anatomically indistinct glomeruli that are responsive to amino acids and bile acids formed only after zebrafish hatched, apparently by segregating from large and diffusely-innervated protoglomeruli. The differentiation of these glomeruli proceeded with conspicuous variation in their numbers and arrangements among larvae and even between the two olfactory bulbs of individual fish. We used transgenic zebrafish to investigate the effects of altered olfactory environments on the development of amino acid-responsive lateral cluster glomeruli, which exist both as large, individually identifiable glomeruli and as smaller indistinct

units. In larvae that were reared in an amino acid-enriched environment, we found no difference in the number or arrangement of the large glomeruli when compared to control, whereas the smaller, anatomically indistinct glomeruli were more numerous and had reduced cross-sectional areas. Collectively, our results suggest that glomeruli in different olfactory pathways emerge via distinct developmental processes either independent of sensory experience or via experience-dependent reorganization of glomerular precursors.

5.2 Introduction

Throughout the animal kingdom, odorants are transduced by large arrays of different olfactory sensory neuron (OSN) types, each of which is defined by its expression of a single functional olfactory receptor (OR; Serizawa et al., 2004). The OSNs appear to be randomly distributed in the sensory epithelium, but their axonal projections into the olfactory bulbs become highly organized, and axons that originate from a particular OSN type converge onto specific spheroidal glomeruli (Sakano, 2010, Mombaerts, 2006). OSNs and glomeruli that process different types of olfactory information, such as pheromonal cues or food odors, constitute separate olfactory pathways (Dulac and Wagner, 2006, Touhara and Vosshall, 2009, Munger et al., 2009, Hildebrand and Shepherd, 1997). In mammals, typical feeding-related odors and non-pheromonal social odors are transduced by a large population of OSN types (~1200) in the main olfactory epithelium. Each OSN type selectively innervates a small number of glomeruli in the main olfactory bulbs (MOB; Vassar et al., 1993, Ressler et al., 1993, Mombaerts, 1996), and each glomerulus appears to include all dendrites of a small set of dedicated bulbar output neurons, the mitral cells (Shepherd, 1972, Dhawale et al., 2010). In contrast, mammalian pheromones are transduced by an unrelated set of chemosensory receptors in the accessory olfactory epithelium, and these cells appear to non-specifically innervate a range of glomeruli in the accessory olfactory bulb (AOB; Rodriguez et al., 1999, Belluscio et al., 1999). Finally, unlike MOB glomeruli, those in the AOB are innervated only broadly by mitral cells, and each mitral cell can innervate multiple glomeruli at once (Mori et al., 1983, Meisami and Safari, 1981, Meisami and Bhatnagar, 1998, Macrides and Schneider, 1982).

Similar to its mammalian counterpart, the zebrafish olfactory system is partitioned into distinct olfactory pathways but both of these are contained in a single compact, and highly accessible olfactory system. Specifically, the mature zebrafish olfactory system contains approximately 280 glomeruli (~140 per olfactory bulb) that are organized based on their selective innervation by distinct OSN populations (Chapter 3, Sato et al., 2005). Glomeruli in the lateral olfactory bulbs are innervated by microvillar OSNs, which are responsive to amino acids that emanate from food sources (Koide et al., 2009, Friedrich and Korsching, 1998, Friedrich and Korsching, 1997). Medial glomeruli are responsive to social odors, such as bile acids that play roles in kin detection (Hara, 1994, Hamdani and Døving, 2007, Friedrich and Korsching, 1998). The medial olfactory bulbs are additionally innervated by putatively pheromone-sensitive crypt sensory neurons (Sorensen et al., 1998, Hamdani and Døving, 2007), and we have recently identified specific glomeruli that are targeted by crypt cell axons (Chapter 3).

In addition to their separation into lateral and medial glomeruli, different types of glomeruli can be discriminated based on several robust anatomical criteria (see Chapter 3 and Chapter 4). For example, we have found that presumptive pheromonal glomeruli are particularly large, are innervated by multiple distinct OSN axon bundles, and are unambiguously identifiable from animal to animal. The remaining glomeruli, viz. those responsive to amino acids and bile acids, are much smaller, anatomically indistinguishable and variable in number and distribution. Armed with this background understanding of the structure of the zebrafish olfactory system, one can now begin to address developmental questions. We therefore ask if large glomeruli develop in the same manner as the small indistinguishable ones, and if they form according to a similar

206

time course and under influence of the same factors.

Currently available data suggest that zebrafish olfactory glomeruli begin to develop approximately 24 hours post fertilization (hpf) as transient pioneer neurons in the olfactory placodes differentiate. The pioneer neurons extend fibrous processes to the developing forebrain (Whitlock and Westerfield, 1998, Hansen and Zeiske, 1993), and by 48hpf axons from newly differentiated OSNs extend along these scaffolds to contact bulbar mitral cells and form anatomically diffuse protoglomeruli (Miyasaka et al., 2005, Li et al., 2005b). Zebrafish protoglomeruli respond only non-selectively to certain classes of odorants (e.g., bile acids), suggesting that they are innervated by multiple OSN types. New glomeruli then arise via progressive subdivision of protoglomeruli after hatching, producing a number of smaller daughter glomeruli that are more narrowly tuned to individual odorants (Li et al., 2005a). Similar processes have been documented in mammals (Potter et al., 2001), and several studies in mice have shown that the restriction of OSN axons to discrete glomeruli is dependent on sensory input (Zou et al., 2004, Oliva et al., 2008, Kerr and Belluscio, 2006). However, it is not known whether these processes underlie the development of all glomeruli, or if there exist different developmental mechanisms in the otherwise distinct main and accessory olfactory pathways.

In the present study we examine the development and, in particular, the postnatal maturation of glomeruli in the entire zebrafish olfactory system. We find that putatively pheromonal glomeruli as well as a small number of amino acid-responsive glomeruli differentiate very early and apparently mature independent of olfactory input. In contrast, the majority of glomeruli develop via observable segregations from larger

protoglomerular structures, often with considerable morphological variation, which we attribute to sensory experience. To our knowledge this is the first study to characterize the development of an entire population of vertebrate glomeruli and to show that glomeruli arise via distinct developmental mechanisms.

5.3 Methods

5.3.1 Animals Used for Morphological Analysis

Adult zebrafish (AB strain, University of Oregon) were maintained according to standard guidelines (Nüsslein-Volhard and Dahm, 2002). Embryos, obtained by breeding adult fish during the first hour of the light period, were kept in tubes with mesh bottoms held in a flow-through nursery unit at 28.5 ^{o}C. The water that was supplied to this unit was not recirculated but was a continuous drip of fresh water that was filtered through a series of sand filters and a charcoal filter. Starting at 5 days post fertilization (dpf), larvae were fed crushed flake food (Omega Sea, Sitka, AK, USA) and Artemia (Salt Creek, Salt Lake City, UT, USA). At 7 dpf the fry were transferred to 1.5 L rearing tanks (Aquatic Habitats, Apopka, FL, USA) connected to the same water source as described above. When necessary, debris was siphoned from these tanks. The developmental stage of embryos ($\leq$ 72 hpf) was determined with reference to standard guidelines (Kimmel et al., 1995), while that of hatched larvae was determined by their body length (Parichy et al., 2009). Brains obtained from larvae of the same developmental stage often varied in size and we therefore also grouped animals according to brain size (Table 5). The number of animals used to produce data shown in this manuscript is listed for every developmental stage in Table 5. All experiments were conducted in accordance with the 'Guide to the Care and Use of Laboratory Animals' established by the Canadian Council for Animal Care.

5.3.2 Tissue Preparation

Embryonic and larval zebrafish were killed by immersion in ice-cold water ($< 4^{o}$C) for ~1 minute (Macdonald, 1999). Whole embryos and heads of larvae were then fixed

by immersion in fresh 2% paraformaldehyde (PFA; Electron Microscopy Sciences, Hartfield, PA, USA) in phosphate buffered saline (PBS; in mM: 100 Na_2HPO_4, 140 NaCl, pH 7.4) for 6 h at room temperature or overnight at 4^oC. After fixation, all tissue was washed 4 times in PBS over 2 hours and then immersed in a PBS-based blocking solution (Kaslin and Panula, 2001) containing 0.25% Triton X-100, 2% dimethyl sulfoxide, 1% normal goat serum and 1% bovine serum albumin (PBS-T; all from Sigma) for $\geq$ 12 hours at 4^oC. Unless noted otherwise, PBS-T was used for all subsequent washing steps (e.g., after primary and secondary antibody incubation), and each washing step consisted of five rinses with PBS-T over a period of approximately 4 hours.

5.3.3 Antibodies and Specificity

We used antibodies that we have previously established as markers for the general structure and functional distribution of glomeruli in the mature zebrafish olfactory system (Table 6, see also Chapter 3 and Chapter 4). Briefly we used a combination of anti-keyhole limpet hemocyanin (KLH) and anti-synaptic vesicle protein 2 (SV_2) to label the presynaptic compartments of glomeruli throughout the olfactory system. We complemented these labels with antibodies against the G-protein α subunits $G_{\alpha\ s/olf}$ and $G_{\alpha o}$ and the calcium binding proteins calretinin and S_{100} (all in Table 6) to selectively label functional subgroups of olfactory glomeruli.

All of these antibodies have been used previously in zebrafish by us and other groups (Table 6), and the labeling that we achieved with these markers was highly consistent with what we expected based on these reports. We thus conducted only negative controls by processing brains (described below) without incubation in primary antibodies. These specimens exhibited no detectable fluorescence.

5.3.4 Immunocytochemistry

Mixtures of two primary antibodies were diluted in PBS-T and tissue was incubated in these solutions for 5-7 days at 4°C with gentle agitation. The tissue was then washed as described above and incubated in a mixture of appropriate secondary goat antibodies conjugated to various Alexa Fluor dyes (1:50 dilution; Invitrogen, Burlington, ON, Canada) for 4-5 days at 4°C.

Before mounting, brains were washed (above) and then immersed for 24 hours in glycerol mountant, a 3:1 solution of glycerol to 0.1M Tris buffer (pH 8.0) containing 2% (w/v) n-propyl gallate (all from Sigma), for 24 hours. Brains were then mounted in fresh glycerol mountant between two coverslips (separated with stacks of coverslip fragments to minimize tissue compression) and sealed with nail polish.

5.3.5 Microscopy, Image Analysis and Processing

Specimens were viewed with a LSM 510 or LSM 510 META laser scanning confocal microscope (Carl Zeiss Inc., Thornwood, NY, USA). Serial optical sections were obtained from the olfactory bulbs at 1μm intervals to a maximum depth of 60-80μm. To achieve optimal visualization of all glomeruli, we remounted and repositioned most specimens and imaged them from ventral, dorsal and lateral viewplanes.

Optical sections were viewed and processed with ImageJ software (http://rsb.info.nih.gov/ij), and glomeruli were identified and mapped based on previously established criteria (Chapter 3). Briefly, glomeruli were counted and measured by stepping through optical sections and tracing outlines of afferent innervation to identified units (in ImageJ). Average counts and sizes were based on observations from at least 5 fish at each developmental stage as listed in Table 5. All glomeruli that could be detected

were included for numerical analyses. Glomeruli that were identified in four or more specimens were assigned specific names (e.g., lateral cluster glomerulus 3 lcG_3), while the remaining units were only assigned to appropriate regions (e.g., lateral cluster glomerulus lcG_x). Glomerular maps thus depict the characteristic arrangement of all repeatedly-identifiable glomeruli plus the average number of glomeruli that were not unambiguously identifiable. Glomerular nomenclature was used as established in Chapter 3 and in (Koide et al., 2009, Dynes and Ngai, 1998, Baier and Korsching, 1994).

Images presented in this report are projections of optical sections to a depth indicated in each figure. Three-dimensional reconstructions of original data were created with the ImageJ 3D viewer (Schmid et al., 2010) and resulting images were adjusted for brightness and contrast in Photoshop. Figure plates were created with InDesign and accompanying drawings were created with Illustrator (all from Adobe Systems Inc., San Jose, CA, USA). Supplemental videos were created with ImageJ and annotated and edited with Apple iMovie.

5.3.6 Animals Used for *In Vivo* Experiments

To study glomerular development and its modifications by experience *in vivo*, we employed readily available transgenic zebrafish lines to drive fluorescence in amino acid-responsive lateral glomeruli as described previously in Koide et al. (2009). Transgenic adult zebrafish containing a GAL4FF transcription activator at the SAGFF27A gene locus and UAS:GFP reporter fish (Asakawa et al., 2008) were maintained according to standard guidelines at the RIKEN Brain Science Institute. 27A-GFP embryos were obtained by crossing GAL4 driver fish with UAS:GFP reporter fish and screened for fluorescence in lateral glomeruli. Positive embryos were maintained at 28.5 $^\circ$C in

zebrafish Ringer's solution (in mM: 39 NaCl, 1.0 KCl, 1.8 CaCl$_2$, and 1.7 HEPES, pH 7.2) supplemented with 100 U/mL penicillin and 100 µg/mL streptomycin. Pigmentation was suppressed by adding 0.002% phenylthiourea (Nacalai Tesque, Kyoto, Japan) to the rearing medium at 12 hours after fertilization.

5.3.7 Olfactory Enrichment Experiments

Immediately after hatching (> 72hpf), individual larvae were imaged with a confocal microscope (see below) and then transferred in pairs to small rectangular mesh chambers (l=4.0cm, w=1.2cm, h=2.0cm) inside a custom-built nursery unit, consisting of a rectangular acrylic tank (l=18cm, w=12cm, h=1.5cm) through which a constant flow (60mL / min) of fresh dechlorinated water at 28.5 ^{o}C was maintained. Single pulses (2.5mL) of an amino acid mixture (Ala, His, Lys, Met, Phe, Trp, and Val, all from Sigma Chemical Co., Tokyo, Japan) were injected into the water inflow of the nursery every 30 minutes for the duration of the experiment (14 days). The final odor concentration that larvae were exposed to was 1µM of each amino acid, and a 10'000-fold clearance of these amino acid stimuli occurred after approximately 4 minutes. A video showing an example of such a trial is supplied as Supplemental Movie 4. Finally, in control experiments, water alone, without amino acids, was injected into the flow.

5.3.8 *In Vivo* Imaging of Glomerular Development

Starting at 3dpf, the olfactory bulbs of larvae were imaged every second day to a maximum of 14 days according to a previously established protocol (Sato et al., 2005). Briefly, fish were anesthetized with 0.016% buffered tricaine (Nacalai Tesque) and placed in a small drop of 3% methyl cellulose (Sigma) in zebrafish Ringer's solution. The fish were carefully positioned with forceps and covered with 2% low melting-point

213

agarose (Sigma) in zebrafish Ringer's solution. Olfactory bulbs were then imaged with a Fluoview 500 confocal laser-scanning microscope (Olympus, Tokyo, Japan) to a maximum depth of 100μm at 1μm intervals. Each larva was imaged from the dorsal and the left lateral aspect in order to get the best image of 27A-GFP labeled lateral cluster glomeruli. After imaging, the larvae were carefully removed from the agarose and returned to the nursery unit. We used a total of 22 fish in these experiments.

5.3.9 Identification of Glomeruli in Transgenic Larvae

In olfactory bulbs of 27A-GFP larvae, only the sensory neuron axons and their terminals were labeled with GFP. We thus used the following criteria to identify glomeruli, consistent with our approach described in Chapters 3 and 4. A glomerulus was expected to be roughly spherical and encapsulated by fluorescent fibers. Furthermore, the structure had to possess a visible afferent stalk that was connected to the olfactory nerve. To confirm that these criteria allowed us to identify glomeruli corresponding to our other anatomical data, we labeled fixed brains from transgenic larvae with the same antibodies described above and compared them with representative data. All image analysis and processing was conducted as described above.

5.3.10 Statistics

Anatomical data obtained from our immunohistochemistry experiments were organized and pooled across animals according to identity of the glomerulus (e.g., lcG_3) or the region in which the glomerulus was located (e.g., lcG_x), separately for each developmental stage. The data presented in this manuscript are means and their standard errors, unless indicated otherwise. To compare numbers and sizes of glomeruli between different developmental stages we conducted analyses of variance (ANOVA) of

developmental stage vs. number *or* area of glomeruli. Data obtained from repeated *in vivo* imaging of the same larvae were similarly treated, but compared via one-way analysis of variance for repeated measures (RM ANOVA). Degrees of anatomical variability among the numbers of glomeruli in certain areas of the olfactory bulbs were furthermore evaluated with Levene's test for equality of variances (see also Chapter 3). All statistics were analyzed with SPSS software (Chicago, IL, USA).

5.4 Results

5.4.1 Organization of Olfactory Glomeruli in Juvenile Zebrafish

The number and organization of olfactory glomeruli in juvenile zebrafish (~ 6 weeks post fertilization) closely resembles that in mature animals, as described in Chapter 3. Specifically, we identified 226.8 ± 17.8 glomeruli in the juvenile olfactory system, with nearly equal numbers in the left (114.8 ± 9.2) and right (112.0 ± 11.6) olfactory bulbs (means and standard deviations from n = 5 animals). The glomeruli clustered in eight anatomically distinct regions (Figures 39 and 40) as discussed below. As in adult animals, the largest glomeruli were scattered throughout the olfactory bulbs individually or in small groups. Six mediodorsal glomeruli (mdG) were located in the dorsal region of each dorsal olfactory bulb (mdG in Figure 39A). Each of these glomeruli was innervated by anatomically distinct fascicles of OSN afferent axons (Figure 39A arrows), some of which could be further differentiated biochemically. For instance, mdG_2 and mdG_5 were selectively innervated by S_{100} IR (Figure 39B) and $G_{\alpha o}$ IR axons (Figure 39C), respectively. The innervation to the remaining mdG was not labeled by these or other OSN axon markers but these glomeruli were nevertheless identifiable because of their stereotypic arrangement.

In the ventral olfactory bulbs, we identified three ventroposterior glomeruli (vpG), with large cross-sectional areas like the mdG (compare cross sectional areas in Table 7). While all vpG were visibly innervated by OSN (see KLH in Figure 40A), none of these axons labeled with antibodies against G-protein α subunits or the calcium binding proteins, and because of this they were difficult to identify in some specimens (see vpG in Figures 40B and 40C). Finally, we consistently identified three large lateral cluster

glomeruli in juvenile zebrafish ($lcG_{1, 3, 4}$ in Figure 40E). The afferent innervation of $lcG_{3,4}$ was strongly calretinin IR (Figure 40F), but the innervation of lcG_1 was $G_{\alpha\ s/olf}$ IR (Figure 40G). Like the other large glomeruli, $lcG_{1,3,4}$ were identifiable in every specimen (Table 7). Collectively, these 12 glomeruli were the largest and most consistently identifiable units in juvenile zebrafish (Table 7), as well as in adult zebrafish (Chapter 3).

In contrast to these few large and individually identifiable glomeruli, the majority of glomeruli were tightly clustered in anatomically separate regions of the olfactory bulbs (see dG, dlG, mG, vlG, vmG, in Figures 39 and 40). These glomeruli were irregularly shaped, smaller than any of the units described above (Table 7) and almost always targeted by OSN axons that labeled with both calretinin and $G_{\alpha\ s/olf}$ antibodies (Figures 39D and 39E and Figures 40B and 40C). These glomeruli were difficult to consistently identify and we often observed variations in their numbers and arrangements, even in the left and right olfactory bulbs of single animals (see vG in Figure 40D and representative raw data in Figure S5). An overall comparison of the between-specimen variance among numbers of glomeruli in dG, dlG, mG, vlG and vmG (Table 7) with variations among large glomeruli (above) was statistically significant ($p < 0.05$; Levene's test), as were individual comparisons between the glomeruli in dG, dlG, mG, vlG and vmG and the large glomeruli (all $p < 0.05$ in Student's t-tests). These results confirm that clusters of some glomeruli are more anatomically variable than others. In the following sections we describe two distinct developmental processes for the large and anatomically invariant glomeruli and the small and anatomically variable units.

217

5.4.2 Normal Development of Mediodorsal Glomeruli (mdG)

The first rudiments of what later became two bilaterally symmetric clusters of large mdG (e.g., Figure 39) were visible at 48hpf, approximately one day before zebrafish hatched. At this time each mdG cluster consisted of three diffuse aggregates of SV_2 IR puncta in the mediodorsal olfactory bulb primordia (Figures $41A_1$ and $41B_1$). The sizes, shapes and arrangements of these mdG rudiments were similar between embryos (compare mdG in Figures $41D_1$ and $41E_1$ with mdG in Figure S6), but they lacked clear innervation by OSN axons, which made it difficult to unambiguously identify the same rudiments in different animals (e.g., mdG_x in Figures $41A_1$ and $41B_1$ and throughout Figure S6). mdG_6, however, could be reliably identified based on its reproducible position as the most ventral glomerulus of this cluster (Figures $41A_1$ and $41B_1$), at 48hpf and during subsequent developmental stages (below).

By 72hpf, we identified approximately five mdG in roughly triangular, nearly bilaterally symmetric clusters that did not differ in number between left (5.0 ± 0.9) and right (5.0 ± 0.9) olfactory bulbs. mdG_2 and mdG_5 were visibly and selectively targeted by S_{100} IR (Figure $41A_2$) and $G_{\alpha o}$ IR (Figure $41B_2$) axons, respectively, while the remaining mdG were exclusively SV_2 IR. From our data, it is unclear how new mdG were added to this cluster between 48 and 72 hpf, but the size of the mdG that were already present at 48 hpf did not change significantly (see cross-sectional area from 48-72 hpf in Figures 42A and 42D). This implies that that no major structural reorganization of pre-existing mdG rudiments occurred and that they presumably did not give rise to new glomeruli.

After hatching, the number and arrangement of the mdG remained remarkably

consistent and they could be increasingly distinguished from one another, based on their clearly separate glomerular tufts, robust position and selective labeling (Figures $41A_3$ and $41B_3$). This observation is also reflected by a visible decrease in the variance in the numbers of mdG that we identified in individual larval stages: beginning in the mid-larval stage there were almost no animals in which we did not identify 12 mdG (6 per olfactory bulb; Figure 42). In Figure 42, it is also important to note that at no time during development did we observe a decrease in mdG cross-sectional area. Instead, the maturation of all mdG was accompanied by a continuous and significant increase in cross-sectional area ($p < 0.05$ for all units, ANOVA), which was particularly visible in and after the mid-larval stage, at which time we observed that the OSN axon innervation to the mdG arrived from multiple distinct axon bundles (see arrows in Figure $41A_{3-4}$). Such innervation patterns persisted throughout later developmental stages, in which mdG were among the largest and most reliably identified glomeruli (Figure 39A-C; Table 7).

5.4.3 Development of Calretinin IR and $G_{\alpha\ s/olf}$ IR Glomeruli

The majority of zebrafish olfactory glomeruli, specifically those that are small and calretinin and $G_{\alpha\ s/olf}$ double IR (e.g., Figures 39 and 40), were undifferentiated and instead consisted of five large and diffuse protoglomeruli in embryonic zebrafish (see dpG, dl$p$G, mpG, vm$p$G and vl$p$G in Figure S7). These protoglomeruli all labeled with calretinin and $G_{\alpha\ s/olf}$ antibodies and were larger than the glomeruli proper of zebrafish embryos (see table in Figure S7G).

Shortly after hatching, we observed progressive subdivisions of the synaptic tufts and innervation of all but one protoglomerulus (vm$p$G, see below). For example, the dorsal protoglomerulus (dpG in Figure $43A_{1,2}$) was replaced by six to seven small,

roughly spherical SV_2 IR tufts that we refer to as dorsal glomeruli (dG). In three-dimensional reconstructions, each dG tuft was clearly visible as a separate spheroidal structure as shown in two different larvae in Figures $43B_1$ and $43C_1$. Numerically, the emergence of dG correlated with a decrease in the cross sectional area of the dpG after hatching (see hatching in Figure 44A). Specifically, the area that was previously occupied by the dpG (469.8 ± 35.2 μm^2 per bulb) was now occupied by dG with a combined cross-sectional area that was nearly eqivalent (522.4 ± 20.9 μm^2 per bulb). Moreover, all newly-formed dG were innervated by both calretinin IR and $G_{\alpha \ s/olf}$ IR axons (Figure $S8A_1$ and $S8B_1$) as was the protoglomerulus previously located in this region (Figure $S7A_1$ and $S7B_1$). Collectively, these data suggest that the dorsal protoglomerulus is replaced by daughter dG after zebrafish hatch. We made nearly identical observations for three additional protoglomeruli, the dl$p$G, mpG and vl$p$G as shown in Figure $43B_2$-C_4 and Figure 44B-D, but for brevity these observations will not be presented in detail.

Glomeruli that originated from large, calretinin IR and $G_{\alpha \ s/olf}$ IR protoglomeruli generally did so with variation in their numbers and distributions. For example, the data shown throughout Figures 43B and 43C are from two larvae of the same clutch, reared together in the same tank. As is evident from the maps and the numbers at the bottom of each panel, the arrangement of daughter glomeruli varied between animals (Figures $43B_1$ and $43C_1$) and also between the two olfactory bulbs of an individual fish (Figures $43B_3$ and $43B_4$). Such variations prevented us from unambiguously assigning identities to most glomeruli, and these are thus denoted 'x' in Figure 43 and other parts of this manuscript.

Anatomical variability was particularly apparent in the OSN innervation of units that emerged well after larvae hatched. The ventromedial glomeruli, for example, developed from bilaterally symmetric ventromedial protoglomeruli (vm$p$G in Figures 45A$_1$ and 45A$_2$). In mid-larvae, the OSN innervation to the vm$p$G reorganized and formed several separate axon stalks that innervated distinct terminal zones, which we refer to as ventromedial glomeruli (see vmG denoted by 'x' in Figures 45B$_1$ and 45B$_2$). This reorganization almost always occurred with visible variation between the olfactory bulbs of individual animals; in the specimen shown in Figure 45B, for example, we identified five vmG with distinct OSN innervation in one olfactory bulb (Figure 45B$_1$), while only a single vmG appeared to have differentiated from an otherwise diffuse aggregate of fibrous processes in the other olfactory bulb (Figure 45B$_2$). Such variation persisted into the juvenile stage, where we often observed different numbers and arrangements of vmG bilaterally in individual animals. Thus, in the specimen shown in Figure 45C, we identified 17 vmG in the left olfactory bulb (Figure 45C$_1$) but only 11 vmG in the right olfactory bulb (Figure 45C$_2$). Similar differences in the number of vmG are also shown in the olfactory bulbs of another zebrafish in Figure S5 (see vmG). Thus, the majority of zebrafish olfactory glomeruli develop from loosely organized protoglomeruli at varying times throughout larval development, with visible variations in numbers and distributions.

5.4.4 Lateral Cluster Glomeruli (lcG) Develop Via Two Mechanisms

The large and stereotypic amino acid responsive lcG$_{3,4}$ (Figure 40 and Table 7) were first identifiable as two irregularly shaped structures in the lateral olfactory bulbs of 48hpf embryos (lcG$_{3,4}$ in Figure 46A). Both glomeruli were connected via separate axon

stalks to the olfactory nerve (arrowheads in Figure 46A) and co-localized with small aggregates of SV_2 IR puncta (white pixels in Figure 46A). By 72hpf, $lcG_{3,4}$ became increasingly compact (Figure 46B) and after hatching they attained a nearly spheroidal shape (Figures $46C_1$ and $46D_1$). In all stages of larval development we identified precisely two $lcG_{3,4}$ per olfactory bulb (see number of $lcG_{3,4}$ in Figures 47A and 47B). As with other large glomeruli (above), the cross-sectional area of $lcG_{3,4}$ increased throughout larval development so that they eventually constituted some of the largest glomeruli in the entire olfactory bulbs (Table 7).

In contrast, additional lateral glomeruli (lcG_x) apparently developed via segregation from a separate lateral protoglomerulus (lpG). This protoglomerulus first emerged between the lcG_3 and lcG_4 starting at 72hpf (Figure 46B). However, immediately after hatching, the cross sectional area of lpG decreased (see lpG in Figures 47C and 47D) and at the same time several lcG_x appeared in its place, between $lcG_{3,4}$ (lcG_x in Figure $46C_{1-2}$). The average cross sectional area of newly formed lcG_x ($58.5 \pm 5.2\mu m^2$) was significantly smaller than that of the lpG ($95.8 \pm 10.7\mu m^2$; $p < 0.05$, ANOVA), suggesting that lcG_x may have separated from lpG. As with other glomeruli that formed via segregation from larger protoglomeruli, the number and distribution of newly formed lcG_x commonly varied. Some early larvae apparently had only two lcG_x per olfactory bulb (Figure $46C_2$) while in others we identified four lcG_x per bulb (Figure $46D_{2-3}$). A comparison of between-specimen variance in the number of lcG_x with that in the number of $lcG_{3,4}$ revealed a highly significant difference ($p < 0.001$; Levene's test), confirming that lcG_x are more variable in number than $lcG_{3,4}$. Collectively, these data thus suggest that the lateral glomeruli develop via two distinct mechanisms that yield either large and

anatomically stereotypic glomeruli ($lcG_{3,4}$) or smaller, anatomically variable glomeruli (lcG_x).

5.4.5 Olfactory Experience Changes Development of lcG_x

The development of glomeruli described thus far occurred under rearing conditions in which fish were raised in tanks that were continuously supplied with fresh water. We next examined the effects of an amino acid-enriched odor environment on the development of lcG, which are all fluorescently labeled and readily accessible for *in vivo* imaging in 27A-GFP transgenic zebrafish (Koide et al., 2009). Figure 48 shows a lateral olfactory bulb of a 27A-GFP larva, oriented and stained in the same manner as for our other anatomical descriptions in Figure 46C and 46D. In agreement with our other results, $lcG_{3,4}$ were brightly labeled by the 27A-GFP transgene (Figures $48A_1$ and $48A_2$) and newly formed lcG_x could be identified between $lcG_{3,4}$ (lcG_x in Figure $48A_2$). The 27A-GFP label overlapped fully with calretinin IR (Figure 48B) and SV_2 IR (Figure 48C), confirming that the structures labeled with the 27A-GFP transgene are lateral glomeruli.

Viewed *in vivo*, $lcG_{3,4}$ were easily identifiable as brightly labeled structures located superficially on the lateral surface of each olfactory bulb (Figure $49A_1$). Throughout our *in vivo* imaging experiment (3-14dpf), the two $lcG_{3,4}$ were always visible, as shown in a series of images obtained from a single control larva in Figure $49A_1$ to $49F_1$. Beneath $lcG_{3,4}$, OSN fibers loosely targeted what appeared to be the lateral protoglomerulus (lpG) in addition to the similarly sized lateral plexus (see lpG and LP in Figure $49B_2$-F_2). It was difficult to identify lcG_x within this diffusely organized neuropil during the first 9dpf (Figure $49A_2$-C_2), but beginning between 9-11dpf we were able to track what appeared to

be a newly emerging lcG_x. Specifically, a small spheroidal structure with a visible connection to the olfactory nerve emerged anterior to the lpG and was visible at 11dpf (lcG_{x1} in Figure 49E$_2$). However, this unit and another potential glomerulus (lcG_{x2}) were difficult to discern from the surrounding neuropil at 14dpf ($lcG_{x1,2}$ in Figure 49F$_2$). In n = 8 control larvae, we observed a significant increase in the number of such lcG_x from 73hpf (0.8 ± 0.4 lpG) to 14dpf zebrafish (3.8 ± 1.2 lcG_x; $p < 0.001$ in RM ANOVA) and these numbers are similar to our other anatomical data discussed above.

The $lcG_{3,4}$ of 27A-GFP larvae that were reared in an enriched amino acid environment developed almost identically to those in control animals. Without exception we identified 2.0 ± 0.0 $lcG_{3,4}$ in experimental animals (n = 8) whenever we imaged them (see image series Figure 50A$_1$ to 50F$_1$). The sizes of lcG_3 and lcG_4 in experimental larvae did not differ from their counterparts in control animals at any time (Figure 51A: $p = 0.441$; Figure 51B: $p = 0.473$ in RM ANOVA). The development of lcG_x, however, was visibly and significantly altered in the enrichment condition. In the animal shown in Figure 50, for example, the first lcG_x were already identifiable at 7dpf as two small spheroidal structures that were connected to the olfactory nerve but distinct from the surrounding neuropil (see $lcG_{x1,2}$ in Figure 50C$_2$). After 7dpf, lcG_{x1-2} persisted and appeared to grow, while additional glomeruli (i.e., lcG_{x3}) appeared nearby (Figure 50D$_2$ to 50F$_2$). In addition, the lateral neuropil in experimental animals appeared to be much more sparsely innervated than in control animals, which allowed us to identify more lcG_x than in control animals (e.g., compare Figure 49D$_2$ and Figure 50D$_2$). Statistical analysis confirmed that from 7dpf onwards, significantly more lcG_X were identifiable in experimental larvae than in control animals from the same clutch (Figure 51C; $p < 0.05$,

RM ANOVA). Furthermore, lcG_X in experimental larvae were smaller than in control larvae, again beginning at 7dpf and persisting throughout the remainder of the experiment (Figure 51D; $p < 0.05$, RM ANOVA). Finally, based on our observation that the lateral neuropil was sparser in experimental than that in control animals, we counted the number of OSN for each group and developmental stage. The number of OSNs increased significantly both groups ($p < 0.001$, RM ANOVA), but there was no difference in the rate of this increase between control and experimental animals (Figure 51E; $p = 0.670$, RM ANOVA).

5.5 Discussion

The mature zebrafish olfactory system contains approximately 140 glomeruli. The majority of these glomeruli are small, anatomically diverse and innervated by the axons of ciliated and microvillous OSNs that label with antibodies against the olfactory G-protein G_{olf} and the calcium binding protein calretinin (Chapters 3 and 4). These glomeruli are involved in processing amino acid odors related to feeding and bile acid odors used in habitat and conspecific (Meyerhof and Korsching, 2009, Hamdani and Døving, 2007, Friedrich and Korsching, 1998, Friedrich and Korsching, 1997). The remaining glomeruli (20%) are large, anatomically stereotypic, and at least in part innervated by the axons of pheromone-responsive crypt sensory neurons (Chapters 3 and 4). In the present study we describe the development of these different types of glomeruli and show that they form via visibly different processes and at separate times during embryonic and larval development. Furthermore, we demonstrate that sensory experience plays a role in the maturation of the small calretinin IR and $G_{\alpha\ s/olf}$ IR glomeruli, but not the large and stereotypic glomeruli. We believe that small and large glomeruli in the zebrafish olfactory bulbs are part of two distinct olfactory pathways, comparable to the glomeruli of mammalian main and accessory olfactory systems, respectively (see also Chapter 3 and 4). We will therefore discuss our results in comparison with their possible mammalian analogues.

5.5.1 Pivotal Roles for ORs in Glomerular Development

The development of olfactory glomeruli in the mammalian MOB of mammals requires the precise routing of thousands of OSN axons from widely scattered somata in the sensory epithelia towards restricted postsynaptic targets in the olfactory bulbs.

Ultimately, all of these axons must be organized so that only those expressing the same OR or similar OR types innervate a single glomerulus (Serizawa et al., 2004, Mombaerts, 2004). This assembly apparently depends on the intrinsic properties and function of ORs that are expressed in developing OSNs and on their axons (Mombaerts, 2006). Specifically, OR-type receptors are coupled to the olfactory-specific G-protein, G_{olf}, which when activated, increases cAMP levels and may thereby recruit cellular messengers and transcription factors (e.g., protein kinase A and CREB) that can initiate the expression of axonal guidance molecules and their receptors on growth cones of OSN axons. Each OR type has a unique molecular makeup, which may translate into unique G_{olf} activity and downstream expression of guidance molecules (Serizawa et al., 2006, Imai et al., 2006, Imai and Sakano, 2007); ingrowing OSN axons will thus extend, along with molecularly similar axons (e.g., through interactions between complementary cell surface molecules) to a separate niche where they form a glomerulus (Schwarting and Henion, 2008, Sakano, 2010, Imai and Sakano, 2007). Alternatively, ORs are also expressed on the surfaces of ingrowing OSN axons (Barnea et al., 2004), and may themselves mediate homophilic and heterophilic interactions between like and unlike axons during glomerular formation (Mombaerts, 2006, Feinstein and Mombaerts, 2004, Feinstein et al., 2004). However, such an additional role for ORs has yet to be demonstrated.

Many of the same guidance and cell adhesion molecules involved in axonal routing in the mammalian olfactory system are also present, and actively involved in olfactory system development in zebrafish (Yanicostas et al., 2009, Stevens and Halloran, 2005, Miyasaka et al., 2005). Our descriptive data show that a rudimentary olfactory system is

present as soon as the first waves of OSN axons arrive in the olfactory bulb primordia, at approximately 48hpf. At this time already, these axons are separated into distinct protoglomeruli that stain selectively, and without overlap, with antibodies against different G-protein α subunits. For example, axons that label with the $G_{\alpha o}$ antibody clearly target a small group of rudimentary glomeruli in the dorsal olfactory bulb primordium, while axons that label with the $G_{\alpha\ s/olf}$ antibody selectively target other protoglomeruli. These and other data (Whitlock and Westerfield, 1998, Dynes and Ngai, 1998) confirm that a rudimentary glomerular map forms intrinsically in zebrafish embryos, and the separation that exists among axons innervating distinct protoglomeruli may be achieved by similar cellular processes as are known in mammals.

5.5.2 Postnatal Refinement and Maturation of Protoglomeruli

The glomerular map that forms during embryonic development of mammals (discussed above) resembles its adult counterpart only vaguely. Specifically, mature MOB glomeruli are selectively innervated by the axons of one or at most a few OSN types, but the protoglomeruli that form during embryonic development appear to be diffusely targeted by axons of many related OSN types (Strotmann and Breer, 2006, Sakano, 2010, Mombaerts, 2006). Protoglomeruli must therefore reorganize as part of their maturation. Zou et al. (2004) demonstrated this process in a transgenic mouse in which select OSN types and their axons are readily visible, observing that different OSN axon types intermingle in diffusely organized protoglomeruli shortly after birth, but reorganize during postembryonic development and eventually route specifically towards certain glomeruli (St John et al., 2003, Potter et al., 2001, Conzelmann et al., 2001). Coincidental with this reorganization, the number of glomeruli increases four to five-fold

(Pomeroy et al., 1990), paralleled by changes in odor-evoked glomerular ensemble activity (Greer et al., 1982).

Similar cellular processes likely underlie the maturation of calretinin IR and $G_{\alpha \, s/olf}$ IR glomeruli in larval zebrafish. Approximately 70 functional ORs are expressed in 72hpf zebrafish (Argo et al., 2003), but there are only ~16 protoglomeruli in the olfactory bulbs at this developmental stage (Dynes and Ngai, 1998). Thus, there must be a significant overlap of dissimilar OSN axon types in the protoglomeruli. Indeed, Li et al., (2005) demonstrated that medial protoglomeruli (viz. calretinin IR and $G_{\alpha \, s/olf}$ IR units) responded to multiple related odors (e.g., bile acids) with overlapping activity foci shortly after hatching, but several days later these activity foci reorganized, becoming smaller and more selective to stimulation by individual odorants (e.g., a single bile acid). Glomerular maturation in zebrafish may thus proceed as follows: 1) different but related OSN axon types (i.e., of the same family) initially innervate a single protoglomerulus; 2) after hatching, these axons reorganize, with functionally similar axons increasingly fasciculating and restricting to appropriate glomeruli (Figure 52A). This is paralleled by 3) a significant decrease in the size of protoglomeruli and 4) the emergence of multiple smaller daughter glomeruli that are in the same location and are targeted by the same classes of OSN axons as the protoglomerulus. This is precisely the developmental sequence we observed for all glomeruli innervated by calretinin IR and $G_{\alpha \, s/olf}$ IR axons (dG, dlG, mG, vlG, vmG) as well as for a portion of the calretinin IR lateral cluster glomeruli (lcG_x).

5.5.3 Experience-Dependent Maturation of Glomeruli

We show that the development of calretinin IR and $G_{\alpha \, s/olf}$ IR glomeruli proceeds with visible differences in the number and distribution of newly formed units. Such differences are apparent between animals and even in the left and right olfactory bulbs of individual larvae. Similar findings have been made in the MOB of mice, and Potter et al (2001) noted that "no two glomeruli look alike, even within an individual mouse" (when referring to the same type of glomerulus). We believe that sensory experience may underlie this anatomical variability.

Genetically silencing OSNs (Zou et al., 2007, Zheng et al., 2000, Zhao and Reed, 2001) or depriving an animal of olfactory input (Zou et al., 2004), appears to prevent the postembryonic deletion of misrouted fibers and removal of ectopic glomeruli, whereas odor stimulation and olfactory conditioning lead to an increase in the number of glomeruli in certain regions of the mammalian MOB (Kerr and Belluscio, 2006). We similarly demonstrate that olfactory enrichment alters the development of the lateral glomeruli (lcG_x), and produces lcG_x that are more numerous and smaller on average than those that developed under standard rearing conditions. It has been reasoned that these differences could reflect effects on the timing of glomerular development (Zou et al., 2004, Kerr and Belluscio, 2006), so that with sufficient time to mature, the numbers and distributions of anatomically variable glomeruli might become increasingly similar between and among individual animals. Our observations on the mature zebrafish olfactory system do not support this hypothesis. Instead, we report that anatomical variability in glomeruli innervated by calretinin IR and $G_{\alpha \, s/olf}$ IR OSN persists throughout development (Chapter 3). We therefore hypothesize that sensory experience not only

affects the timing of glomerular development (e.g., as established in studies cited above), but influences additional cellular processes that ultimately produce a glomerular map that is unique to every animal.

Thus, development of the presynaptic glomerular compartment in the main olfactory system is a two step process in which OR initially guide ingrowing axons to their approximate locations and then sort these according to similar activity profiles as dictated by sensory input. We suggest that the structural variations we and others see in the olfactory system are due, at least in part, to variations in the olfactory environment of developing animals. Given their plasticity, such glomeruli then appear to be well suited to operate in an environment prone to change (e.g., a seasonal food supply) and presumably permit animals to adapt their perception and response to behaviorally relevant stimuli.

5.5.4 Development of Glomeruli in the Accessory Olfactory Bulb

The developmental processes discussed above have been identified in the main olfactory system of mammals or its analogue in zebrafish (our study). Less is known about the development of pheromone-responsive glomeruli in the AOB, but some of the cellular processes described for the MOB above have also been identified in the developing AOB. Belluscio et al. (1999) showed that axons targeting the AOB require functional V1R chemosensory receptor proteins and that deletion of these molecules leads to inappropriate targeting of OSN axons, ectopic glomeruli, and the death of receptor cells. Furthermore, molecules that guide OSN axons to their postsynaptic targets in the MOB are also expressed in the AOB (Knoll et al., 2003, Cloutier et al., 2004, Cloutier et al., 2002). Thus, OR driven 'axon sorting' may also contribute to the

development of AOB glomeruli.

5.5.5 Development of Large, Possibly Pheromonal Glomeruli in Zebrafish

We have previously suggested that large zebrafish glomeruli, like the mdG, are involved in pheromonal processing (Chapters 3), and in the present study we demonstrate that large glomeruli develop differently that the remaining glomeruli. Specifically, the only consistent morphological change that we have identified in developing mdG is significant and continuous growth throughout the course of larval development. Much of this growth may be caused by the arrival of new OSN axons that extend from newly differentiated OSN (Figure 52B), which continue to be added during larval development as the olfactory epithelium (Hansen and Zeiske, 1993).

However, if the mdG are indeed pheromone-responsive, then it is possible that any additional innervation arriving at, and contributing to the growth of these glomeruli could be from different types of chemosensory neurons. Glomeruli in the mammalian AOB are innervated by as many as 20 OSN types (Dulac and Wagner, 2006, Belluscio et al., 1999), and we have similarly observed that most large glomeruli in zebrafish, including the mdG, are innervated by multiple bundles of OSN axons, which could originate from multiple OSN types. Related data describing the development and possible function of mdG$_2$, may further support this idea. Specifically, this glomerulus is innervated by crypt-like sensory neurons (Chapter 3), located in alarm pheromone-responsive medial regions (Chapter 3), and is innervated by mitral cells that project directly to the habenula (Miyasaka et al., 2009), involved in mediating alarm and fear responses (Lee et al., 2010, Agetsuma et al., 2010).

The mdG$_2$ is innervated only by a single OSN axon stalk until the mid-larval and

juvenile stages, at which time we begin to observe that multiple OSN axon bundles innervate this glomerulus (arrows in Figure 41A$_3$, 41A$_4$). The emergence of these axon bundles correlates with a rapid increase in the cross-sectional area of mdG$_2$, and moreover, the onset of visible behavioral responses to alarm pheromone (~48-52dpf; Waldman, 1982). Thus, if like other fish pheromones, alarm pheromone is a blend of chemicals (Sorensen et al., 1998, Døving and Lastein, 2009), then the arrival of new OSN axon types during the mid-larval stage could enable the animal to sense the chemical mixture that constitutes the alarm pheromone and respond with appropriate behaviors.

5.5.6 Conclusion and Future Directions

To our knowledge, this is the first study to examine the development of an entire population of vertebrate glomeruli over an extended period of time. Our data show that there exist distinct developmental mechanisms for different types of glomeruli in the zebrafish olfactory system. Glomeruli that are large and individually identifiable in mature animals are the first ones to develop, and they appear to mature independent of sensory experience. The majority of glomeruli, however, form only after the animals hatch, and mature in an experience-dependent manner. We believe that the early-formed glomeruli may comprise stable olfactory pathways that encode certain odors that animals respond to innately. The remaining glomeruli appear to comprise a dynamic olfactory pathway that can adjust to changing odor environments and thus provide a substrate for olfactory learning.

Table 5. Age and size of zebrafish during larval development. Body length, measured from the lips to the tip of caudal fin served as an initial metric to identify equally-developed animals. Olfactory bulb sizes were then used as another secondary measure to confirm that brains from these animals were similar.

Table 5.

Stage (number of animals)	Approximate Age	Length (mm)	Olfactory Bulb Dimensions (μm)	
			Anterior-Posterior	*Medial-Lateral*
Long-pec embryo (n=8)	48 hpf	3.5	65-75[*]	45-55
Protruding mouth embryo (n=8)	72 hpf	3.5	70-75[*]	60-70
Early larva (EL) (n=10)	5-8 dpf	4.3	65-75 75-85	60-70 65-75
Mid larva (ML) (n=18)	25-30 dpf	5	90-100 100-125 125-150	90-110 110-120 140-150
Juvenile (JU) (n=14)	40-60 dpf	10	190-210	120-220

[*] embryonic olfactory bulbs were measured ventral-dorsal

Table 6. Antibodies and staining protocols used in this study.

Table 6.

Antibody	Immunogen / Host	Source	Fixation	Prior use in fish
*General labels (**1:100 in PBS-T**)*				
Anti-keyhole-limpet-hemocyanin (KLH)	hemocyanin fom keyhole limpets / rabbit	Sigma (H0892)	2% PFA	Riddle and Oakley (1992), Fuller et al (2006)
Anti-synaptic vesicle protein 2 (SV$_2$)	ommata synaptic vesicles / mouse	Developmental Studies Hybridoma Bank (Iowa City, IA, USA)	2% PFA	Koide et al (2009)
*OSN class specific Labels (**1:50-100 in PBS-T**)*				
Anti-G$_{\alpha s/olf}$ (G-protein subunit)	rat c-terminus (seq: 377-394) / rabbit	Santa Cruz Biotech (Santa Cruz, CA, USA) sc-383	2% PFA	Hansen et al (2003), Koide et al (2009)
Anti-G$_{\alpha o}$ (G-protein subunit)	rat divergent domain (seq: 105-124) / rabbit	Santa Cruz Biotech sc-387	2% PFA	Hansen et al (2003)
Anti-calretinin	recombinant human calretinin / mouse	Swant (Bellinzona, Switzerland) 6B3	2% PFA	Miyaska et al (2005), Castro et al (2006)
Anti-S$_{100}$	cow S$_{100}$ protein / rabbit	Dako (Glostrup, Denmark) Z 0311	2% PFA	Germana et al (2004), Sato et al (2005)

Table 7. Summary of numbers, sizes and innervation of glomeruli in the juvenile olfactory system. Data are means and their standard deviations. Note that the 11 largest glomeruli are innervated by only one identified OSN type, while almost all other glomeruli are innervated by calretinin IR and $G_{\alpha\,s/olf}$ IR axons.

Table 7.

Glomeruli (specimens)	Glomeruli per bulb	Average area	Innervation
dG_x (n=5)	17.9 ± 2.7	180 ± 42	calretinin / $G_{\alpha\,s/olf}$
dlG_x (n=4)	36.7 ± 4.5	103 ± 23	calretinin / $G_{\alpha\,s/olf}$
lcG_x (n=5)	8.6 ± 1.6	259 ± 57	calretinin
lcG_1 (n=5)	1 ± 0	555 ± 68	$G_{\alpha\,s/olf}$
lcG_3 (n=5)	1 ± 0	540 ± 60	calretinin
lcG_4 (n=5)	1 ± 0	892 ± 70	calretinin
mdG_1 (n=5)	1 ± 0	443 ± 170	?
mdG_2 (n=5)	1 ± 0	680 ± 143	S_{100}
mdG_3 (n=5)	1 ± 0	439 ± 146	?
mdG_4 (n=5)	1 ± 0	456 ± 130	?
mdG_5 (n=5)	0.9 ± 0.2	375 ± 97	$G_{\alpha 0}$
mdG_6 (n=5)	0.9 ± 0.2	534 ± 131	?
mG_x (n=4)	13.8 ± 2.1	134 ± 31	calretinin / $G_{\alpha\,s/olf}$
vlG_x (n=5)	12.0 ± 3.4	337 ± 77	calretinin / $G_{\alpha\,s/olf}$ *
vmG_x (n=5)	14.7 ± 3.4	128 ± 26	calretinin / $G_{\alpha\,s/olf}$
vpG (n=6)	1 ± 0	695 ± 85	?
$lvpG$ (n=6)	0.8 ± 0.4	695 ± 74	?
$mvpG$ (n=6)	0.8 ± 0.4	865 ± 110	?
Average Number of Glomeruli / Bulb			**115 ± 10**

* vlG were only partially calretinin IR as shown in Figure S2A[1]-A[5]

239

Figure 39. Overview of glomeruli in the dorsal olfactory bulbs of juvenile zebrafish. Glomeruli are arranged in anatomically distinct regions that are traced in dashed outlines. (**A**) The mediodorsal glomeruli (mdG) are traced with solid lines on the left side of **A-C**. mdG$_2$ (**B**) and mdG$_5$ (**C**) are the only glomeruli that are innervated by S$_{100}$ IR and G$_{\alpha o}$ IR axons, respectively. The remaining dorsal glomeruli are located in the dorsal and dorsolateral cluster (dG and dlG) which are uniformly innervated by calretinin IR and anti-G$_{\alpha\ s/olf}$ IR axons (**D**, **E**). (**F**) The diagram depicts the mean number of glomeruli in each cluster and their innervation as indicated by different colors. Scale bar in **E** applies to all panels.
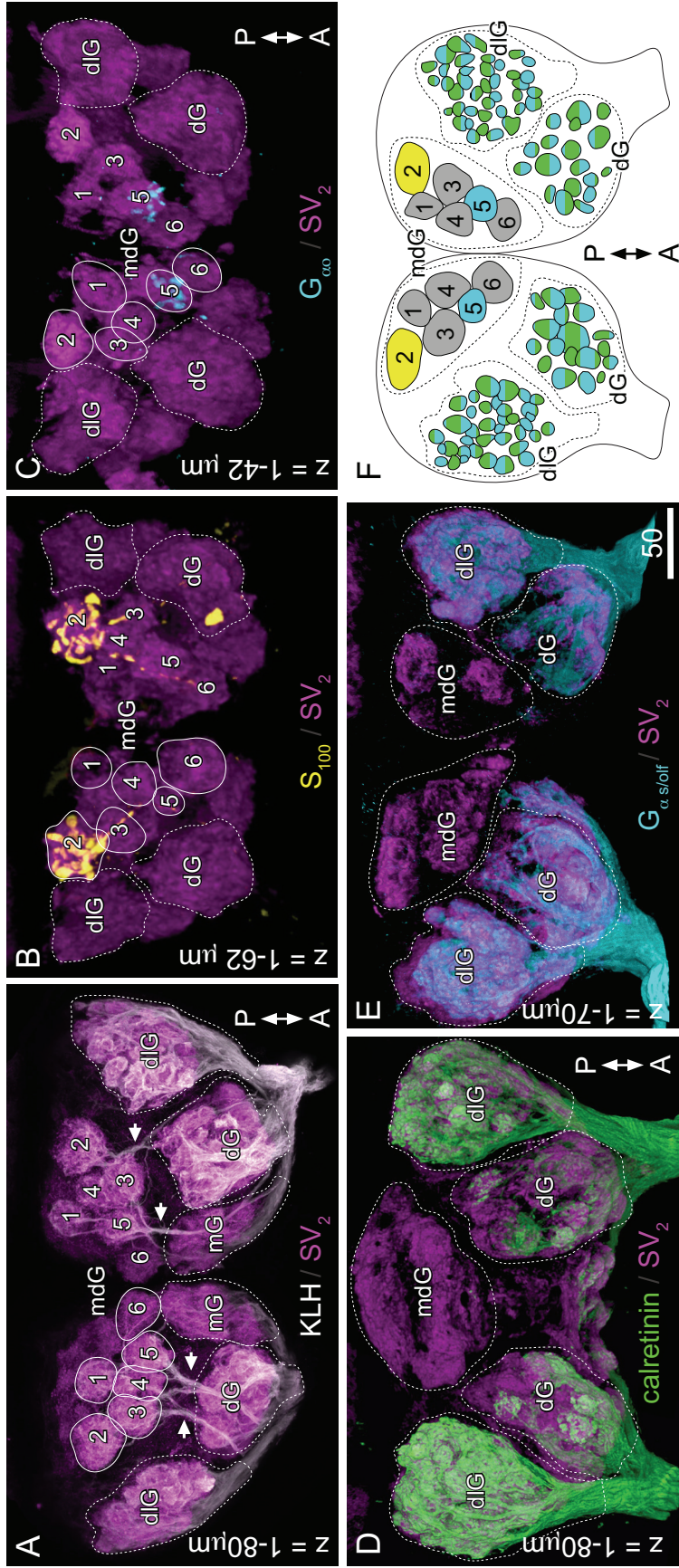
Figure 39. Overview of Glomeruli in the Dorsal Olfactory Bulbs of Juvenile Zebrafish

241

Figure 40. Overview of glomeruli in the ventral (**A-D**) and lateral (**E-G**) olfactory bulbs of juvenile zebrafish. (**A**) The innervation of the large ventroposterior glomeruli (vpG) is only visible in specimens labeled with anti-KLH (**A**). The remaining ventral glomeruli are located in the medial (mG), ventrolateral (vlG) and ventromedial (vmG) clusters that are innervated by calretinin IR (**B**) and $G\alpha_{s/olf}$ IR (**C**) axons. (**E-G**) The lateral olfactory bulbs contain the large $lcG_{1,3,4}$ and some smaller units and a diffusely organized area known as lateral plexus (LP). Individually identifiable glomeruli are traced with solid lines. Diagrams in **D** and **G** depict the mean number of glomeruli in each cluster and their innervation as indicated by different colors. Scale bar in **C** applies to **A** and **B**; scale bar in **F** also applies to **E**.
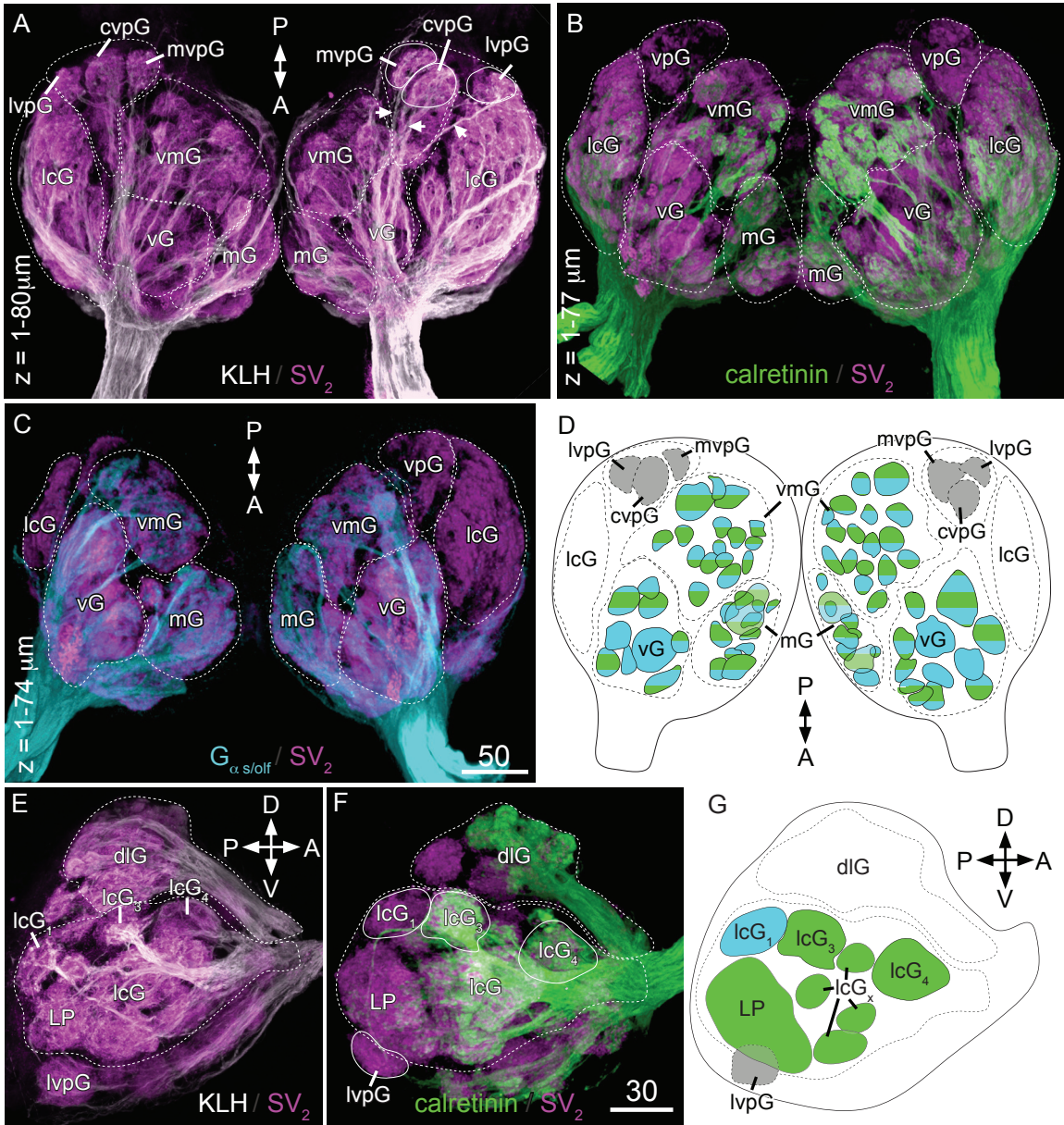
Figure 40. Overview of Glomeruli in the Ventral and Lateral Olfactory Bulbs
of Juvenile Zebrafish

243

Figure 41. Development of mediodorsal glomeruli (mdG) from embryonic to juvenile zebrafish. The mdG were first visible as diffusely organized protoglomeruli at 48hpf (**A**, **B**). At this time the innervation of proto-mdG by OSN axons was unclear. (**A$_2$**, **B$_2$**) By 72hpf, the mdG attained a configuration that was similar to their arrangement in adult zebrafish and this arrangement persisted throughout larval development (**A$_{3-4}$**, **B$_{3-4}$**). Scale bars in the right hand column also apply to panels on the left.
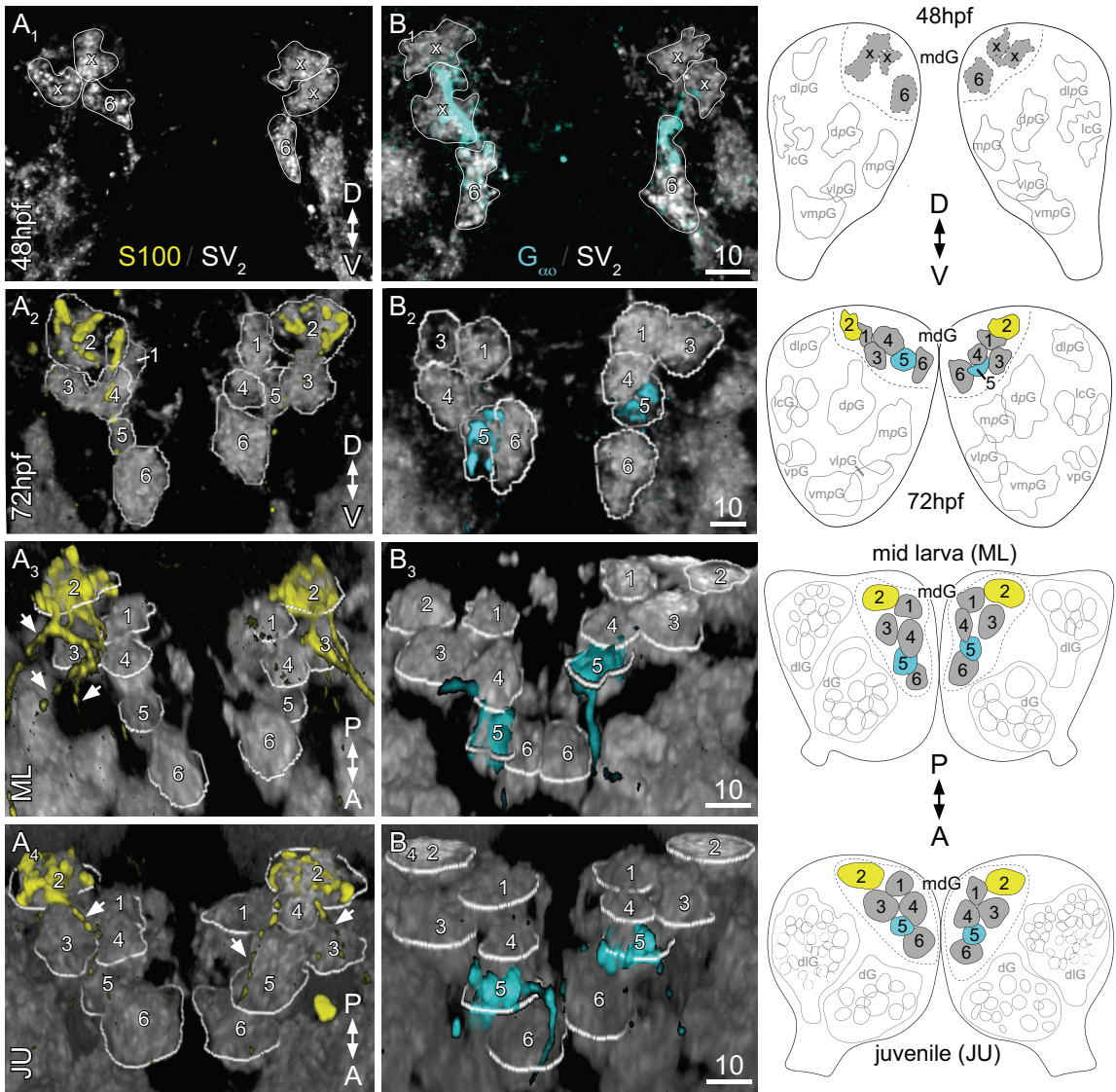
Figure 41. Development of Mediodorsal Glomeruli From Embryonic to Juevnile Zebrafish

Figure 42. Data plots depicting the numbers (colored data points) and sizes (white data points) of mediodorsal glomeruli during larval development. All mdG developed between 48-72hpf and remained identifiable afterwards. Starting in early-larvae (EL) we were able to identify six mdG in nearly every olfactory bulb; all mdG grew with similar timing. Data are mean numbers of mdG from at least 5 animals per developmental stage and their standard errors. LOB and ROB denote left and right olfactory bulbs, respectively.
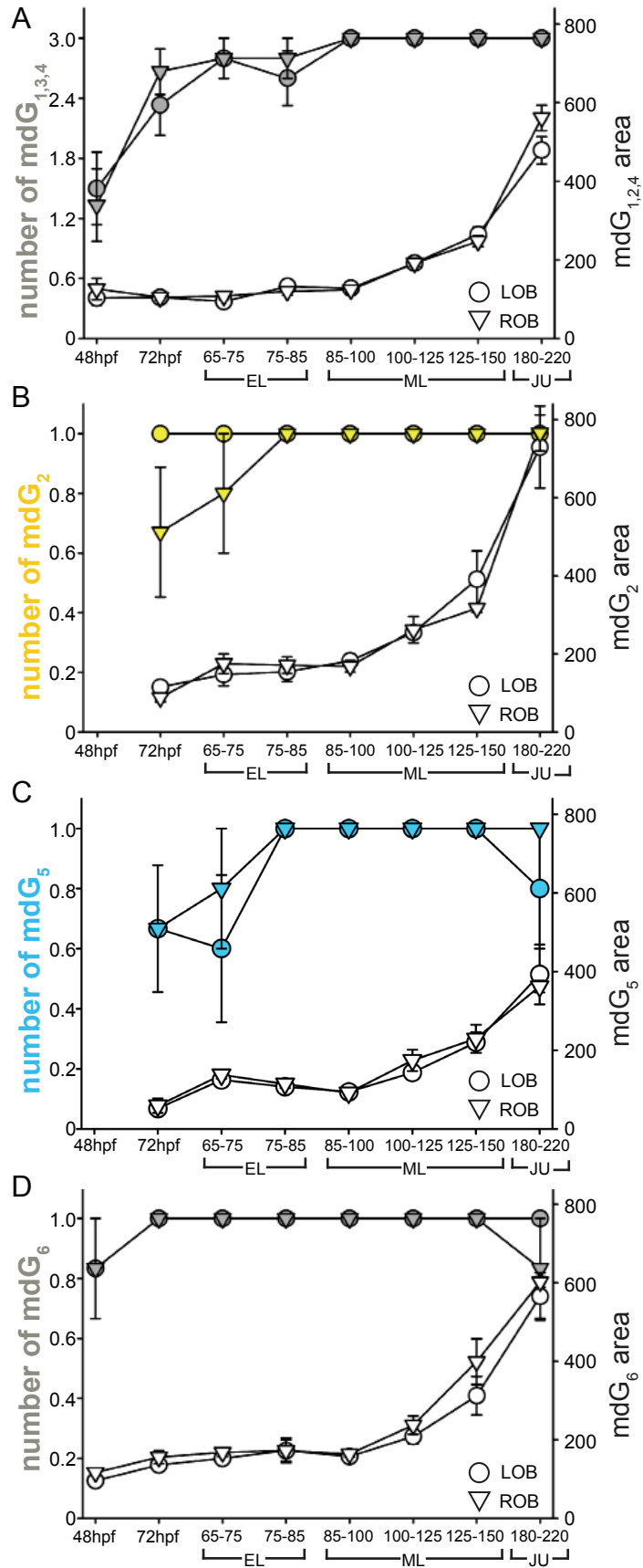
Figure 42. Data Plots Depicting the Numbers and Sizes of Mediodorsal Glomeruli During Larval Development

247

Figure 43. Reorganization of $G_{\alpha\,s/olf}$ IR and calretinin IR protoglomeruli in early larvae. (**A$_1$**, **A$_2$**) Embryonic olfactory primordia are shown as frontal views. (**B$_1$-C$_4$**) Olfactory bulbs of two early larvae are shown as different pitches of maximum projections from dorsal (**B$_1$-C$_2$**) and ventral (**B$_3$-C$_4$**) views rotated along their lateral axis to depict their three dimensional structure. Shortly after hatching, large protoglomeruli (dpG, dl$p$G, mpG and vl$p$G in **A$_1$**, **A$_2$**) gave rise to numerous new glomeruli, shown here as roughly spherical SV$_2$ labeled tufts traced with white outlines and denoted 'x' (**B$_1$-C$_4$**). Numbers of identified glomeruli are indicated at the bottom of each panel. Scale bars in right column also apply to the left column.
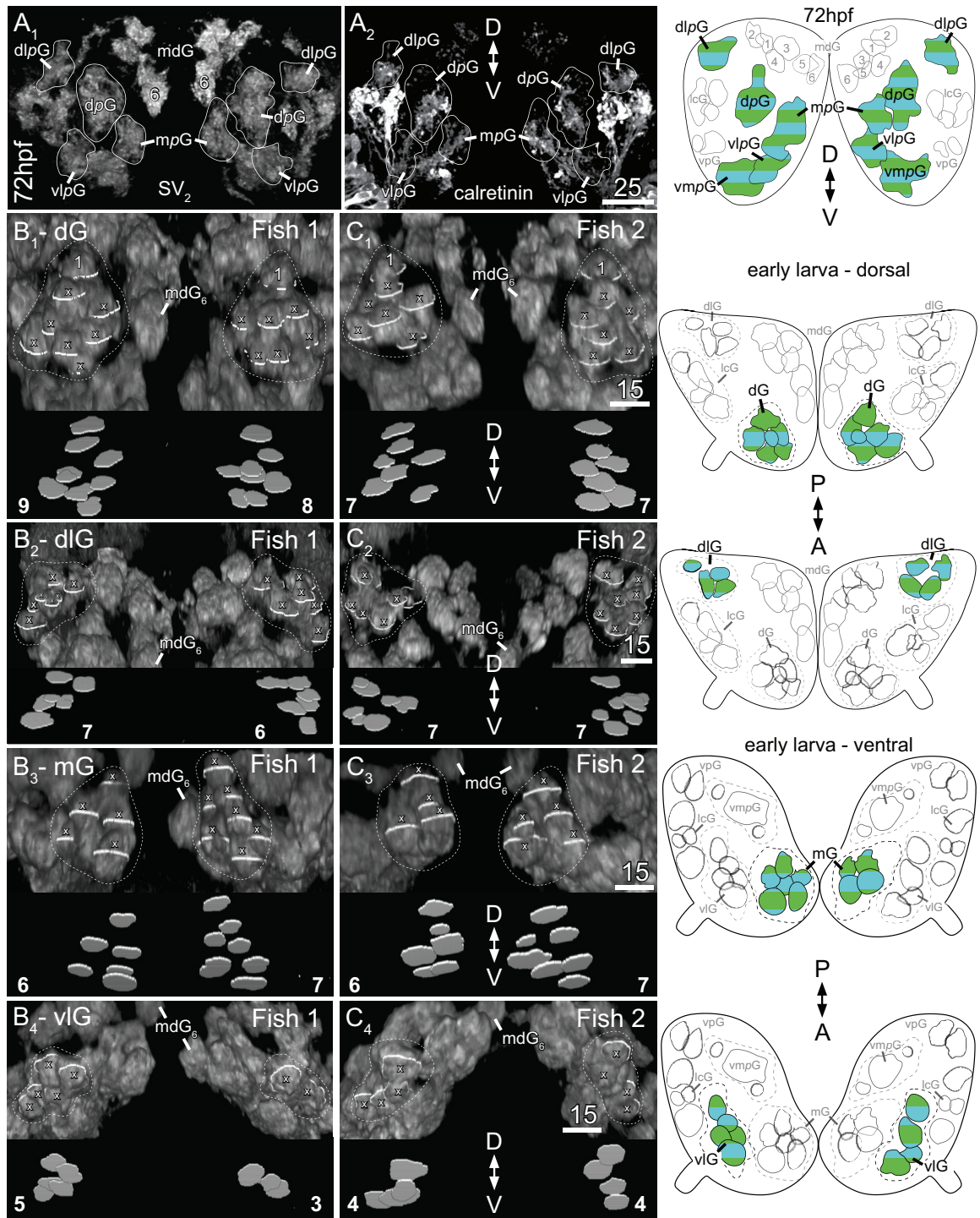
Figure 43. Reorganization of $G_{\alpha s/olf}$ IR and Calretinin IR Protoglomeruli in Early Larvae

249

Figure 44. Data plots depicting the numbers and sizes of $G_{\alpha \text{ s/olf}}$ IR and calretinin IR glomeruli during larval development. All of these glomeruli began to develop after hatching coincidentally with a significant decrease in the cross sectional area of the protoglomerulus (see hatching in plots). The number of glomeruli continued to increase throughout development. Data show the mean number of glomeruli and their standard errors. LOB and ROB denote left and right olfactory bulbs, respectively.
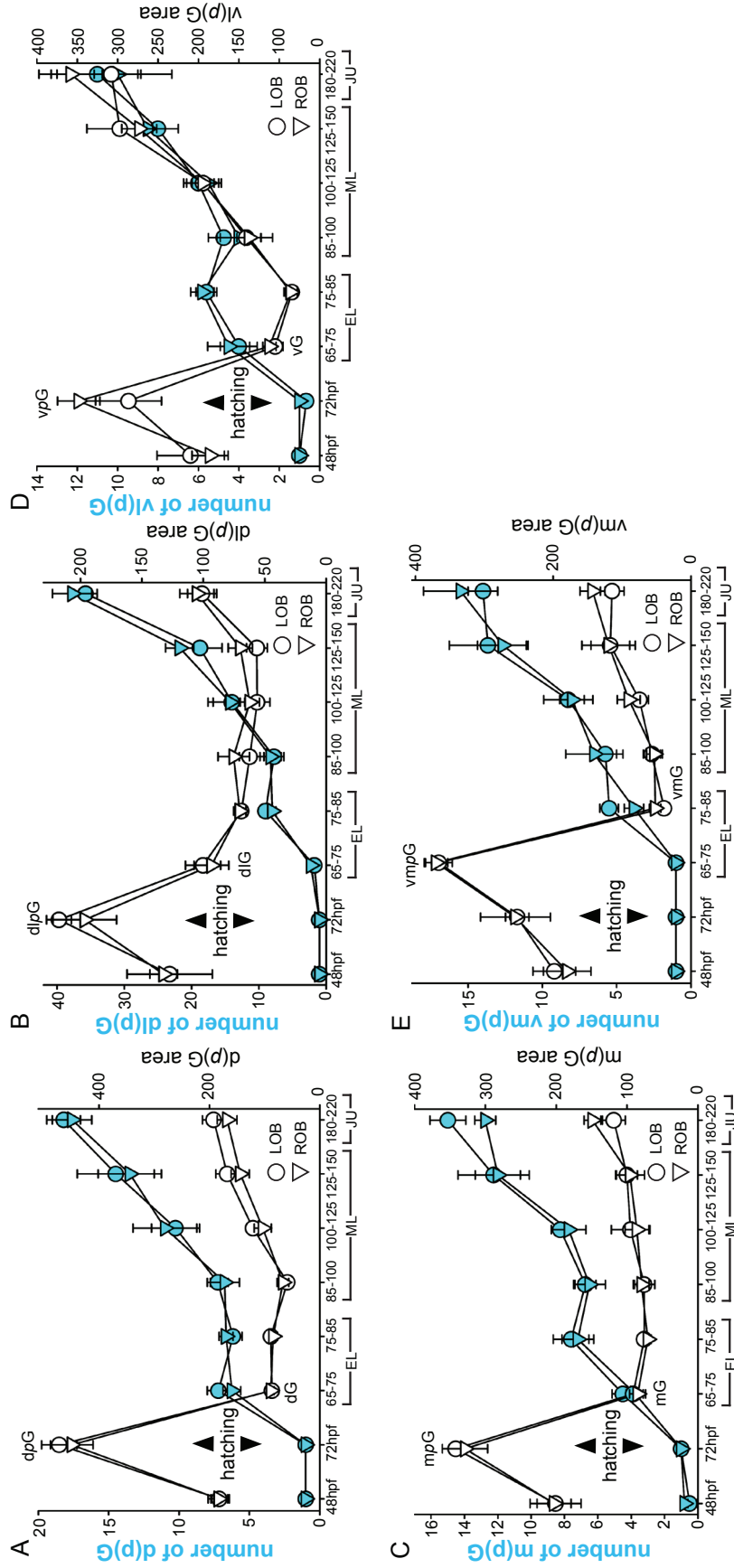
Figure 44. Data Plots Depicting the Numbers and Sizes of $G_{\alpha \, s/olf}$ IR and Calretinin IR Glomeruli During Larval Development

251

Figure 45. Anatomical variations among developing ventromedial glomeruli. **A**, **B**, **C** are maximum ventral projections of whole-mounted olfactory bulbs. **A$_1$-C$_1$** and **A$_2$-C$_2$** are high magnification images of the left and right vmG in single animals at each developmental stage. OSN innervation of the ventromedial olfactory bulb consisted initially of a single protoglomerulus (vm*p*G in **A$_1$**, **A$_2$**) but reorganized to form axon fascicles (arrows) that targeted individual glomeruli (traced outlines). Projection depth of each image is indicated.
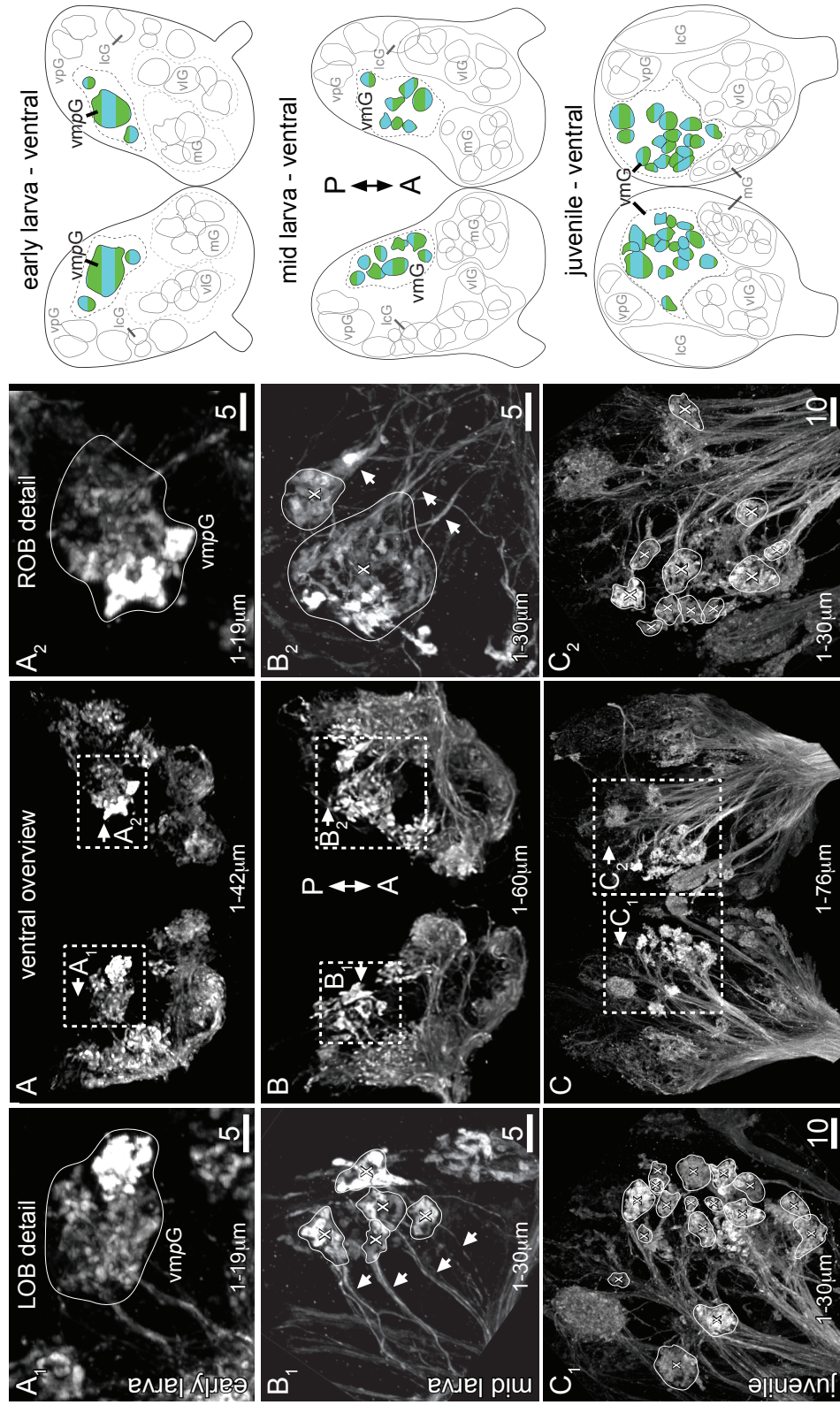
Figure 45. Anatomical Variations Among Developing Ventromedial Glomeruli

253

Figure 46. Development of $lcG_{3,4}$ and lcG_x in the lateral olfactory bulbs. (**A**, **B**) Frontal views of zebrafish embryos and (**C**, **D**) lateral views of the left olfactory bulbs of two early larvae depicting the lateral cluster glomeruli (lcG). (**A**) $lcG_{3,4}$ are visible at 48hpf and remain present throughout subsequent developmental stages (**B**, **C**, **D**). In contrast, lcG_x develop after hatching via a small lateral protoglomerulus (lpG) located between $lcG_{3,4}$ (**B**). The numbers of newly formed lcG_x differed between the olfactory bulbs of different larvae (compare **C**, **D**). The lateral plexus (LP) was a large and diffusely organized structure in which only few glomeruli can be identified. Projection depth of each image is indicated.
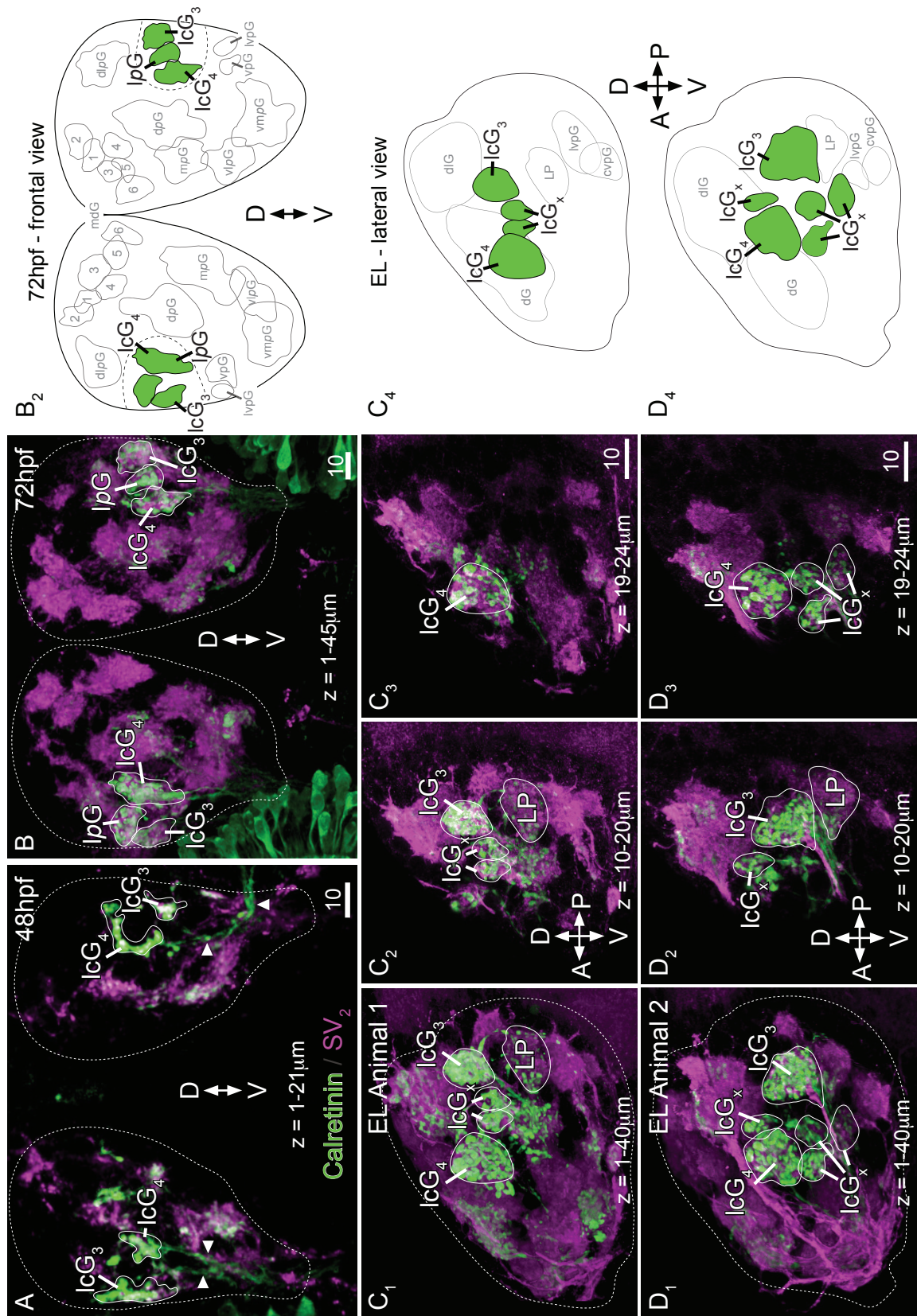
Figure 46. Development of lcG$_{3,4}$ and lcG$_x$ in the Lateral Olfactory Bulbs

255

Figure 47. Data plots depicting the numbers and sizes of lateral glomeruli during larval development. (**A**) lcG_3 and (**B**) lcG_4 were visible in almost all animals at every developmental stage (green data points). Both lcG_3 and lcG_4 grew significantly in and after the mid-larval (ML) stage. lcG_x were not identified at 48hpf (**C**, **D**). Instead, these glomeruli originated from a common precursor (lpG at 72hpf) that became smaller after hatching, coincidental with the formation of lcG_x. The number and cross-sectional area of lcG_x continued to increase throughout larval development. All data are means and their standard errors.
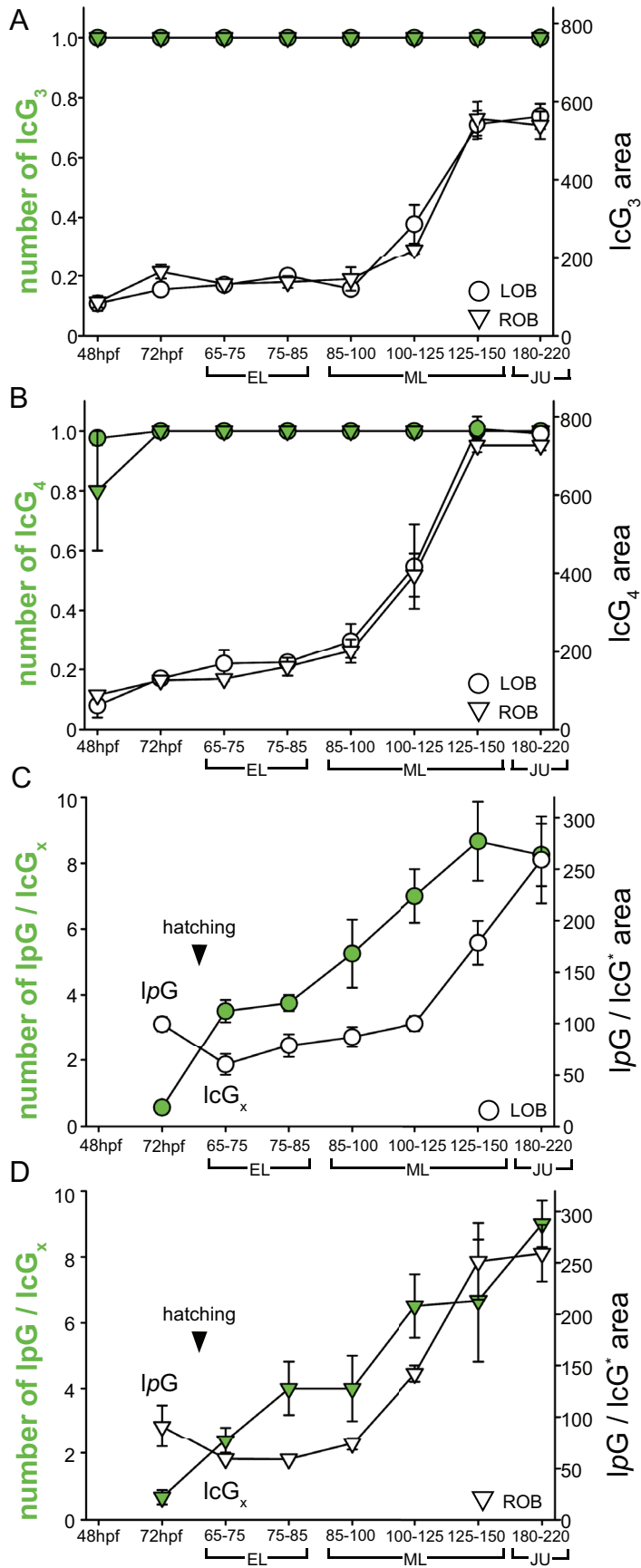
Figure 47. Data Plots Depicting the Numbers and Sizes of Lateral Glomeruli During Larval Development

Figure 48. Overview of a lateral olfactory bulb of a 27A-GFP transgenic zebrafish larva, counterstained with immunohistochemical markers for lcG. (**A$_1$**, **A$_2$**) lcG$_{3,4}$ and lcG$_x$ and the lateral plexus (LP in **A$_3$**) are clearly labeled by the 27A-GFP transgene. In all these structures, the 27A-GFP labeling overlaps with calretinin IR and SV$_2$, confirming that this animal model permits us to study the development of different lcG *in vivo*.
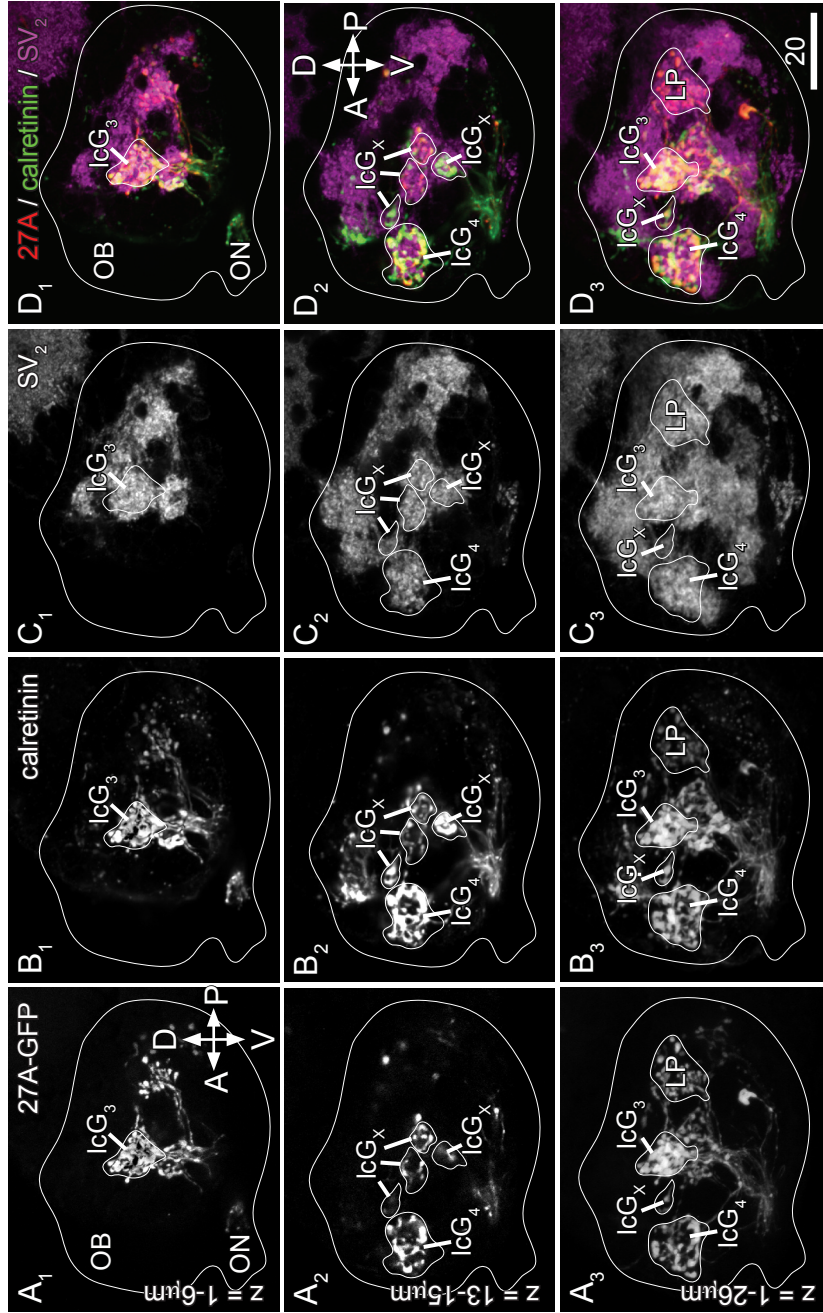
Figure 48. Overview of a Lateral Olfactory Bulb of a 27A-GFP Transgenic Zebrafish Larva Counterstained With Immunohistochemical Markers For IcG

259

Figure 49. Repeated *in vivo* imaging of lateral glomeruli in a 27A-GFP transgenic larva raised in a normal olfactory environment. Images in this figure depict the left lateral olfactory bulb of a single transgenic larvae imaged every second day from 3dpf (**A**) to 14dpf (**F**). OSNs in the olfactory epithelium (OE) are visible on the bottom left of each panel. The top panels (**A$_1$-F$_1$**) show the superficial lateral olfactory bulb, where lcG$_{3,4}$ were prominent anatomical features. Beneath lcG$_{3,4}$ (**A$_2$-F$_2$**) the 27A-GFP transgene labeled many OSN fibers that we interpret to be the lateral protoglomerulus (lpG) and the lateral plexus (LP in **B$_2$**). (**E$_2$**) At 11dpf, a single lcG$_x$ became identifiable anterior to the lpG, but this unit was difficult to identify at later stages. The larva shown in this image series was not exposed to amino acids.
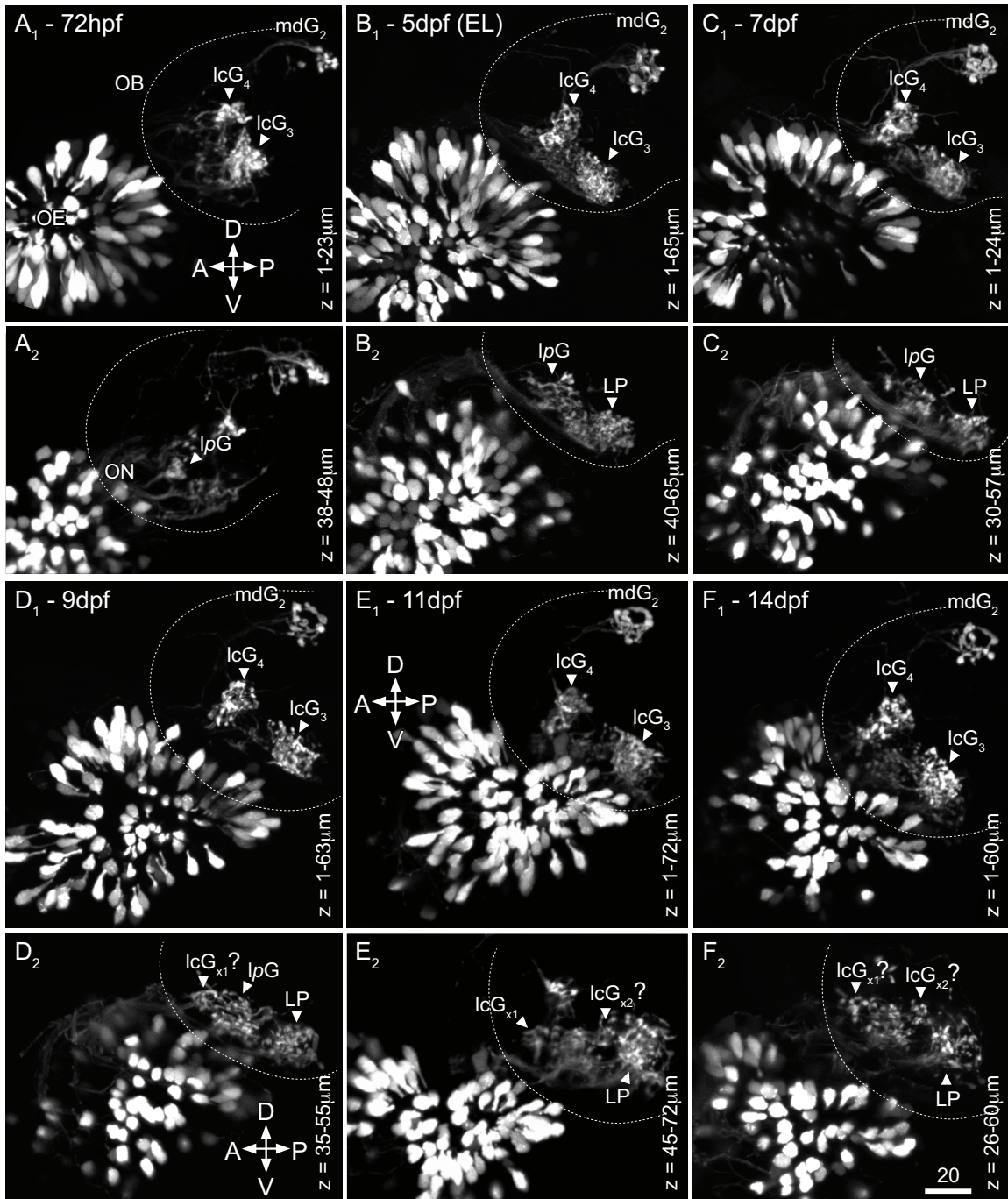
Figure 49. Repeated *In Vivo* Imaging of Lateral Glomeruli in a 27A-GFP Transgenic Larva Raised in a Normal Olfactory Environment

261

Figure 50. Repeated *in vivo* imaging of lateral glomeruli in a 27A-GFP transgenic larva raised in an enriched olfactory environment. Images in this figure depict the left lateral olfactory bulb of a single transgenic larvae imaged every second day from 3dpf (**A**) to 14dpf (**F**). OSN in the olfactory epithelium were brightly labeled and are shown on the bottom left of each panel. The top panels (**A$_1$-F$_1$**) show the superficial lateral olfactory bulbs, where lcG$_{3,4}$ were prominent anatomical features. Beneath lcG$_{3,4}$ (**A$_2$-F$_2$**) the 27A-GFP transgene labeled many OSN fibers that initially terminated in a lateral protoglomerulus (lpG) and lateral plexus (LP in **B$_2$**). Beginning at 7dpf lcG$_x$ became clearly identifiable (**B$_2$**), starting with the emergence of two small glomeruli, lcG$_{x1,2}$. These and additional units remained identifiable during subsequent developmental stages (**D$_2$-F$_2$**).
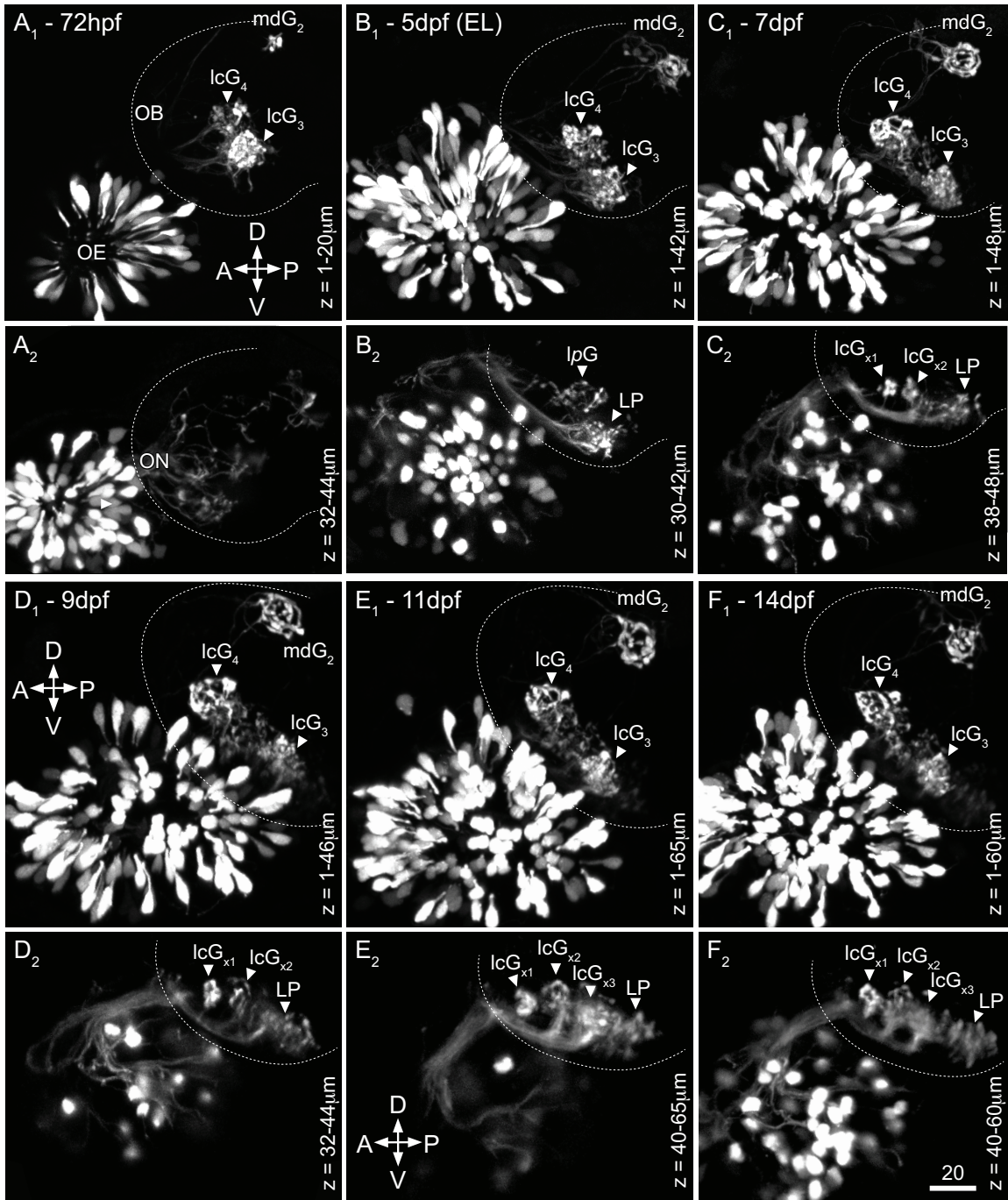
Figure 50. Repeated *In Vivo* Imaging of Lateral Glomeruli in a 27A-GFP Transgenic Larva Raised in an Enriched Olfactory Environment

263

Figure 51. Comparison of morphological features in the lateral olfactory bulbs of control and experimental larvae. The cross-sectional area of lcG_3 (**A**) and lcG_4 (**B**) did not differ between animals in control and experimental groups during any time of the experiment. (**C**) The number and rate of lcG_x development was significantly increased in experimental larvae, but the size of lcG_x was significantly smaller in the experimental group (**D**). (**E**) The number of OSNs and the rate of their development did not differ between control and experimental larvae at any time during the experiment. All data are from n = 8 animals in each group imaged from their left lateral side. Plots show mean data and their standard errors.
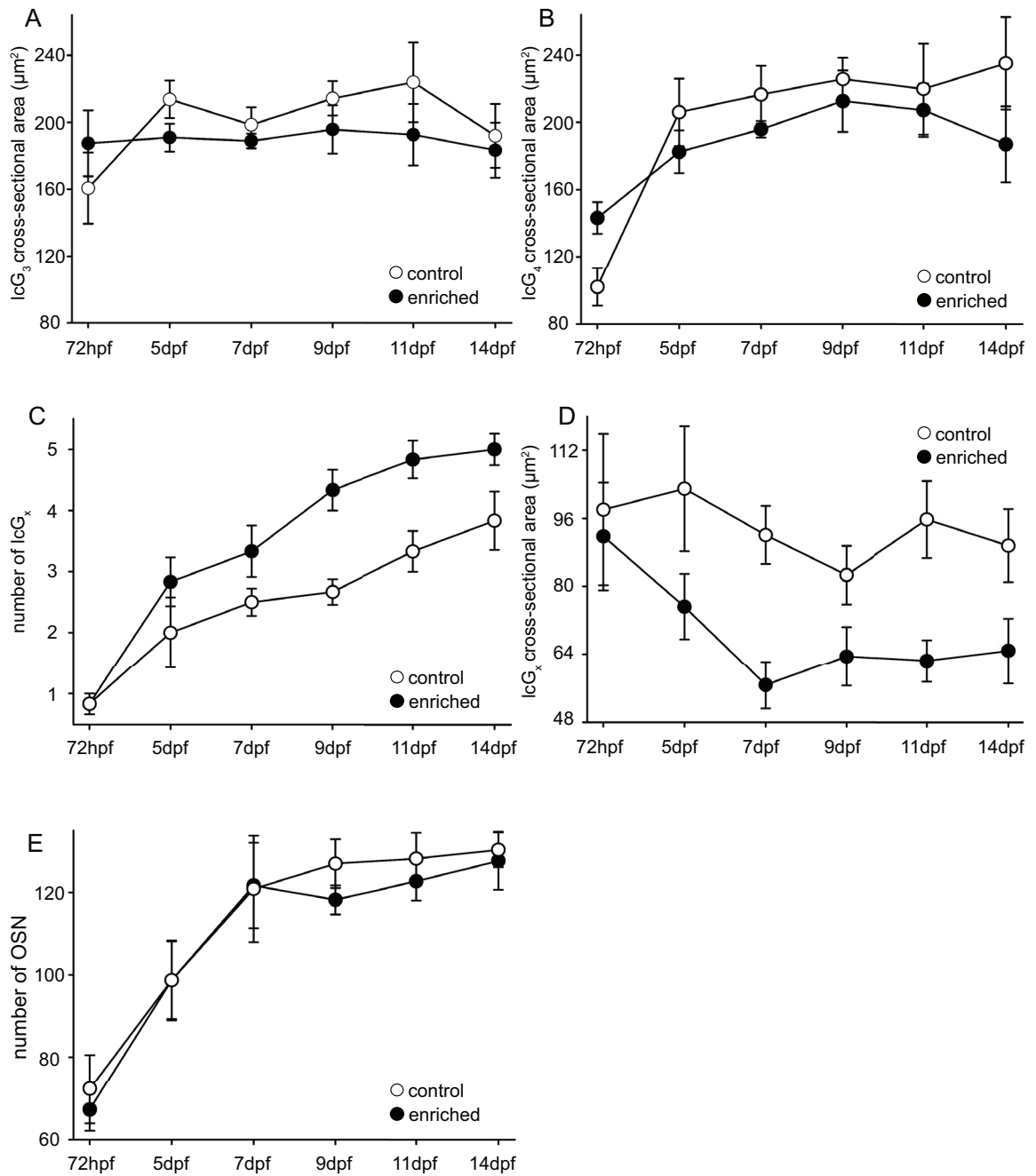
Figure 51. Comparison of Morphological Features in the Lateral Olfactory Bulbs of Control and Experimental Larvae

265

Figure 52. Possible developmental mechanisms underlying the assembly of different types of glomeruli in the zebrafish olfactory system. (**A**) Small and anatomically variable $G_{\alpha\,s/olf}$ IR and calretinin IR glomeruli emerge from common protoglomeruli. (**B**) Large and anatomically stereotypic glomeruli emerge individually after specific routing of their OSN innervation to their postsynaptic targets. Maturation of these glomeruli involves the addition of more axons of the same or other molecular types.

Figure 52. Possible Developmental Mechanims Underlying the Assembly of Different Types of Gomeruli in the Zebrafish Olfactory System

267

Supplemental Figure 5. Sample tracings of ventral glomeruli in the olfactory system of a juvenile zebrafish. Outlines of identified glomeruli are traced in panels **A$_1$** - **A$_4$**, which are projections of 15-25 serial optical sections, acquired at 1µm intervals. Not all glomeruli (e.g., small units) are visible and their outlines are therefore omitted. Glomeruli were often distributed differently in the vG and vmG clusters. The schematic in **A$_5$** summarizes the distributions and the actual numbers of identified glomeruli for the shown specimen. The vpG were not unambiguously identifiable, because neither calretinin IR nor G$_{\alpha\ s/olf}$ IR axons targeted these glomeruli, and glomerular innervation was an important anatomical feature in the identification and detection of individual units.
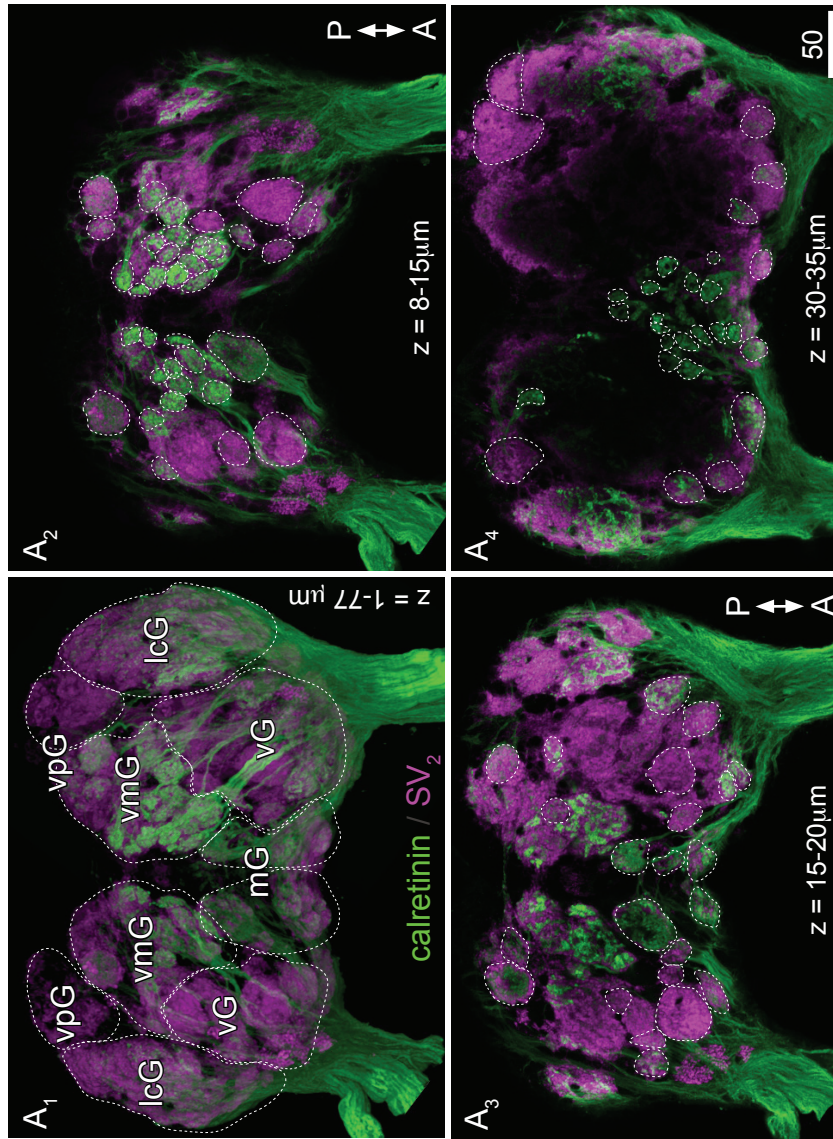
Supplemental Figure S5. Sample Tracings of Ventral Glomeruli in the Olfactory System of a Juvenile Zebrafish

269

Supplemental Figure 6. Frontal views of olfactory bulb primordia from five 48hpf embryos labeled with different antibody combinations. The 48hpf olfactory system contained rudiments of 2-3 mediodorsal glomeruli (see mdG in **A**, **B**, **D**, **E**). A pair of developing lateral cluster glomeruli ($lcG_{3,4}$) was also identifiable in many 48hpf embryos (**A**, **B**). The most prominent structures were 5 large protoglomeruli that were innervated by calretinin IR and $G_{\alpha\ s/olf}$ IR axons (**A**, **B, C**). Neither $G_{\alpha o}$ (**D**) nor S_{100} (**E**) specifically innervated any one glomerulus at 48hpf. (**F**) Mean numbers and cross-sectional areas (plus standard errors) of identified glomeruli are listed.

Supplemental Figure 6. Frontal Views of Olfactory Bulb Primordia From Five 48hpf Embryos Labeled With Different Antibody Combinations

The figure includes the following table (panel F):

Glomeruli (n = X)	Average per Bulb		Innervation
	Number	Area	
m*p*G (4)	0.8 ± 0.2	201 ± 36	calret / G$_{\alpha s/olf}$
d*p*G (5)	1 ± 0	185 ± 12	calret / G$_{\alpha s/olf}$
dl*p*G (5)	1 ± 0	138 ± 19	calret / G$_{\alpha s/olf}$
lcG$_3$ (4)	1 ± 0	93 ± 14	calret
lcG$_4$ (4)	0.9 ± 0.1	81 ± 17	calret
mdG$_x$ (6)	0.9 ± 0.1	133 ± 23	?
mdG$_x$ (6)	0.6 ± 0.5	76 ± 6	?
mdG$_6$ (6)	0.8 ± 0.2	102 ± 11	?
vl*p*G (6)	0.9 ± 0.3	197 ± 79	calret / G$_{\alpha s/olf}$
vm*p*G (6)	1 ± 0	188 ± 81	calret / G$_{\alpha s/olf}$
Average Glomeruli per Bulb			**8.6 ± 0.2**
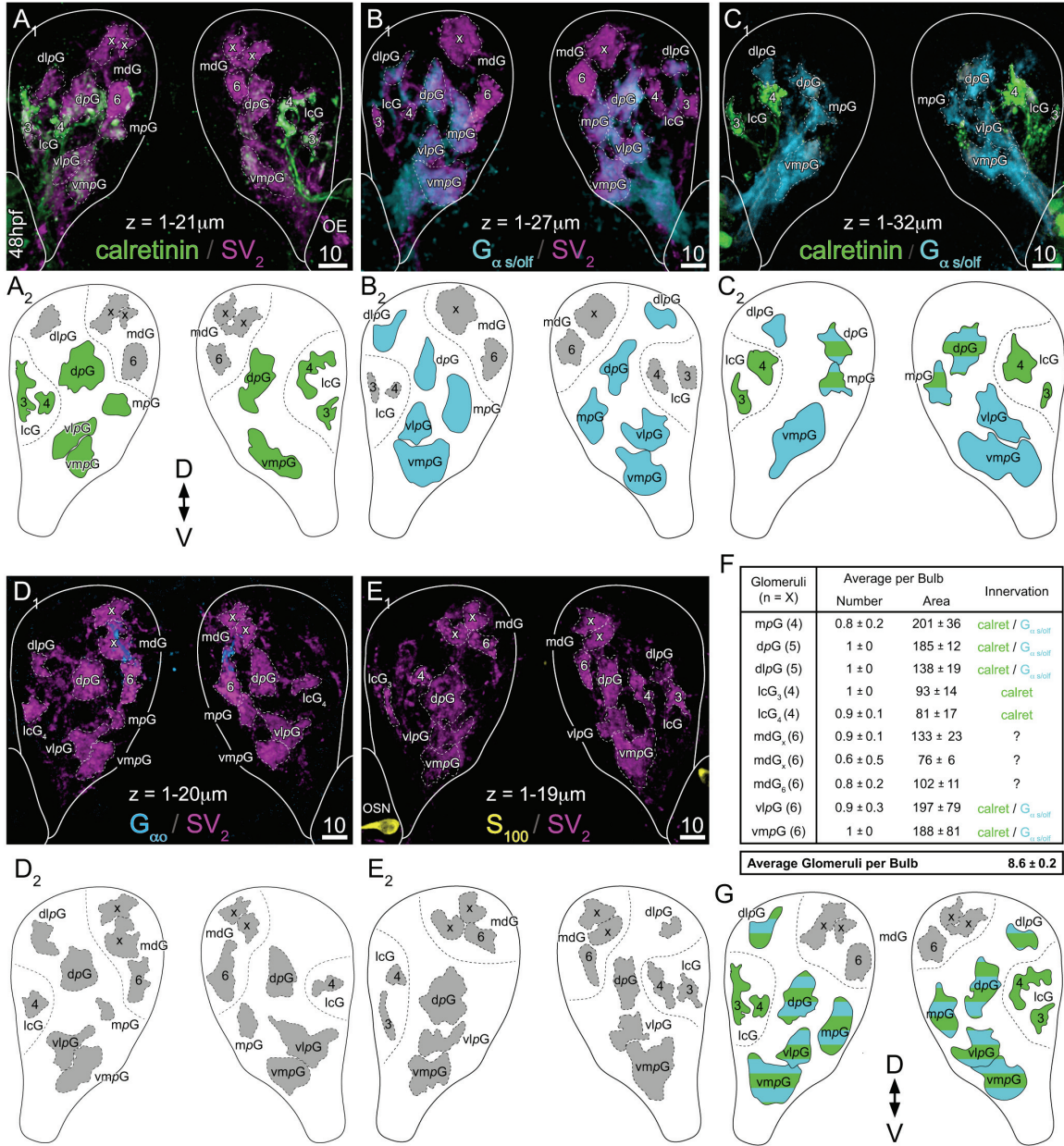
Supplemental Figure 7. Frontal views of olfactory bulb primordia from five 72hpf embryos labeled with different antibody combinations. A_{1-3} and B_{1-3} are subprojections of serial optical sections to show details of glomerular distributions (traced). At this developmental stage, the mdG resembled their mature counterparts and are selectively innervated by S_{100} IR (**D**) and $G_{\alpha o}$ IR axons (**E**). Note the inconsistent calretinin labeling of the mediodorsal glomeruli (compare mdG in **A** and **C**). (**A**, **B**) Five large protoglomeruli occupied most of the 72hpf olfactory bulbs, and these are uniformly innervated by calretinin IR and $G_{\alpha\,s/olf}$ IR axons. (**G**) Mean numbers and cross-sectional areas (plus standard errors) of identified glomeruli are listed.

G

Glomeruli (n=x)	Average per Bulb		Innervation
	Number	Area	
mpG (4)	1 ± 0	346 ± 17	calret / G$_{\alpha\,s/olf}$
dpG (6)	1 ± 0	469 ± 27	calret / G$_{\alpha\,s/olf}$
dl$p$G (6)	1 ± 0	202 ± 15	calret / G$_{\alpha\,s/olf}$
lcG$_3$ (6)	0.9 ± 0.1	129 ± 17	calret
lcG$_4$ (6)	0.9 ± 0.1	115 ± 3	calret
lcG* (6)	0.5 ± 0.2	51 ± 11	calret
lvpG (4)	1 ± 0	61 ± 12	?

continued >>

mdG$_1$ (5)	0.7 ± 0.2	74 ± 8	?
mdG$_2$ (5)	0.8 ± 0.1	82 ± 8	S$_{100}$
mdG$_3$ (5)	1 ± 0	126 ± 14	?
mdG$_4$ (5)	0.7 ± 0.2	61 ± 7	?
mdG$_5$ (5)	0.7 ± 0.2	39 ± 10	G$_{\alpha o}$
mdG$_6$ (5)	1 ± 0	148 ± 11	?
vl$p$G (6)	1 ± 0	368 ± 88	calret / G$_{\alpha\,s/olf}$
vm$p$G (6)	0.8 ± 0.3	323 ± 74	calret / G$_{\alpha\,s/olf}$
vpG (4)	0.8 ± 0.2	71 ± 17	?
Total Number of Glomeruli			**13.8 ± 1.9**
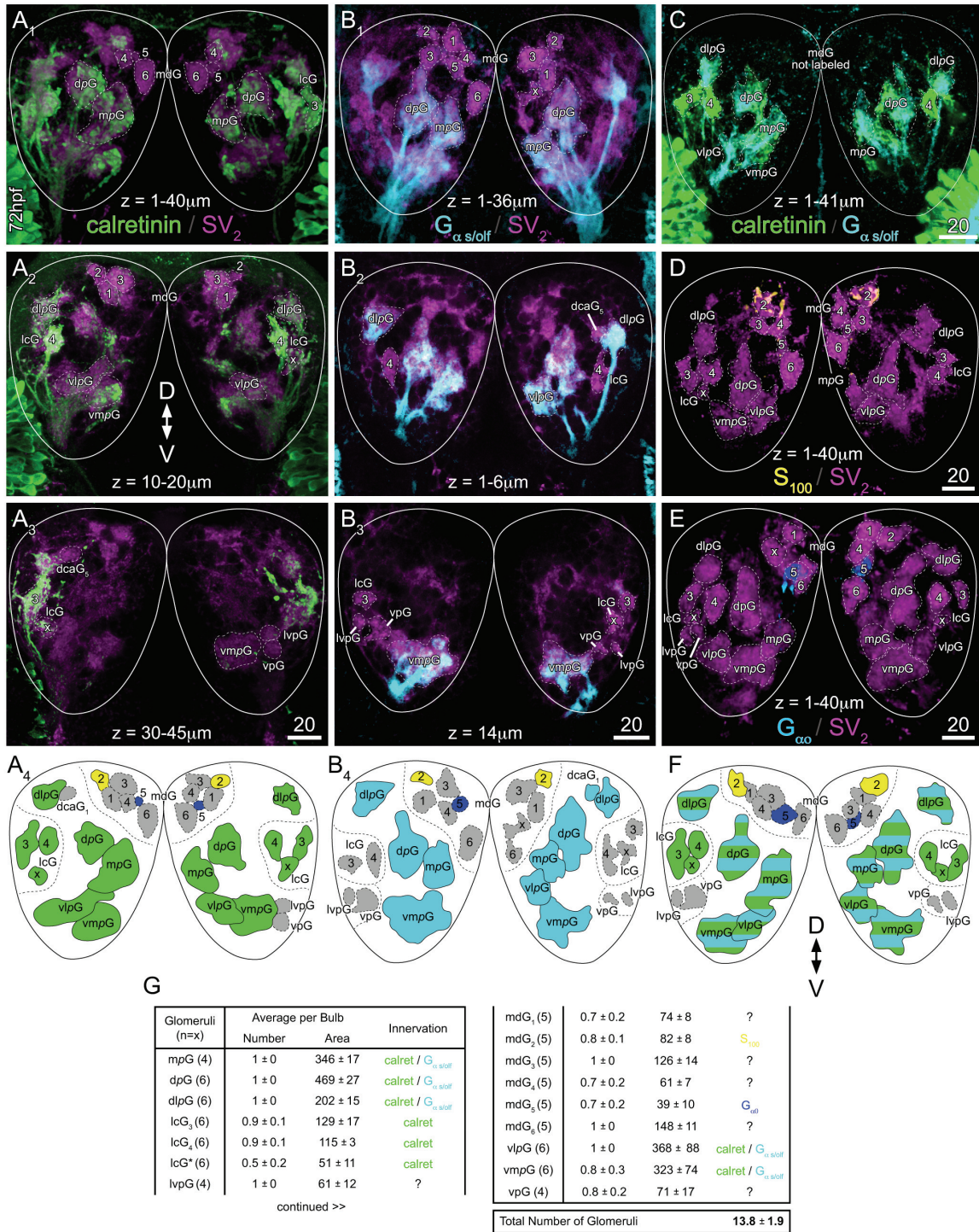
Supplemental Figure S7. Frontal Views of Olfactory Bulb Primordia From Five 72hpf Embryos Labeled With Different Antibody Combinations

273

Supplemental Figure 8. Dorsal olfactory bulbs from four early larvae labeled with different antibody combinations. Numbers were only assigned to glomeruli that were identified unambiguously across specimens, and 'x' denotes other, inconsistently identified units. (**A**, **B**) New glomeruli formed in the dorsal (dG) and dorsolateral (dlG) cluster, which previously consisted of a single protoglomerulus. With the exception of a single glomerulus (dG$_1$), the dorsal and dorsolateral glomeruli labeled with both anti-calretinin and anti-G$\alpha_{s/olf}$. Several small lateral glomeruli appeared to form between pre-existing lcG$_3$ and lcG$_4$ (lcG$_x$ in **A$_3$**, **A$_4$**).
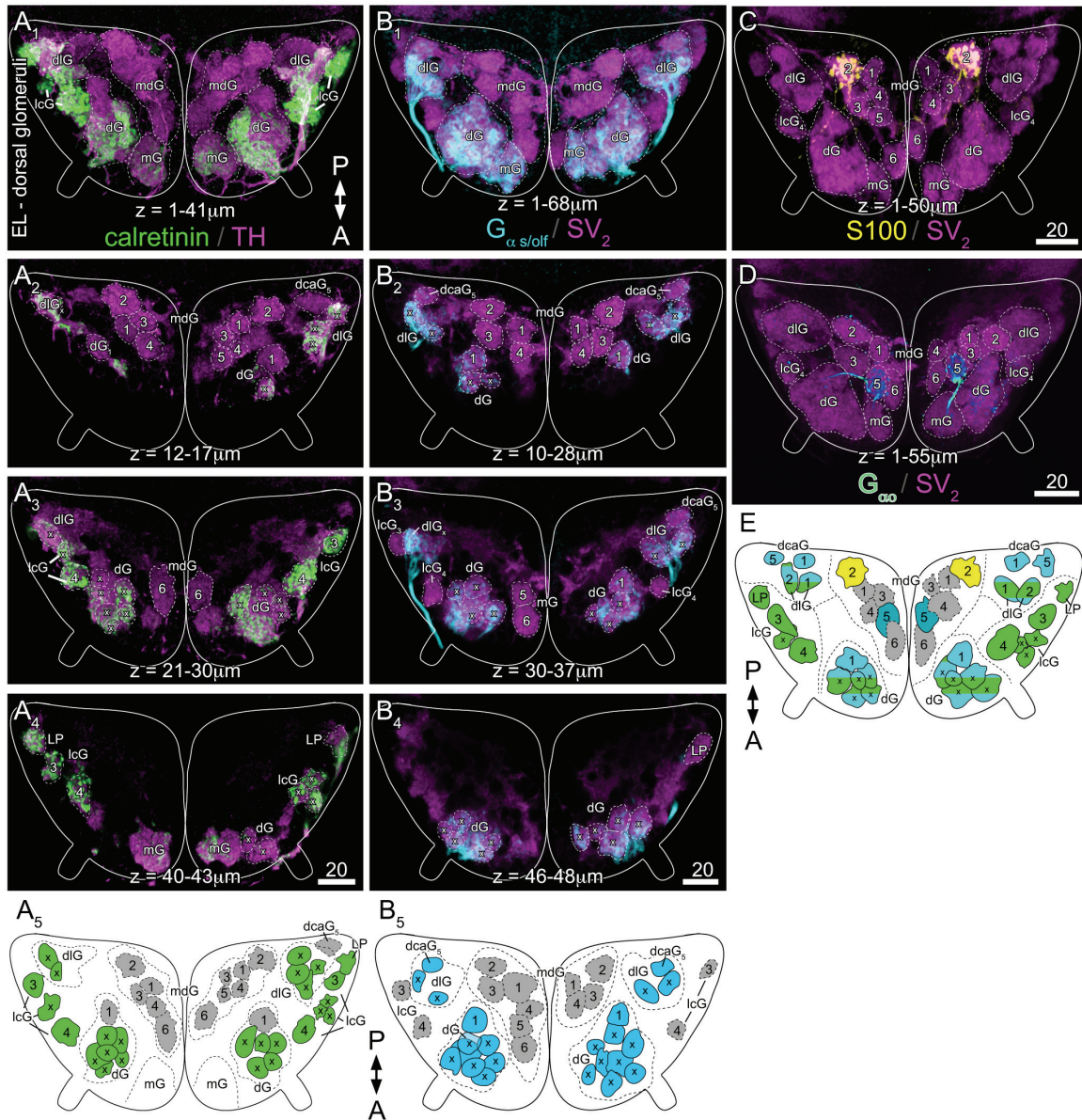
Figure S8 Dorsal Olfactory Bulbs From Four Early Larvae Labeled With Different Antibody Combinations

Chapter 6

Conclusion

6.1 Summary and Conclusion

The objective of this thesis was to identify zebrafish olfactory behaviors that are pre-existing and learned, and to describe the anatomy of olfactory pathways that may underlie these behaviors. In Chapter 2, I describe that zebrafish respond to amino acids, but not a neutral odor, with appetitive swimming behaviors. However, the animals can be conditioned to respond with appetitive behaviors to the neutral odor, demonstrating both a pre-existing and an acquired olfactory behavior. In Chapters 3-4, I characterize the distributions and anatomy of zebrafish olfactory glomeruli, and based on this work I have been able to identify two distinct sets of glomeruli. The first set consists of 25 large and individually identifiable glomeruli, located in reproducible locations throughout the olfactory bulbs of different animals. The other glomeruli are comparably small, anatomically indistinguishable and located in variable arrangements in certain regions of the olfactory bulbs. Finally, in Chapter 5 I provide a description of the development of the different types of glomeruli; I show that the large and stereotypic glomeruli are the first to develop and that they mature apparently independent of sensory experience. In contrast, the small and anatomically variable glomeruli develop only after the animals hatch, and their maturation can be modulated by alterations in the olfactory environment.

Collectively, these results suggest that the olfactory system of zebrafish may be divided into stable and plastic olfactory pathways. The stable olfactory pathway (25 large glomeruli) appears to develop largely under control of preprogrammed genetic events, remains present throughout life, and may serve to inform the animal about certain odors that require appropriate responses during all developmental stages. The plastic olfactory pathway appears to be more dynamic and shaped by the experience of each

animal. Given its plasticity, this latter olfactory pathway could subserve the acquisition of new behavioral responses to learned odorants. I observe both types of olfactory pathways in the medial and lateral olfactory bulbs, suggesting that they are important in social and feeding behaviors. In closing, I will discuss how these two pathways may have produced the pre-existing and conditioned responses to amino acids observed in Chapter 2.

6.2 Neural Substrates for Pre-Existing and Learned Appetitive Behaviors

Amino Acid Attraction Appears to be Innate

The pre-existing amino acid-evoked olfactory behaviors described in Chapter 2 were presumably mediated by the lateral glomeruli. The two amino acids that I used, L-alanine and L-valine, evoke neural activity in the lateral olfactory bulbs of zebrafish (Friedrich and Korsching, 1997) and genetic perturbations of lateral glomeruli interfere with pre-existing attraction of adult zebrafish to amino acids (Koide et al., 2009).

The first lateral glomeruli to develop are lcG_3 and lcG_4 (Chapter 5). At the time of hatching (3dpf), these units are visible in every fish, while the remaining lateral glomeruli only begin to take shape in ensuing days. Prior to this work, these glomeruli had not been identified, but related evidence suggest that lcG_3 and lcG_4 are functional and involved in mediating olfactory behaviors when zebrafish become active at 5dpf. Li et al. (2005) showed that certain regions in the olfactory bulb primordia, which closely correspond to the locations of lcG_3 and / or lcG_4, become responsive to amino acids between 4-5dpf; at 5dpf, these regions respond strongly to several amino acids. At the same time, amino acids apparently evoke swimming behaviors in larvae (Vitebsky et al., 2005, Lindsay and Vogt, 2004), but if the development of the lateral glomeruli is

retarded, as in the *laure* mutant, then larval zebrafish do not respond to amino acids (Vitebsky et al., 2005). These data suggest that the lateral glomeruli become active and involved in producing olfactory behaviors between 4-5dpf.

Zebrafish do not feed until 5-6dpf, and therefore there is little or no time for the animals to make an association between amino acids and the event of feeding. I thus suggest that the attraction of zebrafish to some amino acids is innate, and is relayed by the earliest functional units in the lateral olfactory bulbs, which include lcG$_3$ and lcG$_4$.

A Stable and a Dynamic Lateral Olfactory Pathway

The lateral olfactory bulbs of adult zebrafish contain the largest and most stereotypic glomeruli, namely lcG$_3$ and lcG$_4$ along with anatomically variable lcG$_x$ and the LP. As discussed in Chapter 4, electrophysiological and optical imaging data suggest that these different types of glomeruli serve different roles in olfactory coding, and that a functional dichotomy may exist between certain units in the lateral olfactory bulbs. For example, in an experiment is was demonstrated that 10 of 14 tested amino acids evoked activity in a sharply demarcated 'glomerular modules' (Friedrich and Korsching, 1997), which appear to correlate in position with either the lcG$_3$ or lcG$_4$. However, each amino acid additionally elicits distinct but overlapping activity patterns in surrounding posterolateral regions (Friedrich and Korsching, 1997), which likely resemble the glomerular plexus (see Chapter 3). In Chapter 4 I thus hypothesized that amino acids may be encoded by a) a stable yes / no response by lcG$_3$ and lcG$_4$ in addition to b) a unique combinatorial activity pattern that encodes detailed stimulus information, like exact odor identity and concentration.

What might the role of this redundant or complementary odor code be during learning? Olfactory learning changes odor representations in the olfactory bulb (Wilson and Leon, 1988, Johnson et al., 1995) and presumably also changes the perception of the encoded odors. As Peele et al (2006) have suggested, it may be necessary for an animal to retain certain features of an odor representation as the animal has to compare what it has learned about the stimulus to the original percept in order to know what is new. Indeed, these authors then demonstrated that certain honeybee glomeruli, which notably are innervated by uniglomerular mitral cells (e.g., like lcG_3 and lcG_4), did not change their odor responsiveness after conditioning in an exhaustive array of different learning paradigms. However, other glomeruli involved in processing the conditioned odorants, changed their responsiveness, presumably to encode new stimulus features acquired during learning. I hypothesize that a similar process may underlie my findings in Chapter 2, and based on data collected in this thesis, I suggest that lcG_3 and lcG_4 might represent a similarly stable olfactory pathway and be largely unaffected by the olfactory conditioning. I would, however, expect odor representations in the lcG_x and LP to change. Both of these substrates are highly variable among different animals (Chapter 3), can be changed through environmental enrichment (Chapter 5) and appear to have an integrative capacity as they are innervated by multiglomerular mitral cells that receive input from many different channels (Chapter 4). One possibility is that the repeated pairing of amino acid odors with food rewards could lead to changed integration of inputs representing L-alanine and L-valine; food odors activate the lateral olfactory bulbs very strongly (Tabor et al., 2004; Li et al., 2005), and could shape the processing of amino

acid information if they are co-presented. Given the detailed overview that this thesis now provides over the zebrafish olfactory system, such questions can now be addressed.

Conclusion

In this thesis I have developed a method to study innate and learned appetitive behaviors in zebrafish and created a thorough overview of the development and organization of this animals olfactory system. My work not only provides a basis for future studies aimed at linking the cellular neurobiology of olfaction with whole animal behavior, but also leads to the hypothesis that olfaction may be encoded in parallel pathways that act synergistically to encode recurring and variable olfactory information. Zebrafish are an excellent model to investigate this further, and now that the tools are in place, new experiments can begin.

Bibliography

ACHE, B. W. & YOUNG, J. M. 2005. Olfaction: diverse species, conserved principles. *Neuron,* 48**,** 417-30.

AGETSUMA, M., AIZAWA, H., AOKI, T., NAKAYAMA, R., TAKAHOKO, M., GOTO, M., SASSA, T., AMO, R., SHIRAKI, T., KAWAKAMI, K., HOSOYA, T., HIGASHIJIMA, S. & OKAMOTO, H. 2010. The habenula is crucial for experience-dependent modification of fear responses in zebrafish. *Nat Neurosci,* 13**,** 1354-6.

ALIOTO, T. S. & NGAI, J. 2005. The odorant receptor repertoire of teleost fish. *BMC Genomics,* 6**,** 173.

ALONSO, J. R., LARA, J., MIGUEL, J. J. & AIJON, J. 1987. Ruffed cells in the olfactory bulb of freshwater teleosts. I. Golgi impregnation. *J Anat,* 155**,** 101-7.

APICELLA, A., YUAN, Q., SCANZIANI, M. & ISAACSON, J. S. 2010. Pyramidal cells in piriform cortex receive convergent input from distinct olfactory bulb glomeruli. *J Neurosci,* 30**,** 14255-60.

AREVALO, R., ALONSO, J. R., LARA, J., BRINON, J. G. & AIJON, J. 1991. Ruffed cells in the olfactory bulb of freshwater teleosts. II. A Golgi/EM study of the ruff. *J Hirnforsch,* 32**,** 477-84.

ARGO, S., WETH, F. & KORSCHING, S. I. 2003. Analysis of penetrance and expressivity during ontogenesis supports a stochastic choice of zebrafish odorant receptors from predetermined groups of receptor genes. *Eur J Neurosci,* 17**,** 833-43.

ASAKAWA, K., SUSTER, M. L., MIZUSAWA, K., NAGAYOSHI, S., KOTANI, T., URASAKI, A., KISHIMOTO, Y., HIBI, M. & KAWAKAMI, K. 2008. Genetic dissection of neural circuits by Tol2 transposon-mediated Gal4 gene and enhancer trapping in zebrafish. *Proc Natl Acad Sci U S A,* 105**,** 1255-60.

BAIER, H. & KORSCHING, S. 1994. Olfactory glomeruli in the zebrafish form an invariant pattern and are identifiable across animals. *J Neurosci,* 14**,** 219-230.

BAIER, H., ROTTER, S. & KORSCHING, S. 1994. Connectional topography in the zebrafish olfactory system: random positions but regular spacing of sensory neurons projecting to an individual glomerulus. *Proc Natl Acad Sci U S A,* 91**,** 11646-50.

BAILEY, M. S., PUCHE, A. C. & SHIPLEY, M. T. 1999. Development of the olfactory bulb: evidence for glia-neuron interactions in glomerular formation. *J Comp Neurol,* 415**,** 423-48.

BARNEA, G., O'DONNELL, S., MANCIA, F., SUN, X., NEMES, A., MENDELSOHN, M. & AXEL, R. 2004. Odorant receptors on axon termini in the brain. *Science,* 304**,** 1468.

BELANGER, R. M., SMITH, C. M., CORKUM, L. D. & ZIELINSKI, B. S. 2003. Morphology and histochemistry of the peripheral olfactory organ in the round goby, *Neogobius melanostomus* (Teleostei: Gobiidae). *J Morphol,* 257**,** 62-71.

BELLMANN, D., RICHARDT, A., FREYBERGER, R., NUWAL, N., SCHWARZEL, M., FIALA, A. & STORTKUHL, K. F. 2010. Optogenetically induced olfactory stimulation in *Drosophila* larvae reveals the neuronal basis of odor-aversion behavior. *Front Behav Neurosci,* 4**,** 27.

BELLUSCIO, L., KOENTGES, G., AXEL, R. & DULAC, C. 1999. A map of pheromone receptor activation in the mammalian brain. *Cell,* 97**,** 209-20.

BOECKH, J., ERNST, K. D. & SELSAM, P. 1987. Neurophysiology and neuroanatomy of the olfactory pathway in the cockroach. *Ann N Y Acad Sci,* 510**,** 39-43.

BOZZA, T., MCGANN, J. P., MOMBAERTS, P. & WACHOWIAK, M. 2004. *In vivo* imaging of neuronal activity by targeted expression of a genetically encoded probe in the mouse. *Neuron,* 42**,** 9-21.

BOZZA, T., VASSALLI, A., FUSS, S., ZHANG, J. J., WEILAND, B., PACIFICO, R., FEINSTEIN, P. & MOMBAERTS, P. 2009. Mapping of class I and class II odorant receptors to glomerular domains by two distinct types of olfactory sensory neurons in the mouse. *Neuron,* 61**,** 220-33.

BRENNAN, P. A. & KENDRICK, K. M. 2006. Mammalian social odours: attraction and individual recognition. *Philos Trans R Soc Lond B Biol Sci,* 361**,** 2061-78.

BRUNET, L. J., GOLD, G. H. & NGAI, J. 1996. General anosmia caused by a targeted disruption of the mouse olfactory cyclic nucleotide-gated cation channel. *Neuron,* 17**,** 681-93.

BUCK, L. & AXEL, R. 1991. A novel multigene family may encode odorant receptors: a molecular basis for odor recognition. *Cell,* 65**,** 175-87.

BUCK, L. B. 2004. Olfactory receptors and odor coding in mammals. *Nutr Rev,* 62**,** S184-8.

BYRD, C. A. & BRUNJES, P. C. 1995. Organization of the olfactory system in the adult zebrafish: histological, immunohistochemical, and quantitative analysis. *J Comp Neurol,* 358**,** 247-59.

283

CASTRO, A., BECERRA, M., MANSO, M. J. & ANADON, R. 2006. Calretinin immunoreactivity in the brain of the zebrafish, *Danio rerio*: distribution and comparison with some neuropeptides and neurotransmitter-synthesizing enzymes. II. Midbrain, hindbrain, and rostral spinal cord. *J Comp Neurol,* 494**,** 792-814.

CELIK, A., FUSS, S. H. & KORSCHING, S. I. 2002. Selective targeting of zebrafish olfactory receptor neurons by the endogenous OMP promoter. *Eur J Neurosci,* 15**,** 798-806.

CHEN, W. R. & SHEPHERD, G. M. 2005. The olfactory glomerulus: a cortical module with specific functions. *J Neurocytol,* 34**,** 353-60.

CHRISTENSEN, T. A. & HILDEBRAND, J. G. 1987. Male-specific, sex pheromone-selective projection neurons in the antennal lobes of the moth *Manduca sexta*. *J Comp Physiol A,* 160**,** 553-69.

CHRISTENSEN, T. A. & HILDEBRAND, J. G. 1997. Coincident stimulation with pheromone components improves temporal pattern resolution in central olfactory neurons. *J Neurophysiol,* 77**,** 775-81.

CLOUTIER, J. F., GIGER, R. J., KOENTGES, G., DULAC, C., KOLODKIN, A. L. & GINTY, D. D. 2002. Neuropilin-2 mediates axonal fasciculation, zonal segregation, but not axonal convergence, of primary accessory olfactory neurons. *Neuron,* 33**,** 877-92.

CLOUTIER, J. F., SAHAY, A., CHANG, E. C., TESSIER-LAVIGNE, M., DULAC, C., KOLODKIN, A. L. & GINTY, D. D. 2004. Differential requirements for semaphorin 3F and Slit-1 in axonal targeting, fasciculation, and segregation of olfactory sensory neuron projections. *J Neurosci,* 24**,** 9087-96.

COCKERHAM, R. E., PUCHE, A. C. & MUNGER, S. D. 2009. Heterogeneous sensory innervation and extensive intrabulbar connections of olfactory necklace glomeruli. *PLoS One,* 4**,** e4657.

CONZELMANN, S., MALUN, D., BREER, H. & STROTMANN, J. 2001. Brain targeting and glomerulus formation of two olfactory neuron populations expressing related receptor types. *Eur J Neurosci,* 14**,** 1623-32.

COUTON, L., MINOLI, S., KIEU, K., ANTON, S. & ROSPARS, J. P. 2009. Constancy and variability of identified glomeruli in antennal lobes: computational approach in *Spodoptera littoralis*. *Cell Tissue Res,* 337**,** 491-511.

COX, J. P. 2008. Hydrodynamic aspects of fish olfaction. *J R Soc Interface,* 5**,** 575-93.

CUMMINGS, D. M. & BELLUSCIO, L. 2010. Continuous neural plasticity in the olfactory intrabulbar circuitry. *J Neurosci,* 30**,** 9172-80.

DARLAND, T. & DOWLING, J. E. 2001. Behavioral screening for cocaine sensitivity in mutagenized zebrafish. *Proc Natl Acad Sci U S A,* 98**,** 11691-6.

DERBY, C. D. & SORENSEN, P. W. 2008. Neural processing, perception, and behavioral responses to natural chemical stimuli by fish and crustaceans. *J Chem Ecol,* 34**,** 898-914.

DERJEAN, D., MOUSSADDY, A., ATALLAH, E., ST-PIERRE, M., AUCLAIR, F., CHANG, S., REN, X., ZIELINSKI, B. & DUBUC, R. 2010. A novel neural substrate for the transformation of olfactory inputs into motor output. *PLoS Biol,* 8**,** e1000567.

DHAWALE, A. K., HAGIWARA, A., BHALLA, U. S., MURTHY, V. N. & ALBEANU, D. F. 2010. Non-redundant odor coding by sister mitral cells revealed by light addressable glomeruli in the mouse. *Nat Neurosci,* 13**,** 1404-12.

DØVING, K. B., HANSSON, K. A., BACKSTROM, T. & HAMDANI, H. 2011. Visualizing a set of olfactory sensory neurons responding to a bile salt. *J Exp Biol,* 214**,** 80-7.

DØVING, K. B. & LASTEIN, S. 2009. The alarm reaction in fishes--odorants, modulations of responses, neural pathways. *Ann N Y Acad Sci,* 1170**,** 413-23.

DØVING, K. B., SELSET, R. & THOMMESEN, G. 1980. Olfactory sensitivity to bile acids in salmonid fishes. *Acta Physiol Scand,* 108**,** 123-31.

DULAC, C. 2000. Sensory coding of pheromone signals in mammals. *Curr Opin Neurobiol,* 10**,** 511-8.

DULAC, C. & WAGNER, S. 2006. Genetic analysis of brain circuits underlying pheromone signaling. *Annu Rev Genet,* 40**,** 449-67.

DYNES, J. L. & NGAI, J. 1998. Pathfinding of olfactory neuron axons to stereotyped glomerular targets revealed by dynamic imaging in living zebrafish embryos. *Neuron,* 20**,** 1081-1091.

EDWARDS, J. G., GREIG, A., SAKATA, Y., ELKIN, D. & MICHEL, W. C. 2007. Cholinergic innervation of the zebrafish olfactory bulb. *J Comp Neurol,* 504**,** 631-45.

ELSAESSER, R. & PAYSAN, J. 2007. The sense of smell, its signalling pathways, and the dichotomy of cilia and microvilli in olfactory sensory cells. *BMC Neurosci,* 8 Suppl 3**,** S1.

FEINSTEIN, P., BOZZA, T., RODRIGUEZ, I., VASSALLI, A. & MOMBAERTS, P. 2004. Axon guidance of mouse olfactory sensory neurons by odorant receptors and the β2 adrenergic receptor. *Cell,* 117**,** 833-46.

FEINSTEIN, P. & MOMBAERTS, P. 2004. A contextual model for axonal sorting into glomeruli in the mouse olfactory system. *Cell,* 117**,** 817-31.

FETCHO, J. R., HIGASHIJIMA, S. & MCLEAN, D. L. 2008. Zebrafish and motor control over the last decade. *Brain Res Rev,* 57**,** 86-93.

FINE, J. M., VRIEZE, L. A. & SORENSEN, P. W. 2004. Evidence that petromyzontid lampreys employ a common migratory pheromone that is partially comprised of bile acids. *J Chem Ecol,* 30**,** 2091-110.

FISHMAN, M. C. 2001. Genomics. Zebrafish--the canonical vertebrate. *Science,* 294**,** 1290-1.

FLANAGAN, D. & MERCER, A. R. 1989. An atlas and 3-D reconstruction of the antennal lobes in the work honey bee, *Apis mellifera* (Hymenoptera, Apidae). *Int J Insect Morph Embr,* 18**,** 145-159.

FRIEDRICH, R. W. 2006. Mechanisms of odor discrimination: neurophysiological and behavioral approaches. *Trends Neurosci,* 29**,** 40-7.

FRIEDRICH, R. W. & KORSCHING, S. I. 1997. Combinatorial and chemotopic odorant coding in the zebrafish olfactory bulb visualized by optical imaging. *Neuron,* 18**,** 737-52.

FRIEDRICH, R. W. & KORSCHING, S. I. 1998. Chemotopic, combinatorial, and noncombinatorial odorant representations in the olfactory bulb revealed using a voltage-sensitive axon tracer. *J Neurosci,* 18**,** 9977-88.

FRIEDRICH, R. W. & LAURENT, G. 2001. Dynamic optimization of odor representations by slow temporal patterning of mitral cell activity. *Science,* 291**,** 889-94.

FRONTINI, A., ZAIDI, A. U., HUA, H., WOLAK, T. P., GREER, C. A., KAFITZ, K. W., LI, W. & ZIELINSKI, B. S. 2003. Glomerular territories in the olfactory bulb from the larval stage of the sea lamprey *Petromyzon marinus. J Comp Neurol,* 465**,** 27-37.

FUJITA, I., SORENSEN, P. W., STACEY, N. E. & HARA, T. J. 1991. The olfactory system, not the terminal nerve, functional as the primary chemosensory pathway mediating responses to sex-pheromones in male goldfish. *Brain Behav Evol,* 38**,** 313-321.

FULLER, C. L. & BYRD, C. A. 2005. Ruffed cells identified in the adult zebrafish olfactory bulb. *Neurosci Lett,* 379**,** 190-4.

FULLER, C. L., YETTAW, H. K. & BYRD, C. A. 2006. Mitral cells in the olfactory bulb of adult zebrafish (*Danio rerio*): morphology and distribution. *J Comp Neurol,* 499**,** 218-30.

FUSS, S. H. & KORSCHING, S. I. 2001. Odorant feature detection: activity mapping of structure response relationships in the zebrafish olfactory bulb. *J Neurosci,* 21**,** 8396-407.

GALIZIA, C. G., MCILWRATH, S. L. & MENZEL, R. 1999. A digital three-dimensional atlas of the honeybee antennal lobe based on optical sections acquired by confocal microscopy. *Cell Tissue Res,* 295**,** 383-94.

GALIZIA, C. G. & RÖSSLER, W. 2010. Parallel olfactory systems in insects: anatomy and function. *Annu Rev Entomol,* 55**,** 399-420.

GAUDIN, A. & GASCUEL, J. 2005. 3D atlas describing the ontogenic evolution of the primary olfactory projections in the olfactory bulb of *Xenopus laevis*. *J Comp Neurol,* 489**,** 403-24.

GERMANA, A., PARUTA, S., GERMANA, G. P., OCHOA-ERENA, F. J., MONTALBANO, G., COBO, J. & VEGA, J. A. 2007. Differential distribution of S100 protein and calretinin in mechanosensory and chemosensory cells of adult zebrafish (*Danio rerio*). *Brain Res,* 1162**,** 48-55.

GHYSEN, A. & DAMBLY-CHAUDIERE, C. 2007. The lateral line microcosmos. *Genes Dev,* 21**,** 2118-30.

GREER, C. A., STEWART, W. B., TEICHER, M. H. & SHEPHERD, G. M. 1982. Functional development of the olfactory bulb and a unique glomerular complex in the neonatal rat. *J Neurosci,* 2**,** 1744-59.

HALASZ, N. & GREER, C. A. 1993. Terminal arborizations of olfactory nerve fibers in the glomeruli of the olfactory bulb. *J Comp Neurol,* 337**,** 307-16.

HALL, D. & SUBOSKI, M. D. 1995. Sensory Preconditioning and 2nd-Order Conditioning of Alarm Reactions in Zebra Danio Fish (*Brachydanio-Rerio*). *J Comp Psych,* 109**,** 76-84.

HAMDANI, H., ALEXANDER, G. & DØVING, K. B. 2001a. Projection of sensory neurons with microvilli to the lateral olfactory tract indicates their participation in feeding behaviour in crucian carp. *Chem Senses,* 26**,** 1139-1144.

HAMDANI, H., KASUMYAN, A. & DØVING, K. B. 2001b. Is feeding behaviour in crucian carp mediated by the lateral olfactory tract? *Chem Senses,* 26**,** 1133-1138.

HAMDANI, H. & DØVING, K. B. 2002. The alarm reaction in crucian carp is mediated by olfactory neurons with long dendrites. *Chem Senses,* 27**,** 395-8.

HAMDANI, H. & DØVING, K. B. 2003. Sensitivity and selectivity of neurons in the medial region of the olfactory bulb to skin extract from conspecifics in crucian carp, *Carassius carassius. Chem Senses,* 28**,** 181-9.

HAMDANI, H. & DØVING, K. B. 2007. The functional organization of the fish olfactory system. *Prog Neurobiol,* 82**,** 80-6.

HAMDANI, H., LASTEIN, S., GREGERSEN, F. & DØVING, K. B. 2008. Seasonal variations in olfactory sensory neurons--fish sensitivity to sex pheromones explained? *Chem Senses,* 33**,** 119-23.

HANSEN, A. & FINGER, T. E. 2000. Phyletic distribution of crypt-type olfactory receptor neurons in fishes. *Brain Behav Evol,* 55**,** 100-110.

HANSEN, A., ROLEN, S. H., ANDERSON, K., MORITA, Y., CAPRIO, J. & FINGER, T. E. 2003. Correlation between olfactory receptor cell type and function in the channel catfish. *J Neurosci,* 23**,** 9328-9339.

HANSEN, A., ROLEN, S. H., ANDERSON, K., MORITA, Y., CAPRIO, J. & FINGER, T. E. 2005. Olfactory receptor neurons in fish: Structural, molecular and functional correlates. *Chem Senses,* 30**,** I311-I311.

HANSEN, A. & ZEISKE, E. 1993. Development of the Olfactory Organ in the Zebrafish, *Brachydanio-Rerio. J Comp Neurol,* 333**,** 289-300.

HANSEN, A. & ZIELINSKI, B. S. 2005. Diversity in the olfactory epithelium of bony fishes: development, lamellar arrangement, sensory neuron cell types and transduction components. *J Neurocytol,* 34**,** 183-208.

HANSON, L. R., SORENSEN, P. W. & COHEN, Y. 1998. Sex pheromones and amino acids evoke distinctly different spatial patterns of electrical activity in the goldfish olfactory bulb. *Ann N Y Acad Sci,* 855**,** 521-4.

HANSSON, B. S., LJUNGBERG, H., HALLBERG, E. & LOFSTEDT, C. 1992. Functional specialization of olfactory glomeruli in a moth. *Science,* 256**,** 1313-5.

HARA, T. J. 1994. Olfaction and gustation in fish: an overview. *Acta Physiol Scand,* 152**,** 207-17.

HARA, T. J. 2006. Feeding behaviour in some teleosts is triggered by single amino acids primarily through olfaction. *Journal of Fish Biology,* 68**,** 810-825.

HARDEN, M. V., NEWTON, L. A., LLOYD, R. C. & WHITLOCK, K. E. 2006. Olfactory imprinting is correlated with changes in gene expression in the olfactory epithelia of the zebrafish. *J Neurobiol,* 66**,** 1452-1466.

HASHIGUCHI, Y. & NISHIDA, M. 2007. Evolution of trace amine associated receptor (TAAR) gene family in vertebrates: lineage-specific expansions and degradations of a second class of vertebrate chemosensory receptors expressed in the olfactory epithelium. *Mol Biol Evol,* 24**,** 2099-107.

HASLER, A., SCHOLZ, A. T. & HORRALL, R. M. 1978. Olfactory imprinting and homing in salmon. *Am Sci,* 66**,** 347-55.

HERBERT, P. & ATEMA, J. 1977. Olfactory Discrimination of Male and Female Conspecifics in Bullhead Catfish, *Ictalurus-Nebulosus. Biol Bull,* 153**,** 429-430.

HILDEBRAND, J. G. & SHEPHERD, G. M. 1997. Mechanisms of olfactory discrimination: converging evidence for common principles across phyla. *Annu Rev Neurosci,* 20**,** 595-631.

HU, J., ZHONG, C., DING, C., CHI, Q., WALZ, A., MOMBAERTS, P., MATSUNAMI, H. & LUO, M. 2007. Detection of near-atmospheric concentrations of CO_2 by an olfactory subsystem in the mouse. *Science,* 317**,** 953-7.

HUETTEROTH, W. & SCHACHTNER, J. 2005. Standard three-dimensional glomeruli of the *Manduca sexta* antennal lobe: a tool to study both developmental and adult neuronal plasticity. *Cell Tissue Res,* 319**,** 513-24.

IBBA, I., ANGIOY, A. M., HANSSON, B. S. & DEKKER, T. 2010. Macroglomeruli for fruit odors change blend preference in *Drosophila. Naturwissenschaften,* 97**,** 1059-66.

IGNELL, R., ANTON, S. & HANSSON, B. S. 2001. The antennal lobe of orthoptera - anatomy and evolution. *Brain Behav Evol,* 57**,** 1-17.

IMAI, T. & SAKANO, H. 2007. Roles of odorant receptors in projecting axons in the mouse olfactory system. *Curr Opin Neurobiol,* 17**,** 507-15.

IMAI, T., SUZUKI, M. & SAKANO, H. 2006. Odorant receptor-derived cAMP signals direct axonal targeting. *Science,* 314**,** 657-61.

IWAHORI, N., KIYOTA, E. & NAKAMURA, K. 1987. A Golgi study on the olfactory bulb in the lamprey, *Lampetra japonica. Neurosci Res,* 5**,** 126-39.

JASTREBOFF, P. J., PEDERSEN, P. E., GREER, C. A., STEWART, W. B., KAUER, J. S., BENSON, T. E. & SHEPHERD, G. M. 1984. Specific olfactory receptor populations projecting to identified glomeruli in the rat olfactory bulb. *Proc Natl Acad Sci U S A,* 81**,** 5250-4.

JESUTHASAN, S. J. & MATHURU, A. S. 2008. The alarm response in zebrafish: innate fear in a vertebrate genetic model. *J Neurogenet,* 22**,** 211-28.

JIA, C., CHEN, W. R. & SHEPHERD, G. M. 1999. Synaptic organization and neurotransmitters in the rat accessory olfactory bulb. *J Neurophysiol,* 81**,** 345-55.

JOHNSON, B. A. & LEON, M. 2007. Chemotopic odorant coding in a mammalian olfactory system. *J Comp Neurol,* 503**,** 1-34.

JOHNSON, B. A., WOO, C. C., DUONG, H., NGUYEN, V. & LEON, M. 1995. A learned odor evokes an enhanced Fos-like glomerular response in the olfactory bulb of young rats. *Brain Res,* 699**,** 192-200.

JOHNSON, B. A., WOO, C. C., NINOMIYA-TSUBOI, K. & LEON, M. 1996. Synaptophysin-like immunoreactivity in the rat olfactory bulb during postnatal development and after restricted early olfactory experience. *Brain Res Dev Brain Res,* 92**,** 24-30.

JONES, S. V., CHOI, D. C., DAVIS, M. & RESSLER, K. J. 2008. Learning-dependent structural plasticity in the adult olfactory pathway. *J Neurosci,* 28**,** 13106-11.

KARPATI, Z., OLSSON, S., HANSSON, B. S. & DEKKER, T. 2010. Inheritance of central neuroanatomy and physiology related to pheromone preference in the male European corn borer. *BMC Evol Biol,* 10**,** 286.

KASLIN, J. & PANULA, P. 2001. Comparative anatomy of the histaminergic and other aminergic systems in zebrafish (Danio rerio). *J Comp Neurol,* 440**,** 342-77.

KASOWSKI, H. J., KIM, H. & GREER, C. A. 1999. Compartmental organization of the olfactory bulb glomerulus. *J Comp Neurol,* 407**,** 261-74.

KAZAWA, T., NAMIKI, S., FUKUSHIMA, R., TERADA, M., SOO, K. & KANZAKI, R. 2009. Constancy and variability of glomerular organization in the antennal lobe of the silkmoth. *Cell Tissue Res,* 336**,** 119-36.

KERR, M. A. & BELLUSCIO, L. 2006. Olfactory experience accelerates glomerular refinement in the mammalian olfactory bulb. *Nat Neurosci,* 9**,** 484-6.

KIMMEL, C. B., BALLARD, W. W., KIMMEL, S. R., ULLMANN, B. & SCHILLING, T. F. 1995. Stages of embryonic development of the zebrafish. *Dev Dyn,* 203**,** 253-310.

KISHI, K., MORI, K. & TAZAWA, Y. 1982. Three-dimensional analysis of dendritic trees of mitral cells in the rabbit olfactory bulb. *Neurosci Lett,* 28**,** 127-32.

KLEINEIDAM, C. J., OBERMAYER, M., HALBICH, W. & RÖSSLER, W. 2005. A macroglomerulus in the antennal lobe of leaf-cutting ant workers and its possible functional significance. *Chem Senses,* 30**,** 383-92.

KNOLL, B., SCHMIDT, H., ANDREWS, W., GUTHRIE, S., PINI, A., SUNDARESAN, V. & DRESCHER, U. 2003. On the topographic targeting of basal vomeronasal axons through Slit-mediated chemorepulsion. *Development,* 130**,** 5073-82.

KOBAYAKAWA, K., KOBAYAKAWA, R., MATSUMOTO, H., OKA, Y., IMAI, T., IKAWA, M., OKABE, M., IKEDA, T., ITOHARA, S., KIKUSUI, T., MORI, K. & SAKANO, H. 2007. Innate versus learned odour processing in the mouse olfactory bulb. *Nature,* 450**,** 503-8.

KOIDE, T., MIYASAKA, N., MORIMOTO, K., ASAKAWA, K., URASAKI, A., KAWAKAMI, K. & YOSHIHARA, Y. 2009. Olfactory neural circuitry for attraction to amino acids revealed by transposon-mediated gene trap approach in zebrafish. *Proc Natl Acad Sci U S A,* 106**,** 9884-9.

KORSCHING, S. 2005. Selective imaging of the receptor neuron population in the olfactory bulb of zebrafish and mice. *Chem Senses,* 30 Suppl 1**,** i101-2.

KORSCHING, S. I., ARGO, S., CAMPENHAUSEN, H., FRIEDRICH, R. W., RUMMRICH, A. & WETH, F. 1997. Olfaction in zebrafish: what does a tiny teleost tell us? *Semin Cell Dev Biol,* 8**,** 181-7.

KOSAKA, K., TOIDA, K., MARGOLIS, F. L. & KOSAKA, T. 1997. Chemically defined neuron groups and their subpopulations in the glomerular layer of the rat main olfactory bulb--II. Prominent differences in the intraglomerular dendritic arborization and their relationship to olfactory nerve terminals. *Neurosci,* 76**,** 775-86.

KOSAKA, T. & HAMA, K. 1979. A new type of neuron with a distinctive axon initial segment. *Brain Res,* 163**,** 151-5.

KOSAKA, T. & HAMA, K. 1982a. Structure of the mitral cell in the olfactory bulb of the goldfish (*Carassius auratus*). *J Comp Neurol,* 212**,** 365-84.

KOSAKA, T. & HAMA, K. 1982b. Synaptic organization in the teleost olfactory bulb. *J Physiol (Paris),* 78**,** 707-19.

KOTRSCHAL, K. 2000. Taste(s) and olfaction(s) in fish: a review of specialized subsystems and central integration. *Pflugers Arch,* 439**,** R178-80.

LABERGE, F. & HARA, T. J. 2001. Neurobiology of fish olfaction: a review. *Brain Res Rev,* 36**,** 46-59.

LAISSUE, P. P., REITER, C., HIESINGER, P. R., HALTER, S., FISCHBACH, K. F. & STOCKER, R. F. 1999. Three-dimensional reconstruction of the antennal lobe in *Drosophila melanogaster*. *J Comp Neurol,* 405**,** 543-52.

LASTEIN, S., HAMDANI, H. & DØVING, K. B. 2006. Gender distinction in neural discrimination of sex pheromones in the olfactory bulb of crucian carp, *Carassius carassius*. *Chem Senses,* 31**,** 69-77.

LAURENT, G., STOPFER, M., FRIEDRICH, R. W., RABINOVICH, M. I., VOLKOVSKII, A. & ABARBANEL, H. D. 2001. Odor encoding as an active, dynamical process: experiments, computation, and theory. *Annu Rev Neurosci,* 24**,** 263-97.

LEE, A., MATHURU, A. S., TEH, C., KIBAT, C., KORZH, V., PENNEY, T. B. & JESUTHASAN, S. 2010. The habenula prevents helpless behavior in larval zebrafish. *Curr Biol,* 20**,** 2211-6.

LEI, H., MOONEY, R. & KATZ, L. C. 2006. Synaptic integration of olfactory information in mouse anterior olfactory nucleus. *J Neurosci,* 26**,** 12023-32.

LEINDERS-ZUFALL, T., LANE, A. P., PUCHE, A. C., MA, W., NOVOTNY, M. V., SHIPLEY, M. T. & ZUFALL, F. 2000. Ultrasensitive pheromone detection by mammalian vomeronasal neurons. *Nature,* 405**,** 792-6.

LI, J., MACK, J. A., SOUREN, M., YAKSI, E., HIGASHIJIMA, S., MIONE, M., FETCHO, J. R. & FRIEDRICH, R. W. 2005a. Early development of functional spatial maps in the zebrafish olfactory bulb. *J Neurosci,* 25**,** 5784-5795.

LI, W., SCOTT, A. P., SIEFKES, M. J., YAN, H., LIU, Q., YUN, S. S. & GAGE, D. A. 2002. Bile Acid secreted by male sea lamprey that acts as a sex pheromone. *Science,* 296**,** 138-41.

LIBERLES, S. D. & BUCK, L. B. 2006. A second class of chemosensory receptors in the olfactory epithelium. *Nature,* 442**,** 645-50.

LINDSAY, S. M. & VOGT, R. G. 2004. Behavioral responses of newly hatched zebrafish (Danio rerio) to amino acid chemostimulants. *Chem Senses,* 29**,** 93-100.

LINSTER, C. & CLELAND, T. A. 2010. Decorrelation of Odor Representations via Spike Timing-Dependent Plasticity. *Front Comput Neurosci,* 4**,** 157.

LIPSCHITZ, D. L. & MICHEL, W. C. 2002. Amino acid odorants stimulate microvillar sensory neurons. *Chem Senses,* 27**,** 277-86.

LITTLE, E. E. 1981. Conditioned cardiac response to the olfactory stimuli of amino acids in the channel catfish, *Ictalurus punctatus*. *Physiol Behav,* 27**,** 691-7.

LUO, M. & KATZ, L. C. 2004. Encoding pheromonal signals in the mammalian vomeronasal system. *Curr Opin Neurobiol,* 14**,** 428-34.

LUO, M. 2008. The necklace olfactory system in mammals. *J Neurogenet,* 22**,** 229-38.

MA, M. & SHEPHERD, G. M. 2000. Functional mosaic organization of mouse olfactory receptor neurons. *Proc Natl Acad Sci U S A,* 97**,** 12869-74.

MACDONALD, R. 1999. Zebrafish immunohistochemistry. *Methods Mol Biol,* 127**,** 77-88.

MACRIDES, F. & SCHNEIDER, S. P. 1982. Laminar organization of mitral and tufted cells in the main olfactory bulb of the adult hamster. *J Comp Neurol,* 208**,** 419-30.

MALNIC, B., HIRONO, J., SATO, T. & BUCK, L. B. 1999. Combinatorial receptor codes for odors. *Cell,* 96**,** 713-23.

MAMASUEW, K., BREER, H. & FLEISCHER, J. 2008. Grueneberg ganglion neurons respond to cool ambient temperatures. *Eur J Neurosci,* 28**,** 1775-85.

MANTEIFEL, Y. B. & KARELINA, M. A. 1996. Conditioned food aversion in the goldfish, *Carassius auratus*. *Comp Biochem Physiol A,* 115**,** 31-35.

MASANTE-ROCA, I., GADENNE, C. & ANTON, S. 2005. Three-dimensional antennal lobe atlas of male and female moths, *Lobesia botrana* (Lepidoptera: Tortricidae) and glomerular representation of plant volatiles in females. *J Exp Biol,* 208**,** 1147-59.

MEEKS, J. P., ARNSON, H. A. & HOLY, T. E. 2010. Representation and transformation of sensory information in the mouse accessory olfactory system. *Nat Neurosci,* 13**,** 723-30.

MEISAMI, E. & BHATNAGAR, K. P. 1998. Structure and diversity in mammalian accessory olfactory bulb. *Micro Res Tech,* 43**,** 476-99.

MEISAMI, E. & SAFARI, L. 1981. A quantitative study of the effects of early unilateral olfactory deprivation on the number and distribution of mitral and tufted cells and of glomeruli in the rat olfactory bulb. *Brain Res,* 221**,** 81-107.

MEISTER, M. & BONHOEFFER, T. 2001. Tuning and topography in an odor map on the rat olfactory bulb. *J Neurosci,* 21**,** 1351-60.

MEYERHOF, W. & KORSCHING, S. 2009. Chemosensory systems in mammals, fishes, and insects. Preface. *Results Probl Cell Differ,* 47**,** v-xi.

MIYASAKA, N., MORIMOTO, K., TSUBOKAWA, T., HIGASHIJIMA, S., OKAMOTO, H. & YOSHIHARA, Y. 2009. From the olfactory bulb to higher brain centers: genetic visualization of secondary olfactory pathways in zebrafish. *J Neurosci,* 29**,** 4756-67.

MIYASAKA, N., SATO, Y., YEO, S. Y., HUTSON, L. D., CHIEN, C. B., OKAMOTO, H. & YOSHIHARA, Y. 2005. Robo2 is required for establishment of a precise glomerular map in the zebrafish olfactory system. *Development,* 132**,** 1283-93.

MOMBAERTS, P. 1996. Targeting olfaction. *Curr Opin Neurobiol,* 6**,** 481-6.

MOMBAERTS, P. 2004. Odorant receptor gene choice in olfactory sensory neurons: the one receptor-one neuron hypothesis revisited. *Curr Opin Neurobiol,* 14**,** 31-6.

MOMBAERTS, P. 2006. Axonal wiring in the mouse olfactory system. *Annu Rev Cell Dev Biol,* 22**,** 713-37.

MORI, K., KISHI, K. & OJIMA, H. 1983. Distribution of dendrites of mitral, displaced mitral, tufted, and granule cells in the rabbit olfactory bulb. *J Comp Neurol,* 219**,** 339-55.

MORI, K., TAKAHASHI, Y. K., IGARASHI, K. M. & YAMAGUCHI, M. 2006. Maps of odorant molecular features in the Mammalian olfactory bulb. *Physiol Rev,* 86**,** 409-33.

MORI, K. & YOSHIHARA, Y. 1995. Molecular recognition and olfactory processing in the mammalian olfactory system. *Prog Neurobiol,* 45**,** 585-619.

MORITA, Y. & FINGER, T. E. 1998. Differential projections of ciliated and microvillous olfactory receptor cells in the catfish, *Ictalurus punctatus*. *J Comp Neurol,* 398**,** 539-50.

MOULTON, D. G. 1976. Spatial patterning of response to odors in the peripheral olfactory system. *Physiol Rev,* 56**,** 578-93.

MUNGER, S. D., LEINDERS-ZUFALL, T. & ZUFALL, F. 2009. Subsystem organization of the mammalian sense of smell. *Annu Rev Physiol,* 71**,** 115-40.

NEZLIN, L. P., HEERMANN, S., SCHILD, D. & RÖSSLER, W. 2003. Organization of glomeruli in the main olfactory bulb of *Xenopus laevis* tadpoles. *J Comp Neurol,* 464**,** 257-68.

NEZLIN, L. P. & SCHILD, D. 2000. Structure of the olfactory bulb in tadpoles of *Xenopus laevis*. *Cell Tiss Res,* 302**,** 21-9.

NIKONOV, A. A. & CAPRIO, J. 2001. Electrophysiological evidence for a chemotopy of biologically relevant odors in the olfactory bulb of the channel catfish. *J Neurophysiol,* 86**,** 1869-76.

NIKONOV, A. A. & CAPRIO, J. 2004. Odorant specificity of single olfactory bulb neurons to amino acids in the channel catfish. *J Neurophysiol,* 92**,** 123-34.

NIKONOV, A. A. & CAPRIO, J. 2007a. Highly specific olfactory receptor neurons for types of amino acids in the channel catfish. *J Neurophysiol,* 98**,** 1909-18.

NIKONOV, A. A. & CAPRIO, J. 2007b. Responses of olfactory forebrain units to amino acids in the channel catfish. *J Neurophysiol,* 97**,** 2490-8.

NINKOVIC, J. & BALLY-CUIF, L. 2006. The zebrafish as a model system for assessing the reinforcing properties of drugs of abuse. *Methods,* 39**,** 262-74.

NÜSSLEIN-VOLHARD, C. & DAHM, R. 2002. *Zebrafish: a practical approach,* Oxford, Oxford university press.

OLIVA, A. M., JONES, K. R. & RESTREPO, D. 2008. Sensory-dependent asymmetry for a urine-responsive olfactory bulb glomerulus. *J Comp Neurol,* 510**,** 475-83.

PARICHY, D. M., ELIZONDO, M. R., MILLS, M. G., GORDON, T. N. & ENGESZER, R. E. 2009. Normal table of postembryonic zebrafish development: staging by externally visible anatomy of the living fish. *Dev Dyn,* 238**,** 2975-3015.

PEELE, P., DITZEN, M., MENZEL, R. & GALIZIA, C. G. 2006. Appetitive odor learning does not change olfactory coding in a subpopulation of honeybee antennal lobe neurons. *J Comp Physiol A Neuroethol Sens Neural Behav Physiol,* 192**,** 1083-103.

PIMENTEL, D. O. & MARGRIE, T. W. 2008. Glutamatergic transmission and plasticity between olfactory bulb mitral cells. *J Physiol,* 586**,** 2107-19.

PINCHING, A. J. & POWELL, T. P. 1971. The neuropil of the glomeruli of the olfactory bulb. *J Cell Sci,* 9**,** 347-77.

POMEROY, S. L., LAMANTIA, A. S. & PURVES, D. 1990. Postnatal construction of neural circuitry in the mouse olfactory bulb. *J Neurosci,* 10**,** 1952-66.

POTTER, S. M., ZHENG, C., KOOS, D. S., FEINSTEIN, P., FRASER, S. E. & MOMBAERTS, P. 2001. Structure and emergence of specific olfactory glomeruli in the mouse. *J Neurosci,* 21**,** 9713-23.

PUCHE, A. C. & SHIPLEY, M. T. 2001. Radial glia development in the mouse olfactory bulb. *J Comp Neurol,* 434**,** 1-12.

QUINN, W. G., HARRIS, W. A. & BENZER, S. 1974. Conditioned behavior in *Drosophila melanogaster. Proc Natl Acad Sci U S A,* 71**,** 708-12.

RESSLER, K. J., SULLIVAN, S. L. & BUCK, L. B. 1993. A zonal organization of odorant receptor gene expression in the olfactory epithelium. *Cell,* 73**,** 597-609.

RIDDLE, D. R. & OAKLEY, B. 1992. Immunocytochemical identification of primary olfactory afferents in rainbow trout. *J Comp Neurol,* 324**,** 575-89.

RODRIGUEZ, I., FEINSTEIN, P. & MOMBAERTS, P. 1999. Variable patterns of axonal projections of sensory neurons in the mouse vomeronasal system. *Cell,* 97**,** 199-208.

RONNETT, G. V. & MOON, C. 2002. G proteins and olfactory signal transduction. *Annu Rev Physiol,* 64**,** 189-222.

ROYAL, S. J. & KEY, B. 1999. Development of P2 olfactory glomeruli in P2-internal ribosome entry site-tau-LacZ transgenic mice. *J Neurosci,* 19**,** 9856-64.

RYBAK, J., KUSS, A., LAMECKER, H., ZACHOW, S., HEGE, H. C., LIENHARD, M., SINGER, J., NEUBERT, K. & MENZEL, R. 2010. The Digital Bee Brain: Integrating and Managing Neurons in a Common 3D Reference System. *Front Syst Neurosci,* 4.

SAKANO, H. 2010. Neural map formation in the mouse olfactory system. *Neuron,* 67**,** 530-42.

SATO, K. & SUZUKI, N. 2001. Whole-cell response characteristics of ciliated and microvillous olfactory receptor neurons to amino acids, pheromone candidates and urine in rainbow trout. *Chem Senses,* 26**,** 1145-56.

SATO, Y., MIYASAKA, N. & YOSHIHARA, Y. 2005. Mutually exclusive glomerular innervation by two distinct types of olfactory sensory neurons revealed in transgenic zebrafish. *J Neurosci,* 25**,** 4889-97.

SATOU, M., ANZAI, S. & HURUNO, M. 2005. Long-term potentiation and olfactory memory formation in the carp (*Cyprinus carpio* L.) olfactory bulb. *J Comp Physiol A,* 191**,** 421-34.

SATOU, M., HOSHIKAWA, R., SATO, Y. & OKAWA, K. 2006. An in vitro study of long-term potentiation in the carp (*Cyprinus carpio* L.) olfactory bulb. *J Comp Physiol A,* 192**,** 135-50.

SCHAEFER, M. L., FINGER, T. E. & RESTREPO, D. 2001. Variability of position of the P2 glomerulus within a map of the mouse olfactory bulb. *J Comp Neurol,* 436**,** 351-62.

SCHELLINCK, H. M., FORESTELL, C. A. & LOLORDO, V. M. 2001. A simple and reliable test of olfactory learning and memory in mice. *Chem Senses,* 26**,** 663-72.

SCHMID, B., SCHINDELIN, J., CARDONA, A., LONGAIR, M. & HEISENBERG, M. 2010. A high-level 3D visualization API for Java and ImageJ. *BMC Bioinfo,* 11**,** 274.

SCHWARTING, G. A. & HENION, T. R. 2008. Olfactory axon guidance: the modified rules. *J Neurosci Res,* 86**,** 11-7.

SERIZAWA, S., MIYAMICHI, K. & SAKANO, H. 2004. One neuron-one receptor rule in the mouse olfactory system. *Trends Genet,* 20**,** 648-53.

SERIZAWA, S., MIYAMICHI, K., TAKEUCHI, H., YAMAGISHI, Y., SUZUKI, M. & SAKANO, H. 2006. A neuronal identity code for the odorant receptor-specific and activity-dependent axon sorting. *Cell,* 127**,** 1057-69.

SHARP, F. R., KAUER, J. S. & SHEPHERD, G. M. 1975. Local sites of activity-related glucose metabolism in rat olfactory bulb during olfactory stimulation. *Brain Res,* 98**,** 596-600.

SHEPHERD, G. M. 1972. Synaptic organization of the mammalian olfactory bulb. *Physiol Rev,* 52**,** 864-917.

SHINODA, K., SHIOTANI, Y. & OSAWA, Y. 1989. "Necklace olfactory glomeruli" form unique components of the rat primary olfactory system. *J Comp Neurol,* 284**,** 362-73.

SORENSEN, P. W., CHRISTENSEN, T. A. & STACEY, N. E. 1998. Discrimination of pheromonal cues in fish: emerging parallels with insects. *Curr Opin Neurobiol,* 8**,** 458-67.

SORENSEN, P. W., HARA, T. J. & STACEY, N. E. 1991. Sex-pheromones selectively stimulate the medial olfactory tracts of male goldfish. *Brain Research,* 558**,** 343-347.

SORENSEN, P. W. & STACEY, N. E. 2004. Brief review of fish pheromones and discussion of their possible uses in the control of non-indigenous teleost fishes. *NZ J Marine and Freshwater Res,* 38**,** 399-417.

SPORS, H. & GRINVALD, A. 2002. Spatio-temporal dynamics of odor representations in the mammalian olfactory bulb. *Neuron,* 34**,** 301-15.

ST JOHN, J. A., CLARRIS, H. J., MCKEOWN, S., ROYAL, S. & KEY, B. 2003. Sorting and convergence of primary olfactory axons are independent of the olfactory bulb. *J Comp Neurol,* 464**,** 131-40.

ST JOHN, J. A. & KEY, B. 2001. Chemically and morphologically identifiable glomeruli in the rat olfactory bulb. *J Comp Neurol,* 436**,** 497-507.

STETTLER, D. D. & AXEL, R. 2009. Representations of odor in the piriform cortex. *Neuron,* 63**,** 854-64.

STEVENS, C. B. & HALLORAN, M. C. 2005. Developmental expression of sema3G, a novel zebrafish semaphorin. *Gene Expr Patterns,* 5**,** 647-53.

STEWART, W. B., KAUER, J. S. & SHEPHERD, G. M. 1979. Functional organization of rat olfactory bulb analysed by the 2-deoxyglucose method. *J Comp Neurol,* 185**,** 715-34.

STOWERS, L. & LOGAN, D. W. 2010. Olfactory mechanisms of stereotyped behavior: on the scent of specialized circuits. *Curr Opin Neurobiol,* 20**,** 274-80.

STROTMANN, J. & BREER, H. 2006. Formation of glomerular maps in the olfactory system. *Semin Cell Dev Biol,* 17**,** 402-10.

STROTMANN, J., CONZELMANN, S., BECK, A., FEINSTEIN, P., BREER, H. & MOMBAERTS, P. 2000. Local permutations in the glomerular array of the mouse olfactory bulb. *J Neurosci,* 20**,** 6927-38.

SU, C. Y., MENUZ, K. & CARLSON, J. R. 2009. Olfactory perception: receptors, cells, and circuits. *Cell,* 139**,** 45-59.

SUBOSKI, M. D., BAIN, S., CARTY, A. E., MCQUOID, L. M., SEELEN, M. I. & SEIFERT, M. 1990. Alarm Reaction in Acquisition and Social Transmission of Simulated-Predator Recognition by Zebra Danio Fish (*Brachydanio-Rerio*). *J Comp Psychol,* 104**,** 101-112.

SUH, G. S., BEN-TABOU DE LEON, S., TANIMOTO, H., FIALA, A., BENZER, S. & ANDERSON, D. J. 2007. Light activation of an innate olfactory avoidance response in *Drosophila*. *Curr Biol,* 17**,** 905-8.

SUH, G. S., WONG, A. M., HERGARDEN, A. C., WANG, J. W., SIMON, A. F., BENZER, S., AXEL, R. & ANDERSON, D. J. 2004. A single population of olfactory sensory neurons mediates an innate avoidance behaviour in *Drosophila*. *Nature,* 431**,** 854-9.

SUN, L., WANG, H., HU, J., HAN, J., MATSUNAMI, H. & LUO, M. 2009. Guanylyl cyclase-D in the olfactory CO_2 neurons is activated by bicarbonate. *Proc Natl Acad Sci U S A,* 106**,** 2041-6.

TABOR, R., YAKSI, E., WEISLOGEL, J. M. & FRIEDRICH, R. W. 2004. Processing of odor mixtures in the zebrafish olfactory bulb. *J Neurosci,* 24**,** 6611-6620.

TAKAMI, S. & GRAZIADEI, P. P. 1990. Morphological complexity of the glomerulus in the rat accessory olfactory bulb--a Golgi study. *Brain Res,* 510**,** 339-42.

TAKAMI, S. & GRAZIADEI, P. P. 1991. Light microscopic Golgi study of mitral/tufted cells in the accessory olfactory bulb of the adult rat. *J Comp Neurol,* 311**,** 65-83.

TEICHER, M. H., STEWART, W. B., KAUER, J. S. & SHEPHERD, G. M. 1980. Suckling pheromone stimulation of a modified glomerular region in the developing rat olfactory bulb revealed by the 2-deoxyglucose method. *Brain Res,* 194**,** 530-5.

THOMMESEN, G. 1983. Morphology, distribution, and specificity of olfactory receptor cells in salmonid fishes. *Acta Physiol Scand,* 117**,** 241-9.

TOUHARA, K. & VOSSHALL, L. B. 2009. Sensing odorants and pheromones with chemosensory receptors. *Annu Rev Physiol,* 71**,** 307-32.

TRELOAR, H., WALTERS, E., MARGOLIS, F. & KEY, B. 1996. Olfactory glomeruli are innervated by more than one distinct subset of primary sensory olfactory neurons in mice. *J Comp Neurol,* 367**,** 550-62.

TYLER, W. J., PETZOLD, G. C., PAL, S. K. & MURTHY, V. N. 2007. Experience-dependent modification of primary sensory synapses in the mammalian olfactory bulb. *J Neurosci,* 27**,** 9427-38.

TZSCHENTKE, T. M. 1998. Measuring reward with the conditioned place preference paradigm: a comprehensive review of drug effects, recent progress and new issues. *Prog Neurobiol,* 56**,** 613-72.

UCHIDA, N., TAKAHASHI, Y. K., TANIFUJI, M. & MORI, K. 2000. Odor maps in the mammalian olfactory bulb: domain organization and odorant structural features. *Nat Neurosci,* 3**,** 1035-43.

VALENTINCIC, T. & CAPRIO, J. 1994a. Consummatory feeding behavior to amino acids in intact and anosmic channel catfish *Ictalurus punctatus. Physiol Behav,* 55**,** 857-63.

VALENTINCIC, T. & CAPRIO, J. 1997. Visual and chemical release of feeding behavior in adult rainbow trout. *Chem Senses,* 22**,** 375-82.

VALENTINCIC, T., KRALJ, J., STENOVEC, M. & KOCE, A. 1996. Learned olfactory discrimination of amino acids and their binary mixtures in bullhead catfish (*Ameiurus nebulosus*). *Pflugers Arch,* 431**,** R313-4.

VALENTINCIC, T., KRALJ, J., STENOVEC, M., KOCE, A. & CAPRIO, J. 2000a. The behavioral detection of binary mixtures of amino acids and their individual components by catfish. *J Exp Biol,* 203**,** 3307-17.

VALENTINCIC, T., METELKO, J., OTA, D., PIRC, V. & BLEJEC, A. 2000b. Olfactory discrimination of amino acids in brown bullhead catfish. *Chem Senses,* 25**,** 21-9.

VALENTINCIC, T., MIKLAVC, P., DOLENEK, J. & PLIBEREK, K. 2005. Correlations between Olfactory Discrimination, Olfactory Receptor Neuron Responses and Chemotopy of Amino Acids in Fishes. *Chem Senses,* 30 Suppl 1**,** i312-i314.

VALENTINCIC, T., WEGERT, S. & CAPRIO, J. 1994. Learned olfactory discrimination versus innate taste responses to amino acids in channel catfish (*Ictalurus punctatus*). *Physiol Behav,* 55**,** 865-73.

VALENTINCIC, T. B. & CAPRIO, J. 1994b. Chemical and visual control of feeding and escape behaviors in the channel catfish *Ictalurus punctatus*. *Physiol Behav,* 55**,** 845-55.

VALVERDE, F., SANTACANA, M. & HEREDIA, M. 1992. Formation of an olfactory glomerulus: morphological aspects of development and organization. *Neuroscience,* 49**,** 255-75.

VASSAR, R., CHAO, S. K., SITCHERAN, R., NUNEZ, J. M., VOSSHALL, L. B. & AXEL, R. 1994. Topographic organization of sensory projections to the olfactory bulb. *Cell,* 79**,** 981-91.

VASSAR, R., NGAI, J. & AXEL, R. 1993. Spatial segregation of odorant receptor expression in the mammalian olfactory epithelium. *Cell,* 74**,** 309-18.

VITEBSKY, A., REYES, R., SANDERSON, M. J., MICHEL, W. C. & WHITLOCK, K. E. 2005. Isolation and characterization of the laure olfactory behavioral mutant in the zebrafish, *Danio rerio*. *Dev Dyn,* 234**,** 229-42.

VOSSHALL, L. B., WONG, A. M. & AXEL, R. 2000. An olfactory sensory map in the fly brain. *Cell,* 102**,** 147-59.

WACHOWIAK, M. & COHEN, L. B. 2001. Representation of odorants by receptor neuron input to the mouse olfactory bulb. *Neuron,* 32**,** 723-35.

WACHOWIAK, M. & SHIPLEY, M. T. 2006. Coding and synaptic processing of sensory information in the glomerular layer of the olfactory bulb. *Semin Cell Dev Biol,* 17**,** 411-23.

WACHOWIAK, M., WESSON, D. W., PIREZ, N., VERHAGEN, J. V. & CAREY, R. M. 2009. Low-level mechanisms for processing odor information in the behaving animal. *Ann N Y Acad Sci,* 1170**,** 286-92.

WAGNER, S., GRESSER, A. L., TORELLO, A. T. & DULAC, C. 2006. A multireceptor genetic approach uncovers an ordered integration of VNO sensory inputs in the accessory olfactory bulb. *Neuron,* 50**,** 697-709.

WALDMAN, B. 1982. Quantitative and developmental analyses of the alarm reaction in the zebra danio, *Brachydanio Rerio. Copeia***,** 1-9.

WANG, Z., LI, V., CHAN, G. C., PHAN, T., NUDELMAN, A. S., XIA, Z. & STORM, D. R. 2009. Adult type 3 adenylyl cyclase-deficient mice are obese. *PLoS One,* 4**,** e6979.

WANG, Z., NUDELMAN, A. & STORM, D. R. 2007. Are pheromones detected through the main olfactory epithelium? *Mol Neurobiol,* 35**,** 317-23.

WHITLOCK, K. E. & WESTERFIELD, M. 1998. A transient population of neurons pioneers the olfactory pathway in the zebrafish. *J Neurosci,* 18**,** 8919-8927.

WILSON, D. A. & LEON, M. 1988. Spatial patterns of olfactory bulb single-unit responses to learned olfactory cues in young rats. *J Neurophysiol,* 59**,** 1770-82.

WILSON, R. I. 2008. Neural and behavioral mechanisms of olfactory perception. *Curr Opin Neurobiol,* 18**,** 408-12.

WOO, C. C., COOPERSMITH, R. & LEON, M. 1987. Localized changes in olfactory-bulb morphology associated with early olfactory leraning. *J Comp Neurol,* 263**,** 113-125.

WYATT, T. D. 2010. Pheromones and signature mixtures: defining species-wide signals and variable cues for identity in both invertebrates and vertebrates. *J Comp Physiol A Neuroethol Sens Neural Behav Physiol,* 196**,** 685-700.

WYETH, R. C. & WILLOWS, A. O. D. 2006a. Adaptation of underwater video for near-substratum current measurement. *Biol Bull,* 211**,** 101-105.

WYETH, R. C. & WILLOWS, A. O. D. 2006b. Field behavior of the nudibranch mollusc *Tritonia diomedea. Biol Bull,* 210**,** 81-96.

YAKSI, E., JUDKEWITZ, B. & FRIEDRICH, R. W. 2007. Topological Reorganization of Odor Representations in the Olfactory Bulb. *PLoS Biol,* 5**,** e178.

YAMBE, H., KITAMURA, S., KAMIO, M., YAMADA, M., MATSUNAGA, S., FUSETANI, N. & YAMAZAKI, F. 2006. L-Kynurenine, an amino acid identified as a sex pheromone in the urine of ovulated female masu salmon. *Proc Natl Acad Sci U S A,* 103**,** 15370-4.

YANICOSTAS, C., HERBOMEL, E., DIPIETROMARIA, A. & SOUSSI-YANICOSTAS, N. 2009. Anosmin-1a is required for fasciculation and terminal targeting of olfactory sensory neuron axons in the zebrafish olfactory system. *Mol Cell Endocrinol,* 312**,** 53-60.

YOKOI, M., MORI, K. & NAKANISHI, S. 1995. Refinement of odor molecule tuning by dendrodendritic synaptic inhibition in the olfactory bulb. *Proc Natl Acad Sci U S A,* 92**,** 3371-5.

YUAN, Q. 2009. Theta bursts in the olfactory nerve paired with beta-adrenoceptor activation induce calcium elevation in mitral cells: a mechanism for odor preference learning in the neonate rat. *Learn Mem,* 16**,** 676-81.

ZHAO, H. & REED, R. R. 2001. X inactivation of the OCNC1 channel gene reveals a role for activity-dependent competition in the olfactory system. *Cell,* 104**,** 651-60.

ZHENG, C., FEINSTEIN, P., BOZZA, T., RODRIGUEZ, I. & MOMBAERTS, P. 2000. Peripheral olfactory projections are differentially affected in mice deficient in a cyclic nucleotide-gated channel subunit. *Neuron,* 26**,** 81-91.

ZHENG, L. M., RAVEL, N. & JOURDAN, F. 1987. Topography of centrifugal acetylcholinesterase-positive fibres in the olfactory bulb of the rat: evidence for original projections in atypical glomeruli. *Neurosci,* 23**,** 1083-93.

ZHOU, Z., XIONG, W., ZENG, S., XIA, A., SHEPHERD, G. M., GREER, C. A. & CHEN, W. R. 2006. Dendritic excitability and calcium signalling in the mitral cell distal glomerular tuft. *Eur J Neurosci,* 24**,** 1623-32.

ZIPPEL, H. P., SORENSEN, P. W. & HANSEN, A. 1997. High correlation between microvillous olfactory receptor cell abundance and sensitivity to pheromones in olfactory nerve-sectioned goldfish. *J Comp Physiol A,* 180**,** 39-52.

ZIPPEL, H. P., VOIGT, R., KNAUST, M. & LUAN, Y. 1993. Spontaneous behavior, training and discrimination-training in goldfish using chemosensory stimuli. *J Comp Physiol A,* 172**,** 81-90.

ZOU, D. J., CHESLER, A. & FIRESTEIN, S. 2009. How the olfactory bulb got its glomeruli: a just so story? *Nat Rev Neurosci,* 10**,** 611-8.

ZOU, D. J., CHESLER, A. T., LE PICHON, C. E., KUZNETSOV, A., PEI, X., HWANG, E. L. & FIRESTEIN, S. 2007. Absence of adenylyl cyclase 3 perturbs peripheral olfactory projections in mice. *J Neurosci,* 27**,** 6675-83.

ZOU, D. J., FEINSTEIN, P., RIVERS, A. L., MATHEWS, G. A., KIM, A., GREER, C. A., MOMBAERTS, P. & FIRESTEIN, S. 2004. Postnatal refinement of peripheral olfactory projections. *Science,* 304**,** 1976-9.

ZUFALL, F. & LEINDERS-ZUFALL, T. 2007. Mammalian pheromone sensing. *Curr Opin Neurobiol,* 17**,** 483-9.

Appendix 1

Supplemental Movies

Supplemental Movie 1. A projection through serial confocal sections obtained by viewing whole mounted olfactory bulbs from their dorsal surfaces. Each olfactory bulb was imaged separately with a 25X oil immersion objective and the video is a composite of two raw image stack projections recorded with ImageJ software and assembled to their final format in Apple keynote. The specimens are labeled with anti-calretinin (red) and anti-KLH (grey) antibodies. Tracings were performed manually and each glomerulus was assigned a number, in order of their identification. Individual glomeruli were identified after such an analysis was performed. Notice that not all glomeruli are traced in this image series; each series was viewed 2-3 separate times to ensure that all glomeruli had been identified. Images shown in this video had only been viewed once. The tissue shown in the movie is the same as in Figure 15. We recommend viewing the movie with VLC video player, ImageJ or Itunes.

Supplemental Movie 2. A projection through serial optical sections obtained by viewing whole mounted olfactory bulbs from their ventral surfaces. The olfactory bulbs were from the same specimen but were each imaged separately with a 25X oil immersion objective. Each bulb is labeled with calretinin (red) and $G_{\alpha\ s/olf}$ (green) antibodies. Much of the ventral surface is covered in thick fiber bundles that project towards glomeruli in the ventromedial or ventroposterior regions. Beneath these fibers bundles are the ventral glomeruli (vG) that are almost exclusively $G_{\alpha\ s/olf}$ IR. Examples of ventral glomeruli are traced and annotated. Also shown are the stereotypic vtG_2 and the medial glomeruli. Note that these glomeruli also contain several exclusively $G_{\alpha\ s/olf}$ IR glomeruli. The tissue shown in the movie is the same as in Figure 22. We recommend viewing the movie with VLC video player, ImageJ or Itunes.

Supplemental Movie 3. Three dimensionally reconstructed single dorsal olfactory bulb of a female zebrafish. The image on the left of the reconstruction shows the main divisions of the dorsal olfactory bulb, the dorsal (dG), dorsolateral (dlG) mediodorsal (mdG) and dorsal cluster associated (dcaG) glomeruli. All glomeruli but the dcaG are located in a thin sheet on the surface of the olfactory bulbs. The dcaG are located beneath this sheet and extend caudally. This olfactory bulb was labeled with anti KLH

antibodies. The tissue shown in the movie is the same as in Figure 15. We recommend viewing the movie with VLC video player, ImageJ or Itunes.

Supplemental Movie 4. For olfactory enrichment experiments fish were housed individually or in pairs in small chambers in a flow-through nursery system. Odorants (shown in the video as red dye) were administered as brief pulses every 30 minutes for the duration of the experiment. We recommend viewing the movie with VLC video player, ImageJ or Itunes.

Appendix 2

Copyright Release for Material Presented in
Chapter 2

This is a License Agreement between Oliver R Braubach ("You") and Elsevier ("Elsevier") provided by Copyright Clearance Center ("CCC"). The license consists of your order details, the terms and conditions provided by Elsevier, and the payment terms and conditions.

All payments must be made in full to CCC. For payment instructions, please see information listed at the bottom of this form.

Supplier	Elsevier Limited The Boulevard,Langford Lane Kidlington,Oxford,OX5 1GB,UK
Registered Company Number	1982084
Customer name	Oliver R Braubach
Customer address	5850 College Street
	Halifax, NS B3H1X5
License number	2600000215378
License date	Feb 01, 2011
Licensed content publisher	Elsevier
Licensed content publication	Behavioural Brain Research
Licensed content title	Olfactory conditioning in the zebrafish (*Danio rerio*)
Licensed content author	Oliver R. Braubach, Heather-Dawn Wood, Simon Gadbois, Alan Fine, Roger P. Croll
Licensed content date	2 March 2009
Licensed content volume number	198
Licensed content issue number	1
Number of pages	9
Start Page	190
End Page	198
Type of Use	reuse in a thesis/dissertation
Portion	full article
Format	electronic
Are you the author of this Elsevier article?	Yes
Will you be translating?	No
Order reference number	
Title of your	Development, Organization and Plasticity of the Zebrafish Olfactory

thesis/dissertation	System
Expected completion date	Feb 2011
Estimated size (number of pages)	350
Elsevier VAT number	GB 494 6272 12
Permissions price	0.00 USD
VAT/Local Sales Tax	0.0 USD / 0.0 GBP
Total	0.00 USD
Terms and Conditions	

INTRODUCTION

1. The publisher for this copyrighted material is Elsevier. By clicking "accept" in connection with completing this licensing transaction, you agree that the following terms and conditions apply to this transaction (along with the Billing and Payment terms and conditions established by Copyright Clearance Center, Inc. ("CCC"), at the time that you opened your Rightslink account and that are available at any time at http://myaccount.copyright.com).

GENERAL TERMS

2. Elsevier hereby grants you permission to reproduce the aforementioned material subject to the terms and conditions indicated.

3. Acknowledgement: If any part of the material to be used (for example, figures) has appeared in our publication with credit or acknowledgement to another source, permission must also be sought from that source. If such permission is not obtained then that material may not be included in your publication/copies. Suitable acknowledgement to the source must be made, either as a footnote or in a reference list at the end of your publication, as follows:

"Reprinted from Publication title, Vol /edition number, Author(s), Title of article / title of chapter, Pages No., Copyright (Year), with permission from Elsevier [OR APPLICABLE SOCIETY COPYRIGHT OWNER]." Also Lancet special credit - "Reprinted from The Lancet, Vol. number, Author(s), Title of article, Pages No., Copyright (Year), with permission from Elsevier."

4. Reproduction of this material is confined to the purpose and/or media for which permission is hereby given.

5. Altering/Modifying Material: Not Permitted. However figures and illustrations may be altered/adapted minimally to serve your work. Any other abbreviations, additions, deletions and/or any other alterations shall be made only with prior written authorization of Elsevier Ltd. (Please contact Elsevier at permissions@elsevier.com)

6. If the permission fee for the requested use of our material is waived in this instance, please be advised that your future requests for Elsevier materials may attract a fee.

7. Reservation of Rights: Publisher reserves all rights not specifically granted in the combination of (i) the license details provided by you and accepted in the course of this licensing transaction, (ii) these terms and conditions and (iii) CCC's Billing and Payment terms and conditions.

8. License Contingent Upon Payment: While you may exercise the rights licensed immediately upon issuance of the license at the end of the licensing process for the transaction, provided that you have disclosed complete and accurate details of your proposed use, no license is finally effective unless and until full payment is received from you (either by publisher or by CCC) as provided in CCC's Billing and Payment terms and conditions. If full payment is not received on a timely basis, then any license preliminarily granted shall be deemed automatically revoked and shall be void as if never granted. Further, in the event that you breach any of these terms and conditions or any of CCC's Billing and Payment terms and conditions, the license is automatically revoked and shall be void as if never granted. Use of materials as described in a revoked license, as well as any use of the materials beyond the scope of an unrevoked license, may constitute copyright infringement and publisher reserves the right to take any and all action to protect its copyright in the materials.

9. Warranties: Publisher makes no representations or warranties with respect to the licensed material.

10. Indemnity: You hereby indemnify and agree to hold harmless publisher and CCC, and their respective officers, directors, employees and agents, from and against any and all claims arising out of your use of the licensed material other than as specifically authorized pursuant to this license.

11. No Transfer of License: This license is personal to you and may not be sublicensed, assigned, or transferred by you to any other person without publisher's written permission.

12. No Amendment Except in Writing: This license may not be amended except in a writing signed by both parties (or, in the case of publisher, by CCC on publisher's behalf).

13. Objection to Contrary Terms: Publisher hereby objects to any terms contained in any purchase order, acknowledgment, check endorsement or other writing prepared by you, which terms are inconsistent with these terms and conditions or CCC's Billing and Payment terms and conditions. These terms and conditions, together with CCC's Billing and Payment terms and conditions (which are incorporated herein), comprise the entire agreement between you and publisher (and CCC) concerning this licensing transaction. In the event of any conflict between your obligations established by these terms and conditions and those established by CCC's Billing and Payment terms and conditions, these terms and conditions shall control.

14. Revocation: Elsevier or Copyright Clearance Center may deny the permissions described in this License at their sole discretion, for any reason or no reason, with a full refund payable to you. Notice of such denial will be made using the contact information provided by you. Failure to receive such notice will not alter or invalidate the denial. In no event will Elsevier or Copyright Clearance Center be responsible or liable for any costs, expenses or damage incurred by you as a result of a denial of your permission request, other than a refund of the amount(s) paid by you to Elsevier and/or Copyright Clearance Center for denied

310

permissions.

LIMITED LICENSE

The following terms and conditions apply only to specific license types:

15. **Translation**: This permission is granted for non-exclusive world **English** rights only unless your license was granted for translation rights. If you licensed translation rights you may only translate this content into the languages you requested. A professional translator must perform all translations and reproduce the content word for word preserving the integrity of the article. If this license is to re-use 1 or 2 figures then permission is granted for non-exclusive world rights in all languages.

16. **Website**: The following terms and conditions apply to electronic reserve and author websites:
Electronic reserve: If licensed material is to be posted to website, the web site is to be password-protected and made available only to bona fide students registered on a relevant course if:
This license was made in connection with a course,
This permission is granted for 1 year only. You may obtain a license for future website posting,
All content posted to the web site must maintain the copyright information line on the bottom of each image,
A hyper-text must be included to the Homepage of the journal from which you are licensing at http://www.sciencedirect.com/science/journal/xxxxx or the Elsevier homepage for books at http://www.elsevier.com , and
Central Storage: This license does not include permission for a scanned version of the material to be stored in a central repository such as that provided by Heron/XanEdu.

17. **Author website** for journals with the following additional clauses:

All content posted to the web site must maintain the copyright information line on the bottom of each image, and
he permission granted is limited to the personal version of your paper. You are not allowed to download and post the published electronic version of your article (whether PDF or HTML, proof or final version), nor may you scan the printed edition to create an electronic version,
A hyper-text must be included to the Homepage of the journal from which you are licensing at http://www.sciencedirect.com/science/journal/xxxxx , As part of our normal production process, you will receive an e-mail notice when your article appears on Elsevier's online service ScienceDirect (www.sciencedirect.com). That e-mail will include the article's Digital Object Identifier (DOI). This number provides the electronic link to the published article and should be included in the posting of your personal version. We ask that you wait until you receive this e-mail and have the DOI to do any posting.
Central Storage: This license does not include permission for a scanned version of the material to be stored in a central repository such as that provided by Heron/XanEdu.

18. **Author website** for books with the following additional clauses:
Authors are permitted to place a brief summary of their work online only.
A hyper-text must be included to the Elsevier homepage at http://www.elsevier.com

311

All content posted to the web site must maintain the copyright information line on the bottom of each image
   You are not allowed to download and post the published electronic version of your chapter, nor may you scan the printed edition to create an electronic version.
Central Storage: This license does not include permission for a scanned version of the material to be stored in a central repository such as that provided by Heron/XanEdu.

19. **Website** (regular and for author): A hyper-text must be included to the Homepage of the journal from which you are licensing at http://www.sciencedirect.com/science/journal/xxxxx. or for books to the Elsevier homepage at http://www.elsevier.com

20. **Thesis/Dissertation**: If your license is for use in a thesis/dissertation your thesis may be submitted to your institution in either print or electronic form. Should your thesis be published commercially, please reapply for permission. These requirements include permission for the Library and Archives of Canada to supply single copies, on demand, of the complete thesis and include permission for UMI to supply single copies, on demand, of the complete thesis. Should your thesis be published commercially, please reapply for permission.

21. **Other Conditions**:

v1.6